Theoretical, Numerical, and Semi-Analytical Treatment of Different Variants of Non-Linear Coagulation Equations

THESIS

Submitted in partial fulfillment of the requirements
for the degree of

DOCTOR OF PHILOSOPHY

by

SONALI KAUSHIK
ID No. 2018PHXF0023P

under the supervision of

Prof. Rajesh Kumar

BIRLA INSTITUTE OF TECHNOLOGY & SCIENCE PILANI
PILANI - 333031, India

2023

BIRLA INSTITUTE OF TECHNOLOGY AND SCIENCE, PILANI

CERTIFICATE

This is to certify that the thesis titled **"Theoretical, Numerical, and Semi-Analytical Treatment of Different Variants of Non-Linear Coagulation Equations"** submitted by **Ms. Sonali Kaushik**, ID No. **2018PHXF0023P** for award of Ph.D. of the Institute embodies original work done by her under my supervision.

Signature of the Supervisor
Name: **PROF. RAJESH KUMAR**
Designation: **Associate Professor**

Date: **18 May 2023**

Acknowledgments

First, I would like to start with a beautiful saying by Indian mathematician Aryabhatta- "*Life is a math equation, in order to gain the most, you have to know how to convert negatives into positives*".

I thank my supervisor, Prof. Rajesh Kumar, whose calmness and expertise were pivotal in pursuing my research work and completing my thesis compilation. His extremely observant feedback, constant support, and fruitful discussions enabled me to become a calmer open-minded researcher and sharpen my mental strength.

I extend my sincere gratitude to Vice-Chancellor Prof. V. Ramgopal Rao and Director Prof. Sudhirkumar Barai, BITS Pilani, Pilani Campus, for providing a peaceful environment to complete my thesis work. I also thank Prof. Shamik Chakraborty, Associate Dean, AGSRD, and Prof. Ashish Tiwari for his continuous support as the DRC convener. I express my heartiest thanks to my DAC members, Dr. Sangita Yadav and Dr. Gaurav Dwivedi, Assistant Professors, Department of Mathematics, BITS Pilani, Pilani Campus, for providing invaluable suggestions for my Ph.D. thesis.

I am grateful to Prof. Balram Dubey (former HoD), Prof. Bhupendra Kumar Sharma (former HoD), and present HoD, Prof. Devendra Kumar, for providing me with all the necessary research facilities and a healthy working environment.

I acknowledge all the faculty members of the Mathematics Department, BITS Pilani, Pilani Campus, for their direct and indirect encouragement, support, and guidance during the entire journey of my doctoral work.

I thankfully acknowledge Prof. Fernando Pestana da Costa, Professor, IST, Lisbon, for providing valuable inputs for some of the theoretical results in this work. Having collaborated with him, I learned a lot from his expert comments, and the constructive discussions helped me polish my understanding of discrete models. I also thank Prof. Ankik Kumar Giri, Associate Professor, IIT Roorkee, for his constant encouragement and guidance during my Ph.D. My sincere regards go to the esteemed examiners for providing precise feedback and for offering a substantial intellectual rationale for the contents of the thesis.

The credit also goes to all my colleagues, staff, and dear friends whose constant support and motivation in all crucial moments made this journey joyful. I will never forget the wonderful time I spent with my dear friends Barkha, Kapil, Sugandha, Komal, Pallav, Swati, Deepak, Shilpa, and helpful juniors Sanjiv, Gourav, Umesh, Saddam, and Shweta.

My heartiest appreciation goes to my family, whose blessings and motivation helped me with my humble academic achievements. I would like to thank my grandparents, Mr. Anand Prakash Sharma and Mrs. Kailashvati Devi Sharma, for providing a happy and satisfying childhood. I thank my parents, Mr. Man Mohan Kaushik and Mrs. Mamta Rani Kaushik, for their unconditional love and for inspiring me to commence my Ph.D. journey. My father, a Lecturer, is my life coach, and his beautiful Hindi stories and poems have upskilled my emotional quotient. Being a mathematics Lecturer herself, my mother is my first teacher and has taught me the importance of discipline. I am very much thankful to my brother, Er. Bhaskar Kaushik for fun-filled discussions and reverse psychology motivation which has inspired me to challenge my mental abilities. I thank my best friend and husband, Mr. Saurav Mitra for always cheering me up in adverse situations, and tolerating my flare for storytelling. This work would not have been possible without my parents, supervisor, and teachers' endless support and encouragement. In the end, I thankfully acknowledge everyone who contributed directly or indirectly to the completion of this thesis work.

Place: Pilani

Date: 18/05/2023

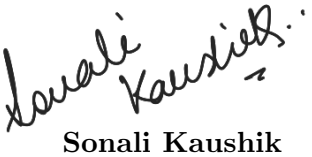

Sonali Kaushik

Abstract

This thesis mainly focuses on the coagulation equations such as the Safronov-Dubovski coagulation equation (SDCE) and Smoluchowski's coagulation equation which are relevant to astrophysics, particle physics, and other fields of sciences. The SDCE includes two major events: coagulation followed by collision. There are various examples of the phenomena explained by SDCE, namely, the formation of the protoplanetary disk around a star, the collision of asteroids, and the development of Saturn's rings. The real-world problems caused by particle coagulation such as the health hazards of sand and dust storms, nano-metal dust explosions, and the impact on glacier mass as a result of volcanic dust accumulation. Smoluchowski's equation has a diverse range of applications, such as in the field of biopharmaceuticals, the financial sector, aerosol science, and marine sciences.

The thesis initially investigates the theoretical, numerical, and steady-state behavior of the SDCE. The theoretical analysis deals with the establishment of existence, uniqueness, and mass conservation results for the SDCE for the unbounded kernel of the form $\min\{i,j\}V_{i,j} \leq (i+j)\ \forall\ i,j \geq 1$. For the existence part, Helly's selection theorem is implemented and Gronwall's lemma is used to establish the uniqueness. Moreover, it is also shown that the obtained unique solution is mass conserving. Further, the definition of the kernel is extended to $V_{i,j} \leq (i+j)\ \forall\ i,j \geq 1$, and the global existence, density conservation of the solutions are discussed. In addition, the existence and density conservation results are also examined in the case of a non-conservative approximation of the finite-dimensional system for both the above-mentioned parameters. Furthermore, the differentiability of the solution is proved for the generalized class $V_{i,j} \leq (i^\alpha + j^\alpha)$, $0 \leq \alpha \leq 1$ which contains the above kernel. Finally, the uniqueness of solution is established for the coagulation kernel of the type $V_{i,j} \leq \min\{i^\eta, j^\eta\}$ such that $0 \leq \eta \leq 2$.

After the theoretical analysis, the steady-state behavior of SDCE is investigated for the parameters $V_{i,j} = C_V(i^\beta j^\gamma + i^\gamma j^\beta)$ when $0 \leq \beta \leq \gamma \leq 1$, $\forall\, i,j \in \mathbb{N}$, $C_V \in \mathbb{R}^+$. By assuming the boundedness of the second moment and that the solution is differentiable, the existence of a unique steady-state solution is established. Since the model is nonlinear and analytical solutions are not available for such cases, numerical simulations are performed to justify the theoretical findings. Four different test cases are considered by taking physically relevant kernels such as $V_{i,j} = 2, (i+j), 8i^{1/2}j^{1/2}$ and $2ij$ along with various initial conditions. It is observed that when the number of equations is increased, the oscillations arise, but settle down when time progresses, confirming the presence of

steady-state.

The thesis further deals with the introduction of a novel semi-analytical technique called the optimized decomposition method (ODM) to compute solutions of Smoluchowski's coagulation equation and 1D Burgers' equation. Further, it focuses on developing a technique based on ODM suitable to solve two and three-dimensional systems. The series solutions computed using ODM are shown to converge to the exact solution and the theoretical error bounds are obtained. In the case of the coagulation equation, the theoretical results are validated using numerical examples for scientifically relevant aggregation kernels for which the exact solutions are available. Additionally, the ODM approximated results are compared with the solutions obtained using the Adomian decomposition method (ADM). The novel method is found to be superior to ADM for the examples considered and thus established as an improved and efficient method for solving Smoluchowski's equation. In the case of 1D Burgers' equation, it is shown that ODM enjoys better estimates than ADM. In most cases, it is observed that the series solution converges towards the exact solution. Moreover, in all the examples, the proposed method is shown to provide good accuracy with the exact solutions.

Finally, the thesis deals with implementing a Laplace transform approach based on ODM called the Laplace optimized decomposition method (LODM) to solve Smoluchowski's coagulation equation. In addition, the Laplace Adomian decomposition method (LADM) is applied to the fragmentation equation and solution expressions are obtained. The convergence analysis is also conducted to obtain the error bound for the omitted terms in both cases. Several numerical test cases are also presented to validate our theoretical findings. In the case of the coagulation problem, LODM solutions are also compared with the finite volume method results. Furthermore, the closed-form solutions are obtained in all the cases for the fragmentation equation. The methods are found to be highly accurate to solve these partial integro-differential equations.

Contents

List of Figures

List of Tables

Dedicated to

My Parents and Brother... who inspired me to commence this journey!

My Supervisor... who made it possible!!

Chapter 1

Introduction

"*Since Newton, mankind has come to realize that the laws of physics are always expressed in the language of differential equations*" -Steven Strogatz.

Particles may change their properties in a system due to various physical, chemical, or biological factors. The processes such as coagulation, fragmentation, growth, and nucleation are part of a population balance equation (PBE). The model has several applications in modeling real-world phenomena including milling process [1], protein filament division [2], fluidized bed wet granulation [3], fibrin clot formation [4] and coagulation of magnetic nanoflowers in biofluids [5], among many others (see [6] for a detailed survey on applications). *Aggregation* or *coagulation* is a process where two or more particles combine together to form a larger particle (as shown in Figure 1.1(a)). Here, the total number of particles decreases while the total mass remains conserved. In a *fragmentation* or *breakage* process, particles break into two or more fragments due to the external forces or collision between the particles (see Figure 1.1(b)). The total number of particles in a fragmentation process increases while the total mass remains constant. In a *growth* process, the particles grow when the molecular matter is added to the surface of a particle (as shown in Figure 1.1(c)). Growth has no effect on the number of particles but the total volume increases. The formation of a new particle by condensation or crystallization is called *nucleation* and has a significant effect on the total number of particles but less on the total volume (see Figure 1.1(d)).

This thesis mainly focuses on the different variants of coagulation equations relevant to particle physics and astrophysics, i.e., Smoluchowski's coagulation and the Safronov-Dubovski coagulation equation (SDCE). Smoluchowski's equation has a diverse range of applications, such as in the field of bio-pharmaceuticals [7], financial sector [8], aerosol science [9], marine sciences [10]. The SDCE includes two major events, collision followed by coagulation. There are various examples of the phenomenon explained by

SDCE, namely, the collision of asteroids [11], formation of Saturn's rings [12], formation of protoplanetary disc around a newly formed star [13]. There are several real-world problems caused by particle coagulation such as the health hazards of sand and dust storms [14], the analysis of nano-metal dust explosions [15], and the impact on glacier mass as a result of volcanic dust accumulation [16]. This thesis deals with the theoretical, numerical, and steady-state analysis of the SDCE. In addition, the semi-analytical approaches for solving the pure coagulation as well as the fragmentation equations are discussed. The following objectives are fulfilled in this thesis:

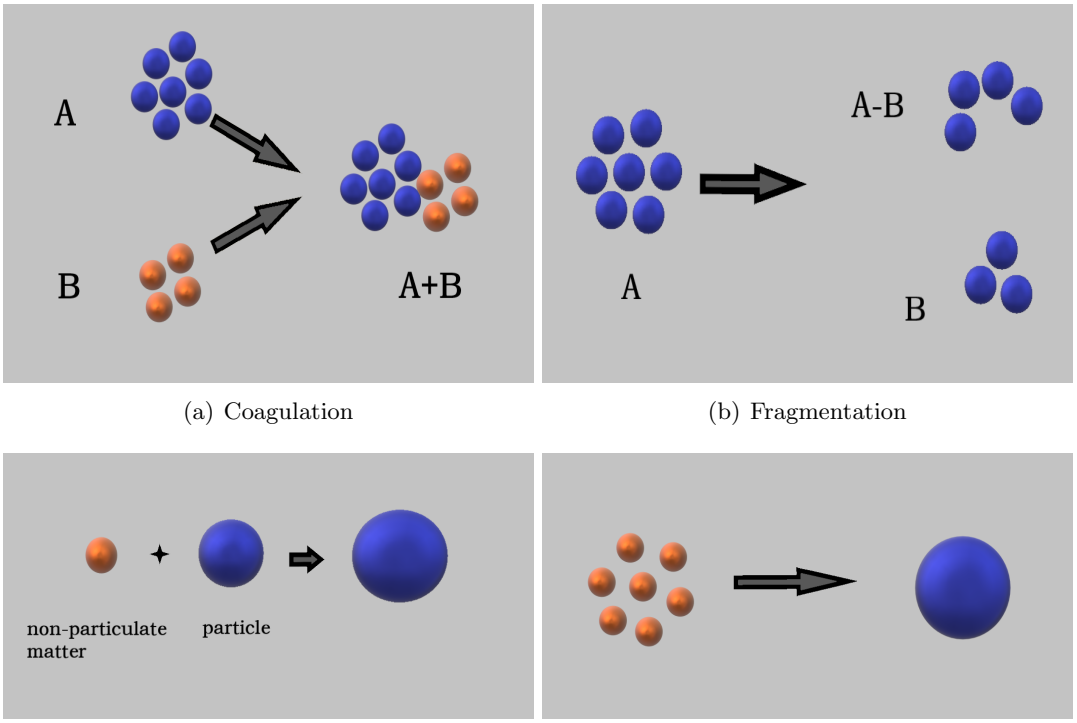

(a) Coagulation (b) Fragmentation

(c) Growth (d) Nucleation

FIGURE 1.1: Particulate processes

1.1 Objectives of Thesis

1. To prove the existence, uniqueness, and mass conservation in case of the conservative as well as non-conservative finite dimensional systems for the unbounded coagulation kernel $V_{i,j} \leq \frac{(i+j)}{\min\{i,j\}} \ \forall \ i,j \geq 1$ for the Safronov-Dubovski coagulation equation.

2. To establish the existence and differentiability of mass-conserving solutions for the Safronov-Dubovski coagulation equation when $V_{i,j} \leq (i+j) \ \forall \ i,j \in \mathbb{N}$.

3. To study the steady-state behavior of solution theoretically and numerically for the Safronov-Dubovski coagulation equation in case of constant, sum, and product kernels, i.e., $V_{i,j} = 2,\ \ (i+j),\ \ 8i^{1/2}j^{1/2}\ \ \&\ \ 2ij\ \forall\ i,j \geq 1$.

4. To implement the novel efficient semi-analytical technique called the optimized decomposition method (ODM) to solve Smoluchowski's coagulation equation for the parameters $V(x,y) = 1$, $(x+y)$, xy and to extend the method to solve the 2D and 3D Burgers equations.

5. To conduct a novel convergence analysis for the series solution computed using Laplace optimized decomposition method (LODM) and Laplace Adomian decomposition method (LADM) for Smoluchowski's coagulation and pure fragmentation equations, respectively.

1.2 Requisite Models

In this section, we shall describe the models that are discussed in the thesis starting with the non-linear coagulation equations, i.e., the Safronov-Dubovski coagulation equation and Smoluchowski's coagulation equation, which are at the center of our analysis.

1.2.1 Safronov-Dubovski Coagulation Equation

The Safronov-Dubovski coagulation equation (SDCE) is the discrete version of a coagulation model, proposed in astrophysics by Oort et al. [17] in 1946 to describe the process of aggregation of protoplanetary bodies. It was then written in a more amenable form by Safronov [18] in 1972. Hence, it was named Oort-Hulst-Safronov (OHS) coagulation equation and is given by

$$\partial_t f(t,x) = -\partial_x \left(f(t,x) \int_0^x yV(x,y)f(t,y)dy \right) - f(t,x) \int_x^\infty V(x,y)f(t,y)dy, \quad (1.1)$$

for $t \in (0,\infty)$ and $x \in \mathbb{R}^+$. The kernel, $V(x,y)$ is non-negative, symmetric, and defines the rate of coagulation of particles. The first term on the right-hand side of the above equation describes the formation of clusters of size x from smaller clusters. The second term deals with the disappearance of clusters of size x by sedimentation on larger clusters. SDCE is a particular case of a two-parameter family of discrete coagulation models introduced by Dubovski [19] where a link with OHS is highlighted. The SDCE, an infinite system of ordinary differential equations that has been studied by various

authors [19–21] is written as

$$\frac{df_i(t)}{dt} = \underbrace{f_{i-1}(t)\sum_{j=1}^{i-1} jV_{i-1,j}f_j(t)}_{(i)} - \underbrace{f_i(t)\sum_{j=1}^{i} jV_{i,j}f_j(t)}_{(ii)} - \underbrace{\sum_{j=i}^{\infty} V_{i,j}f_i(t)f_j(t)}_{(iii)}, \tag{1.2}$$

for $t \in [0,\infty)$, $i,j \in \mathbb{N}$ and with the initial condition

$$f_i(0) = f_i^0 \geq 0. \tag{1.3}$$

Here, $f_i(t)$ is the concentration of particles of size i at time t and $V_{i,j}$ is the intensity rate of collisions when particles of sizes i and j collide to form a particle of size $(i+j)$ and is called the coagulation kernel. It is assumed to be symmetric, i.e, $V_{i,j} = V_{j,i}$ and non-negative, i.e., $V_{i,j} \geq 0$. SDCE describes the evolution of a disperse system (like clouds, interstellar gases, etc) where the binary collision of particles of masses im_0 and jm_0, $i \geq j$ leads to the merging of the smaller particles to a bigger particle in the following way: A collision of an i-mer and a j-mer yields fragmentation of j-mer into j-monomers. Note that m_0 is the mass of the tiniest particle in the system. Each of these j-monomers combines to a different i-mer and therefore, gives j new $(i+1)$-mers from one collision event. The underlying dynamics of the equation are explained in a simplified way in Figure 1.2. The terms, in order of their presence in the equation, explain the following scenarios: (i) merging of an $(i-1)$-mer and a dust particle (monomer) to generate a cluster of mass im_0, (ii) removal of i-mers from the system due to the creation of particles with mass bigger than im_0, and (iii) breaking of an i-mer into monomers and combining with different j-mers.

There are various physical properties of the solution that can be investigated with the help of its moments, which are also extremely useful tools to handle related mathematical problems. The r^{th} moment of a solution $f = (f_i)$ of (1.2) is defined by

$$M_r(f(t)) = M_r(t) := \sum_{i=1}^{\infty} i^r f_i(t). \tag{1.4}$$

Putting $r = 0$ gives the zeroth moment, denoted as $M_0(t)$, which determines the total number of particles in the system, per unit volume. Taking $r = 1$ in (1.4) we get the first moment $M_1(t)$, which can be physically interpreted as the mass of the system per unit volume. We expect the mass to be a conserved quantity, i.e., $M_1(t) = M_1(0)$, for kernels with slowly increasing rate of coagulation. Though the physical relevance of the second moment has not been much discussed in the literature, it can be interpreted as the energy dissipated in the process [22].

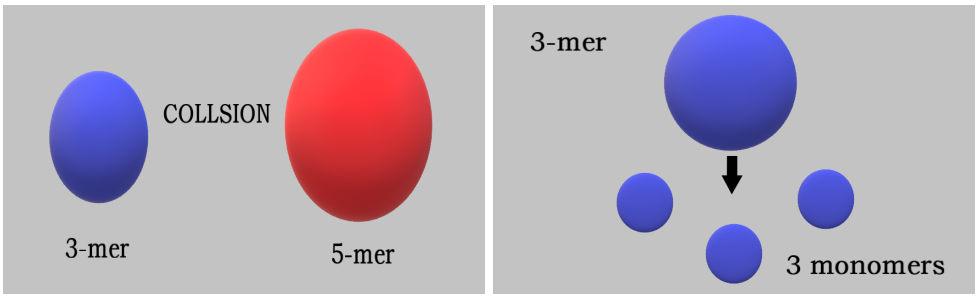

(a) Step 1 (b) Step 2

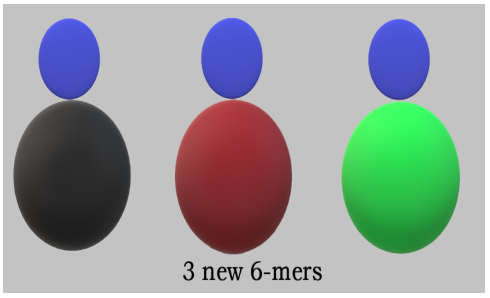

(c) Step 3

FIGURE 1.2: An example of the dynamics of Safronov-Dubovski coagulation equation

1.2.2 Coagulation and Fragmentation Equations

Smoluchowski [23] in 1917, proposed the infinite set of the non-linear differential equations for coagulation based on the Brownian motion of particles as

$$\frac{du_i(t)}{dt} = \frac{1}{2}\sum_{j=1}^{i-1} a_{i-j,j}u_{i-j}(t)u_j(t) - \sum_{j=1}^{\infty} a_{i,j}u_i(t)u_j(t).$$

Here, $u_i(t)$, $i \geq 1$ are the densities of particles of discrete size i at time t and $a_{i,j}$ is the coagulation kernel. It is non-negative and symmetric, i.e., $a_{i,j} \geq 0$ and $a_{i,j} = a_{j,i}$ $\forall$ $i, j \geq 1$. The continuous version of this equation was given by Müller [24] in 1928 as

$$\frac{\partial u(t,x)}{\partial t} = \frac{1}{2}\int_0^x a(x-y,y)u(t,x-y)u(t,y)dy - u(t,x)\int_0^\infty a(x,y)u(t,y)dy. \quad (1.5)$$

Here, $u(t,x)$ denotes the number of particles of size $x > 0$ at time $t \geq 0$. Similar to the discrete case, the kernel a is non-negative and symmetric, i.e., $a(x,y) = a(y,x)$. The first term on the right-hand side of the above equation describes the creation of particles of size x when two particles of masses $x-y$ and y collide. The second integral shows the disappearance of particles of size x after colliding with any particle of size y. The

pure breakage equation is written as

$$\frac{\partial u(t,x)}{\partial t} = \int_x^\infty \phi(y)b(x,y)u(t,y)dy - \phi(x)u(t,x), \tag{1.6}$$

where the first expression on the right side defines the breakage of a particle of size $y > x$ to generate a particle of size x and the second one is symbolic of the death of a particle with size x when it breaks. The term $\phi(x)$ is the selection function that describes the rate at which particles of size x are selected to break. The breakage function $b(x,y)$ for a given $y > 0$ gives the size distribution of particle sizes $x \in (0,y)$ resulting from the breakage of a particle of size y. The breakage function has the following properties

$$\int_0^y b(x,y)dx = \bar{N}(y) \quad \text{and} \quad \int_0^y xb(x,y)dx = y, \quad y \in (0,\infty),$$

where $\bar{N}(y)$ defines the total number of fragments of y.

1.2.3 Burgers Equation

The Burgers equation (BE) is a fundamental partial differential equation in the turbulence model [25], fluid mechanics [26] and has applications in various areas of applied mathematics such as gas dynamics, traffic flow, non-linear acoustics, and cancer growth modelling (see studies [27–30] and references cited therein for details). Owing to the real-world applications of the equation, it piques interest to explore new and efficient methods to solve Burgers equation. The equation explains the following scenario: consider a viscous fluid having an initial speed $\hat{w_0}(x)$, passing through an ideal pipe with negligible diameter. Then, the rate of change in the distance travelled by the fluid along the pipe at each point $(\hat{x},\hat{t})$ as time passes is described by the Burgers equation (BE) [25, 31] written as

$$\frac{\partial \hat{w}}{\partial \hat{t}} + \hat{w}\frac{\partial \hat{w}}{\partial \hat{x}} = \hat{\nu}\frac{\partial^2 \hat{w}}{\partial \hat{x}^2} + \hat{f}(\hat{x},\hat{t}), \tag{1.7}$$

with the initial data

$$\hat{w}(x,0) = \hat{w_0}(x). \tag{1.8}$$

In 1995, Esipov [32] introduced the system of two-dimensional BE expressed as

$$\begin{aligned}
\frac{\partial \hat{w}}{\partial \hat{t}} + \hat{w}\frac{\partial \hat{w}}{\partial \hat{x}} + \hat{v}\frac{\partial \hat{w}}{\partial \hat{y}} &= \hat{\nu}\left(\frac{\partial^2 \hat{w}}{\partial \hat{x}^2} + \frac{\partial^2 \hat{w}}{\partial \hat{y}^2}\right), \\
\frac{\partial \hat{v}}{\partial \hat{t}} + \hat{w}\frac{\partial \hat{v}}{\partial \hat{x}} + \hat{v}\frac{\partial \hat{v}}{\partial \hat{y}} &= \hat{\nu}\left(\frac{\partial^2 \hat{v}}{\partial \hat{x}^2} + \frac{\partial^2 \hat{v}}{\partial \hat{y}^2}\right),
\end{aligned} \tag{1.9}$$

with the initial values

$$\hat{w}(\hat{x},\hat{y},0)=\hat{f}_1(\hat{x},\hat{y}),\qquad \hat{v}(\hat{x},\hat{y},0)=\hat{f}_2(\hat{x},\hat{y}), \tag{1.10}$$

and boundary values

$$\hat{w}(\hat{x},\hat{y},\hat{t})=\hat{g}_1(\hat{x},\hat{y},\hat{t}),\qquad \hat{v}(\hat{x},\hat{y},\hat{t})=\hat{g}_2(\hat{x},\hat{y},\hat{t}). \tag{1.11}$$

Consider 3D Burgers equation, see [33]

$$\frac{\partial}{\partial\hat{t}}\hat{w}(\hat{x},\hat{y},\hat{z},\hat{t})=\hat{w}\frac{\partial\hat{w}}{\partial\hat{x}}+\hat{\nu}\left(\frac{\partial^2\hat{w}}{\partial\hat{x}^2}+\frac{\partial^2\hat{w}}{\partial\hat{y}^2}+\frac{\partial^2\hat{w}}{\partial\hat{z}^2}\right), \tag{1.12}$$

together with the initial condition $\hat{w}(\hat{x},\hat{y},\hat{z},0)=\hat{\phi}(\hat{x},\hat{y},\hat{z})$. The explanation of the

TABLE 1.1: Nomenclature

Parameter	Description	Dimension
$\hat{\mathbf{x}}$	spatial coordinates	$[L]$
$\hat{t}$	time	$[T]$
$\hat{\nu}$	kinematic viscosity	$[L^2T^{-1}]$
R_e	Reynold's number	Dimensionless
$\hat{\mathbf{w}}(\hat{\mathbf{x}},\hat{t})$	unknown velocity functions	$[LT^{-1}]$
$\hat{\mathbf{w}}_0(\hat{\mathbf{x}})$	initial speed	$[LT^{-1}]$
$\hat{f}(\hat{x},\hat{t})$	non-homogenous term	$[LT^{-2}]$

quantities involved in the above equations is part of the TABLE 1.1. The governing equations (1.7), (1.9), and (1.12) are converted to dimensionless form by defining the variables

$$\mathbf{x}=\frac{\hat{\mathbf{x}}}{\hat{\mathbf{l}}},\quad t=\frac{\hat{t}}{\hat{k}},\quad \nu=\frac{\hat{\nu}}{\hat{l}^2\hat{k}^{-1}},\quad c=\frac{\hat{w}-\hat{w}_0}{\hat{w}_0},\quad \text{and}\quad f=\frac{\hat{f}}{\hat{l}\hat{k}^{-2}},$$

where $\hat{\mathbf{l}}$ and $\hat{k}$ are the reference length and time scales, respectively. The dimensionless Burgers equations, which are the main focus of this work, are then represented in the following forms:

$$\frac{\partial w}{\partial t}+w\frac{\partial w}{\partial x}=\nu\frac{\partial^2 w}{\partial x^2}+f(x,t), \tag{1.13}$$

with the initial data

$$w(x,0)=w_0(x), \tag{1.14}$$

for the single variable and for the two variables, it is expressed as

$$\begin{aligned} \frac{\partial w}{\partial t} + w\frac{\partial w}{\partial x} + v\frac{\partial w}{\partial y} &= \nu\left(\frac{\partial^2 w}{\partial x^2} + \frac{\partial^2 w}{\partial y^2}\right), \\ \frac{\partial v}{\partial t} + w\frac{\partial v}{\partial x} + v\frac{\partial v}{\partial y} &= \nu\left(\frac{\partial^2 v}{\partial x^2} + \frac{\partial^2 v}{\partial y^2}\right), \end{aligned} \tag{1.15}$$

with the initial values

$$w(x, y, 0) = f_1(x, y), \quad v(x, y, 0) = f_2(x, y), \quad \forall (x, y) \in D \tag{1.16}$$

and boundary values

$$w(x, y, t) = g_1(x, y, t), \quad v(x, y, t) = g_2(x, y, t), \quad \forall (x, y) \in \partial D, \tag{1.17}$$

where ∂D is the boundary of $D = \{(x, y) : x, y \in [a, b]\}$, $\nu = \frac{1}{Re}$. The values $f_i(x, y)$ and $g_i(x, y, t)$ are assumed to be smooth enough and satisfy the conditions $g_i(x, y, 0) = f_i(x, y)$ so that the coupled equations (1.15)-(1.17) admit a smooth solution. The 3D Burgers equation can be written in dimensionless form as

$$\frac{\partial}{\partial t} w(x, y, z, t) = w\frac{\partial w}{\partial x} + \nu\left(\frac{\partial^2 w}{\partial x^2} + \frac{\partial^2 w}{\partial y^2} + \frac{\partial^2 w}{\partial z^2}\right), \tag{1.18}$$

together with the initial condition $w(x, y, z, 0) = \phi(x, y, z)$. The equations (1.13), (1.15), and (1.18) become the *inviscid* BE when $\nu = 0$ and *viscous* BE for $\nu = 1$. Furthermore, if the viscous term is not included, i.e., *inviscid* case, the equations are hyperbolic, and if included, the equations are of parabolic type.

1.3 Kernels

In this section, we list a few important coagulation parameters:

Sum Kernel

The sum kernel, see Figure 1.3 (i), is given by

$$V_{i,j} = (i + j). \tag{1.19}$$

Brownian Kernel

The Brownian coagulation kernel, with continuum regime, is plotted in Figure 1.3 (ii) and is described by

$$V_{i,j} = (i^{1/3} + j^{1/3})(i^{-1/3} + j^{-1/3}). \tag{1.20}$$

Through Figure 1.3 (ii), we can see that for smaller-sized particles, the interaction is low

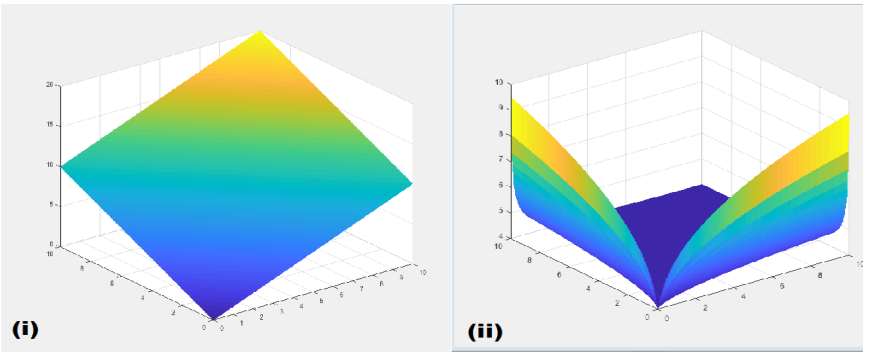

FIGURE 1.3: Sum kernel and Brownian kernel

but as the size of the particle keeps on increasing, the interaction between the particles increases. The reason for this kind of behavior is characterized by the multiplicative nature of the kernel.

Shear Kernel

The Shear kernel, with a non-linear velocity profile, is shown in Figure 1.4 (i) and is defined by

$$V_{i,j} = (i^{1/3} + j^{1/3})^7. \tag{1.21}$$

Gravitational Kernel

The gravitational kernel (see Figure 1.4 (ii)), which explains gravitational settling with particles larger than $\approx 50\ \mu m$, is described by

$$V_{i,j} = (i^{1/3} + j^{1/3})^2 |i^{1/3} - j^{1/3}|. \tag{1.22}$$

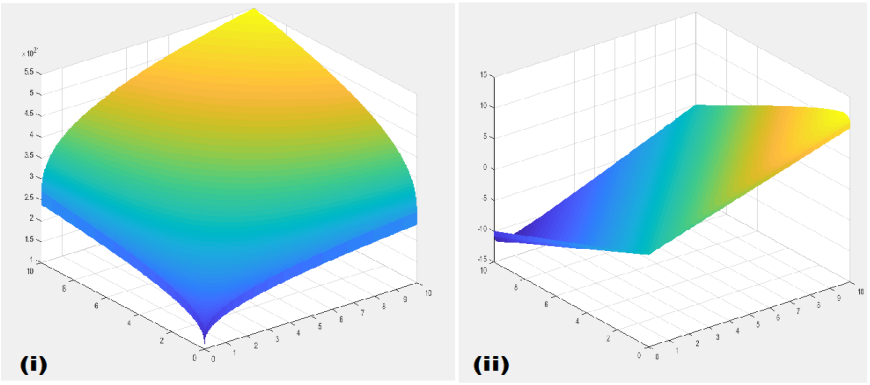

FIGURE 1.4: Shear kernel and gravitational kernel

Diffusion Kernel

It explains the controlled growth of supported metal crystallites and is given by, see Figure 1.5

$$V_{i,j} = (i^{-2/3} + j^{-2/3}). \tag{1.23}$$

All the above kernels can be defined in continuous settings accordingly. Some breakage

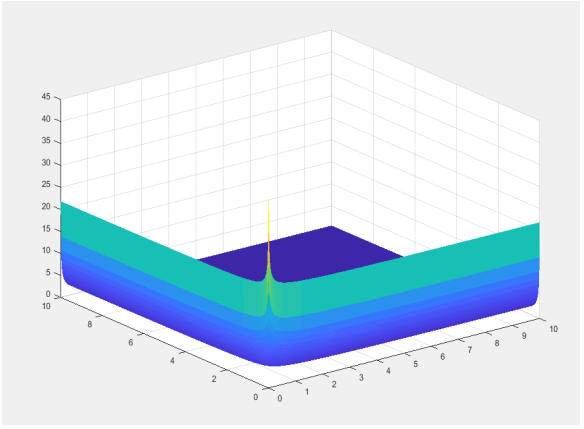

FIGURE 1.5: Diffusion kernel

and selection functions are defined by $b(x, y) = \frac{2}{y}, \frac{2}{y^2}, \frac{3x}{y^2}, \frac{4x^2}{y^3}$ and $\phi(x) = x, x^2, x^3, x^4$, respectively.

1.4 Applications

There are various applications of the above-mentioned coagulation-fragmentation equations, which include the following:

Protoplanetary Disk

A protoplanetary disk is a rotating circumstellar disk of dense gas and 'dust' surrounding a young newly formed star, as shown in Figure 1.6(a). It is formed by the coagulation of larger particles in space with 'dust'(the smallest particle in the system). The formation of this protoplanetary disk can be explained through the Coagulation-Disintegration model [13]. In 2011, Rolf Olsen presented pictures of a protoplanetary disk around the star β-pictoris as shown in Figure 1.6(a).

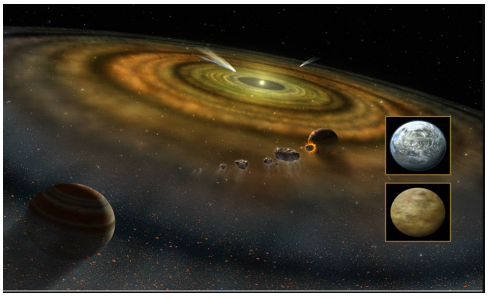

(a) Protoplanetary disk around a star

(b) Asteroid collision

(c) Schooling of fish

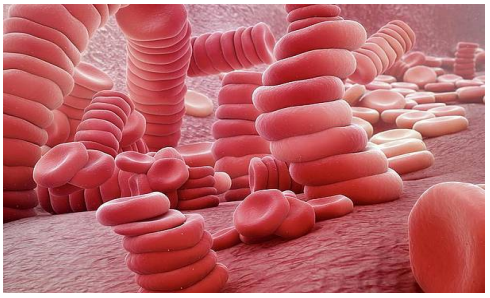

(d) Rouleaux formations

FIGURE 1.6: Some applications of coagulation processes

Asteroid Collision

In space, the asteroids collide with each other and also with other planets, as shown in Figure 1.6(b). Recent news about the collision of a 150 km asteroid with Earth could have been the reason for the coagulation of so much dust that it resulted in the ice age, and climate variation between Antarctica and the equator (see [34]).

Schooling of Fish

Fish form groups due to social reasons, which is called shoaling. If this group moves in the same direction, then it is called 'schooling' as shown in Figure 1.6(c). In [10], Niwa et al. explained this behavior using Smoluchowski's coagulation equation.

Rouleaux Formations

Rouleaux (singular is rouleau) are stacks or aggregations of red blood cells (RBCs) that form because of the unique discoid shape of the cells in vertebrates as shown in Figure 1.6(d). The flat surface of the discoid RBCs gives them a large surface area to make contact with and stick to each other; thus forming a rouleau. They occur when the plasma protein concentration is high, and, because of them, the ESR (erythrocyte sedimentation rate) is also increased. This is a nonspecific indicator of the presence of disease.

1.5 Existing Literature

Let us now provide the literature survey for each of the models considered in this thesis.

1.5.1 Safronov-Dubovski Coagulation Equation

In 2003, Lachowicz et al. [35] showed the relation between the Smoluchowski coagulation (1.5) and the OHS coagulation equations (1.1). They proved the existence of solutions when $V(x,y) \in W^{1,\infty}_{loc}([0,\infty)^2)$ and $\partial_x V(x,y) \geq -\alpha$, in particular, for $V(x,y) \leq (1+x)(1+y)$, $V(x,y) \leq G(1+x+y)$. The authors have also provided the results for gelation in finite time, i.e. $T_{gel} < +\infty$ by taking $V(x,y) \leq (1+x)(1+y)$ and $V(x,y) \geq A(xy)^{\frac{\lambda}{2}}$, $\lambda \in (1,2]$. In 2005, Laurençot [36] discussed the convergence to the self-similar solutions of Eq. (1.1) with constant kernel and extended the results for multiplicative kernel

$$V(x,y) = xy,$$

in 2006 [37]. Another interesting result in this direction is found in [38] where the authors proved the existence of self-similar profiles with a finite first moment for the additive kernel, i.e.,

$$V(x,y) = x^\lambda + y^\lambda, \quad \lambda = (0,1).$$

Bagland [21] established the existence of a solution for the SDCE in case of the bounded kernel

$$\lim_{j\to\infty} \frac{V_{i,j}}{j} = 0.$$

In 2014, Davidson [20] has proved the global existence for an unbounded kernel of the type

$$jV_{i,j} \leq M, \quad j \leq i \quad \text{and} \quad V_{i,j} \leq C_V h_i h_j \quad \text{such that} \quad \frac{h_i}{i} \to 0.$$

The author discussed the mass conservation when $h_i \leq i^{1/2}$ and the uniqueness of the solution for the bounded kernel, i.e., $0 \leq V_{i,j} \leq C_V, C_V \in \mathbb{R}^+$. This equation has not been explored much and hence is the focus of our analysis in this thesis.

1.5.2 Coagulation and Fragmentation Equations

Several researchers have studied the global existence, mass-conservation, uniqueness, and self-similar solutions for the coagulation (1.5) and fragmentation equations (1.6) (see [39–48] and the references therein for details). In general, it is not easy to find a solution for the aggregation and breakage problems considering physical kernels. Therefore, numerical and semi-analytical methods are used to find the solution numerically and in analytic approximate forms, respectively. It is proven that the FVM is more suitable for solving such a model due to the conservative formulation of the equation. Filbet and Laurençot [49] were the first to develop such a numerical scheme in 2004 for solving coagulation and binary breakage problem. Further, Bourgade et al. [50] discussed the convergence of finite volume approximated solution towards a weak solution of the continuous problem in weighted L^1 space under the condition that kernels are locally bounded. Several articles are available on the consistency and convergence analysis of FVM for solving such non-linear models, see [51, 52] and further citations for more details. The semi-analytical approaches do not rely on nonphysical assumptions like discretization, linearization, estimating the initial term, or a set of basis functions, they allow us to solve both linear and non-linear initial and boundary value problems. These methods are widely used to calculate series approximated solutions for the coagulation equation (1.5) which include the Laplace decomposition method [53], tensor decomposition [54], HPM [55, 56], Laplace-variational iteration method (LVIM) [57], ADM [58], VIM [59]. HPM was used in [55] to obtain the series solution for (1.5) for $a(x, y) = 1$, $a(x, y) = xy$ with $u_0(x) = e^{-x}, (e^{-x}/x)$, respectively. Kaur et al. [56] analyzed the convergence of series solution computed using HPM for the Eq. (1.5) considering two additional coagulation kernels namely sum and Ruckenstein kernel, i.e.,

$$a(x, y) = (x + y), \quad (x^{2/3} + y^{2/3}),$$

with initial value $u_0(x) = e^{-x}$. The authors in [56] also dealt with the breakage problem (1.6) using HPM for the parameters

$$\phi(x) = x^{\alpha}, \quad b(x,y) = \frac{\alpha}{y}\left(\frac{x}{y}\right)^{\alpha-2} \quad \forall \ 1 \leq \alpha \leq 2 \ \text{ with } \ u_0(x) = e^{-x}, \delta(x-1). \tag{1.24}$$

Hammouch and Toufika [57] established that the Laplace-variational iteration method (LVIM) is more efficient compared to HPM for the problem (1.5). The other homotopy methods are also among the popular ones to analyze the series solutions of (1.5), namely, HAM, optimal homotopy asymptotic method (OHAM), and the homotopy analysis transform method (HATM) (see [60, 61]). Singh et al. [58] implemented ADM for $a(x,y) = 1, (x+y), xy$ with $u(0,x) = e^{-x}, \frac{e^{-x}}{x}$. and

$$\phi(x) = x^3, x^4, \quad b(x,y) = \frac{3x}{y^2}, \frac{4x^2}{y^3} \ \text{ with } \ u_0(x) = e^{-x}. \tag{1.25}$$

Hasseine et al. [59] established the comparison between the semi-analytical solutions obtained using VIM, HPM, and ADM for $a(x,y) = xy$ with $u_0 = e^{-x}$. Hasseine et al. [62] implemented VIM and ADM for the breakage equation (1.6) when $\alpha = 1, 2$ in (1.24). The authors in [59] analyzed three semi-analytical methods namely VIM, HPM, and ADM for the parameters same as in (1.24) and product coagulation kernel with $u_0(x) = e^{-x}$. In [63], ADM solution is compared with a collocation method result for $\phi(x) = x$ and x^2 for $u_0(x) = xe^{-x}$. The authors in [64] used ADM and HPM to compute the series solutions for a kernel relevant in milling processes (see [65]), i.e, $\phi(x) = x, \quad b(x,y) = \frac{12(y-x)}{x^3}$. Very recently in 2022, the authors [66] have used HAM to obtain the solutions for the Ruckenstein kernel for Eq. (1.5) and for the parameters as in (1.24) for Eq. (1.6) along with parameters same as in (1.25). A method suggested by Odibat [67, 68] in 2020, known as ODM, was implemented on the non-linear ODEs and PDEs. The fundamental aspect of the ODM is the linear approximation of the nonlinear operator, which is used to decompose the solution into series form.
It has been shown in recent works [69–71] that the addition of the Laplace transformation on the ADM approach (LADM) provided better accuracy than ADM. In 2022, Beghami et al. [72] developed a new series solution method based on ODM called the Laplace optimized decomposition method (LODM) to solve the system of partial differential equations of fractional order with great accuracy.

1.5.3 Burgers Equation

Due to the vast range of applicability of these equations in natural world phenomena, many researchers have contributed to their numerical and theoretical analysis. From the numerical point of view, Zhang and Wang [73] introduced a compact predictor-corrector

finite difference scheme for the viscous 1D BE. In [74], the authors used the finite volume method for the non-linear advective terms in (1.13) by the fifth-order weighted upwind compact scheme. In 2021, the article [75] focused on computing the numerical solutions of the 1D Burgers equation by calculating Chebyshev polynomials and using the tau spectral method. In 2022, the authors [76] applied Lax–Friedrichs, and Lax–Wendroff schemes to obtain the numerical solutions of the inviscid 1D BE. An efficient technique such as Lucas polynomials coupled with the finite difference method is implemented on the one and two-dimensional time-fractional Burgers equation [77]. There are other approaches that can be used to solve the Burgers equation such as the Mittag-Leffler kernel approach [78], using nonlocal symmetries arising from the inverse potential system [79], and the quadratic-linear schemes [80]. In the case of the 2D Burgers problem (1.15), recently in 2022, Hussein and Kashkool [81] presented a continuous and discrete-time weak Galerkin finite element scheme for the coupled problem while Zhang et al. [82] developed a high-order implicit weighted compact non-linear scheme. In [83], two-dimensional BE (1.15) is solved using Lucas and Fibonacci polynomials by converting the equation into algebraic equations. In addition to the above approaches, the finite difference method and the method of lines are also used to compute the numerical solution of (1.15) (see [84, 85] and the references cited in the papers).

However, the above investigations require physical changes such as linearization, discretization, and theoretical assumptions related to non-linearities. To avoid these issues, the researchers make use of semi-analytical methods that do not require complicated discretization and assumptions on the parameters. During the last several decades, many authors have studied solutions to the 1D BE using various methodologies, including Backlund transformation [86], Elzaki transformation, homotopy perturbation method (HPM) [87], the tanh method [88], the sine cosine method [89], and the Laplace transformation method [90]. There are other semi-analytical schemes implemented on fractional Burgers equation such as HPM [91], optimal perturbation iteration method [92], and the energy boundary function method [93]. Further, Asmouh et al. [94] developed a higher-order isogeometric modified method of characteristics for the 2D BE (1.15) which is a very efficient method for the coupled problem and the authors established it using several test cases. The other methods that are implemented on (1.15) are the homotopy analysis method [95], the variational iteration technique [96, 97], the discrete Adomian decomposition method [98] and the Adomian-Padé technique [99]. For a more detailed review of the several methods applied to the Burgers equation, we refer the readers to the review paper [100].

1.6 Plan of Thesis

This thesis deals with the theoretical, numerical, and steady-state analysis of the Safronov-Dubovski coagulation equation (1.2). In addition, the semi-analytical approaches for solving the pure coagulation (1.5) as well as fragmentation equations (1.6) are discussed. In the following, a summary of each chapter in the thesis is presented:

Chapter 2 presents the existence, uniqueness, and mass conservation of the solution of the Safronov-Dubovski coagulation equation (1.2)- (1.3) in the case of an unbounded kernel of the type $V_{i,j} \leq \frac{(i+j)}{\min\{i,j\}}$ for every $i, j \in \mathbb{N}$. Helly's selection theorem and the contraction mapping theorem are pivotal for establishing these results. The existence and mass conservation are dealt with for both the conservative and non-conservative finite dimensional systems.

In Chapter 3, we extend the definition of the kernel to $V_{i,j} \leq (i + j)$ for all $i, j \geq 1$, i.e., the sum kernel and establish the existence and mass conservation results for the conservative as well as non-conservative approximations to the infinite system of ODEs (1.2). In this case, we prove the differentiability of the solution and the conditions under which all solutions conserve density. The differentiability results are established for the generalized class $V_{i,j} \leq (i^{\alpha} + j^{\alpha})$, where $0 \leq \alpha \leq 1$ and the boundedness of the $(\alpha+1)^{th}$ moment is pivotal in establishing that the solution is first-order differentiable and the derivative is continuous.

The numerical and steady-state analysis of SDCE (1.2)- (1.3) for standard physical parameters such as the constant, sum, and product kernel, i.e., $V_{i,j} = 2,\ \ (i+j),\ \ 8i^{1/2}j^{1/2}$, and $2ij\ \forall\ i, j \geq 1$ are discussed in Chapter 4. In addition, we investigate the oscillatory behavior of the solutions for these parameters. Due to the complexity of the expressions in the equation, a novel moment method is found to be most suitable to study steady-state behavior. In light of these expressions, the explicit fourth-order Runge-Kutta method is implemented to compute the numerical solutions which are compared with the analytical solutions calculated using the method of moments.

The aim of Chapter 5 is the development and implementation of a novel semi-analytical approach called the optimized decomposition method (ODM) to solve the non-linear Smoluchowski's coagulation problem (1.5) and its novel extension to the system of PDEs for solving 2D (1.15) and 3D viscous Burgers' equations (1.18). Also, we study the convergence analysis for the series solutions obtained using ODM and compute the error

estimates. The applications of ODM to calculate the series solutions of one-dimensional inviscid and viscous Burgers equations are also part of this chapter. The results for Smoluchowski's equation and 1D Burgers equation are compared to the existing Adomian decomposition method (ADM) and the scheme gives nice accuracy with the exact solution. The proposed method is implemented to solve the two and three dimensional Burgers equations and the technique proved to be very efficient.

In the final Chapter 6, Laplace transform-based methods called the Laplace optimized decomposition method (LODM) and Laplace Adomian decomposition method (LADM) are applied to the pure coagulation (1.5) and fragmentation (1.6) equations, respectively. A novel convergence analysis for the approximated solutions is conducted to obtain the theoretical error estimates for the two methods. The schemes are found to be highly efficient and accurate to solve these problems by comparing the numerical simulations with the available exact solutions or the error between the approximate results.

In the end, some conclusions and future works are summarized.

Chapter 2

Existence, Uniqueness, and Mass Conservation for Safronov-Dubovski Coagulation Equation [1]

The Safronov-Dubovski coagulation equation is given by

$$\frac{df_i(t)}{dt} = f_{i-1}(t)\sum_{j=1}^{i-1} jV_{i-1,j}f_j(t) - f_i(t)\sum_{j=1}^{i} jV_{i,j}f_j(t) - \sum_{j=i}^{\infty} V_{i,j}f_i(t)f_j(t), \tag{2.1}$$

for $t \in [0,\infty)$, $i,j \geq 1$ and with initial datum

$$f_i(0) = f_{in}. \tag{2.2}$$

Here, $f_i(t)$ is the concentration of particles of size i at time t and $V_{i,j}$ is the intensity rate of collisions when particles of sizes i and j collide to form a particle of size $(i+j)$ and is called the coagulation kernel. It is assumed to be symmetric, i.e, $V_{i,j} = V_{j,i}$ and non-negative, i.e., $V_{i,j} \geq 0$. Our main aim in this work is to derive the existence, mass conservation, and uniqueness results for the unbounded kernel of the form $\min\{i,j\}V_{i,j} \leq (i+j)\ \forall\ i,j \in \mathbb{N}$. The parameters which are covered under the umbrella of the said kernel are $V_{i,j} = i^{-2/3} + j^{-2/3}\ \forall\ i,j \geq 1$ which explains the 'Diffusion-controlled growth of supported metal crystallites' (see [101]), $V_{i,j} = i^{1-\alpha}j^{-\alpha} + i^{-\alpha}j^{1-\alpha}$ and $V_{i,j} = (i+j)^{1-\alpha}(ij)^{-\alpha}$, where $\alpha \geq 1$.

The chapter is organized as follows: Section 2.1 defines basic definitions and theorems that are relevant for chapters 2, 3, and 4. In Section 2.2, the finite-dimensional system is presented along with the statement and proofs of various lemmas that are required

[1] A considerable part of this chapter is published in *Acta Applicandae Mathematicae*, **179(1)**, 1-21, 2022.

to exemplify the major developments of the work. Section 2.3 has two subsections, first one investigates the existence of the solution while the mass-conserving properties of the solution are dealt with in the other subsection. Section 2.4 explores the uniqueness of the solution $f_i(t)$. The existence and density conservation for the non-conservative approximation of the Eqs. (2.1)-(2.2) are analyzed in the last section, Section 2.5.

2.1 Preliminaries

Definition 2.1. (see [[102], Definition 4.18]) For a function $f : X \to Y$ with metric spaces (X, d_1) and (Y, d_2), f is called *uniformly continuous* if for every real number $\epsilon > 0$, there exists a real number $\delta > 0$ such that for every $x, y \in X$ with $d_1(x, y) < \delta$, we have $d_2(f(x), f(y)) < \epsilon$.

Definition 2.2. (see [103]) For a function $f : X \to Y$ with metric spaces (X, d_1) and (Y, d_2), f is called *Lipshitz continuous* if there exists a real constant $K \geq 0$ such that, $\forall x, y \in X$,

$$d_2(f(x), f(y)) \leq K d_1(x, y).$$

Such K is called Lipshitz constant for f and f is called $K-$ Lipshitz.

Definition 2.3. (see [[104], page 108]) Let, (X, d) be a metric space and I be an interval in the real line $\mathbb{R}$. A function $f : I \to X$ is *absolutely continuous* on I if for every positive number ϵ, there is a positive number δ such that whenever a finite sequence of disjoint sub-intervals (x_k, y_k) of I with $x_k < y_k \in I$ satisfies $\sum_k (y_k - x_k) < \delta$, then

$$\sum_k d(f(y_k), f(x_k)) < \epsilon.$$

Remark 2.4. Note here that every absolute continuous function (over a compact interval) is uniformly continuous and therefore continuous. Every (globally) Lipshitz continuous function is absolutely continuous.

Definition 2.5. (see [[102], Definition 7.19]) A sequence $\{f_n : \mathbb{R} \to \mathbb{R}\}$ of functions is *uniformly bounded* if there exists a constant $C \geq 0$, such that $\forall\ n$, we have $\sup_{x \in \mathbb{R}} |f_n(x)| \leq C$.

Definition 2.6. (see [[105], page 137-139]) The *total variation* of the complex-valued measure μ is the set function

$$|\mu|(E) = \sup_P \sum_{A \in P} \|\mu(A)\|, \quad \forall E,$$

where the sum is taken over all the partitions P of a measurable set E into a countable number of disjoint measurable subsets.

Definition 2.7. (see [[102], Definition 9.22]) A *contraction mapping* on a metric space (M, d) is a function f from M to itself with the property that there is some real number $0 \leq k < 1$ so that $\forall\ x, y \in M$,

$$d(f(x), f(y)) \leq k\, d(x, y).$$

Remark 2.8. It is worth noting that every contraction mapping is Lipshitz continuous and hence uniformly continuous.

Definition 2.9. (see, [46])

(a) Let $p \in [1, \infty)$. A sequence (f_n) in $L_p(\Omega)$ converges *weakly* to f (written as $f_n \rightharpoonup f$) in $L_p(\Omega)$ if

$$\lim_{n\to\infty} \int_\Omega f_n(x)\varphi(x)\ d\mu(x) = \int_\Omega f(x)\varphi(x)\ d\mu(x)$$

for all $\varphi \in L_q$, where $q = \infty$ when $p = 1$ and $q = \frac{p}{p-1}$ when $p \in (1, \infty)$.

(b) A sequence (f_n) in $L_\infty(\Omega)$ converges $*$ weakly to f (written as $f_n \overset{*}{\rightharpoonup} f$) in $L_\infty(\Omega)$ if

$$\lim_{n\to\infty} \int_\Omega f_n(x)\varphi(x)\ d\mu(x) = \int_\Omega f(x)\varphi(x)\ d\mu(x)$$

for all $\varphi \in L_1(\Omega)$.

Lemma 2.10. *(see [106]) Gronwall's Lemma: Assume $f : [0, T] \to \mathbb{R}$ is a bounded non-negative measurable function, $g : [0, T] \to \mathbb{R}$ is a non-negative integrable function and $k \geq 0$ is a constant with the property that $f(t) \leq k + \int_0^t g(s)f(s)ds$, then*

$$f(t) \leq k \exp\left(\int_0^t g(s)ds\right).$$

Lemma 2.11. *(see [[107], page 468]) Let $\vartheta_1, \vartheta_2 \in L_1(\Omega)$ be such that $\vartheta_1 \leq \vartheta_2$ a.e. Then, the set $K = \{f \in L_1(\Omega) : \vartheta_1 \leq f \leq \vartheta_2 \text{ a.e.}\}$ is compact in weak topology $\sigma(L_1, L_\infty)$.*

Lemma 2.12. *(see [[107], page 468]) Let (f_n) be a bounded sequence in $L_1(\Omega)$ such that $\int_A f_n$ converges to a finite limit $\ell(A)$, for every measurable set $A \subset \Omega$. Then, there exists some $f \in L_1(\Omega)$ such that $f_n \rightharpoonup f$.*

Lemma 2.13. *(see [[107], page 125]) Let (f_n) be a sequence in $L_1(\Omega)$ with $|\Omega| < \infty$ and $f \in L_1(\Omega)$. Then, the following properties are equivalent:*

(a) $f_n \rightharpoonup f$ in $\sigma(L_1, L_\infty)$

(b) $\int_\Omega |f_n| < C$ and $\int_\omega f_n \to \int_\omega f$, $\forall \omega \subset \Omega$, ω measurable and $|\omega| < \infty$.

Lemma 2.14. *(see [[107], page 125]) Let (f_n) be a sequence of functions in $L_1(\Omega)$ with $|\Omega| = \infty$ and $f(x) \in L_1(\Omega)$ such that*

(a) $f_n \geq 0 \quad \forall n$ *and* $f \geq 0$ *a.e. on* Ω,

(b) $\int_\Omega f_n \to \int_\Omega f$,

(c) $\int_\omega f_n \to \int_\omega f, \ \forall \omega \subset \Omega, \ \omega$ *measurable and* $|\omega| < \infty$.

Then, $f_n \rightharpoonup f$ *in* $L_1(\Omega)$ *with respect to the weak topology* $\sigma(L_1, L_\infty)$.

Theorem 2.15. *(see [[108]) Picard Lindelöf theorem: Consider the initial value problem (IVP),*

$$y' = f(t, y(t)), \quad y(t_0) = y_0,$$

and suppose, f *is* Lipshitz continuous *in* y *and continuous in* t*, then for some* $\varepsilon > 0$*, there exists a unique solution* $y(t)$ *to the IVP on the interval* $[t_0 - \varepsilon, t_0 + \varepsilon]$.

Theorem 2.16. *(see [102]) Helly's selection theorem: Let,* U *be an open subset in* $\mathbb{R}$ *and let* $f_n : U \to \mathbb{R}, n \in \mathbb{N}$ *be a sequence of functions. Suppose that:*

(a) $\{f_n\}$ *has uniformly bounded total variation on any* W *that is compactly embedded in* U*. That is, for all sets* $W \subset U$ *with compact closure* $\bar{W} \subset U$*,*

$$\sup_{n \in \mathbb{N}} \left(\|f_n\|_{L^1(W)} + \|\frac{df_n}{dt}\|_{L^1(W)} \right) < \infty,$$

where the derivative is taken in sense of tempered distributions.

(b) $\{f_n\}$ *is uniformly bounded at a point, i.e., for some* $t \in U, \{f_n(t) | n \in \mathbb{N}\} \subset \mathbb{R}$ *is a bounded set.*

Then $\exists$ *a subsequence* $f_{n_k}, k \in \mathbb{N}$ *of* $\{f_n\}$ *and a function* $f : U \to \mathbb{R}$ *locally of bounded variation, such that* f_{n_k} *converges to* f *pointwise and* $\{f_n\}$ *converges to* f *locally in* L^1*, i.e., for all* W *compactly embedded in* U*,*

$$\lim_{k \to \infty} \int_W |f_{n_k}(x) - f(x)| dx = 0.$$

Theorem 2.17. *(see [[102], Theorem 9.23]) Contraction Mapping Theorem: Let,* (X, d) *be a non-empty complete metric space with a contraction mapping* $T : X \to X$*. Then,* T *admits a unique fixed point* x^* *in* X*. Furthermore,* x^* *can be found as follows: start with an arbitrary element* $x_0 \in X$ *and define a sequence* $(x_n)_{n \in \mathbb{N}}$ *by* $x_n = T(x_{n-1})$ *for* $n \geq 1$*, then* $x_n \to x^*$ *as* $n \to \infty$*. The theorem is also known as the Banach fixed point theorem.*

Theorem 2.18. *(see [109]) Lebesgue Dominated Convergence Theorem: Suppose* g *is Lebesgue integrable on* E *and the sequence of functions* $\{f_n\}$ *are such that* $|f_n(x)| \leq g(x)$

a.e. on E for all $n \in \mathbb{N}$ and $\{f_n\}$ converges pointwise to f a.e. on E, then f is Lebesgue integrable on E and

$$\lim_{n\to\infty} \int_E f_n dx = \int_E f dx.$$

In the weak compactness sense, the properties of L_1 spaces differ from properties of L_p, $1 < p < \infty$, spaces. In particular, L_1 being non-reflexive, its unit ball is not weakly compact. Kakutani's theorem [[107], Theorem 3.17] and the reflexivity of $L_p(\Omega)$, $p \in (1, \infty)$, see [[107], Theorem 4.10] warrant that any bounded sequence in $L_p(\Omega)$ has a subsequence that converges weakly in $L_p(\Omega)$. The bounded sets of L_1 do not play an important role with respect to the weak topology of L_1 space because L_1 is not reflexive. In the following, the Dunford-Pettis theorem provides an important characterization of weakly compact sets in L_1. The weak compactness argument in L_1 space is used to prove the existence of a weak solution to the age/size-structured population models, see [43, 110–114].

Theorem 2.19. *(see [115]) De La Vallée Poussin Theorem: Let $\mathcal{F}$ be a subset of $L^1(\Omega)$. The following two statements are equivalent:*
(a) $\mathcal{F}$ is uniformly integrable.
(b) $\mathcal{F}$ is a bounded subset of $L^1(\Omega)$ and there exists a convex function $\gamma \in C^\infty([0,\infty)])$ such that $\gamma(0) = \gamma'(0) = 0$, γ' is a concave function, $\gamma'(r) > 0$ if $r > 0, \lim_{r\to\infty} \frac{\gamma(r)}{r} = \lim_{r\to\infty} \gamma'(r) = \infty$, and $\sup_{f\in\mathcal{F}} \int_\Omega \gamma(|f|) d\mu < \infty$.

Example 2.1. *(See [[107], page 122]) Consider the sequence (g_n) of functions in $L_1(0,1)$ and defined by $g_n(x) = ne^{-nx}$. Then,*

(a) $g_n \to 0$ a.e.

(b) g_n is bounded.

(c) $g_n \nrightarrow 0$ strongly.

(d) $g_n \nrightarrow 0$ weakly $\sigma(L_1, L_\infty)$.

Example 2.2. *(See [[107], page 122]) Consider the sequence (f_n) of functions in $L_p(0,1)$, $1 < p < \infty$, and defined by $f_n(x) = n^{1/p} e^{-nx}$. Then,*

(a) $f_n \to 0$ a.e.

(b) f_n is bounded.

(c) $f_n \nrightarrow 0$ strongly.

(d) $f_n \rightharpoonup 0$ weakly $\sigma(L_p, L_q)$, where $\frac{1}{p} + \frac{1}{q} = 1$.

Example 2.3. *(See [[116], page 181]) Let $X = L_1([0, 2\pi])$. Then, the sequence $f_n(x) = \sin nx$ converges weakly to 0 in $L_1([0, 2\pi])$.*

2.2 Finite Dimensional System and Required Results

Let us now proceed to establish our findings: consider the weighted ℓ_1 space of real sequences,

$$X = \{z = (z_k) : ||z|| < \infty\},$$

with the norm defined by

$$||z|| = \sum_{k=1}^{\infty} k|z_k|, \tag{2.3}$$

such that $(X, ||\cdot||)$ is a Banach space. The solution of the Safronov-Dubovski coagulation equation when $\min\{i,j\}jV_{i,j} \leq (i+j)$ is defined to be in the space

$$X^+ = \{z \in X : z \geq 0\}.$$

Definition 2.20. Solution: The solution $f = (f_i)$ of the equation (2.1) on $[0,T)$ where $0 < T \leq \infty$ is a function $f : [0,T) \to X^+$ such that

1. For every i, $f_i \in C([0,T))$ and

$$\sup_{t\in[0,T)} \|f(t)\| < \infty.$$

2. For $i \in \mathbb{N}$ and $\forall\ t \in [0,T)$

$$\int_0^t \sum_{j=1}^{\infty} V_{i,j} f_j(s) ds < \infty.$$

3. For all i and $\forall\, t \in [0,T)$

$$f_i(t) = f_i(0) + \int_0^t f_{i-1}(s) \sum_{j=1}^{i-1} jV_{i-1,j} f_j(s) - f_i(s) \sum_{j=1}^{i} jV_{i,j} f_j(s) - \sum_{j=i}^{\infty} V_{i,j} f_i(s) f_j(s) ds := A(f)_i(t), \tag{2.4}$$

where A is a non-linear operator.

The r_{th} moment is defined by

$$M_r(t) = \sum_{i=1}^{\infty} i^r f_i(t). \tag{2.5}$$

In order to study the infinite system of ordinary differential equations, it is customary to convert the existing system into a finite system and further take the limit of the finite system to crawl our way up to the infinite one. The finite-dimensional system for the

equation (2.1) is given below as

$$\frac{df_1}{dt} := f_1^o = -V_{1,1}f_1^2 - f_1\sum_{j=1}^{n-1} V_{1,j}f_j, \tag{2.6}$$

$$\frac{df_i}{dt} := f_i^o = f_{i-1}\sum_{j=1}^{i-1} jV_{i-1,j}f_j - f_i\sum_{j=1}^{i} jV_{i,j}f_j - \sum_{j=i}^{n-1} V_{i,j}f_if_j, \tag{2.7}$$

when $2 \leq i \leq n-1$ and

$$\frac{df_n}{dt} := f_n^o = f_{n-1}\sum_{j=1}^{n-1} jV_{n-1,j}f_j, \tag{2.8}$$

with the initial condition

$$f_i(0) = f_i^0 \geq 0, \qquad \text{for } 1 \leqslant i \leqslant n. \tag{2.9}$$

The finite-dimensional system (2.6)-(2.9) will be examined to extend the results for the infinite-dimensional Safronov-Dubovski equation. To check whether the truncation is suitable for an aggregation system, i.e., obeys the dissipation law, we shall compute the rate of change in the zeroth moment. For this, take

$$\frac{dM_0^n}{dt} = \frac{d}{dt}\sum_{i=1}^{n} f_i^n(t) := \sum_{i=1}^{n} f_i^o = f_1^o + f_2^o + f_3^o + \cdots + f_{n-2}^o + f_{n-1}^o + f_n^o$$

$$= \left(-f_1\sum_{j=1}^{1} jV_{1,j}f_j - f_1\sum_{j=1}^{n-1} V_{1,j}f_j\right) + \left(f_1\sum_{j=1}^{1} jV_{1,j}f_j - f_2\sum_{j=1}^{2} jV_{2,j}f_j - f_2\sum_{j=2}^{n-1} V_{2,j}f_j\right)$$

$$+ \cdots + \left(f_{n-3}\sum_{j=1}^{n-3} jV_{n-3,j}f_j - f_{n-2}\sum_{j=1}^{n-2} jV_{n-2,j}f_j - f_{n-2}\sum_{j=n-2}^{n-1} V_{n-2,j}f_j\right)$$

$$+ \left(f_{n-2}\sum_{j=1}^{n-2} jV_{n-2,j}f_j - f_{n-1}\sum_{j=1}^{n-1} jV_{n-1,j}f_j - \sum_{j=n-1}^{n-1} f_{n-1}V_{n-1,j}f_j\right) + \left(f_{n-1}\sum_{j=1}^{n-1} jV_{n-1,j}f_j\right).$$

On simplifying the above expression, one can obtain

$$\frac{dM_0^n}{dt} = -\sum_{i=1}^{n-1}\sum_{j=i}^{n-1} V_{i,j}f_if_j.$$

Hence,

$$\frac{dM_0^n}{dt} \leq 0. \tag{2.10}$$

Thus, the number of particles in the truncated system decreases, serving us right to use this finite-dimensional system. Further, it is important to derive the r_{th} moment for detailed analysis of the salient components, that is, the first and the second moments.

Using the definition (2.5), the rate of change in the truncated r_{th} moment is defined as follows

$$\frac{dM_r^n(f)}{dt} = \frac{d}{dt}\sum_{i=1}^{n} i^r f_i = \sum_{i=1}^{n} g_i f_i^o,$$

where g_i is a non-negative sequence. Putting the values of f_i^o in the above equation yields

$$\begin{aligned}\frac{dM_r^n(f)}{dt} = g_1\left(-f_1\sum_{j=1}^{1} jV_{1,j}f_j - f_1\sum_{j=1}^{n-1} V_{i,j}f_j\right) + g_2\left(f_1\sum_{j=1}^{1} jV_{1,j}f_j - f_2\sum_{j=1}^{2} jV_{2,j}f_j - f_2\sum_{j=2}^{n-1} V_{2,j}f_j\right)\\ +g_3\left(f_2\sum_{j=1}^{2} jV_{2,j}f_j - f_3\sum_{j=1}^{3} jV_{3,j}f_j - f_3\sum_{j=3}^{n-1} V_{3,j}f_j\right) + \cdots\\ +g_{n-1}\left(f_{n-2}\sum_{j=1}^{n-2} jV_{n-2,j}f_j - f_{n-1}\sum_{j=1}^{n-1} jV_{n-1,j}f_j - f_{n-1}\sum_{j=n-1}^{n-1} V_{n-1,j}f_j\right) + g_n f_{n-1}\sum_{j=1}^{n-1} jV_{n-1,j}f_j.\end{aligned}$$

Thus

$$\frac{dM_r^n(f)}{dt} = \sum_{i=1}^{n-1}(g_{i+1}-g_i)\sum_{j=1}^{i} jV_{i,j}f_i f_j - \sum_{i=1}^{n-1}\sum_{j=i}^{n-1} g_i V_{i,j} f_i f_j. \tag{2.11}$$

Below some important lemmas are stated and proved that are required to achieve the main outcomes of this work.

Lemma 2.21. *The system of equations (2.6 - 2.9) has a unique solution for the kernel* $min\{i,j\}V_{i,j} \le (i+j)$ *and* $f_i(t) \ge 0$, *with* $t \ge 0$, $1 \le i \le n$ *and*

$$\sum_{i=1}^{n} i f_i(t) = \sum_{i=1}^{n} i f_i(0), \quad i.e., \quad M_1^n(t) = M_1^n(0). \tag{2.12}$$

Proof. The existence and uniqueness of local solutions to (2.6)–(2.9) is an easy consequence of the Picard-Lindelöf Theorem 2.15 since the RHS of each of (2.6)–(2.8) is a polynomial (as a function of the components f_i of the solution vector $f = f_i(\cdot)$. The non-negativity of the solutions can be proved by the standard procedure of adding a positive ε to the right-hand side of all equations and, being $f^\varepsilon = (f_i^\varepsilon)$ the corresponding solution. If f^ε satisfy, for some $t_0 > 0$, $f_i^\varepsilon(t_0) > 0$ and $f_j^\varepsilon(t_0) = 0$ for some $j \in \{1,\ldots,n\}$, then $\frac{d}{dt}f_j^\varepsilon(t_0) > 0$, and thus the solution is non-negative for $t > t_0$. Passing to the limit $\varepsilon \to 0$ proves the result (see [117, Theorem III-4-5]). The relation (2.12) follows by putting $r = 1$ and $g_i = i$ in (2.11). Finally, the Lipschitz continuity of the RHS of (2.6)–(2.8) follows from the non-negativity of the solution and the bound

$$f_i(t) \le i^{-1}\sum_{i=1}^{n} i f_i(0).$$

In addition to this, we can also establish the Lipschitz continuity by proving that the non-linear operator A defined in (8) is a contraction mapping (proved in Section 2.4). Thus, the global existence and uniqueness of the finite-dimensional system (2.6)–(2.9) hold by using the Picard-Lindelöf Theorem 2.15. □

As in [118], let us define the terms $X_m^n(t)$ and $x_m^n(t)$ where $m \geq 1$ as

$$X_m^n(t) := \sum_{i=m}^{n} g_i f_i^n(t), \tag{2.13}$$

and for the particular value of $g_i = i$, it is

$$x_m^n(t) := \sum_{i=m}^{n} i f_i^n(t). \tag{2.14}$$

Following (2.11), $x_m^{on}(t)$ can be defined by

$$x_m^{on}(t) = \sum_{i=m}^{n-1} \sum_{j=1}^{i} j V_{i,j} f_i^n f_j^n + m f_{m-1} \sum_{j=1}^{m-1} j V_{m-1,j} f_j - \sum_{i=m}^{n-1} \sum_{j=i}^{n-1} i V_{i,j} f_i^n f_j^n. \tag{2.15}$$

Assume $2m < n$ and putting $g_i = i$ when $m \leq i \leq 2m$ and $g_i = 2m$ when $2m+1 \leq i \leq n$ in (2.13) give us the expression for $q_m^n(t)$ as

$$\sum_{i=m}^{2m} i f_i^n(t) + 2m \sum_{i=2m+1}^{n} f_i^n(t) := q_m^n(t) \tag{2.16}$$

and therefore,

$$\sum_{i=m}^{2m} i f_i^{on}(t) + 2m \sum_{i=2m+1}^{n} f_i^{on}(t) = q_m^{on}(t). \tag{2.17}$$

Expanding and simplifying the above equation reduces to

$$\begin{aligned} q_m^{on}(t) = m f_{m-1}^n \sum_{j=1}^{m-1} j V_{m-1,j} f_j^n(t) + \sum_{i=m}^{2m-1} f_i^n(t) \sum_{j=1}^{i} j V_{i,j} f_j^n(t) \\ - \sum_{i=m}^{2m} \sum_{j=i}^{n-1} i f_i^n(t) V_{i,j} f_j^n(t) - 2m \sum_{i=2m+1}^{n-1} \sum_{j=i}^{n-1} V_{i,j} f_i^n(t) f_j^n(t), \end{aligned} \tag{2.18}$$

which can be further written as

$$\begin{aligned} q_m^{on}(t) = m f_{m-1}^n(t) \sum_{j=1}^{m-1} j V_{m-1,j} f_j^n(t) + \sum_{W_1} A_{i,j} V_{i,j} f_i^n(t) f_j^n(t) \\ + \sum_{W_2} B_{i,j} V_{i,j} f_i^n(t) f_j^n(t) + \sum_{W_3} C_{i,j} V_{i,j} f_i^n(t) f_j^n(t), \end{aligned}$$

where, $A_{i,j} = j$ when $i \geq m, j \leq m$, $B_{i,j} = -i$ when $i \leq 2m, j \geq 2m$ and $C_{i,j} = -2m$, when $i > 2m, j > 2m$. Now, for the proof of existence result, the introduction of another term $D_m^n(t)$ is required which is defined by

$$D_m^n(t) = e^{-t}\left[\sum_{i=m}^{n} i f_i^n(t) + (2m+2)M_1^n(0)^2\right]. \tag{2.19}$$

The following lemma will be useful in the application of Helly's selection theorem for the sequence $f^n = \{f_i^n\}$ later on.

Lemma 2.22. *Let, $min\{i,j\}V_{i,j} \leq (i+j)$, $i,j \geq 1$ and $D_m^n(t)$ is defined in (2.19). Then,*

$$\frac{dD_m^n(t)}{dt} \leq 0. \tag{2.20}$$

Proof. Differentiating (2.19) both sides with respect to t and using (2.14) and (2.15) yield

$$\begin{aligned}
\frac{dD_m^n(t)}{dt} &= e^{-t}\left[\sum_{i=m}^{n-1}\sum_{j=1}^{i} jV_{i,j}f_i^n(t)f_j^n(t) + mf_{m-1}^n(t)\sum_{j=1}^{m-1} jV_{m-1,j}f_j^n(t) - \sum_{i=m}^{n-1}\sum_{j=i}^{n-1} iV_{i,j}f_i^n(t)f_j^n(t)\right] \\
&\quad - e^{-t}\left[\sum_{i=m}^{n} i f_i^n(t) + (2m+2)M_1^n(0)^2\right] \\
&\leq e^{-t}\left[\sum_{i=m}^{n-1}\sum_{j=1}^{i} jV_{i,j}f_i^n(t)f_j^n(t) + mf_{m-1}^n(t)\sum_{j=1}^{m-1} jV_{m-1,j}f_j^n(t) - (2m+2)M_1^n(0)^2\right].
\end{aligned}$$

Putting the bounds for the kernel $V_{i,j}$ gives us

$$\begin{aligned}
\frac{dD_m^n(t)}{dt} &\leq e^{-t}\left[\sum_{i=m}^{n-1}\sum_{j=1}^{i}(i+j)f_i^n(t)f_j^n(t) + mf_{m-1}^n(t)\sum_{j=1}^{m-1}(m-1+j)f_j^n(t) - (2m+2)M_1^n(0)^2\right] \\
&\leq e^{-t}\left[\sum_{i=m}^{n-1}\sum_{j=1}^{i} 2ijf_i^n(t)f_j^n(t) + 2mf_{m-1}^n(t)(m-1)\sum_{j=1}^{m-1} f_j^n(t) - (2m+2)M_1^n(0)^2\right] \\
&\leq e^{-t}\left[2M_1^n(0)^2 + 2mM_1^n(0)^2 - (2m+2)M_1^n(0)^2\right].
\end{aligned}$$

This completes the proof of Lemma 2.22 as

$$\frac{dD_m^n(t)}{dt} \leq 0.$$

□

Now, all the necessary information is gathered to proceed with the main outcomes of the chapter, i.e., the global existence result for (2.1)-(2.2) considering the conservative as well as the non-conservative truncations.

2.3 Existence and Mass Conservation

When an equation has the capability of governing a particular phenomenon, it creates immense opportunities for its mathematical analysis. The first step of this analysis is the existence theory which answers the most relevant question, does this equation possesses a solution, and under what conditions it exists? The result depends on various factors, space that is taken into consideration, the defined norm, and the domain of dependence in terms of space as well as time. As far as the existing theory is concerned, here it is for an equation governed by the collision of particles followed by the coagulation of monomers with other particles. So, the existence of solutions should also be affected by the rate of interaction between particles, i.e., the physical kernel $V_{i,j}$ and the initial concentration of particles, $f(0)$. In this section, the global existence theorem, the corollary to the existence theorem, and the density conservation result are discussed for the equation (2.1).

2.3.1 Existence

In the following theorem, the existence result is stated and discussed.

Theorem 2.23. *Let,* $f(0) \in X^+$, $\sum_{i=1}^{\infty} i|f_i(0)| < \infty$ *and the kernel* $V_{i,j}$ *satisfy* $min\{i,j\}V_{i,j} \leq (i+j)$, $\forall\ i,j \in \mathbb{N}^+$, *then* $\exists$ *a solution* f *of (2.1) on* $\mathbb{R}^+ \cup \{0\}$.

Proof. The truncated system (2.6 - 2.9) has a unique solution by Lemma 2.21 and

$$\sum_{i=1}^{n} i f_i^n(t) = \sum_{i=1}^{n} i f_i(0) \quad \forall\, t \geq 0.$$

Consider $f^n(t) \in X^+$ if $f^n(t) = f_i^n(t)$ when $1 \leq i \leq n$ and $f^n(t) = 0$ when $i > n$ and it implies that

$$\|f^n(t)\| \leq \|f(0)\| \ \text{ and } \ 0 \leq f_i^n(t) \leq i^{-1}||f_0||. \tag{2.21}$$

By Lemma 2.22 and Eqn (2.12) for each m, the functions $D_m^n(.)$ are of uniformly bounded variation on $[0,\infty)$. Hence, by Helly's selection theorem, $\exists$ a subsequence '$\tilde{D}_m^n$' of D_m^n such that

$$\tilde{D}_m^n(t) \to D_m(t) \ \text{ as } \ n \to \infty \ \text{ for each } \ t \geq 0,$$

for some D_m of bounded variation. By the definition of $D_m^n(t)$, we obtain the following expression for $f_i^n(t)$

$$f_i^n(t) = i^{-1}e^t\left[D_i^n(t) - D_{i+1}^n(t)\right] + 2i^{-1}M_1^n(0)^2.$$

It follows that there exists a subsequence '$\tilde{f}^n$' of f^n and functions $f_i : [0,\infty) \to \mathbb{R}$ each of bounded variation on every compact subset of $[0,\infty)$ such that

$$\tilde{f}_i^n(t) \to f_i(t) \quad \text{as} \quad n \to \infty \quad \text{for each} \quad t \geq 0.$$

Thus,

$$f_i(t) \geq 0 \quad \text{and} \quad ||f(t)|| \leq ||f(0)||. \tag{2.22}$$

Our goal is to prove that this limit function f is a solution of the initial value problem (2.1)–(2.2), i.e., fulfills the conditions in Definition 2.20. This will be done by passing to the limit $n \to \infty$ in the integrated version of the truncated problem (2.6–2.9). To do this, and also to satisfy condition 2 in Definition 2.20, we need to prove that, for every fixed $i \in \mathbb{N}$, $T \geq 0$, and $\varepsilon > 0$, there exists m and N_0, with $N_0 > m \geq i$, such that, for all $n > N_0$,

$$\int_0^T x_m^n(t)dt < \varepsilon. \tag{2.23}$$

In order to prove this, let us integrate (2.15) in $[0,t]$ which yields

$$\begin{aligned}
x_m^n(t) &= x_m^n(0) + \int_0^t \left(\sum_{i=m}^{n-1}\sum_{j=1}^{i} jV_{i,j}f_i^n(s)f_j^n(s) + mf_{m-1}\sum_{j=1}^{m-1} jV_{m-1,j}f_j - \sum_{i=m}^{n-1}\sum_{j=i}^{n-1} iV_{i,j}f_i^n(s)f_j^n(s) \right) ds \\
&= x_m^n(0) + \int_0^t \left(\sum_{i=m}^{2m-1}\sum_{j=1}^{i} jV_{i,j}f_i^n(s)f_j^n(s) + \sum_{i=2m}^{2m}\sum_{j=1}^{i} jV_{i,j}f_i^n(s)f_j^n(s) \right) ds \\
&\quad + \int_0^t \left(\sum_{i=2m+1}^{n-1}\sum_{j=1}^{i} jV_{i,j}f_i^n(s)f_j^n(s) + mf_{m-1}\sum_{j=1}^{m-1} jV_{m-1,j}f_j \right) ds \\
&\quad - \int_0^t \left(\sum_{i=m}^{2m}\sum_{j=i}^{n-1} iV_{i,j}f_i^n(s)f_j^n(s) + \sum_{i=2m+1}^{n-1}\sum_{j=i}^{n-1} iV_{i,j}f_i^n(s)f_j^n(s) \right) ds.
\end{aligned}$$

Using (2.18), one can write

$$\begin{aligned}
x_m^n(t) &= x_m^n(0) + \int_0^t q_m^{on}(s)ds + \int_0^t \left(\sum_{i=2m}^{2m}\sum_{j=1}^{i} jV_{i,j}f_i^n(s)f_j^n(s) + \sum_{i=2m+1}^{n-1}\sum_{j=1}^{i} jV_{i,j}f_i^n(s)f_j^n(s) \right) ds \\
&\quad - \int_0^t \left(\sum_{i=2m+1}^{n-1}\sum_{j=i}^{n-1} iV_{i,j}f_i^n(s)f_j^n(s) - 2m\sum_{i=2m+1}^{n-1}\sum_{j=i}^{n-1} V_{i,j}f_i^n(s)f_j^n(s) \right) ds.
\end{aligned}$$

Simplification of the fourth term of the above equation yields

$$\begin{aligned}\sum_{i=2m+1}^{n-1}\sum_{j=1}^{i} jV_{i,j}f_i^n(s)f_j^n(s) &= \sum_{i=2m+1}^{n-1}\sum_{j=1}^{2m} jV_{i,j}f_i^n(s)f_j^n(s) + \sum_{i=2m+1}^{n-1}\sum_{j=2m+1}^{i} jV_{i,j}f_i^n(s)f_j^n(s)\\ &= \sum_{i=2m+1}^{n-1}\sum_{j=1}^{2m} jV_{i,j}f_i^n(s)f_j^n(s) + \sum_{j=2m+1}^{n-1}\sum_{i=j}^{n-1} jV_{i,j}f_i^n(s)f_j^n(s)\\ &= \sum_{i=2m+1}^{n-1}\sum_{j=1}^{2m} jV_{i,j}f_i^n(s)f_j^n(s) + \sum_{i=2m+1}^{n-1}\sum_{j=i}^{n-1} iV_{j,i}f_j^n(s)f_i^n(s). \quad (2.24)\end{aligned}$$

Using (2.24) in the expansion of $x_m^n(t)$ gives us

$$\begin{aligned}x_m^n(t) = x_m^n(0) + \int_0^t q_m^{on}(s)ds + \int_0^t \left(\sum_{i=2m}^{2m}\sum_{j=1}^{i} jV_{i,j}f_i^n(s)f_j^n(s)\right) ds\\ + \int_0^t \left(\sum_{i=2m+1}^{n-1}\sum_{j=1}^{2m} jV_{i,j}f_i^n(s)f_j^n(s) + 2m\sum_{i=2m+1}^{n-1}\sum_{j=i}^{n-1} V_{i,j}f_i^n(s)f_j^n(s)\right) ds. \quad (2.25)\end{aligned}$$

By (2.21), (2.22), and the pointwise convergence of f_i^n to f_i we conclude that, for all $t \in [0,T]$, $\forall \varepsilon > 0, \forall p > \frac{4\|f_0\|}{\varepsilon}, \exists N_0 : \forall n > N_0$,

$$\sum_{i=1}^{\infty}|f_i^n(t) - f_i(t)| = \sum_{i=1}^{p-1}|f_i^n(t) - f_i(t)| + \sum_{i=p}^{\infty}|f_i^n(t) - f_i(t)| < \frac{\varepsilon}{2} + \frac{2}{p}\|f_0\| < \varepsilon,$$

which allows us to let $n \to \infty$ in the definition of $q_m^n(t)$ in (2.16), getting, for all $t \in [0,T]$

$$\sum_{i=m}^{2m} if_i(t) + 2m\sum_{i=2m+1}^{\infty} f_i(t) = q_m(t) \le \sum_{i=m}^{\infty} if_i(t), \quad (2.26)$$

so that

$$\lim_{m\to\infty} q_m(t) = 0, \quad |q_m(t)| \le \text{constant}, \quad t \in [0,T].$$

Therefore, given $\varepsilon > 0$, $\exists\ M, N_0$ with $N_0 > M$ such that for all $m > M, n > N_0, n \ge 2m+1$, one can write

$$\int_0^T q_m^o(t)dt < \varepsilon, \quad (2.27)$$

and

$$x_m^n(0) = \sum_{i=m}^{n} if_i(0) < \varepsilon. \quad (2.28)$$

By applying (2.27) and (2.28) in the equation of $x_m^n(t)$ for $t \in [0,T]$ yield

$$x_m^n(t) < 2\varepsilon + \int_0^t \left(\sum_{i=2m}^{2m} \sum_{j=1}^{i} jV_{i,j} f_i^n(s) f_j^n(s) \right) ds$$
$$+ \int_0^t \left(\sum_{i=2m+1}^{n-1} \sum_{j=1}^{2m} jV_{i,j} f_i^n(s) f_j^n(s) + 2m \sum_{i=2m+1}^{n-1} \sum_{j=i}^{n-1} V_{i,j} f_i^n(s) f_j^n(s) \right) ds.$$

Putting $jV_{i,j} \leq (i+j)$ when $j \leq i$ and $iV_{i,j} \leq (i+j)$ when $i \leq j$ in the above equation simplify to

$$\begin{aligned} x_m^n(t) &\leq 2\varepsilon + \int_0^t \left(\sum_{i=2m}^{2m} \sum_{j=1}^{i} (i+j) f_i^n(s) f_j^n(s) \right) ds \\ &+ \int_0^t \left(\sum_{i=2m+1}^{n-1} \sum_{j=1}^{2m} (i+j) f_i^n(s) f_j^n(s) + 2m \sum_{i=2m+1}^{n-1} \sum_{j=i}^{n-1} \frac{(i+j)}{i} f_i^n(s) f_j^n(s) \right) ds \\ &\leq 2\varepsilon + \int_0^t \left(\sum_{i=m}^{n} \sum_{j=1}^{i} 2i f_i^n(s) f_j^n(s) + \sum_{i=m}^{n} \sum_{j=1}^{2m} 2i f_i^n(s) f_j^n(s) + 2M \sum_{i=m}^{n} \sum_{j=i}^{n-1} 2j f_i^n(s) f_j^n(s) \right) ds. \end{aligned}$$

One can easily compute using (2.21)

$$x_m^n(t) \leq 2\varepsilon + \int_0^t \left(4\|f(0)\| x_m^n(s) + 4m\|f(0)\| x_m^n(s)\right) ds.$$

Thanks to Gronwall's lemma to get

$$x_m^n(t) \leq k_1 \varepsilon, \tag{2.29}$$

where $k_1 = c(T, \|f(0)\|)$, which gives that

$$\int_0^t x_M^n dt < k_1 T \varepsilon.$$

Since, $f_i^n(t)$ is pointwise convergent to $f_i(t)$, the above expression entails

$$\int_0^T \sum_{i=M}^{\infty} i f_i(t) dt < \varepsilon.$$

When $V_{i,j} \leq \frac{i+j}{\min\{i,j\}}$, the following holds

$$\int_0^T \sum_{j=1}^{\infty} V_{i,j} f_j(t) dt < \infty \quad \forall \ i. \tag{2.30}$$

For any $n > l$, $t \in [0, T)$, one can write

$$\left| f_i^n(t) - f_i(0) - \int_0^t \left(f_{i-1}^n(s) \sum_{j=1}^{i-1} j V_{i-1,j} f_j^n - f_i^n(s) \sum_{j=1}^{i} j V_{i,j} f_j^n(s) - f_i^n(s) \sum_{j=i}^{l} V_{i,j} f_j^n(s) \right) ds \right|$$
$$\leq |f_i^n(t)| + |f_i(0)| + \int_0^t \left(f_{i-1}^n(s) \sum_{j=1}^{i-1} j V_{i-1,j} f_j^n - f_i^n(s) \sum_{j=1}^{i} j V_{i,j} f_j^n(s) - f_i^n(s) \sum_{j=i}^{l} V_{i,j} f_j^n(s) \right) ds.$$

Now, letting $l \to \infty$ and further using (2.14) and the equations (2.28) and (2.29), one can obtain

$$\left| f_i^n(t) - f_i(0) - \int_0^t \left(f_{i-1}^n(s) \sum_{j=1}^{i-1} j V_{i-1,j} f_j^n - f_i^n(s) \sum_{j=1}^{i} j V_{i,j} f_j^n(s) - f_i^n(s) \sum_{j=i}^{\infty} V_{i,j} f_j^n(s) \right) ds \right|$$
$$\leq x_m^n(t) + \varepsilon + \int_0^t x_m^{on}(s) ds \leq \varepsilon + 2k_1 \varepsilon.$$

Taking $n \to \infty$ yields

$$\left| f_i(t) - f_i(0) - \int_0^t \left(f_{i-1}(s) \sum_{j=1}^{i-1} j V_{i-1,j} f_j - f_i(s) \sum_{j=1}^{i} j V_{i,j} f_j(s) - f_i(s) \sum_{j=i}^{\infty} V_{i,j} f_j(s) \right) ds \right|$$
$$\leq (1 + 2k_1)\varepsilon.$$

Using the arbitrariness of ε, the solution $f_i(t)$ can be defined as

$$f_i(t) = f_i(0) + \int_0^t f_{i-1}(s) \sum_{j=1}^{i-1} j V_{i-1,j} f_j - f_i(s) \sum_{j=1}^{i} j V_{i,j} f_j(s) - f_i(s) \sum_{j=i}^{\infty} V_{i,j} f_j(s) ds.$$

□

Below an important result of strong convergence of subsequence f^{n_k} to the solution f is established.

2.3.1.1 Corollary to Existence Theorem

Corollary 2.24. *Let f^{n_k} be the corresponding pointwise convergent subsequence of solutions to the finite-dimensional system (2.6 – 2.9). Then, $f^{n_k} \to f$ in X uniformly on compact subsets of $[0, \infty)$.*

Proof. To prove the above result, first we show that $f_i^{n_k}(t) \to f_i(t)$ for each i uniformly on the compact subsets of $[0,\infty)$. For this, it is sufficient to prove that for each $m > 1$

$$z_m^{n_k}(t) := e^{-t}\left[M_1^n(t) - \sum_{i=1}^{m-1} i f_i^{n_k}(t) + 4M_1^n(0)^2\right],$$

converges to $z_m(t) = e^{-t}\left[M_1(t) - \sum_{i=1}^{m-1} i f_i(t) + 4M_1(0)^2\right]$ uniformly on compact subsets of $[0,T)$. This follows by the pointwise convergence of $z_m^{n_k}(t)$ to $z_m(t)$ and

$$\frac{dz_m^{n_k}(t)}{dt} \leq 0, \qquad n \geq M, \;\; t \in [0,T],$$

where the second equation follows from the results by Lemma 2.21 and Lemma 2.22. Let, $K \subset [0,\infty)$ be compact and $t_{n_k} \to t$ in K, then

$$\lim_{n\to\infty} \|f^{n_k}(t_{n_k})\| = \lim_{n\to\infty} \sum_{i=1}^{\infty} i f_i^{n_k}(t_{n_k}) = \lim_{n\to\infty} \sum_{i=1}^{\infty} i f_i(t_{n_k}) = \sum_{i=1}^{\infty} i f_i(t) = \|f(t)\|,$$

which ensures

$$\|f^{n_k}\| \to \|f\|.$$

Therefore

$$f^{n_k} \to f,$$

in $C(K,X)$. □

To move further, in the following subsection, the mass conservation of the Safronov-Dubovski coagulation equation is discussed.

2.3.2 Density Conservation

Another interesting phenomenon to discuss for the equation (2.1) is the rate of change of the mass in the system. The total mass of the system may or may not be conserved, i.e., there might be certain situations in which the initial mass of the system is greater than the mass at any time during the process. Therefore in this subsection, the mass for the Safronov-Dubovski coagulation equation is investigated for the kernel $V_{i,j}$ satisfying $V_{i,j} \leq \frac{(i+j)}{\min\{i,j\}}$.

Theorem 2.25. *Let $f_i(t)$ be the solution of (2.1) when $V_{i,j} \leq \frac{(i+j)}{min\{i,j\}}$, then the total mass of the system remains conserved, i.e.,*

$$\sum_{i=1}^{\infty} i f_i(t) = \sum_{i=1}^{\infty} i f_i(0) \quad or \quad M_1(t) = M_1(0), \tag{2.31}$$

when $t \in [0, \infty)$.

Proof. Following (2.29), it is given that for $n \geq m$

$$x_m^n(t) \leq k_1 \varepsilon,$$

which implies that

$$\sum_{i=m}^{n} i f_i^n \leq k_1 \varepsilon. \tag{2.32}$$

Letting $n \to \infty$ and using the convergence of $f^n \to f$ entails

$$\sum_{i=m}^{\infty} i f_i \leq k_1 \varepsilon. \tag{2.33}$$

If $f_i^n(t) := 0$ when $i > n$, it yields for $n \geq m$

$$\left| \sum_{i=1}^{\infty} i \left(f_i^n(t) - f_i(t) \right) \right| \leq \left| \sum_{i=1}^{m-1} i \left(f_i^n(t) - f_i(t) \right) \right| + \sum_{i=m}^{n} i f_i^n(t) + \sum_{i=m}^{n} i f_i(t) + \sum_{i=n}^{\infty} i f_i(t). \tag{2.34}$$

Using (2.32) and (2.33) in (2.34), one can achieve

$$\left| \sum_{i=1}^{\infty} i \left(f_i^n(t) - f_i(t) \right) \right| \leq \left| \sum_{i=1}^{m-1} i \left(f_i^n(t) - f_i(t) \right) \right| + 2k_1 \varepsilon.$$

Taking $n \to \infty$ followed by using

$$\sum_{i=1}^{\infty} i f_i^n(t) = \sum_{i=1}^{\infty} i f_i(0),$$

on lhs of the above equation, it reduces to

$$\left| \sum_{i=1}^{\infty} i \left(f_i(0) - f_i(t) \right) \right| \leq 2k_1 \varepsilon.$$

As ε is arbitrary, the desired result is obtained. □

Finally, the uniqueness result is developed in the following section.

2.4 Uniqueness

When an equation has a unique solution, it becomes more relevant and trustworthy for calculating the analytical solutions and comparing them with the numerical solutions.

The statement and proof of uniqueness result are given through the following theorem.

Theorem 2.26. *Let, $f_i(t)$ be a solution of the equation (2.1) with $V_{i,j}$ being the coagulation kernel such that $min\{i,j\}V_{i,j} \leq (i+j)\ \forall\ i,j \in \mathbb{N}$ and initial mass $M_1(0) = \sum_{i=1}^{\infty} i f_i(0) < \infty$, then the solution $f_i(t)$ is unique.*

Proof. To prove the uniqueness theorem, the continuity and the non-negativity of $f_i(t)$ when $\min\{i,j\}V_{i,j} \leq (i+j)$ are required. The non-negativity of $f_i(t)$ follows from (2.22), and the continuity follows from the existence theorem. Let $f_i(t)$ and $g_i(t)$ be two solutions of the Safronov-Dubovski coagulation equation with the same initial condition, i.e.,

$$f_i(0) = g_i(0). \tag{2.35}$$

Considering $h(t)$ as

$$h(t) = \sum_{i=1}^{\infty} |f_i(t) - g_i(t)|,$$

where $f_i(t)$ is given by the equation (2.4). Then,

$$h(t) = \sum_{i=1}^{\infty} \Bigg| f_i(0) + \int_0^t f_{i-1}(s) \sum_{j=1}^{i-1} V_{i-1,j} j f_j(s) - f_i(s) \sum_{j=1}^{i} V_{i,j} j f_j(s) - \sum_{j=i}^{\infty} V_{i,j} f_i(s) f_j(s) ds$$
$$- g_i(0) - \int_0^t g_{i-1}(s) \sum_{j=1}^{i-1} V_{i-1,j} j g_j(s) + g_i(s) \sum_{j=1}^{i} V_{i,j} j g_j(s) + \sum_{j=i}^{\infty} V_{i,j} g_i(s) g_j(s) ds \Bigg|.$$

Using the equation (2.35), replacing $i-1$ by i' and then taking $i' \to i$ in the first and fourth sums, the above equation becomes,

$$h(t) \leq 2 \sum_{i=1}^{\infty} \left| \int_0^t \left(f_i(s) \sum_{j=1}^{i} j V_{i,j} f_j(s) - g_i(s) \sum_{j=1}^{i} j V_{i,j} g_j(s) \right) ds \right|$$
$$+ \sum_{i=1}^{\infty} \left| \int_0^t \left(\sum_{j=i}^{\infty} V_{i,j} g_i(s) g_j(s) - V_{i,j} f_i(s) f_j(s) \right) ds \right|.$$

Putting $\min\{i,j\}V_{i,j} \leq (i+j)$ in the equation above yields,

$$h(t) \leq \int_0^t \left(\sum_{i=1}^{\infty} \sum_{j=1}^{i} (i+j) |g_i(s) - f_i(s)||g_j(s) + f_j(s)| + \sum_{i=1}^{\infty} \sum_{j=1}^{i} (i+j) |g_i(s) + f_i(s)||g_j(s) - f_j(s)| \right) ds$$
$$+ \int_0^t \left(\sum_{i=1}^{\infty} \sum_{j=i}^{\infty} \frac{(i+j)}{2} |g_i(s) - f_i(s)||g_j(s) + f_j(s)| + \sum_{i=1}^{\infty} \sum_{j=i}^{\infty} \frac{(i+j)}{2} |g_i(s) + f_i(s)||g_j(s) - f_j(s)| \right) ds.$$

Using symmetry in the first and the fourth sums lead to,

$$h(t) \leq \int_0^t \left(\sum_{i=1}^{\infty} \sum_{j=i}^{\infty} 2j|g_i(s) - f_i(s)||g_j(s) + f_j(s)| + \sum_{i=1}^{\infty} \sum_{j=1}^{i} 2i|g_i(s) + f_i(s)||g_j(s) - f_j(s)| \right) ds$$
$$+ \int_0^t \left(\sum_{i=1}^{\infty} \sum_{j=i}^{\infty} j|g_i(s) - f_i(s)||g_j(s) + f_j(s)| + \sum_{i=1}^{\infty} \sum_{j=1}^{i} i|g_i(s) + f_i(s)||g_j(s) - f_j(s)| \right) ds.$$

Thus, using the definition of norm and the definition of $h(t)$, one can write,

$$h(t) \leq \int_0^t 6||f + g||h(s)ds,$$

which, by using Theorem 2.25, reduces to

$$h(t) \leq 12M_1(0) \int_0^t h(s)ds.$$

Hence, equation (2.22), the continuity of $f_i(t)$ and the Gronwall's lemma ensure that $h(t) \equiv 0$ for $0 \leq t \leq T$, which implies that $f_i(t) = g_i(t)\ \forall\ i$ and $\forall\ 0 \leq t \leq T$. Since T is arbitrary, this shows that the solution is unique. □

2.5 Non-Conservative Truncation

In this section, we explore a more realistic interpretation of our problem (2.1)-(2.2), through the analysis of a finite-dimensional system that does not conserve mass. We establish the global existence and density conservation of a solution to (2.1)-(2.2) using the results on the non-conservative truncation. Such a type of analysis is conducted by several researchers (see [101] [119], [120] and references therein).

Required Results

Here, in this subsection, we present an approximating system of equations that do not conserve the first moment. The system is hence called *non-conservative* and is defined as

$$\frac{df_i^n}{dt} = F_i^n(f), \qquad \text{for } 1 \leq i \leq n, \tag{2.36}$$

where

$$F_1^n(f) := -V_{1,1}f_1^2 - f_1\sum_{j=1}^{n} V_{1,j}f_j \tag{2.37}$$

$$F_i^n(f) := f_{i-1}\sum_{j=1}^{i-1} jV_{i-1,j}f_j - f_i\sum_{j=1}^{i} jV_{i,j}f_j - f_i\sum_{j=i}^{n} V_{i,j}f_j, \quad \text{for } 2 \le i \le n-1, \tag{2.38}$$

$$F_n^n(f) := f_{n-1}\sum_{j=1}^{n-1} jV_{n-1,j}f_j \tag{2.39}$$

with the initial conditions

$$f_i(0) = f_i^0 \ge 0, \qquad \text{for } 1 \le i \le n. \tag{2.40}$$

We compute the i^{th} moment of the solution of the finite-dimensional system which aids in computing its zeroth and first moments.

Lemma 2.27. *Let $f = (f_i)_{i\in\{1,\dots,n\}}$ be a solution of (2.36)-(2.39) defined in an open interval I containing 0. Let $g = (g_i)$ be a real sequence. Then*

$$\frac{dM_g^n}{dt} = \sum_{i=1}^{n-1}|g_{i+1} - g_i|\sum_{j=1}^{i} jV_{i,j}f_if_j - \sum_{i=1}^{n-1}\sum_{j=i}^{n} g_iV_{i,j}f_if_j. \tag{2.41}$$

Proof. Using the expressions (2.37)–(2.39), one can obtain

$$\frac{dM_g^n}{dt} = \sum_{i=1}^{n} g_iF_i^n(f) = \underbrace{g_1\Big(-V_{1,1}f_1^2 - f_1\sum_{j=1}^{n} V_{1,j}f_j\Big)}_{I} + \underbrace{g_n\Big(f_{n-1}\sum_{j=1}^{n-1} jV_{n-1,j}f_j\Big)}_{II}$$
$$+ \underbrace{\sum_{i=2}^{n-1} g_i\Big(f_{i-1}\sum_{j=1}^{i-1} jV_{i-1,j}f_j - f_i\sum_{j=1}^{i} jV_{i,j}f_j - f_i\sum_{j=i}^{n} V_{i,j}f_j\Big)}_{III}.$$

To obtain the desired result, some simple but careful computations are required. One can proceed as follows: expand III for each i, then combine the first term in I and the first term in III_1, where III_k, $k = 1, 2, \cdots, (n-1)$ denotes sub-brackets of III. Further, merge the second term of III_1 with the first term of III_2 and the second term of III_2 with the first term of III_3. Finally, combine II and the second term of $III_{(n-1)}$. □

The rate of change in the number of particles of the finite-dimensional system can be calculated by putting $g_i = 1$ in (2.41) and the non-negativity of f_i, f_j and $V_{i,j}$ yield

$$\frac{dM_0^n}{dt} = \sum_{i=1}^{n} F_i^n = -\sum_{i=1}^{n-1}\sum_{j=i}^{n} V_{i,j}f_if_j \le 0$$

and thus $M_0^n(t) \leq M_0^n(0)\ \forall t \in I \cap \{t \geq 0\}$ which ensures that the above-mentioned truncation is valid. Taking $g_1 = i$ in (2.41), we obtain

$$\frac{dM_1^n(t)}{dt} = \sum_{i=1}^{n} iF_i^n = \sum_{i=1}^{n-1}\sum_{j=1}^{i} jV_{i,j}f_i f_j - \sum_{i=1}^{n-1}\sum_{j=i}^{n} iV_{i,j}f_i f_j.$$

Now, adding and subtracting some terms, changing the order of summation, and replacing $i \leftrightarrow j$ in the second term, it is easy to see that

$$\frac{dM_1^n(t)}{dt} = -\sum_{j=1}^{n-1} jV_{n,j}f_n f_j \leq 0, \tag{2.42}$$

which means that solutions to the truncated system do not conserve mass, i.e.,

$$F_1^n(t) \leq M_1^n(0), \quad \text{for any } t. \tag{2.43}$$

When the approximating system does not conserve the first moment, the global existence of the solution is established by the application of Helly's theorem (see [121]) to $\{f_i^n(t)\}$. The theorem requires us to prove that the truncated solution is of locally bounded total variation and uniformly bounded at a point. This is achieved by the application of Lemma 2.30, discussed later on. In addition to this, we make use of the refined version of De la Vallée- Poussin theorem (see [115, 119]), which ensures that if f_i^0 is in weighted L^1 space, there exists a non-negative convex function $\gamma \in G$ where

$$G := \{\gamma \in C^1([0,\infty)) \cap W^{1,\infty}_{loc}(0,\infty) : \gamma(0) = 0, \gamma'(0) \geq 0, \gamma' \text{ is concave and } \lim_{r\to\infty} \frac{\gamma(r)}{r} = \infty\},$$

satisfying certain properties given by the following proposition.

Proposition 2.28. *Let, $i, j \geq 1$ and $\gamma \in G$, then the following holds true*

$$0 \leq \gamma(i+1) - \gamma(i) \leq \frac{(3i+1)\gamma(1) + 2\gamma(i)}{(i+1)}.$$

Proof. The proof is provided in Lemma A.2 in [122]. □

Now, the results which will be useful in proving the existence are presented below.

Lemma 2.29. *Consider $T \in (0,\infty)$, $t \in [0,T]$ and $\gamma \in G$,*

$$\sum_{i=1}^{n} \gamma(i) f_i^n(t) \leq Q(T) \quad \text{and} \tag{2.44}$$

$$0 \leq \int_0^t \left(\sum_{i=1}^{n-1}\sum_{j=i}^{n} \gamma(i) V_{i,j} f_i^n(h) f_j^n(h) \right) dh \ \leq Q(T), \tag{2.45}$$

where $Q(T)$ depends only on $\gamma(1), ||f_0||$ and $M_0(0)$.

Proof. Using $g_i = \gamma(i)$ in the equation (2.41) leads to

$$\sum_{i=1}^{n}\gamma(i)f_i^n(t) = \sum_{i=1}^{n}\gamma(i)f_i^0 + \int_0^t \Big(\sum_{i=1}^{n-1}|\gamma(i+1)-\gamma(i)|\sum_{j=1}^{i} jV_{i,j}f_i^n(h)f_j^n(h) - \sum_{i=1}^{n-1}\sum_{j=i}^{n}\gamma(i)V_{i,j}f_i^n(h)f_j^n(h)\Big)dh. \tag{2.46}$$

Since $\gamma(k)$ and f_i^n for $k = i, j$ are non-negative, the above expression simplifies to

$$\sum_{i=1}^{n}\gamma(i)f_i^n(t) \le \sum_{i=1}^{n}\gamma(i)f_i^0 + \int_0^t \Big(\sum_{i=1}^{n-1}|\gamma(i+1)-\gamma(i)|\sum_{j=1}^{i} jV_{i,j}f_i^n(h)f_j^n(h)\Big)dh.$$

Using Proposition 2.28, replacing $jV_{i,j} \le (i+j)$ will give us

$$\begin{aligned}\sum_{i=1}^{n}\gamma(i)f_i^n(t) &\le \sum_{i=1}^{n}\gamma(i)f_i^0 + \int_0^t \Big(\sum_{i=1}^{n-1}\sum_{j=1}^{i}[(3i+1)\gamma(1)+2\gamma(i)]2f_i^n(h)f_j^n(h)\Big)dh \\ &\le \sum_{i=1}^{n}\gamma(i)f_i^0 + \int_0^t \Big(Q_1(T)+Q_2(T)\sum_{i=1}^{n}\gamma(i)f_i^n(h)\Big)dh,\end{aligned}$$

where $Q_1(T) = 2\gamma(1)M_0(0)(M_0(0)+3\|f_0\|)$ and $Q_2(T) = 4M_0(0)$. Finally, an application of Gronwall's inequality proves (2.44) where $Q(T) = \sum_{i=1}^{n}\gamma(i)f_i^0 + \frac{Q_1(T)}{Q_2(T)}\left(e^{TQ_2(T)}-1\right)$. Combining (2.44) and (2.46) leads to

$$\int_0^t \left(\sum_{i=1}^{n-1}\sum_{j=i}^{n}\gamma(i)V_{i,j}f_i^n(h)f_j^n(h)\right)dh \le Q(T),$$

which establishes (2.45). □

Lemma 2.30. *Consider $T \in (0,\infty)$, $i \in \mathbb{N}$. The following result holds true for a constant $\tilde{Q}(T)$ which depends on $||f_0||$ and T:*

$$\sup_{0\le t\le T}\int_0^t \left|\frac{df_i^n}{dt}\right|dh = \tilde{Q}(T). \tag{2.47}$$

Proof. Using the equations (2.36) and (2.38) provide

$$\begin{aligned}\int_0^t \left|\frac{df_i^n}{dt}\right|dh &\le \int_0^t \Big(\Big|f_{i-1}^n(h)\sum_{j=1}^{i-1} jV_{i-1,j}f_j^n(h)\Big| + \Big|f_i^n(h)\sum_{j=1}^{i} jV_{i,j}f_j^n(h)\Big| + \Big|f_i^n(h)\sum_{j=i}^{\infty}V_{i,j}f_j^n(h)\Big|\Big)dh \\ &= \int_0^t \Big(2\Big|f_i^n(h)\sum_{j=1}^{i} jV_{i,j}f_j^n(h)\Big| + \Big|f_i^n(h)\sum_{j=i}^{\infty}V_{i,j}f_j^n(h)\Big|\Big)dh \\ &\le 6||f_0||\,M_0(0)\,T.\end{aligned}$$

Also, the absolute values of the equations (2.37) and (2.39) can easily be shown bounded by $2||f_0||^2+||f_0||\,M_0(0)$ and $2||f_0||M_0(0)$, respectively, which completes the proof of the lemma. □

Existence

This section is devoted to proving the global existence of a solution for the problem (2.1)-(2.2) using the existing results for the non-conservative truncation.

Theorem 2.31. *Consider $f \in X^+$ and $V_{i,j} \leq \frac{(i+j)}{\min\{i,j\}}$ $\forall i,j$. Suppose that $f_i^n(t)$ and f_i^0 are the solution and initial condition of the non-conservative approximation (2.36)-(2.39), then there exists a solution of the discrete OHS equation (2.1)-(2.2) in $\mathbb{R}^+$.*

Proof. Let, (E,σ,M) be a measure space with $E=\mathbb{N}, \sigma=\{S : S\subset\mathbb{N}\}$ and the measure M defined by

$$M(S)=\sum_{i\in S} f_i^0.$$

Since, $f^0\in X^+$, we get $z\mapsto z\in L^1(E,\sigma,M)$. Then by the refined version of De la Vallée-Poussin theorem, there exists a function $\gamma_0\in G$ such that $z\mapsto\gamma_0(z)\in L^1(E,\sigma,M)$ meaning that

$$\sum_{i=1}^{\infty}\gamma_0(i)f_i^0<\infty. \tag{2.48}$$

Using the equation (2.43) and Lemma 2.30, the sequence is locally bounded and absolutely continuous in $(0,T)$ for every $i\geq 1$ and $T\in(0,\infty)$. Thus, by Helly's theorem, there exists a subsequence of $\{f_i^n\}$ denoted as $\{\hat{f}_i^n\}$ and a sequence $\{f_i\}$ of functions of locally bounded variation such that

$$\lim_{n\to\infty}\hat{f}_i^n=f_i(t),\quad \forall i\geq 1, t\geq 0. \tag{2.49}$$

Also, if we let $f_i^n=0$ when $i>n$,

$$||f^n(t)||=\sum_{i=1}^{n} i f_i^n(t)\leq\sum_{i=1}^{n} i f_{0i}^n\leq||f_0|| \tag{2.50}$$

which, followed by the use of (2.49) gives the non-negativity of the solution $f_i(t)$. Further, since, $\gamma_0\in G$, equation (2.48) and Lemma 2.29 yield the following

$$\sum_{i=1}^{n}\gamma_0(i)f_i^n(t)\leq Q(T)\quad\&\quad 0\leq\int_0^T\sum_{i=1}^{n-1}\sum_{j=i}^{n}\gamma_0(i)V_{i,j}f_i^n(h)f_j^n(h)dh\leq Q(T), \tag{2.51}$$

for every $n \geq 2, t \in [0,T]$ where $T \in [0,\infty)$. If we take $T \in (0,\infty)$ and $m \geq 2$, then using the above equation (2.51) and the non-negativity of $\gamma(i)$ give us

$$\sum_{i=1}^{m} \gamma_0(i) f_i^n(t) \leq Q(T) \quad \& \quad 0 \leq \int_0^T \sum_{i=1}^{m-1} \sum_{j=i}^{m} \gamma_0(i) V_{i,j} f_i^n(h) f_j^n(h) dh \leq Q(T). \tag{2.52}$$

Using (2.49), passing the limit as $n \to \infty$ in equation (2.51) and $m \to \infty$ in (2.52) yield

$$\sum_{i=1}^{\infty} \gamma_0(i) f_i(t) \leq Q(T) \quad \& \quad 0 \leq \int_0^T \sum_{i=1}^{\infty} \sum_{j=i}^{\infty} \gamma_0(i) V_{i,j} f_i(h) f_j(h) dh \leq Q(T). \tag{2.53}$$

Following on the lines of [123], the application of (2.50), (2.53), the definition of the kernel and the properties of γ_0 confirm the Definition 2.20(2) as

$$\int_0^T \sum_{j=1}^{\infty} V_{i,j} f_j(h) dh < \infty. \tag{2.54}$$

Now, by the definition of $V_{i,j}$ and Eqn. (2.50), we have

$$\sum_{j=i}^{n} V_{i,j} f_i^n f_j^n \leq 2||f_0||M_0(0).$$

Further, using (2.49) followed by the Lebesgue-dominated convergence theorem, the following holds

$$\lim_{n\to\infty} \int_0^T \Big(\sum_{j=i}^{n} V_{i,j} f_i^n f_j^n - \sum_{j=i}^{\infty} V_{i,j} f_i f_j \Big)(h) dh = 0. \tag{2.55}$$

The relations, (2.49), (2.43), (2.50) and (2.55) lead to the fulfilment of Definition 2.4(3). Consequently using (2.54), the Definition 2.4(1) follows, hence establishing the existence result for the problem (2.1)-(2.2) in $\mathbb{R}^+$. □

Density Conservation

Here, density conservation is demonstrated for the non-mass conserving truncation by the following result.

Theorem 2.32. *Let $V_{i,j} \leqslant \frac{(i+j)}{\min\{i,j\}}$ for all natural numbers i and j. Let $f = (f_i) \in X^+$ be a solution of the Safronov-Dubovski equation (2.1) satisfying all the conditions of Theorem 2.31. Additionally, if*

$$V_{n,j} \to 0 \ \text{ as } \ n \to \infty \ \text{ for every } \ j \in [1,(n-1)], \tag{2.56}$$

holds, then the solution is density conserving satisfying

$$\sum_{i=1}^{\infty} i f_i(t) = \sum_{i=1}^{\infty} i f_i(0). \tag{2.57}$$

Proof. To establish density conservation, let us consider

$$\Big|\sum_{i=1}^{\infty} i f_i(t) - \sum_{i=1}^{\infty} i f_i(0)\Big| = \Big|(\sum_{i=1}^{m} + \sum_{i=m+1}^{\infty}) i f_i(t) - (\sum_{i=1}^{m} + \sum_{i=m+1}^{\infty}) i f_i(0)\Big|. \tag{2.58}$$

Now, writing the equation (2.42) as

$$\sum_{i=1}^{n} i f_i(0) = \sum_{i=1}^{m} i f_i^n(t) + \sum_{i=m+1}^{n} i f_i^n(t) - \sum_{j=1}^{n-1} j V_{n,j} f_n^n(t) f_j^n(t). \tag{2.59}$$

Using (2.59) in (2.58), one can obtain

$$\begin{aligned}\Big|\sum_{i=1}^{\infty} i f_i(t) - \sum_{i=1}^{\infty} i f_i(0)\Big| \leq \sum_{i=1}^{m} i\Big|f_i(t) - f_i^n(t)\Big| + \sum_{i=m+1}^{\infty} i f_i(t) + \sum_{i=m+1}^{n} i f_i^n(t) + \sum_{i=n+1}^{\infty} i f_i(0) \\ + \Big|f_n^n(t) \sum_{j=1}^{n-1} j V_{n,j} f_j^n(t)\Big|. \end{aligned} \tag{2.60}$$

Before passing the limit $n \to \infty$, the boundedness of the last expression in the above equation needs to be dealt with and is given as

$$\Big|f_n^n(t) \sum_{j=1}^{n-1} j V_{n,j} f_j^n(t)\Big| \leq 2||f_0||M_0(0).$$

Further, having (2.56), (2.49) and then passing the limit in (2.60) provide

$$\lim_{n\to\infty} \Big|\sum_{i=1}^{\infty} i f_i(t) - \sum_{i=1}^{\infty} i f_i(0)\Big| \leq \sup_{i\geq m} \frac{2i f_i^n(t)\gamma_0(i)}{\gamma_0(i)}.$$

Hence, the first result given in equation (2.53), and the properties of γ_0 lead to our claim. □

Chapter 3

Theoretical Analysis of Safronov-Dubovski Coagulation Equation for Sum Kernel [1]

Let us define the Safronov-Dubovski coagulation equation for $t \in [0, \infty)$ and $i \in \mathbb{N}$ as

$$\frac{df_i(t)}{dt} = \delta_{i\geq 2} f_{i-1}(t) \sum_{j=1}^{i-1} j V_{i-1,j} f_j(t) - f_i(t) \sum_{j=1}^{i} j V_{i,j} f_j(t) - \sum_{j=i}^{\infty} V_{i,j} f_i(t) f_j(t), \tag{3.1}$$

where $\delta_P = 1$ if P is true, and zero otherwise. The Eqn.(3.1) deals with the change in concentration of i-clusters, and, consequently, the focus of our study is the qualitative behavior of $f_i(t)$ to the initial value problems defined by this system with initial conditions

$$f_i(0) = f_{0i} \geq 0. \tag{3.2}$$

In this chapter, we study the existence of mass-conserving solutions to the initial value problem (3.1)-(3.2) with rate kernels satisfying $V_{i,j} \leq (i + j)$, $\forall i, j \in \mathbb{N}$, and initial condition with finite initial mass. To establish the regularity of the solutions, we need to consider a balance between a more restrictive class of kernels $V_{i,j} \leq i^\alpha + j^\alpha$, for $\alpha \in [0, 1]$, $\forall i, j \in \mathbb{N}$, and initial condition with some finite higher moment. The uniqueness result is also established for a restrictive class of kernels, i.e., $V_{i,j} \leq C_V \min\{i^\eta, j^\eta\}, 0 \leq \eta \leq 2$, $\forall i, j \in \mathbb{N}$, $C_V \in \mathbb{R}^+$. The boundedness of a higher moment in finite time played a significant role in proving uniqueness.

[1] A considerable part of this chapter is accepted in *Portugaliae Mathematica*

Let us now define some basic notations and notions that are needed throughout. Similar to Chapter 2, the set of finite mass sequences and the norm are defined by

$$X = \{z = (z_k) : ||z|| < \infty\}, \quad \text{with} \quad ||z|| := \sum_{k=1}^{\infty} k|z_k|, \tag{3.3}$$

where $(X, \|\cdot\|)$ is a Banach space. For analysis, we often consider the non-negative cone

$$X^+ = \{f = (f_i) \in X : f_i \geq 0\}. \tag{3.4}$$

Further, we shall need to define the solution of (3.1)-(3.2) and is written as:

Definition 3.1. The solution $f = (f_i)$ of the initial value problem (3.1)–(3.2) on $[0, T)$ where $0 < T < \infty$, is a function $f : [0, T) \to X^+$ with the following properties

(a) $\forall\, i,\ f_i$ is continuous,

(b) $\int_0^t \sum_{j=1}^{\infty} V_{i,j} f_j(s) ds < \infty$ for every i and $\forall\ 0 \leq t < T$,

(c) $\forall\, i$ and $\forall\, 0 \leq t < T$

$$f_i(t) = f_{0i} + \int_0^t \Big(\delta_{i\geq 2} f_{i-1} \sum_{j=1}^{i-1} j V_{i-1,j} f_j - f_i \sum_{j=1}^{i} j V_{i,j} f_j - f_i \sum_{j=i}^{\infty} V_{i,j} f_j \Big)(s) ds, \tag{3.5}$$

where $\delta_P = 1$ if P is true, and is zero otherwise.

The chapter is organized into six sections. The Section 3.1 discusses the preliminary results required to establish the main results of the work. Section 3.2 deals with the existence of the solution and its corollary. Further, in Section 3.3, density conservation is shown for all the solutions of the given equation and the regularity result is proved in Section 3.4. Furthermore, the statement and proof of the uniqueness theorem are part of Section 3.5. Finally, in Section 3.6, the qualitative behavior of the solution in case of the non-conservative truncation is discussed.

3.1 A Finite-Dimensional Truncation

Our general approach in this work is similar to the one in the previous chapter which is considering a finite n-dimensional truncation of (3.1) and, after obtaining appropriate *a priori* estimates for its solutions, passing to the limit $n \to \infty$ and getting corresponding results for (3.1). In this section, we introduce a truncated system of the SDCE and study some useful results about the moments of its solutions. The finite n-dimensional

truncated system for the equation (3.1) that we shall consider corresponds to assuming that no particles with a size larger than n can exist initially or be formed by the dynamics. Thus, for the phase variable $f = (f_1, f_2, \ldots, f_n)$ the system is

$$\frac{df_i}{dt} = f_i^n(f), \qquad \text{for } 1 \le i \le n, \tag{3.6}$$

where

$$f_1^n(f) := -V_{1,1}f_1^2 - f_1\sum_{j=1}^{n-1} V_{1,j}f_j \tag{3.7}$$

$$f_i^n(f) := f_{i-1}\sum_{j=1}^{i-1} jV_{i-1,j}f_j - f_i\sum_{j=1}^{i} jV_{i,j}f_j - f_i\sum_{j=i}^{n-1} V_{i,j}f_j, \quad \text{for } 2 \le i \le n-1, \tag{3.8}$$

$$f_n^n(f) := f_{n-1}\sum_{j=1}^{n-1} jV_{n-1,j}f_j. \tag{3.9}$$

From what is stated above the initial conditions of interest are

$$f_i(0) = f_i^0 \ge 0, \qquad \text{for } 1 \le i \le n. \tag{3.10}$$

It can be observed here that we have truncated the last sum up to $n-1$, not n. This is done to make sure that the truncation conserves mass which will be beneficial in proving the existence result. The solutions to (3.6)–(3.10) exist and are unique which can be proved using the fact that the right side contains polynomials and the Picard-Lindelöf theorem. The solutions are also non-negative, established by the addition of positive ε to the right part of all equations. Now, if f^ε satisfies $f_i^\varepsilon(t_0) > 0$ for some $t_0 \in \mathbb{R}^+ - \{0\}$ and $f_j^\varepsilon(t_0) = 0$ for every $j \in \{1, \ldots, n\}$, then $\frac{d}{dt}f_j^\varepsilon(t_0) > 0$. Finally, taking $\varepsilon \to 0$ gives the non-negativity (see [117, Theorem III-4-5]). In the analysis of coagulation-type systems, estimating the time evolution of moments of solution is of paramount importance. For the truncated system, and in a way analogous to the r^{th} moments, we consider the quantities

$$M_g^n(t) := \sum_{i=1}^{n} g_i f_i(t), \tag{3.11}$$

where $g = (g_i)$ is a non-negative sequence. The following result on the evolution of M_g^n will be relevant:

Lemma 3.2. *Let $f = (f_i)_{i\in\{1,\ldots,n\}}$ be a solution of (3.6)–(3.10) defined in an open interval I containing 0. Let $g = (g_i)$ be a real sequence. Then*

$$\frac{dM_g^n}{dt} = \sum_{i=1}^{n-1}\sum_{j=i}^{n-1}(ig_{j+1} - ig_j - g_i)V_{i,j}f_if_j. \tag{3.12}$$

Proof. The proof follows on the same lines of proof of the Eq. (2.5). □

Now, for $g_p := (i^p)$, consider the simplified notation $M_p^n := M_{g_p}^n$. It is clear from (3.12) that, for all $t \in I$,

$$\frac{dM_0^n(t)}{dt} \leq 0 \tag{3.13}$$

and thus $M_0^n(t) \leq M_0^n(0)$, for all $t \in I \cap \{t \geq 0\}$. This *a priori* bound implies that non-negative solutions of the truncated systems (3.6)–(3.9) are globally defined forward in time, i.e., $I \supset [0, +\infty)$. Taking $g = g_1$ in (3.12), we immediately conclude that, for all t

$$\frac{dM_1^n(t)}{dt} = 0, \tag{3.14}$$

which means that solutions to the truncated system conserve mass. For further reference, this is stated in the next lemma.

Lemma 3.3. *Solutions to Cauchy problems for the truncated systems (3.6)–(3.9) are globally defined forward in time and mass conserving, i.e.,*

$$M_1^n(t) = M_1^n(0), \quad \forall t \geq 0. \tag{3.15}$$

For the existence proof let us consider $x_m^n(t)$ defined as in [118] by

$$x_m^n(t) := \sum_{i=m}^{n} i f_i^n(t), \tag{3.16}$$

where $f^n = (f_1^n, \ldots, f_n^n)$ is a solution of the n-dimensional truncated system (3.6)–(3.9). From these expressions, we immediately obtain

$$\frac{dx_m^n(t)}{dt} = \Big(\sum_{i=m}^{n-1} \sum_{j=1}^{i} j V_{i,j} f_i^n f_j^n + m f_{m-1}^n \sum_{j=1}^{m-1} j V_{m-1,j} f_j^n - \sum_{i=m}^{n-1} \sum_{j=i}^{n-1} i V_{i,j} f_i^n f_j^n \Big)(t). \tag{3.17}$$

Assume now $2m < n$ and consider the function $q_m^n(\cdot)$ defined by

$$q_m^n(t) := \sum_{i=m}^{2m} i f_i^n + 2m \sum_{i=2m+1}^{n} f_i^n, \tag{3.18}$$

where, again $f^n = (f_1^n, \ldots, f_n^n)$ is a solution of the n-dimensional truncated system. Then, after a few algebraic manipulations, we get

$$\begin{aligned}\frac{dq_m^n(t)}{dt} &= \sum_{i=m}^{2m} i f_i^n + 2m \sum_{i=2m+1}^{n} f_i^n \\ &= m f_{m-1}^n(t) \sum_{j=1}^{m-1} j V_{m-1,j} f_j^n(t) + \sum_{i=m}^{2m-1} f_i^n(t) \sum_{j=1}^{i} j V_{i,j} f_j^n(t) - \\ &\quad - \sum_{i=m}^{2m} \sum_{j=i}^{n-1} i f_i^n(t) V_{i,j} f_j^n(t) - 2m \sum_{i=2m+1}^{n-1} \sum_{j=i}^{n-1} V_{i,j} f_i^n(t) f_j^n(t). \end{aligned} \tag{3.19}$$

Finally, so that we can take $n \to \infty$ (or, eventually, only on a subsequence $n_k \to \infty$), we make use of the following lemma.

Lemma 3.4. *Take $f_0 = (f_{0i}) \in X^+$ and, for each $n \in \mathbb{N}$, consider the point $f_0^n \in X^+$ defined by $f_0^n = (f_{01}, f_{02}, \ldots, f_{0n}, 0, 0, \ldots)$ and let it be identified with the point of $\mathbb{R}^n$ obtained by discarding the j^{th} components, for $j > n$. Let f^n be the solution of the n-dimensional truncated system (3.6)–(3.9) when $V_{i,j} \leq (i + j)$ with initial condition $f^n(0) = f_0^n$ such that (3.15) holds, then f^n is relatively compact in $C([0, T])$.*

Proof. Using the truncated system (3.7-3.9) and mass conservation of this system (see (3.15)), it can be shown that $\exists$ a constant $C > 0$ such that $\forall\ n \geq i \geq 1$,

$$\sup_{t \geq 0} \left(f_i^n(t) + \left| \frac{df_i^n(t)}{dt} \right| \right) \leq C M_1(0)^2.$$

Thus, Ascoli theorem gives the intended result. □

Now, we have gathered all the required information to proceed with the existence results.

3.2 Existence Result for the Cauchy Problem

We can now prove the existence of global solutions for the Cauchy problem (3.1)–(3.2).

Theorem 3.5. *Let, $V_{i,j}$ be nonnegative, symmetric for the exchange of i with j, and satisfy $V_{i,j} \leq (i+j)$, $\forall\ i, j$, and let $f_0 = (f_{0i}) \in X^+$, $M_1(0) < \infty$. Then, $\exists$ a non-negative solution of (3.1)–(3.2) defined globally.*

Proof. Let n be an arbitrarily fixed positive integer and let f_0^n be defined as in the statement of Lemma 3.4. As we stated above, following (3.10), the initial value problem

(3.6)–(3.10) has a unique solution, $f^n = (f_i^n)_{1\le i\le n}$, which is globally defined, non-negative and, by Lemma 3.3, density conserving. By defining $f_i^n(t) = 0$ when $i > n$ we can consider $f^n(t)$ as an element of X^+ for all t, and thus

$$\|f^n(t)\| = \sum_{i=1}^{\infty} i f_i^n(t) = \sum_{i=1}^{n} i f_i^n(t) = \sum_{i=1}^{n} i f_{0i}^n = \sum_{i=1}^{n} i f_{0i} \le \sum_{i=1}^{\infty} i f_{0i} = \|f_0\|. \tag{3.20}$$

By Lemma 3.4 and (3.15) for each i, $\exists$ a subsequence of f^n (not relabelled) & a function $f_i : [0,\infty) \to \mathbb{R}$, which are of bounded variation on each subset of $[0,\infty)$, such that $f_i^n(t)$ converges to $f_i(t)$ as n approaches ∞, for every $t \in \mathbb{R}^+$. Thus $\forall\ t \ge 0$,

$$f_i(t) \ge 0 \quad \text{and} \quad ||f(t)|| \le ||f_0||. \tag{3.21}$$

Our goal is to prove that this limit function f is a mild solution of the initial value problem (3.1)–(3.2), i.e., fulfills the conditions in Definition 3.1. This will be done by passing to the limit $n \to \infty$ in the integrated version of the truncated problem (3.6)–(3.10), namely

$$f_i^n(t) = f_{0i} + \int_0^t \left(f_{i-1}^n(s) \sum_{j=1}^{i-1} j V_{i-1,j} f_j^n(s) - f_i^n(s) \sum_{j=1}^{i} j V_{i,j} f_j^n(s) - f_i^n(s) \sum_{j=i}^{n-1} V_{i,j} f_j^n(s) \right) ds. \tag{3.22}$$

To do this, and also to satisfy condition (b) in Definition 3.1, we need to prove that, for every fixed $i \in \mathbb{N}$, $T \ge 0$, and $\varepsilon > 0$, there exists m and n_0, with $n_0 > m \ge i$, such that, for all $n > n_0$,

$$\int_0^T x_m^n(t)dt \le \varepsilon, \tag{3.23}$$

where x_m^n is defined in (3.16). This can be achieved by integrating (3.17) in $[0,t]$ and using (3.19) as

$$\begin{aligned} x_m^n(t) &= x_m^n(0) + \int_0^t \Bigg(\sum_{i=m}^{n-1} \sum_{j=1}^{i} j V_{i,j} f_i^n(s) f_j^n(s) + m f_{m-1}^n \sum_{j=1}^{m-1} j V_{m-1,j} f_j^n - \\ &\qquad - \sum_{i=m}^{n-1} \sum_{j=i}^{n-1} i V_{i,j} f_i^n(s) f_j^n(s) \Bigg) ds \\ &= x_m^n(0) + q_m^n(t) - q_m^n(0) + \int_0^t \Bigg(f_{2m}^n(s) \sum_{j=1}^{2m} j V_{2m,j} f_j^n(s) + \sum_{i=2m+1}^{n-1} \sum_{j=1}^{i} j V_{i,j} f_i^n(s) f_j^n(s) - \\ &\qquad - \sum_{i=2m+1}^{n-1} \sum_{j=i}^{n-1} i V_{i,j} f_i^n(s) f_j^n(s) + 2m \sum_{2m+1}^{n-1} \sum_{j=i}^{n-1} V_{i,j} f_i^n(s) f_j^n(s) \Bigg) ds. \end{aligned}$$

Some algebraic manipulations of the second double sum above provide

$$\sum_{i=2m+1}^{n-1}\sum_{j=1}^{i} jV_{i,j}f_i^n(s)f_j^n(s) = \sum_{i=2m+1}^{n-1}\sum_{j=1}^{2m} jV_{i,j}f_i^n(s)f_j^n(s) + \sum_{i=2m+1}^{n-1}\sum_{j=i}^{n-1} iV_{j,i}f_j^n(s)f_i^n(s).$$

Substituting this into the above expression for $x_m^n(t)$ gives

$$x_m^n(t) = x_m^n(0) + q_m^n(t) - q_m^n(0) + \int_0^t \Bigg(\sum_{i=2m}^{n-1}\sum_{j=1}^{2m} jV_{i,j}f_i^n(s)f_j^n(s) + \\ + 2m\sum_{i=2m+1}^{n-1}\sum_{j=i}^{n-1} V_{i,j}f_i^n(s)f_j^n(s)\Bigg)ds. \quad (3.24)$$

By (3.20), (3.21), and the pointwise convergence of f_i^n to f_i we conclude that, for all $t \in [0,T]$, $\forall \varepsilon > 0, \forall p > \frac{4\|f_0\|}{\varepsilon}$, $\exists n_0$ such that $\forall n > n_0$,

$$\sum_{i=1}^{\infty}|f_i^n(t) - f_i(t)| = \sum_{i=1}^{p-1}|f_i^n(t) - f_i(t)| + \sum_{i=p}^{\infty}|f_i^n(t) - f_i(t)| < \frac{\varepsilon}{2} + \frac{2}{p}\|f_0\| < \varepsilon,$$

that enables us to take $n \to \infty$ in the definition of $q_m^n(t)$ in (3.18) and yields

$$q_m^n(t)[n\to\infty] \sum_{i=m}^{2m} if_i(t) + 2m\sum_{i=2m+1}^{\infty} f_i(t) =: q_m(t) \le \sum_{i=m}^{\infty} if_i(t), \quad (3.25)$$

and so $\lim_{m\to\infty} q_m(t) = 0$ and $|q_m(t)| \le \|f_0\|$, for all $t \in [0,T]$. Therefore, $\forall \varepsilon > 0$, $\exists M, n_0$ with $n_0 > M$, such that, $\forall m > M$, $n > n_0$ and $n \ge 2m+1$,

$$q_m^n(t) \le \frac{1}{3}\varepsilon, \quad (3.26)$$

and

$$q_m^n(0) \le \frac{1}{3}\varepsilon. \quad (3.27)$$

By (3.26), (3.27), and using the assumption $V_{i,j} \le (i+j)$ we can estimate the right-hand side of (3.24) as follows (redefining)

$$\begin{aligned} x_m^n(t) &\le \varepsilon + \int_0^t \Bigg(\sum_{i=2m}^{n-1}\sum_{j=1}^{2m} j(i+j)f_i^n(s)f_j^n(s) + 2m\sum_{i=2m+1}^{n-1}\sum_{j=i}^{n-1}(i+j)f_i^n(s)f_j^n(s)\Bigg)ds \\ &\le \varepsilon + \int_0^t \Bigg(2\sum_{i=2m}^{n-1}\sum_{j=1}^{2m} ijf_i^n(s)f_j^n(s) + 4m\sum_{i=2m+1}^{n-1}\sum_{j=i}^{n-1} if_i^n(s)f_j^n(s)\Bigg)ds \\ &\le \varepsilon + \int_0^t \Bigg(2\sum_{i=m}^{n} if_i^n(s)\sum_{j=1}^{n} jf_j^n(s) + 4\sum_{i=m}^{n} if_i^n(s)\sum_{j=i}^{n} jf_j^n(s)\Bigg)ds \\ &\le \varepsilon + 6\|f_0\|\int_0^t x_m^n(s)ds. \end{aligned}$$

Hence, thanks to Gronwall's lemma, we get, for all $t \in [0, T]$,

$$x_m^n(t) \leq k_1 \varepsilon \tag{3.28}$$

where $k_1 = e^{6||f_0||T}$, which implies that $\forall \varepsilon > 0, \exists M, n_0$ with $n_0 > M$, such that, $\forall m > M$, $n > n_0$ and $n \geq 2m + 1$,

$$\int_0^t x_m^n(s)ds \leq \varepsilon k_1 T, \quad \text{for all } t \in [0, T]. \tag{3.29}$$

Since, $f_i^n(t)$ is point-wise convergent to $f_i(t)$, the above expression entails that, for all $\varepsilon > 0$, there exists M such that, for all $m > M$, we have

$$\int_0^T \sum_{i=m}^{\infty} i f_i(t)dt \leq \varepsilon.$$

Hence, when $V_{i,j} \leq (i + j)$ for all $i \geq 1$,

$$\int_0^T \sum_{j=1}^{\infty} V_{i,j} f_j(t)dt < \infty, \tag{3.30}$$

thus establishing (b) in Definition 3.1. Now, for every fixed i, take $n > i$ sufficiently large and for any ℓ such that $i < \ell < n - 1$, write (3.22) as

$$\begin{aligned}\left| f_i^n(t) - f_i(0) - \int_0^t \Big(f_{i-1}^n(s) \sum_{j=1}^{i-1} j V_{i-1,j} f_j^n - f_i^n(s) \sum_{j=1}^{i} j V_{i,j} f_j^n(s) - f_i^n(s) \sum_{j=i}^{\ell} V_{i,j} f_j^n(s) \Big) ds \right| \\ = f_i^n(s) \int_0^t \sum_{j=\ell+1}^{n-1} V_{i,j} f_j^n(s)ds \;\leq\; 2\|f_0\| \int_0^t x_{\ell+1}^n(s)ds.\end{aligned}$$

Thus, from (3.29), for all $\varepsilon > 0$, there exists M such that, for all $\ell + 1 > M$ and all n sufficiently large, the right-hand side can be bounded above by $2\varepsilon\|f_0\|k_1 T$. Considering that each sum on the left-hand side has a fixed and finite number of terms, that $f_j^n(s) \to f_j(s)$ pointwise as $n \to \infty$, and each of the three terms inside the integral is bounded by $2\|f_0\|^2$, we can use the dominated convergence theorem and take $n \to \infty$ to conclude that, for every $\varepsilon > 0$, there exists M such that, for all $\ell \geq M$, we have

$$\begin{aligned}\left| f_i(t) - f_i(0) - \int_0^t \Big(f_{i-1}(s) \sum_{j=1}^{i-1} j V_{i-1,j} f_j - f_i(s) \sum_{j=1}^{i} j V_{i,j} f_j(s) - f_i(s) \sum_{j=i}^{\ell} V_{i,j} f_j(s) \Big) ds \right| \\ \leq 2\varepsilon\|f_0\|k_1 T.\end{aligned}$$

Hence, by the arbitrariness of ε, we can let $\ell \to \infty$ and conclude that $f = (f_i)$ satisfy (3.5), which completes the proof. □

Next, we establish that the subsequence f^{n_k} of solutions to the truncated system which converges to the solution f of (3.1)-(3.2) actually does so in the strong topology of X, uniformly for t in compact subsets of $[0,\infty)$.

Corollary 3.6. *Let f^{n_k} be the pointwise convergent subsequence of solutions to (3.8 – 3.10). Then, $f^{n_k} \to f$ in X uniformly on compact subsets of $[0,\infty)$.*

Proof. To prove this, we prove that $f_i^{n_k}(t) \to f_i(t)$ for each i uniformly on the compact subsets of $[0,\infty)$. For this, let n_k be n and for each $I < m$

$$z_m^n(t) := e^{-t}\left[M_1^n(t) - \sum_{i=1}^{m-1} i f_i^n(t) + (2m+2)M_1^n(0)^2\right]. \tag{3.31}$$

Now, differentiating (3.31) gives

$$\frac{dz_m^n(t)}{dt} = e^{-t}\left[\frac{dM_1^n(t)}{dt} - \sum_{i=1}^{m-1} i\frac{df_i^n(t)}{dt}\right] - e^{-t}\left[M_1^n(t) - \sum_{i=1}^{m-1} i f_i^n(t) + (2m+2)M_1^n(0)^2\right] \tag{3.32}$$

where

$$\frac{d}{dt}\sum_{i=1}^{m-1} i f_i^n(t) = \sum_{i=1}^{m-2}\sum_{j=1}^{i} jV_{i,j} f_i^n f_j^n - \sum_{i=1}^{m-1}\sum_{j=i}^{n-1} iV_{i,j} f_i^n f_j^n - (m-1)f_{m-1}^n \sum_{j=1}^{m-1} jV_{m-1,j} f_j^n. \tag{3.33}$$

Using the above expression, Lemma 3.3 and $V_{i,j} \le (i+j)\ \forall\ i,j$ in (3.32), one can obtain

$$\frac{dz_m^n(t)}{dt} \le e^{-t}\left[\sum_{i=1}^{m-1}\sum_{j=i}^{n-1} j(i+j) f_i^n f_j^n + (m-1)f_{m-1}^n \sum_{j=1}^{m-1} j(m-1+j) f_j^n - 2M_1^n(0)^2 - 2mM_1^n(0)^2\right].$$

Some simplifications guarantee that

$$\frac{dz_m^n(t)}{dt} \le 0, \quad n \ge m,\ \ t \in [0,T].$$

Hence, $z_m^n(t) \to z_m(t)$ uniformly on compact subsets of $[0,T)$ where

$$z_m(t) := e^{-t}\left[M_1(t) - \sum_{i=1}^{m-1} i f_i(t) + (2m+2)M_1(0)^2\right].$$

Let, $K \subset [0,\infty)$ be compact and $t_n \to t$ in K, then

$$\lim_{n\to\infty} \|f^n(t_n)\| = \lim_{n\to\infty} \sum_{i=1}^{\infty} i f_i^n(t_n) = \sum_{i=1}^{\infty} i f_i(t) = \|f(t)\|$$

which ensures that $\|f^n\| \to \|f\|$ in $C(K,X)$. □

3.3 All Solutions Conserve Density

In this section, we prove that under the assumption on the rate coefficients we have been using, all solutions of (3.1)-(3.2) conserve density.

Let $f = (f_i) \in X^+$ be a solution of (3.5) in $[0, T]$. Multiplying equation (3.5) by g_i and adding from $i = 1$ to n, we have, after some algebraic manipulations, for all $t \in [0, T]$,

$$\sum_{i=1}^{n} g_i f_i(t) - \sum_{i=1}^{n} g_i f_{0\,i} = \int_0^t \sum_{i=1}^{n}\sum_{j=i}^{n} (jg_{i+1} - jg_i - g_j) V_{i,j} f_i(s) f_j(s) ds$$
$$- \int_0^t \sum_{j=1}^{n}\sum_{i=n+1}^{\infty} g_j V_{i,j} f_i(s) f_j(s) ds - \int_0^t g_{n+1} f_n(s) \sum_{j=1}^{n} j V_{n,j} f_j(s) ds. \quad (3.34)$$

We start by observing that, taking $g_i \equiv i$ in (3.34) concludes that

$$\sum_{i=1}^{n} i f_i(t) \leq \sum_{i=1}^{n} i f_{0\,i} \leq \|f_0\|,$$

and, as this inequality is valid for all n, we can take the limit as $n \to \infty$ and conclude the *a priori* bound $\|f(t)\| \leq \|f_0\|$. We now use (3.34) to prove that, under the assumed conditions on $V_{i,j}$, all solutions conserve density.

Theorem 3.7. *Let $V_{i,j} \leq (i + j)$ for all i and j. Let $f = (f_i) \in X^+$ be a solution of the Safronov-Dubovski equation (3.1). Then the total density of f is constant.*

Proof. Let $A \in \mathbb{N}$ be fixed, and consider the sequence $(g_i^A) \in \ell^\infty$ defined by

$$g_i^A = i \wedge A, \quad (3.35)$$

where $a \wedge b = \min\{a, b\}$. Then

$$jg_{i+1}^A - jg_i^A - g_j^A = \begin{cases} -A & \text{on } \{(i,j) : A \leq i \leq j \leq n\}, \\ 0 & \text{on } \{(i,j) : 1 \leq i \leq A-1 \text{ and } i \leq j \leq n\}, \end{cases}$$

and (3.34) becomes, for $n > A$,

$$\sum_{i=1}^{n} g_i^A f_i(t) - \sum_{i=1}^{n} g_i^A f_{0\,i} = \tag{3.36}$$

$$= -\int_0^t A \sum_{j=A}^{n} \sum_{i=A}^{j} V_{i,j} f_i(s) f_j(s) ds \tag{3.37}$$

$$-\int_0^t \left(\sum_{j=1}^{A} \sum_{i=n+1}^{\infty} j V_{i,j} f_i(s) f_j(s) + A \sum_{j=A+1}^{n} \sum_{i=n+1}^{\infty} V_{i,j} f_i(s) f_j(s) \right) ds \tag{3.38}$$

$$-\int_0^t A f_n(s) \sum_{j=1}^{n} j V_{n,j} f_j(s) ds. \tag{3.39}$$

We first estimate the term in (3.37):

$$\begin{aligned} A \sum_{j=A}^{n} \sum_{i=A}^{j} V_{i,j} f_i f_j &\le A \sum_{j=A}^{n} f_j \sum_{i=A}^{j} i f_i + A \sum_{j=A}^{n} j f_j \sum_{i=A}^{j} f_i \\ &= A \sum_{j=A}^{n} \frac{1}{j} j f_j \sum_{i=A}^{j} i f_i + A \sum_{j=A}^{n} j f_j \sum_{i=A}^{j} \frac{1}{i} i f_i \\ &\le 2 \sum_{j=A}^{n} j f_j \sum_{i=A}^{n} i f_i \\ &\le 2 \sum_{j=A}^{\infty} j f_j \sum_{i=A}^{\infty} i f_i. \end{aligned} \tag{3.40}$$

Thus, $f \in X^+$ implies that (3.40) converges to zero as $A \to \infty$. Furthermore, since (3.40) is bounded above by $2\|f_0\|^2$, the dominated convergence theorem implies that, for all $\varepsilon > 0$ there exists A_0 such that, for all $n > A \ge A_0$ the absolute value of (3.37) is smaller than $\frac{\varepsilon}{5}$. Consider now (3.38). For the first double sum, observe that for $n > A$,

$$\begin{aligned} \sum_{j=1}^{A} \sum_{i=n+1}^{\infty} j V_{i,j} f_i f_j &\le \sum_{j=1}^{A} j f_j \sum_{i=n+1}^{\infty} i f_i + \sum_{j=1}^{A} j^2 f_j \sum_{i=n+1}^{\infty} f_i \\ &\le \|f_0\| \sum_{i=n+1}^{\infty} i f_i + \sum_{j=1}^{A} j^2 f_j \frac{1}{n+1} \sum_{i=n+1}^{\infty} i f_i \\ &\le \|f_0\| \sum_{i=n+1}^{\infty} i f_i + \frac{A}{A+1} \sum_{j=1}^{A} j f_j \sum_{i=n+1}^{\infty} i f_i \\ &\le \|f_0\| \sum_{i=n+1}^{\infty} i f_i + \|f_0\| \sum_{i=n+1}^{\infty} i f_i \\ &\le 2\|f_0\| \sum_{i=n+1}^{\infty} i f_i. \end{aligned} \tag{3.41}$$

For the second double sum in (3.38) we have a similar estimate:

$$\begin{aligned} A\sum_{j=A+1}^{n}\sum_{i=n+1}^{\infty} V_{i,j}f_if_j &\le A\sum_{j=A+1}^{n} f_j\sum_{i=n+1}^{\infty} if_i + A\sum_{j=A+1}^{n} jf_j\sum_{i=n+1}^{\infty} f_i \\ &\le \frac{A}{A+1}\sum_{j=A+1}^{n} jf_j\sum_{i=n+1}^{\infty} if_i + A\sum_{j=A+1}^{n} jf_j\frac{1}{n+1}\sum_{i=n+1}^{\infty} if_i \\ &\le \|f_0\|\sum_{i=n+1}^{\infty} if_i + \frac{A}{n+1}\|f_0\|\sum_{i=n+1}^{\infty} if_i \\ &\le 2\|f_0\|\sum_{i=n+1}^{\infty} if_i. \end{aligned} \tag{3.42}$$

Thus, by (3.41) and (3.42), we conclude that the integrand function in (3.38) is bounded by $4\|f_0\|^2$ and converges pointwise to zero as $n\to\infty$, for each fixed A. Hence, again by the dominated convergence theorem, we conclude that, as previously, for all $\varepsilon>0$, there exists A_0 such that, for all $n>A_0$, the absolute value of the integral (3.38) is smaller than $\frac{\varepsilon}{5}$. Finally, let us consider (3.39)

$$\begin{aligned} Af_n\sum_{j=1}^{n} jV_{n,j}f_j &\le Af_n\sum_{j=1}^{n} j(n+j)f_j \\ &\le 2Anf_n\sum_{j=1}^{n} jf_j \\ &\le 2\|f_0\|Anf_n. \end{aligned} \tag{3.43}$$

Clearly, for each fixed A, (3.43) converges to zero as $n\to\infty$ and it is bounded above by $A\|f_0\|^2$, and so the dominated convergence theorem implies that, for every $\varepsilon>0$, there exits $A_0=A_0(\varepsilon)$ such that, for any fixed $A>A_0$, there exists $n_0=n_0(\varepsilon,A)$ such that, for all $n>n_0\vee A$, the absolute value of (3.39) is smaller than $\frac{\varepsilon}{5}$.

To estimate (3.36) observe that, for every $n>A$, we can write

$$\left|\sum_{i=1}^{n} g_i^A f_i(t) - \sum_{i=1}^{n} g_i^A f_{0\,i}\right| \ge \left|\sum_{i=1}^{A} if_i(t) - \sum_{i=1}^{A} if_{0\,i}\right| - A\left|\sum_{i=A+1}^{n} f_i(t) - \sum_{i=A+1}^{n} f_{0\,i}\right|,$$

and thus,

$$\left|\sum_{i=1}^{A} if_i(t) - \sum_{i=1}^{A} if_{0\,i}\right| \le \sum_{i=A+1}^{\infty} if_i(t) + \sum_{i=A+1}^{\infty} if_{0\,i} + \left|\sum_{i=1}^{n} g_i^A f_i(t) - \sum_{i=1}^{n} g_i^A f_{0\,i}\right|. \tag{3.44}$$

Now, for every $\varepsilon>0$ there exists A_0 such that, for all $A>A_0$, each of the first two sums in the right-hand side of (3.44) can be made smaller than $\frac{\varepsilon}{5}$, and since the estimates of (3.37)-(3.39) obtained previously allow us to have the last term in the right-hand side

of (3.44) is smaller than $\frac{3}{5}\varepsilon$, we conclude that

$$\forall \varepsilon > 0,\ \exists A_0 : \forall A > A_0,\ \left| \sum_{i=1}^{A} i f_i(t) - \sum_{i=1}^{A} i f_{0\,i} \right| < \varepsilon,$$

which proves the result. □

3.4 Differentiability

This section is devoted to proving that the solution of the S-D model is first-order differentiable if the rate coefficients satisfy $V_{i,j} \leq i^\alpha + j^\alpha$ for $\alpha \in [0,1]$. This requires the boundedness of $(\alpha+1)$-moments of the solutions and an invariance result, which are proved below in Lemma 3.8 and Theorem 3.9, respectively.

Lemma 3.8. *Let the non-negative kernel $V_{i,j}$ satisfy $V_{i,j} \leq i^\alpha + j^\alpha$, for all $i, j \geq 1$, and for some fixed $0 \leq \alpha \leq 1$. For any $T \in (0,\infty)$, let f be a solution to (3.1)-(3.2) in $[0,T]$ with initial condition $f_0 \in X^+$. If the $(\alpha+1)$-moment of f_0, $M_{1+\alpha}(f_0)$, is bounded, then the $(\alpha+1)$-moment of $f(t)$ is also bounded for all $t \in [0,T]$.*

Proof. Let $f = (f_i)$ be a solution of (3.1)-(3.2) in $[0,T]$ with initial condition f_0. By (3.5) adding the components from $i = 1$ to n, we have, for all $t \in [0,T]$,

$$\sum_{i=1}^{n} i^{1+\alpha} f_i(t) + \int_0^t \sum_{i=1}^{n} \sum_{j=i}^{\infty} i^{i+\alpha} V_{i,j} f_i(s) f_j(s) ds + \int_0^t (n+1)^{1+\alpha} f_n(s) \sum_{j=1}^{n} j V_{n,j} f_j(s) ds$$
$$= \sum_{i=1}^{n} i^{1+\alpha} f_{0\,i} + \int_0^t \sum_{i=1}^{n} \sum_{j=1}^{i} (j(i+1)^{1+\alpha} - j i^{1+\alpha}) V_{i,j} f_i(s) f_j(s) ds. \quad (3.45)$$

Due to the non-negativity of solutions, (3.45) implies that

$$\sum_{i=1}^{n} i^{1+\alpha} f_i(t) \leq \sum_{i=1}^{n} i^{1+\alpha} f_{0\,i} + \int_0^t \sum_{i=1}^{n} \sum_{j=1}^{i} (j(i+1)^{1+\alpha} - j i^{1+\alpha}) V_{i,j} f_i(s) f_j(s) ds. \quad (3.46)$$

Since $\alpha \in [0,1]$ and $i \geq 1$ we have $(i+1)^{1+\alpha} - i^{1+\alpha} \leq (1+\alpha) i^\alpha + \frac{(1+\alpha)\alpha}{2!}$, and so,

$$j((i+1)^{1+\alpha} - i^{1+\alpha}) V_{i,j} \leq (1+\alpha) j i^{2\alpha} + (1+\alpha) j^{1+\alpha} i^\alpha + \frac{(1+\alpha)\alpha}{2!} j i^\alpha + \frac{(1+\alpha)\alpha}{2!} j^{1+\alpha},$$

from where, using $\sum_{i=1}^{n} i f_i(s) \leq \|f_0\|$, we obtain

$$\begin{aligned}
&\sum_{i=1}^{n}\sum_{j=1}^{i}(j(i+1)^{1+\alpha} - ji^{1+\alpha})V_{i,j}f_i(s)f_j(s) \\
&\leq \frac{1}{2}(1+\alpha)\alpha\|f_0\|^2 + \frac{1}{2}(1+\alpha)(4+\alpha)\|f_0\|\sum_{i=1}^{n} i^{1+\alpha}f_i(s) \\
&\leq \|f_0\|^2 + 5\|f_0\|\sum_{i=1}^{n} i^{1+\alpha}f_i(s)
\end{aligned}$$

which, upon substitution in (3.46), gives

$$\sum_{i=1}^{n} i^{1+\alpha}f_i(t) \leq \sum_{i=1}^{n} i^{1+\alpha}f_{0\,i} + \|f_0\|^2 T + \int_0^t 5\|f_0\|\sum_{i=1}^{n} i^{1+\alpha}f_i(s)ds.$$

Hence, by Gronwall's lemma, we conclude that, for all $t \in [0,T]$ and $n \geq 1$,

$$\begin{aligned}
\sum_{i=1}^{n} i^{1+\alpha}f_i(t) &\leq \Big(\sum_{i=1}^{n} i^{1+\alpha}f_{0\,i} + T\|f_0\|^2\Big)e^{5\|f_0\|t} \\
&\leq (M_{1+\alpha}(f_0) + T\|f_0\|^2)e^{5\|f_0\|t},
\end{aligned} \tag{3.47}$$

where the inequality (3.47) is due to the assumption about the boundedness of the $(1+\alpha)$-moment of the initial condition f_0. Since the right-hand side of (3.47) does not depend on n we conclude that the same is valid in the limit $n \to \infty$, which proves the result. □

An important result regarding the evaluation of the higher moments of the solution is analyzed here.

Theorem 3.9. *Assume (g_i) be a real-valued non-negative sequence such that $g_i = O(i^{\alpha+1})$. Let f be a solution of (3.1) when $V_{i,j} \leq i^{\alpha}+j^{\alpha}$, $\alpha \in [0,1]$ under the assumption that $M_{\alpha+1}(f_0)$ is bounded on some interval $[0,T)$, for $0 < T \leq \infty$. Let $0 \leq t_1 < t_2 < T$. If the following hypotheses hold*

$(H1)$

$$\int_{t_1}^{t_2}\sum_{i=1}^{\infty}\sum_{j=1}^{i} j(g_{i+1}-g_i)V_{i,j}f_j(s)f_i(s)ds < \infty \tag{3.48}$$

$(H2)$

$$\int_{t_1}^{t_2}\sum_{i=1}^{\infty}\sum_{j=1}^{i} g_j V_{i,j}f_i(s)f_j(s)ds < \infty \tag{3.49}$$

then, for every $m \in \mathbb{N}$,

$$\begin{aligned}\sum_{i=m}^{\infty} g_i f_i(t_2) - \sum_{i=m}^{\infty} g_i f_i(t_1) = &\int_{t_1}^{t_2} \sum_{i=m}^{\infty} \sum_{j=1}^{i} (jg_{i+1} - jg_i - g_j) V_{i,j} f_i(s) f_j(s) ds \\ &+ \delta_{m\geq 2} \int_{t_1}^{t_2} \sum_{i=m}^{\infty} \sum_{j=1}^{m-1} g_j V_{i,j} f_i(s) f_j(s) ds \\ &+ \delta_{m\geq 2} \int_{t_1}^{t_2} g_m f_{m-1}(s) \sum_{j=1}^{m-1} j V_{m-1,j} f_j(s) ds\end{aligned} \tag{3.50}$$

where $\delta_P = 1$ *if* P *holds, and is equal to zero otherwise.*

Proof. Take positive integers $m < n$. Multiplying each equation in (3.5) by g_i and summing over i from m to n, we obtain

$$\sum_{i=m}^{n} g_i f_i(t_2) - \sum_{i=m}^{n} g_i f_i(t_1) = \int_{t_1}^{t_2} \sum_{i=m}^{n} \sum_{j=1}^{i} (jg_{i+1} - jg_i - g_j) V_{i,j} f_i(s) f_j(s) ds \tag{3.51}$$

$$+ \delta_{m\geq 2} \int_{t_1}^{t_2} \sum_{i=m}^{n} \sum_{j=1}^{m-1} g_j V_{i,j} f_i(s) f_j(s) ds \tag{3.52}$$

$$+ \delta_{m\geq 2} \int_{t_1}^{t_2} g_m f_{m-1}(s) \sum_{j=1}^{m-1} j V_{m-1,j} f_j(s) ds \tag{3.53}$$

$$- \int_{t_1}^{t_2} \sum_{i=m}^{n} \sum_{j=n+1}^{\infty} g_i V_{i,j} f_i(s) f_j(s) ds \tag{3.54}$$

$$- \int_{t_1}^{t_2} g_{n+1} f_n(s) \sum_{j=1}^{n} j V_{n,j} f_j(s) ds. \tag{3.55}$$

We need to prove that, as $n \to \infty$, the integrals in (3.54) and (3.55) converge to zero, and the other integrals converge to the corresponding ones on the right-hand side of (3.50).

Using $(H2)$ by interchanging the order of summation and replacing i for j and then following (a) in Definition 3.1, one can obtain

$$\lim_{n\to\infty} \int_{t_1}^{t_2} \sum_{i=m}^{n} \sum_{j=n+1}^{\infty} g_i V_{i,j} f_i(s) f_j(s) ds = 0 \tag{3.56}$$

which proves the convergence of (3.54) to zero. With $g_i = 1$ we can write (3.51)-(3.55) as follows

$$\sum_{i=m}^{n} f_i(t_2) - \sum_{i=m}^{n} f_i(t_1) = \int_{t_1}^{t_2} \sum_{i=m}^{n} \sum_{j=1}^{i} (-V_{i,j} f_i(s) f_j(s)) ds + \delta_{m\geq 2} \int_{t_1}^{t_2} \sum_{i=m}^{n} \sum_{j=1}^{m-1} V_{i,j} f_i(s) f_j(s) ds$$
$$+ \delta_{m\geq 2} \int_{t_1}^{t_2} f_{m-1}(s) \sum_{j=1}^{m-1} j V_{m-1,j} f_j(s) ds - \int_{t_1}^{t_2} \sum_{i=m}^{n} \sum_{j=n+1}^{\infty} V_{i,j} f_i(s) f_j(s) ds$$
$$- \int_{t_1}^{t_2} f_n(s) \sum_{j=1}^{n} j V_{n,j} f_j(s) ds.$$

Further, thanks to relation $(H2)$ and the fact that $g_j = O(j^{\alpha+1})$, the last two integrals in the above expression tend to zero as $n \to \infty$. Therefore,

$$\sum_{i=m}^{\infty} f_i(t_2) - \sum_{i=m}^{\infty} f_i(t_1) = \int_{t_1}^{t_2} \sum_{i=m}^{\infty} \sum_{j=1}^{i} (-V_{i,j}) f_i(s) f_j(s) ds + \delta_{m\geq 2} \int_{t_1}^{t_2} \sum_{i=m}^{\infty} \sum_{j=1}^{m-1} V_{i,j} f_i(s) f_j(s) ds$$
$$+ \delta_{m\geq 2} \int_{t_1}^{t_2} f_{m-1}(s) \sum_{j=1}^{m-1} j V_{m-1,j} f_j(s) ds. \tag{3.57}$$

For $p = 1, 2$, consider,

$$|g_{n+1}| \sum_{i=n+1}^{\infty} f_i(t_p) \leq C(n+1)^{\alpha+1} \sum_{i=n+1}^{\infty} f_i(t_p)$$
$$\leq C \sum_{i=n+1}^{\infty} i^{\alpha+1} f_i(t_p)$$

for $C \in \mathbb{R}^+$ and thus Lemma 3.8 guarantees that

$$\lim_{n\to\infty} |g_{n+1}| \sum_{i=n+1}^{\infty} f_i(t_p) = 0. \tag{3.58}$$

Replacing m by $n+1$ in (3.57), multiplying both sides by g_{n+1}, letting $n \to \infty$, and using $(H2)$ together with (3.58) confirms that

$$\int_{t_1}^{t_2} g_{n+1} f_n(s) \sum_{j=1}^{n} j V_{n,j} f_j(s) ds \to 0. \tag{3.59}$$

By Definition 3.1, the boundedness of $f_i(t)$, $(H1)$ and $(H2)$, we conclude that

$$\int_{t_1}^{t_2} \sum_{i=m}^{n} \sum_{j=1}^{i} (j g_{i+1} - j g_i - g_j) V_{i,j} f_i(s) f_j(s) ds \to \int_{t_1}^{t_2} \sum_{i=m}^{\infty} \sum_{j=1}^{i} (j g_{i+1} - j g_i - g_j) V_{i,j} f_i(s) f_j(s) ds \tag{3.60}$$

and

$$\delta_{m\geq 2}\int_{t_1}^{t_2}\sum_{i=m}^{n}\sum_{j=1}^{m-1} g_j V_{i,j} f_i(s) f_j(s) ds \to \delta_{m\geq 2}\int_{t_1}^{t_2}\sum_{i=m}^{\infty}\sum_{j=1}^{m-1} g_j V_{i,j} f_i(s) f_j(s) ds. \tag{3.61}$$

Thus, using Definition 3.1 together with equations (3.56), (3.59)-(3.61) and the bounded convergence theorem, the result follows. □

Finally, the following proposition is discussed which is essential in showing that the solution of SDCE is first-order differentiable.

Proposition 3.10. *Let* $\{V_{i,j}\}_{i,j\in\mathbb{N}}$ *be non-negative and* $V_{i,j} \leq i^\alpha + j^\alpha$, $0 \leq \alpha \leq 1$. *Let* $f = (f_i)$ *be a solution on some interval* $[0, T[$, *where* $0 < T \leq \infty$, *of the equation (3.1) with initial condition* f_0 *and having bounded* $M_{\alpha+1}(f_0)$. *Then, the series* $\sum_{j=1}^{i} jV_{i,j} f_j(t) f_i(t)$ *and* $\sum_{j=i}^{\infty} V_{i,j} f_j(t) f_i(t)$ *are absolutely continuous on the compact sub-intervals of* $[0, T[$.

Proof. Let, (g_i) satisfy the conditions in the statement of Theorem 3.9. For $(H1)$ to hold, proving the boundedness of the series $\sum_{i=1}^{\infty}\sum_{j=1}^{i} j(g_{i+1} - g_i)V_{i,j} f_i(t) f_j(t)$ is enough. Using the fact that $g_{i+1} - g_i = O(i^\alpha)$, we have the following

$$\begin{aligned}\sum_{i=1}^{\infty}\sum_{j=1}^{i} j(g_{i+1} - g_i)V_{i,j} f_i f_j &\leq \sum_{i=1}^{\infty}\sum_{j=1}^{i} Cji^\alpha V_{i,j} f_i f_j \\ &\leq \sum_{i=1}^{\infty}\sum_{j=1}^{i} Cji^\alpha(i^\alpha + j^\alpha) f_i f_j \quad \leq \sum_{i=1}^{\infty}\sum_{j=1}^{i} C(ji^{\alpha+1} + i^\alpha j^{\alpha+1}) f_i f_j\end{aligned}$$

for C being some positive constant. Hence, by Lemma 3.8 and Section 3.3, one can obtain

$$\sum_{i=1}^{\infty}\sum_{j=1}^{i} j(g_{i+1} - g_i)V_{i,j} f_i f_j \leq 2CN_{\alpha+1}M_1(0). \tag{3.62}$$

Thus, $(H1)$ holds true. Further, to establish the relation $(H2)$, consider the expression,

$$\begin{aligned}\sum_{i=1}^{\infty}\sum_{j=1}^{i} g_j V_{i,j} f_i(s) f_j(s) &\leq \sum_{i=1}^{\infty}\sum_{j=1}^{i} C[j^{2\alpha+1} + i^\alpha j^{\alpha+1}] f_i f_j \\ &\leq 2CN_{\alpha+1}M_1(0)\end{aligned}$$

which is finite by Lemma 3.8. Therefore, all hypotheses of Theorem 3.9 are satisfied for any $t_1, t_2 \in [0, T)$. Hence, considering $m = 1$ for $t \in [0, T)$, equation (3.50) implies the uniform convergence of the series $\sum_{i=1}^{\infty} g_i f_i(t)$. Since, the series $\sum_{j=1}^{i} jV_{i,j} f_j(t)$ is bounded by this series, as $jV_{i,j} = O(i^{\alpha+1})$ when $j < i$, we conclude the uniform convergence of $\sum_{j=1}^{i} jV_{i,j} f_j(t)$. Now, the boundedness of $f_i(t)$ ensures the absolute continuity

of $\sum_{j=1}^{i} jV_{i,j}f_j(t)f_i(t)$. Also, the series $\sum_{j=i}^{\infty} V_{i,j}f_j(t)$ is bounded by $\sum_{j=1}^{\infty} g_j f_j(t)$, which yields its uniform convergence. Finally, the boundedness of $f_i(t)$ gives the desired result. □

The Definition 3.1 (a), hypotheses $(H1)-(H2)$ of Theorem 3.9 and Proposition 3.10 ensure that the solution f is differentiable in the classical sense in $[0,T[$.

3.5 Uniqueness

In this section, we discuss the uniqueness of solutions for the SDCE for a restrictive class of kernels. It should be mentioned here that it was not easy to deal with $V_{i,j} \leq C_V(i+j)$ $\forall i,j$, so the kernel was restricted to establish uniqueness.

Theorem 3.11. *Let, the kernel* $V_{i,j} \leq (i+j)$ *only when* $j<i$, *and* $V_{i,j} \leq C_V \min\{i^\eta, j^\eta\}, 0 \leq \eta \leq 2$ *valid* $\forall i,j \in \mathbb{N}$, $C_V \in \mathbb{R}^+$. *If the Lemma 3.8 holds, then the equations* (3.1)-(3.2) *have a unique solution in* X^+.

Proof. We shall use an approach that revolves around defining a function (say $u(t)$) that is a difference of two solutions of the equation (3.1) (let f_i and ρ_i), both satisfying the initial condition (3.2). Furthermore, it makes use of the properties of the signum function such as

- $(P1)$ $(\mathcal{C}(t))\frac{d\mathcal{C}(t)}{dt} = \frac{d|\mathcal{C}(t)|}{dt}$,
- $(P2)$ $(a)(b) = (ab)$ and $|a| = a(a)$ for any real numbers a, b.

Our goal here is to use Gronwall's lemma to the function $u(t)$ to reach at the required result. Define

$$u(t) := \sum_{i=1}^{\infty} |f_i(t) - \rho_i(t)| = \sum_{i=1}^{\infty} |u_i(t)|. \tag{3.63}$$

Using the expression of the equation (3.1), we obtain

$$\begin{aligned}\frac{du_i(t)}{dt} = &\left(\delta_{i\geq 2} f_{i-1}(t) \sum_{j=1}^{i-1} jV_{i-1,j}f_j(t) - f_i(t)\sum_{j=1}^{i} jV_{i,j}f_j(t) \sum_{j=i}^{\infty} V_{i,j}f_i(t)f_j(t)\right)\\ &- \left(\delta_{i\geq 2}\rho_{i-1}(t)\sum_{j=1}^{i-1} jV_{i-1,j}\rho_j(t) - \rho_i(t)\sum_{j=1}^{i} jV_{i,j}\rho_j(t) - \sum_{j=i}^{\infty} V_{i,j}\rho_i(t)\rho_j(t)\right).\end{aligned}$$

Multiplying both sides by $(u_i(t))$ and then using $(P1)$, the above equation reduces to

$$\frac{d}{dt}|u_i(t)| = (u_i(t))\Big(\delta_{i\geq 2} f_{i-1}(t)\sum_{j=1}^{i-1} jV_{i-1,j} f_j(t) - f_i(t)\sum_{j=1}^{i} jV_{i,j} f_j(t) - \sum_{j=i}^{\infty} V_{i,j} f_i(t) f_j(t)\Big)$$
$$- (u_i(t))\Big(\delta_{i\geq 2}\rho_{i-1}(t)\sum_{j=1}^{i-1} jV_{i-1,j}\rho_j(t) - \rho_i(t)\sum_{j=1}^{i} jV_{i,j}\rho_j(t) - \sum_{j=i}^{\infty} V_{i,j}\rho_i(t)\rho_j(t)\Big).$$

Further, integrating both sides, using $u(0) = 0$ and summing over i from 1 to ∞ yield

$$u(t) = \int_0^t \sum_{i=1}^{\infty}(u_i(h)\Big(\delta_{i\geq 2} f_{i-1}(h)\sum_{j=1}^{i-1} jV_{i-1,j} f_j(h) - f_i(h)\sum_{j=1}^{i} jV_{i,j} f_j(h) - \sum_{j=i}^{\infty} V_{i,j} f_i(h) f_j(h)\Big)dh$$
$$- \int_0^t \sum_{i=1}^{\infty}(u_i(h)\Big(\delta_{i\geq 2}\rho_{i-1}(h)\sum_{j=1}^{i-1} jV_{i-1,j}\rho_j(h) - \rho_i(h)\sum_{j=1}^{i} jV_{i,j}\rho_j(h) - \sum_{j=i}^{\infty} V_{i,j}\rho_i(h)\rho_j(h)\Big)dh.$$

Replacing $i-1$ by i', then changing i' by i in the first and fourth sums and finally using

$$(f_i\, f_j - \rho_i\, \rho_j)(t) = (f_i\, u_j + \rho_j\, u_i)(t),$$

simplify to

$$u(t) = \int_0^t \Big(\sum_{i=1}^{\infty}\Big((u_{i+1})(\delta_{i\geq 1}\sum_{j=1}^{i} jV_{i,j}(f_i u_j + \rho_j u_i)) - (u_i)(\sum_{j=1}^{i} jV_{i,j}(f_i\, u_j + \rho_j\, u_i))$$
$$- (u_i)(\sum_{j=i}^{\infty} V_{i,j}(f_i\, u_j + \rho_j\, u_i))\Big)\Big)(h)dh.$$

Using $(P1)$ and $(P2)$, one can obtain the following expression

$$u(t) \leq \int_0^t \Big(\Big(\sum_{i=1}^{\infty}\sum_{j=1}^{i} jV_{i,j}(|u_j|\, f_i + |u_i|\,\rho_j)\Big) - \Big(\sum_{i=1}^{\infty}\sum_{j=1}^{i} jV_{i,j}((u_i)\, u_j\, f_i + |u_i|\,\rho_j)\Big)$$
$$- \Big(\sum_{i=1}^{\infty}\sum_{j=i}^{\infty} V_{i,j}((u_i)\, u_j\, f_i + |u_i|\,\rho_j)\Big)\Big)(h)dh.$$

Now, canceling the second and fourth expressions and estimating the summations will give us

$$u(t) \ \leq \int_0^t \Big(2\sum_{i=1}^{\infty}\sum_{j=1}^{i} jV_{i,j}|u_j|\, f_i + \sum_{i=1}^{\infty}\sum_{j=i}^{\infty} V_{i,j}|u_j|\, f_i\Big)(h)dh.$$

Finally, inserting the value of $V_{i,j}$, we write

$$u(t) \leq \int_0^t \left(2\sum_{i=1}^{\infty}\sum_{j=1}^{i} j(i+j)|u_j|\, f_i + \sum_{i=1}^{\infty}\sum_{j=i}^{\infty} C_V i^{\eta}|u_j|\, f_i \right)(h)dh.$$

The application of Lemma 3.8 for $\alpha = 1$ leads to

$$u(t) \leq \int_0^t (4M_2 + C_V M_2)u(h)dh.$$

The application of Gronwall's lemma enables us to have $u(t) \equiv 0$ which implies that $f_i(t) = \rho_i(t)\ \forall\ 0 \leq t \leq T$. Since, T is arbitrary, we get uniqueness of $f_i(t)$. □

3.6 Non-Conservative Truncation

Required Results

Here, in this subsection, we present an approximating system of equations that do not conserve the first moment. The system is hence called *non-conservative* and is defined same as in equations (2.37)-(2.40)]. We compute the i^{th} moment of the solution of the finite-dimensional system defined as

$$\frac{dM_g^n}{dt} = \sum_{i=1}^{n-1} |g_{i+1} - g_i| \sum_{j=1}^{i} jV_{i,j} f_i f_j - \sum_{i=1}^{n-1}\sum_{j=i}^{n} g_i V_{i,j} f_i f_j. \tag{3.64}$$

which aids in computing its zeroth and first moments and can be followed from Lemma 2.21

When the approximating system does not conserve the first moment, the global existence of the solution is established by the application of Helly's theorem (see [121]) to $\{f_i^n(t)\}$. The theorem requires us to prove that the truncated solution is of locally bounded total variation and uniformly bounded at a point. This is achieved by the application of Lemma 3.14, discussed later on. In addition to this, we make use of the refined version of De la Vallée- Poussin theorem (see [115, 119]), which ensures that if f_i^0 is in weighted L^1 space, there exists a non-negative convex function $\gamma \in G$ where

$$G := \{\gamma \in C^1([0,\infty)) \cap W^{1,\infty}_{loc}(0,\infty) : \gamma(0) = 0, \gamma'(0) \geq 0, \gamma' \text{ is concave and } \lim_{r\to\infty} \frac{\gamma(r)}{r} = \infty\},$$

satisfying certain properties given by the following proposition.

Proposition 3.12. *Let, $i, j \geq 1$ and $\gamma \in G$, then the following holds true*

$$0 \leq \gamma(i+1) - \gamma(i) \leq \frac{(3i+1)\gamma(1) + 2\gamma(i)}{(i+1)}.$$

Proof. The proof can be adapted from Lemma A.2 in [122]. □

Now, the results which will be useful in proving the existence are presented below.

Lemma 3.13. *Consider $T \in (0, \infty)$, $t \in [0, T]$ and $\gamma \in G$ and $V_{i,j} \leq (i+j)$ $\forall i, j \geq 1$, then we have*

$$\sum_{i=1}^{n} \gamma(i) f_i^n(t) \leq Q(T) \quad \text{and} \tag{3.65}$$

$$0 \leq \int_0^t \left(\sum_{i=1}^{n-1} \sum_{j=i}^{n} \gamma(i) V_{i,j} f_i^n(h) f_j^n(h) \right) dh \ \leq Q(T), \tag{3.66}$$

where $Q(T)$ depends only on $\gamma(1), ||f_0||$ and $M_0(0)$.

Proof. Using $g_i = \gamma(i)$ in the equation (3.64) leads to

$$\sum_{i=1}^{n} \gamma(i) f_i^n(t) = \sum_{i=1}^{n} \gamma(i) f_i^0 + \int_0^t \Big(\sum_{i=1}^{n-1} |\gamma(i+1) - \gamma(i)| \sum_{j=1}^{i} j V_{i,j} f_i^n(h) f_j^n(h) - \sum_{i=1}^{n-1} \sum_{j=i}^{n} \gamma(i) V_{i,j} f_i^n(h) f_j^n(h) \Big) dh. \tag{3.67}$$

Since $\gamma(k)$ and f_i^n for $k = i, j$ are non-negative, the above expression simplifies to

$$\sum_{i=1}^{n} \gamma(i) f_i^n(t) \leq \sum_{i=1}^{n} \gamma(i) f_i^0 + \int_0^t \Big(\sum_{i=1}^{n-1} |\gamma(i+1) - \gamma(i)| \sum_{j=1}^{i} j V_{i,j} f_i^n(h) f_j^n(h) \Big) dh.$$

Using Proposition 3.12, replacing $V_{i,j} \leq (i+j)$ will give us

$$\begin{aligned} \sum_{i=1}^{n} \gamma(i) f_i^n(t) &\leq \sum_{i=1}^{n} \gamma(i) f_i^0 + \int_0^t \Big(\sum_{i=1}^{n-1} \sum_{j=1}^{i} [(3i+1)\gamma(1) + 2\gamma(i)] 2 f_i^n(h) f_j^n(h) \Big) dh \\ &\leq \sum_{i=1}^{n} \gamma(i) f_i^0 + \int_0^t \Big(Q_1(T) + Q_2(T) \sum_{i=1}^{n} \gamma(i) f_i^n(h) \Big) dh, \end{aligned}$$

where $Q_1(T) = 2\gamma(1) M_0(0)(M_0(0) + 3\|f_0\|)$ and $Q_2(T) = 4\|f_0\|$. Finally, an application of Gronwall's inequality proves (3.65) where $Q(T) = \sum_{i=1}^{n} \gamma(i) f_i^0 + \frac{Q_1(T)}{Q_2(T)} \left(e^{T Q_2(T)} - 1 \right)$. Combining (3.65) and (3.67) leads to

$$\int_0^t \left(\sum_{i=1}^{n-1} \sum_{j=i}^{n} \gamma(i) V_{i,j} f_i^n(h) f_j^n(h) \right) dh \leq Q(T),$$

which establishes (3.66). □

Lemma 3.14. *Consider $T \in (0,\infty)$, $i \in \mathbb{N}$. The following result holds true for a constant $\tilde{Q}(T)$ which depends on $||f_0||$ and T:*

$$\sup_{0\le t\le T}\int_0^t \Big|\frac{df_i^n}{dt}\Big|dh = \tilde{Q}(T). \tag{3.68}$$

Proof. Using the equations (2.36) and (2.38) yield

$$\begin{aligned}\int_0^t \Big|\frac{df_i^n}{dt}\Big|dh &\le \int_0^t \Big(\Big|f_{i-1}^n(h)\sum_{j=1}^{i-1} jV_{i-1,j}f_j^n(h)\Big| + \Big|f_i^n(h)\sum_{j=1}^{i} jV_{i,j}f_j^n(h)\Big| + \Big|f_i^n(h)\sum_{j=i}^{\infty} V_{i,j}f_j^n(h)\Big|\Big)dh\\ &= \int_0^t \Big(2\Big|f_i^n(h)\sum_{j=1}^{i} jV_{i,j}f_j^n(h)\Big| + \Big|f_i^n(h)\sum_{j=i}^{\infty} V_{i,j}f_j^n(h)\Big|\Big)dh\\ &\le 4\|f_0\|^2T + 2||f_0||\,M_0(0)\,T.\end{aligned}$$

Also, the absolute values of the equations (2.37) and (2.39) can easily be shown bounded by $2||f_0||^2+||f_0||\,M_0(0)$ and $2||f_0||^2$, respectively, which completes the proof of the lemma. □

Existence

This section is devoted to prove the global existence of a solution for non-conservative truncation.

Theorem 3.15. *Consider $f \in X^+$ and $V_{i,j} \le (i+j)\ \ \forall i,j$. Suppose that $f_i^n(t)$ and f_i^0 are the solution and initial condition of the non-conservative approximation (2.36)-(2.39), then there exists a solution of the discrete OHS equation (3.1)-(3.2) in $\mathbb{R}^+$.*

Proof. The proof follows the same pattern and the same bounds are obtained in the case of the considered kernel as in Chapter 2 [Theorem 2.31]. □

Density Conservation

Here, density conservation is demonstrated for the non-mass conserving truncation by the following result.

Theorem 3.16. *Let $V_{i,j} \le (i+j)$ for all natural numbers i and j. Let $f = (f_i) \in X^+$ be a solution of the Safronov-Dubovski equation (3.1) satisfying all the conditions of Theorem 3.15. Additionally, if*

$$V_{n,j} \to 0 \ \text{ as } \ n \to \infty \ \text{ for every } \ j \in [1,(n-1)], \tag{3.69}$$

holds, then the solution is density conserving satisfying

$$\sum_{i=1}^{\infty} i f_i(t) = \sum_{i=1}^{\infty} i f_i(0). \tag{3.70}$$

Proof. To establish density conservation, let us consider

$$\Big|\sum_{i=1}^{\infty} i f_i(t) - \sum_{i=1}^{\infty} i f_i(0)\Big| = \Big|(\sum_{i=1}^{m} + \sum_{i=m+1}^{\infty}) i f_i(t) - (\sum_{i=1}^{m} + \sum_{i=m+1}^{\infty}) i f_i(0)\Big|. \tag{3.71}$$

Now, writing the equation (2.42) as

$$\sum_{i=1}^{n} i f_i(0) = \sum_{i=1}^{m} i f_i^n(t) + \sum_{i=m+1}^{n} i f_i^n(t) - \sum_{j=1}^{n-1} j V_{n,j} f_n^n(t) f_j^n(t). \tag{3.72}$$

Using (3.72) in (3.71), one can obtain

$$\begin{aligned}\Big|\sum_{i=1}^{\infty} i f_i(t) - \sum_{i=1}^{\infty} i f_i(0)\Big| \le \sum_{i=1}^{m} i\Big|f_i(t) - f_i^n(t)\Big| + \sum_{i=m+1}^{\infty} i f_i(t) + \sum_{i=m+1}^{n} i f_i^n(t) + \sum_{i=n+1}^{\infty} i f_i(0) \\ + \Big|f_n^n(t) \sum_{j=1}^{n-1} j V_{n,j} f_j^n(t)\Big|.\end{aligned} \tag{3.73}$$

Before passing the limit $n \to \infty$, the boundedness of the last expression in the above equation needs to be dealt with and is given as

$$\Big|f_n^n(t) \sum_{j=1}^{n-1} j V_{n,j} f_j^n(t)\Big| \le 2||f_0||^2.$$

Further, having (3.69), then passing the limit in (3.73) and using (2.49) provide

$$\lim_{n\to\infty} \Big|\sum_{i=1}^{\infty} i f_i(t) - \sum_{i=1}^{\infty} i f_i(0)\Big| \le \sup_{i\ge m} \frac{2 i f_i^n(t) \gamma_0(i)}{\gamma_0(i)}.$$

Hence, the first result is given in equation (2.53), and the properties of γ_0 lead to accomplishing our claim. □

Chapter 4

Steady-State Solution for Safronov-Dubovski Coagulation Equation[1]

Let us consider the SDCE written as

$$\frac{df_1(t)}{dt} = -V_{1,1}f_1^2(t) - f_1(t)\sum_{j=1}^{\infty} V_{1,j}f_j(t) \tag{4.1}$$

$$\frac{df_i(t)}{dt} = f_{i-1}\sum_{j=1}^{i-1} jV_{i-1,j}f_j - f_i\sum_{j=1}^{i} jV_{i,j}f_j - f_i\sum_{j=i}^{\infty} V_{i,j}f_j(t), \quad i > 1 \tag{4.2}$$

with the initial datum as

$$f_i(0) = f_{in}, \quad \forall i \geq 1. \tag{4.3}$$

The chapter attempts to understand the steady-state behavior of the solutions of SDCE for the coagulation kernel $V_{i,j} = C_V(i^\beta j^\gamma + i^\gamma j^\beta)$ when $0 \leq \beta \leq \gamma \leq 1$, $\forall\, i, j \in \mathbb{N}$, $C_V \in \mathbb{R}^+$. The kernel covers a wide variety of physical parameters including the constant, sum, and product kernels. The theoretical investigation into the existence of the unique steady-state is carried out for these kernels. The solutions for the equation (4.1)-(4.2) are numerically plotted to ensure steady-state behavior. The motivation for this work comes from the steady-state analysis done by Wattis [13] on the discrete coagulation-disintegration model developed in 2012 and the work by Ghosh et al. [124] where the same analysis was investigated for the continuous coagulation-fragmentation equation.

The chapter is organized in the following order. Section 4.1 includes the characterization of the steady-state solution while in Section 4.2, the existence and uniqueness results

[1]The work in this chapter is published in *Int. J. of Dynamical Systems and Differential Equations*, 13(2), 144-163, 2023.

are discussed. Finally, some numerical observations and verification of theoretical results are reported in Section 4.3.

4.1 Characterization of Steady-State

The steady state refers to a phase in the dynamics of the system wherein the solution does not change with time. The steady state for the system that we are concerned with, would mean that the concentration of the particles in the system does not vary as time changes. This section is devoted to such an analysis for the Safrononv-Dubovski coagulation equation (4.1)-(4.3) when the rate of collision between the particles is given by the following general classes of the kernel,

$$V_{i,j} = C_V(i^\beta j^\gamma + i^\gamma j^\beta),\ 0 \le \beta \le \gamma \le 1. \tag{4.4}$$

By using the above expression for $V_{i,j}$, the equations (4.1)-(4.2) simplify to

$$\frac{df_1(t)}{dt} = -2C_V f_1(t)^2 - C_V f_1(t) \sum_{j=1}^{\infty} (j^\gamma + j^\beta) f_j(t), \tag{4.5}$$

$$\begin{aligned}\frac{df_i(t)}{dt} = f_{i-1}(t) \sum_{j=1}^{i-1} C_V \left((i-1)^\beta j^{\gamma+1} + (i-1)^\gamma j^{\beta+1}\right) f_j(t) - f_i(t) \sum_{j=1}^{i} C_V \left(i^\beta j^{\gamma+1} + i^\gamma j^{\beta+1}\right) f_j(t) \\ - f_i(t) \sum_{j=i}^{\infty} C_V \left(i^\beta j^\gamma + i^\gamma j^\beta\right) f_j(t),\ \ i > 1.\end{aligned} \tag{4.6}$$

Now, the steady-state solution will be the one when the left part of the equation (4.6) will tend to zero (assuming that $f_i(t)$ is differentiable). Rearranging the terms in the above expression, one can easily obtain the value of $f_i(t)$. For the sake of notations, let us denote this solution as c_i, which yields the following equation

$$c_i = c_{i-1} \frac{\sum_{j=1}^{i-1} \left((i-1)^\beta j^{\gamma+1} + (i-1)^\gamma j^{\beta+1}\right) c_j}{\left(i^\beta \sum_{j=1}^{i} j^{\gamma+1} c_j + i^\gamma \sum_{j=1}^{i} j^{\beta+1} c_j + i^\beta \sum_{j=i}^{\infty} j^\gamma c_j + i^\gamma \sum_{j=i}^{\infty} j^\beta c_j\right)}, \qquad i \ge 2. \tag{4.7}$$

To analyze the steady-state solution, we adopt an approach that involves defining some summation terms in the equation, which will enable easy retrieval of the explicit expression of the steady-state solution. The summations in the denominator are defined as

$$L_a = \sum_{j=1}^{i} j^a c_j, \qquad a \le 2 \tag{4.8}$$

and

$$U_b = \sum_{j=i}^{\infty} j^b c_j, \qquad b \leq 2. \tag{4.9}$$

The aforementioned sums are finite as a consequence of the assumption that the second moment is bounded and expressed as

$$M_2 = \sum_{i=1}^{\infty} i^2 c_i \leq K, \tag{4.10}$$

where $K \in \mathbb{R}^+$. Based on the equations (4.8)-(4.9), (4.7) can be written as

$$c_i = c_{i-1} \frac{\sum_{j=1}^{i-1} \left((i-1)^\beta j^{\gamma+1} + (i-1)^\gamma j^{\beta+1}\right) c_j}{(i^\beta L_{\gamma+1} + i^\gamma L_{\beta+1} + i^\beta U_\gamma + i^\gamma U_\beta)}, \qquad i \geq 2. \tag{4.11}$$

For theoretical and numerical analysis, we shall assume $c_1 = f_1(0) \geq 0$. For any $\beta, \gamma \geq 0$, $i \geq 2$, and $j \geq 1$, the numerator consists of two summands and the denominator involves the finite quantities. Hence, we can define a nonlinear operator A as

$$A(c)_i := c_{i-1} \frac{\sum_{j=1}^{i-1} \left((i-1)^\beta j^{\gamma+1} + (i-1)^\gamma j^{\beta+1}\right) c_j}{(i^\beta L_{\gamma+1} + i^\gamma L_{\beta+1} + i^\beta U_\gamma + i^\gamma U_\beta)}, \qquad i \geq 2, \tag{4.12}$$

such that $A : l_{1,i} \to l_{1,i}$ (proved later) where the norm on $l_{1,i}$ is defined as

$$||z|| = \sum_{i=1}^{\infty} i^\gamma |z_i|, \qquad \gamma \leq 1. \tag{4.13}$$

4.2 Existence and Uniqueness of Steady-State

In this section, we apply the contraction mapping theorem to prove that there exists a unique fixed point of the operator A. For this, we shall first prove that A maps $l_{1,i}$ to itself. For this, we show

$$||A(c) - c_1|| < b, \qquad \text{where} \qquad [c_1 - b, c_1 + b].$$

We have,

$$\begin{aligned} ||A(c) - c_1|| &= \sum_{i=2}^{\infty} i^\gamma \left| \frac{\sum_{j=1}^{i-1} ((i-1)^\beta j^{\gamma+1} + (i-1)^\gamma j^{\beta+1}) c_{i-1} c_j}{(L_{\gamma+1} i^\beta + L_{\beta+1} i^\gamma + i^\beta U_\gamma + i^\gamma U_\beta)} \right| \\ &\leq \sum_{i=2}^{\infty} i^\gamma \left| \frac{\sum_{j=1}^{i-1} ((i-1)^\beta j^{\gamma+1} + (i-1)^\gamma j^{\beta+1}) c_{i-1} c_j}{i^\beta (L_{\gamma+1} + L_{\beta+1} + U_\gamma + U_\beta)} \right| \qquad \text{wlog} \quad \text{let} \quad \beta \leq \gamma. \end{aligned}$$

Replacing $(i-1)$ by i', then taking $i' \leftrightarrow i$ and using $(i+1)^\gamma \leq (i+1)$, one can easily obtain

$$||A(c) - c_1|| \leq \frac{\sum_{i=1}^{\infty}\sum_{j=1}^{i}(i+1)(j^{\gamma+1}+i^\gamma j)c_i c_j}{(L_{\gamma+1}+L_{\beta+1}+U_\gamma+U_\beta)}.$$

Further, changing the order of integration and $i \leftrightarrow j$ yields

$$||A(c) - c_1|| \leq \frac{\sum_{i=1}^{\infty}\sum_{j=i}^{\infty}2(j+1)j^\gamma i c_i c_j}{(L_{\gamma+1}+L_{\beta+1}+U_\gamma+U_\beta)} \leq \frac{4M_1(0)U_{\gamma+1}}{(L_{\gamma+1}+L_{\beta+1}+U_\gamma+U_\beta)}.$$

So, we obtain the condition on b, L_a, U_b as

$$\frac{4M_1(0)U_{\gamma+1}}{b(L_{\gamma+1}+L_{\beta+1}+U_\gamma+U_\beta)} < 1. \tag{4.14}$$

Now, we shall proceed towards proving that A is a contraction mapping in the following theorem.

Theorem 4.1. *Let the steady-state solution $c_i \geq 0 \quad \forall\ i \geq 1$ and the following condition*

$$4U_{\gamma+1} < L_{\gamma+1}+L_{\beta+1}+U_\gamma+U_\beta, \tag{4.15}$$

holds where $U_{\gamma+1}, L_{\gamma+1}, L_{\beta+1}, U_\gamma$ as well as U_β can be derived from (4.8)-(4.9). Then A is a contraction mapping.

Proof. The result is established by applying the contraction mapping theorem to the operator A. For this, we prove that $A : l_{1,i} \to l_{1,i}$ is a contraction mapping with respect to the norm defined in (4.13). Consider, c_i and d_i be two solutions satisfying the equation (4.7) such that $c_1 = d_1$ and hence, we get

$$||A(c)-A(d)|| = |c_1-d_1| + \sum_{i=2}^{\infty} i^\gamma \left| \frac{\sum_{j=1}^{i-1}((i-1)^\beta j^{\gamma+1}+(i-1)^\gamma j^{\beta+1})c_{i-1}c_j - \sum_{j=1}^{i-1}((i-1)^\beta j^{\gamma+1}+(i-1)^\gamma j^{\beta+1})d_{i-1}d_j}{(L_{\gamma+1}i^\beta + L_{\beta+1}i^\gamma + i^\beta U_\gamma + i^\gamma U_\beta)} \right|.$$

Now, let us assume wlog that $\beta \leq \gamma$ which simplifies the above equation to

$$||A(c) - A(d)|| \leq \sum_{i=1}^{\infty} i^\gamma \left| \frac{\sum_{j=1}^{i-1}((i-1)^\beta j^{\gamma+1}+(i-1)^\gamma j^{\beta+1})c_{i-1}c_j - \sum_{j=1}^{i-1}((i-1)^\beta j^{\gamma+1}+(i-1)^\gamma j^{\beta+1})d_{i-1}d_j}{i^\beta(L_{\gamma+1}+L_{\beta+1}+U_\gamma+U_\beta)} \right|.$$

Using the formula, $ab - cd = \frac{(a-c)(b+d)+(a+c)(b-d)}{2}$, one can obtain

$$\begin{aligned} ||A(c) - A(d)|| &\leq \frac{\sum_{i=1}^{\infty} i^\gamma \sum_{j=1}^{i-1}((i-1)^\beta j^{\gamma+1}+(i-1)^\gamma j^{\beta+1})\left[|c_{i-1}-d_{i-1}|\,|c_j+d_j| + |c_{i-1}+d_{i-1}|\,|c_j-d_j|\right]}{2i^\beta(L_{\gamma+1}+L_{\beta+1}+U_\gamma+U_\beta)} \\ &=: \frac{S_1+S_2+S_3+S_4}{2(L_{\gamma+1}+L_{\beta+1}+U_\gamma+U_\beta)}. \end{aligned} \tag{4.16}$$

Let us analyze these terms one by one. For the first term S_1,

$$\sum_{i=1}^{\infty} i^{\gamma} \frac{\sum_{j=1}^{i-1}(i-1)^{\beta} j^{\gamma+1} |c_{i-1} - d_{i-1}|\,|c_j + d_j|}{i^{\beta}} \leq \sum_{i=1}^{\infty}\sum_{j=1}^{i-1} i^{\gamma} j^{\gamma+1} |c_{i-1} - d_{i-1}|\,|c_j + d_j|$$
$$\leq \sum_{i=1}^{\infty}\sum_{j=1}^{i} i^{\gamma}(i-1)^{\gamma} j |c_{i-1} - d_{i-1}|\,|c_j + d_j|.$$

Further, replacing $i-1$ by i' and then $i' \to i$ and some simplifications lead to

$$S_1 \leq \sum_{i=1}^{\infty}\sum_{j=i}^{\infty} i^{\gamma} j^{\gamma+1} |c_i - d_i|\,|c_j + d_j|.$$

Using the positivity of the steady state solution, the above equation reduces to

$$S_1 \leq 2\, U_{\gamma+1} ||c - d||. \tag{4.17}$$

Now, the second sum S_2 can be evaluated as

$$S_2 = \sum_{i=1}^{\infty} i^{\gamma} \frac{\sum_{j=1}^{i-1}(i-1)^{\gamma} j^{\beta+1} |c_{i-1} - d_{i-1}|\,|c_j + d_j|}{i^{\beta}} \leq \frac{\sum_{i=1}^{\infty}\sum_{j=1}^{i} i^{\gamma}(i-1)^{\gamma} j i^{\beta} |c_{i-1} - d_{i-1}|\,|c_j + d_j|}{i^{\beta}},$$

which can be further made easier as

$$S_2 \leq \sum_{i=1}^{\infty}\sum_{j=i}^{\infty} i^{\gamma}(i-1)^{\gamma} j |c_{i-1} - d_{i-1}|\,|c_j + d_j|$$
$$\leq 2\, U_{\gamma+1}\, ||c - d||. \tag{4.18}$$

Further, consider the term S_3 which is written as

$$S_3 = \frac{\sum_{i=1}^{\infty} i^{\gamma} \sum_{j=1}^{i-1}(i-1)^{\beta} j^{\gamma+1} |c_{i-1} + d_{i-1}|\,|c_j - d_j|}{i^{\beta}} \leq \sum_{i=1}^{\infty}\sum_{j=1}^{i} i^{\gamma}(i-1)^{\gamma+1} |c_{i-1} + d_{i-1}|\,|c_j - d_j|.$$

Using the symmetricity of the summation on the right side of the inequality yields

$$S_3 \leq \sum_{j=1}^{\infty}\sum_{i=j}^{\infty} j^{\gamma}(i-1)^{\gamma+1} |c_{i-1} + d_{i-1}|\,|c_j - d_j|.$$

Changing the order of variables in the above expression, letting $i - 1 = i'$ and then replacing $i' = i$, one can easily obtain

$$S_3 \leq \sum_{j=1}^{\infty}\sum_{i=j}^{\infty} j^{\gamma} i^{\gamma+1} |c_i + d_i|\,|c_j - d_j| \leq 2U_{\gamma+1} ||c - d||. \tag{4.19}$$

Finally, S_4 can be interpreted as

$$\begin{aligned} S_4 &= \sum_{i=1}^{\infty} i^{\gamma} \frac{\sum_{j=1}^{i-1}(i-1)^{\gamma} j^{\beta+1} |c_{i-1}+d_{i-1}|\,|c_j-d_j|}{i^{\beta}} \\ &\leq \sum_{i=1}^{\infty} i^{\gamma} \frac{\sum_{j=1}^{i-1}(i-1)^{\gamma} j(i-1)^{\beta} |c_{i-1}+d_{i-1}|\,|c_j-d_j|}{i^{\beta}} \\ &\leq \sum_{i=1}^{\infty} i^{\gamma} \sum_{j=1}^{i-1}(i-1)^{\gamma+1} |c_{i-1}+d_{i-1}|\,|c_j-d_j| \\ &\leq \sum_{i=1}^{\infty} i^{\gamma} \sum_{j=1}^{i}(i-1)^{\gamma+1} |c_{i-1}+d_{i-1}|\,|c_j-d_j|. \end{aligned}$$

Furthermore, after some simple computations and changing the order of variables, the above can be rewritten as

$$\begin{aligned} S_4 &\leq \sum_{i=1}^{\infty} \sum_{j=i}^{\infty} j^{\gamma}(i-1)^{\gamma+1} |c_{i-1}+d_{i-1}|\,|c_j-d_j| \\ &\leq 2\,U_{\gamma+1}\,||c-d||. \end{aligned} \tag{4.20}$$

Substituting all the relations (4.17)-(4.20) in the main expression (4.16), one gets

$$||A(c)-A(d)|| \leq \frac{8U_{\gamma+1}}{2(L_{\gamma+1}+L_{\beta+1}+U_{\gamma}+U_{\beta})}\,||c-d||.$$

Following the condition (4.15) stated in Theorem 4.1 above implies that the non-linear operator $A : l_{1,i} \to l_{1,i}$ has a contraction mapping. Since $l_{1,i}$ is a complete metric space, the contraction mapping theorem states the operator A has only one fixed point, and therefore, the steady-state solution c_i is unique for any $b > M_1(0)$. □

The result proved above depends solely on the fact that the condition (4.15) holds. For this condition, the values of the terms $U_{\gamma+1}$, $L_{\gamma+1}$, $L_{\beta+1}$, U_{γ} and U_{β} are needed which require the values of the solution $f_i(t)$. The discrete OHS equation is a coupled system due to the term

$$\sum_{j=i}^{\infty} C_V(i^{\beta}j^{\gamma} + i^{\gamma}j^{\beta}) f_i(t) f_j(t), \quad 0 \leq \beta \leq \gamma \leq 1$$

and can be converted to a non-coupled system by altering it as

$$\left(\sum_{j=1}^{\infty} - \sum_{j=1}^{i-1}\right) C_V(i^{\beta}j^{\gamma} + i^{\gamma}j^{\beta}) f_i(t) f_j(t).$$

Thus, using the above expression, the computations for calculating the solutions $f_i(t)$ involve the zeroth and first moments, but not explicitly. The expression of $f_i(t)$ also

involves the solutions up to $f_{i-1}(t)$. The presence of these moments creates various problems while evaluating $f_i(t)$ as we have

$$\frac{df_i(t)}{dt} = \left(f_{i-1} \sum_{j=1}^{i-1} j V_{i-1,j} f_j - f_i \sum_{j=1}^{i} j V_{i,j} f_j - f_i \sum_{j=i}^{\infty} V_{i,j} f_j \right)(t).$$

Now, if we put $V_{i,j} = C_V$ (constant kernel), then

$$\frac{df_i(t)}{dt} = C_V \left(f_{i-1} \sum_{j=1}^{i-1} j f_j - f_i \sum_{j=1}^{i} j f_j - M_0 f_i + f_i \sum_{j=1}^{i-1} f_j \right)(t).$$

Since, (4.1)-(4.2) is a coagulation equation, it is obvious from the article [20] that $M_0(t) \leq M_0(0)$. Hence, the exact solution is not easily tractable. Furthermore, for the sum kernel, i.e., $V_{i,j} = C_V(i+j)$, the expression is written as

$$\frac{df_i(t)}{dt} = C_V \left(\sum_{j=1}^{i-1} j(i-1+j) f_{i-1} f_j - \sum_{j=1}^{i} j(i+j) f_i f_j - M_0 i f_i - M_1 f_i + \sum_{j=1}^{i-1} C_V (i+j) f_i f_j \right)(t).$$

The above term involves the zeroth and the first moments, where even if $M_1(t)$ is assumed to be constant, the presence of $M_0(t)$ makes it difficult to obtain the explicit value of the exact solution. For the product kernel $V_{i,j} = C_V ij$, the solution appears as

$$\frac{df_i(t)}{dt} = C_V \left(f_{i-1} \sum_{j=1}^{i-1} (i-1) j^2 f_j - f_i \sum_{j=1}^{i} i j^2 f_j - M_1 i f_i + f_i \sum_{j=1}^{i-1} ij f_j \right)(t).$$

Now, the loss of mass for this kernel is registered in [125], i.e., $M_1(t) \leq M_1(0)$, and therefore, the exact solution cannot be obtained. Finally, for any kernel with $0 < \beta \leq \gamma < 1$, the two expressions given as

$$\sum_{j=1}^{\infty} j^{\beta} f_j(t) \quad \text{and} \quad \sum_{j=1}^{\infty} j^{\gamma} f_j(t)$$

are clearly bounded by $M_1(t)$. We have explored some analytical methods to establish a comparison with the numerical solutions. The method of moments (MOM) was used to calculate the analytical solutions for all the cases and it was observed that the scheme is unable to calculate the general value of $f_i(t)$. So, the authors decided to compute the value of f_1 and then use it to calculate the higher $f_i's$. However, the calculations in MATLAB© (dsolve) show that in case of $V_{i,j} = 2$, $f_i(0) = (1/2)^i$ and $V_{i,j} = 2ij$, $f_i(0) = e^{-i^2}$, the values of f_2 are not real. In addition, for $V_{i,j} = (i+j)$ and $f_i(0) = e^{-i}$, the value of f_2 was reported to be 'empty'. Therefore, in absence of the exact solutions, the analytical values of f_1 for each case are compared with that of its numerical counterparts

in Figures 4.1(d), 4.4(c), and 4.7(c). The numerical solutions show nice accuracy with the analytical ones for all the examples and the plots can be further improved by increasing the value of N.

4.3 Numerical Results

In this section, we consider four different test cases of numerical examples to verify the theoretical observations. The solutions $f_i(t)$ are evaluated using the fourth-order explicit Runge-Kutta method (ODE45) in MATLAB©. The examples presented below discuss the properties of the solution when constant, sum and product kernels are taken. The analysis also includes the type of kernels discussed by Davidson [20].

Test Case 1: Constant Kernel

Putting $\beta = 0$, $\gamma = 0$, $C_V = 1$ in (4.4), the kernel $V_{i,j} = 2$ is obtained. The other parameters used in the computations are initial condition $f_i(0) = \frac{1}{2^i}$ and $c_1 = 0.5$:
Figure 4.1 presents the concentration plots for the constant kernel $V_{i,j} = 2$ with Figure 4.1(a) depicting the normalized solution with respect to (wrt) size when $1 \leq N \leq 50$ at various time durations. The Figures 4.1(b) and 4.1(c) show the plots of normalized solutions wrt time when $t \in [0, 60]$ and log-linear plot of the concentration when $t \in [0, 100]$, respectively. The analytical value of f_1 is compared with the numerical solution in Figure 4.1(d) for $N = 20$ and it is visualized that they are in good agreement with each other. In all the figures, we can see as time increases, the concentration of the particles decreases. The Figures 4.2(a) and 4.2(b) represent the condition (4.15) plot which confirms the steady-state and the normalized moments of the non-normalized solution, respectively. The presence of a steady-state solution is visualized in Figure 4.3. The Figure 4.3(b) depicts the plot of the normalized $f_i(t)$ when $N \in [1, 500]$. Interestingly, it can be seen that oscillations start to appear as the value of N exceeds ≈ 320, but as the value of t increases, the oscillations start to relax and a steady state is reached. The Figures 4.3(c) and 4.3(d) are the flag-bearers for the case $N \in [1, 1000]$ and since, this case is computationally very expensive, the calculations are done only up to $t = 200$. The said figures show that for the same values of N, as time progresses (from $t = 100$ to $t = 200$), the oscillations start to settle and the authors are imperative that the concentration will reach the steady state when the value of t is increased further.
In addition to this, in Table 4.1, values of $M_2(t)$ are summarized for three different initial conditions. It is observed that when $N = 100$, very mild differences in the numerical values are obtained for all the three cases $(a), (b), (c)$ when $t = 100$ and $t = 1000$. Moreover, for large values of N, for instance, $N = 500$, this similarity is observed for

a large time scales. Hence, it is certain that the steady-state behavior of the SDCE is achieved.

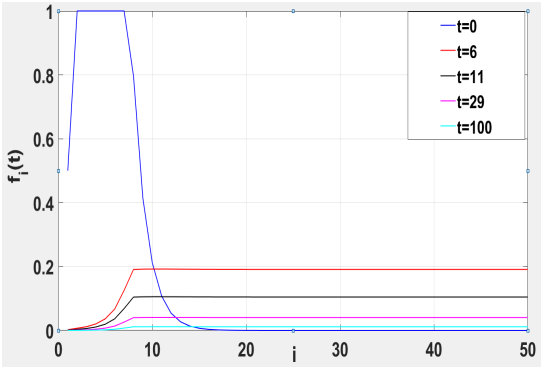

(a) Normalised concentration wrt size

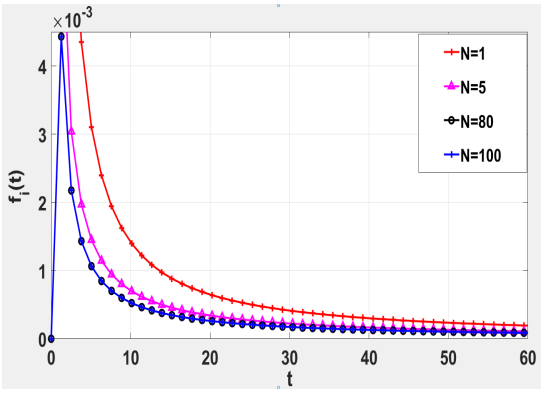

(b) Normalized concentration wrt time

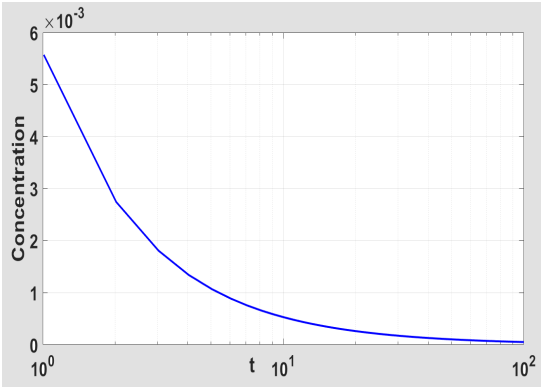

(c) Log-linear plot of concentration

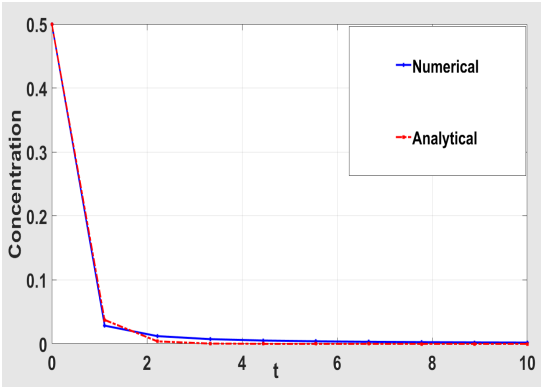

(d) Plot for f_1 when $N = 20$

FIGURE 4.1: Concentration plots for $V_{i,j} = 2$

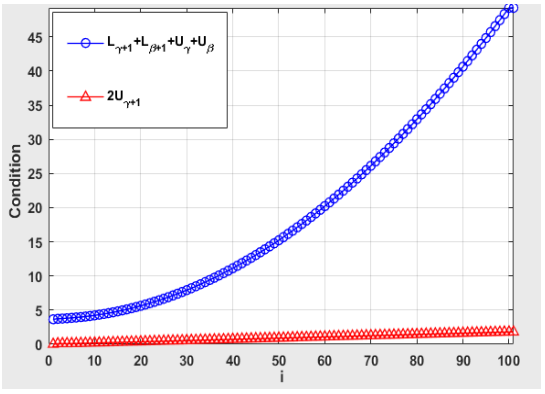

(a) Condition (4.15) plot

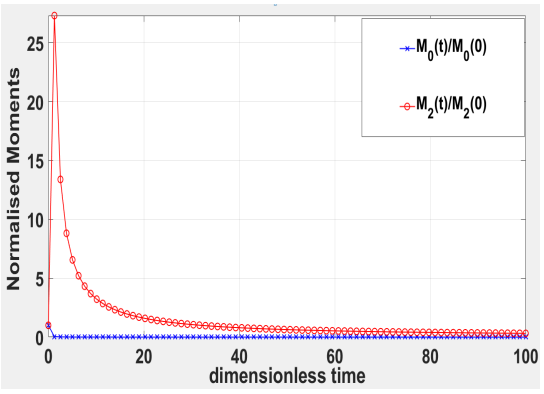

(b) Normalized moments

FIGURE 4.2: Condition (4.15) plot and normalized moments for $V_{i,j} = 2$

Test Case 2: Sum Kernel

Considering $\beta = 0$, $\gamma = 1$, $C_V = 1$ leads to the sum kernel $V_{i,j} = (i + j)$. The initial

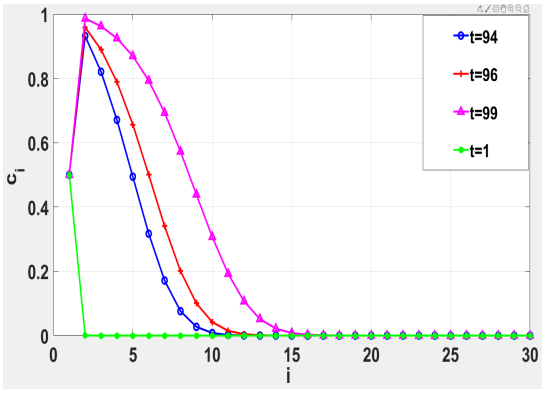

(a) Steady-state solution wrt size

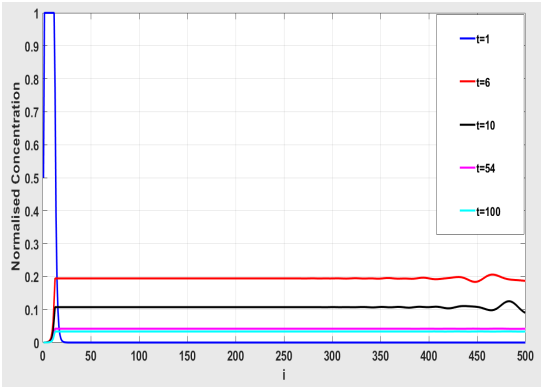

(b) Solution wrt size for $N = 500$ up to $t = 100$

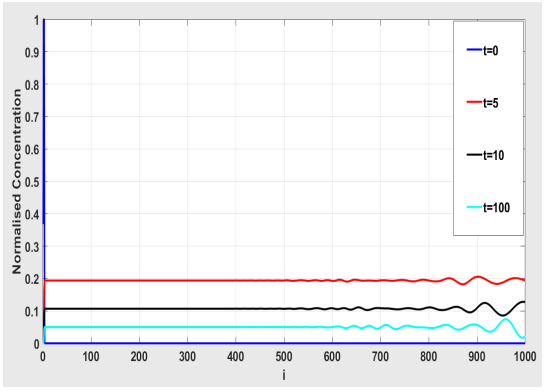

(c) Solution wrt size for $N = 1000$ up to $t = 100$ units of time

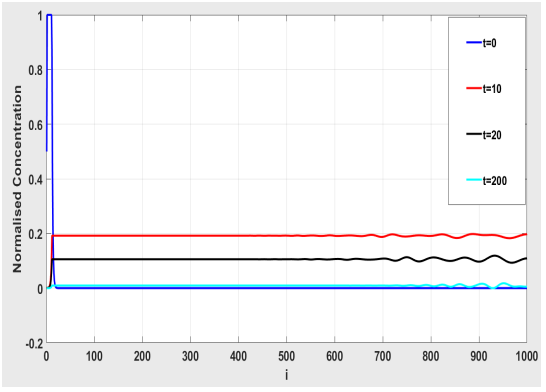

(d) Solution wrt size for 1000 equations up to 500 units of time

FIGURE 4.3: Steady-state solution for $V_{i,j} = 2$

condition $f_i(0) = e^{-i}$ is taken along with $c_1 = 1/e$:

The Figure (4.4) presents the normalized solutions at various time durations for $N = 80, 100$; a log-log plot of the non-normalized solution and comparison of analytical (MOM) f_1 with the numerical one for $N = 100$. It is clear that the numerical solution provides good accuracy with the analytical one. Figure 4.5(a) proves that the condition (4.15) holds for the sum kernel which guarantees the uniqueness of a steady-state solution. The normalized moments displayed in Figure 4.5(b) indicates that they also tend to reach steady-state. The normalized concentration plots in the Figures 4.6(b) and 4.6(c) show that the oscillations start to appear near $N \approx 100$ and as the value of N is increased up to 500, the oscillations become more prominent for lower t but as time increases, the oscillations start to fade out.

It should be noted that similar results are observed for the initial condition $f_i(0) = \frac{1}{2^i}$ as well. Also, the qualitative behavior of the concentration with respect to size is similar to the previous case and therefore, plots are omitted here. Further, the values of the second moment are computed which aids in evaluating the numerical bound for it. Again, it is evident from Table 4.2 that the values of the second moment are almost similar for small

N after a certain point in time. For large N, the time taken by the system to achieve a certain level of energy is different for every initial condition. For example, $f_i(0) = e^{-i}$ takes maximum time (t=1000) to reach the approximate value 0.5, which is estimated at $t = 300$ for the other two initial conditions, see Table 4.2.

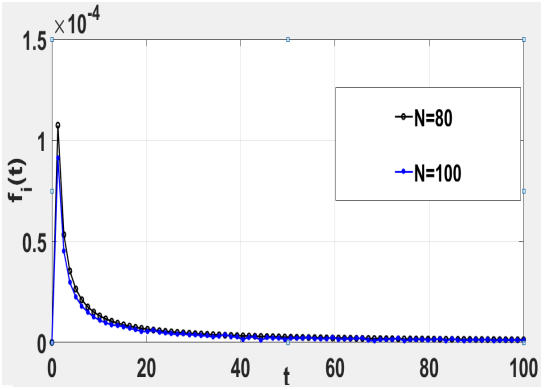

(a) Normalized $f_i(t)$ wrt time at $N = 80, 100$

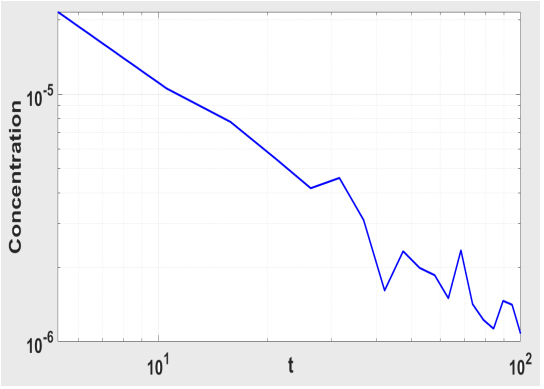

(b) Log-log plot of solution at $N = 100$

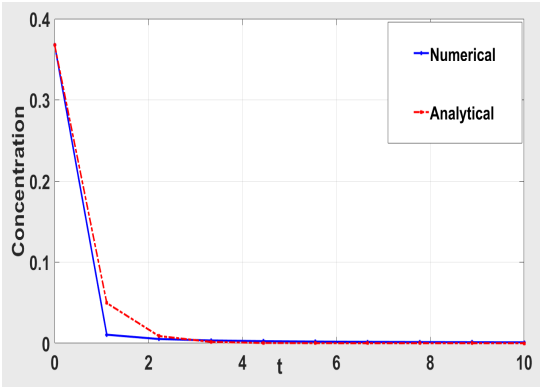

(c) f_1 plot for $N = 100$

FIGURE 4.4: Concentration plots for $V_{i,j} = (i + j)$

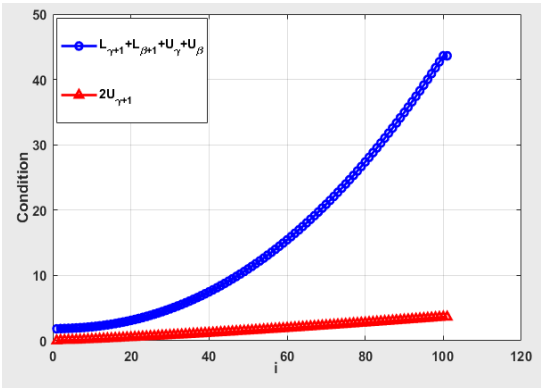

(a) Condition (4.15) plot

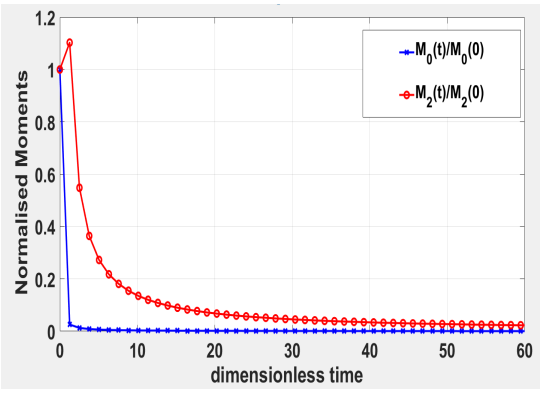

(b) Normalized moments

FIGURE 4.5: Condition (4.15) plot and normalized moments for $V_{i,j} = (i + j)$

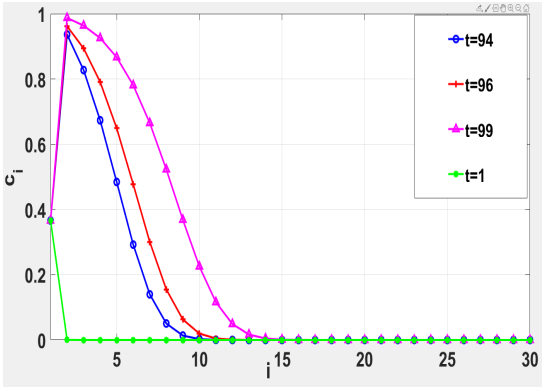

(a) c_i wrt i

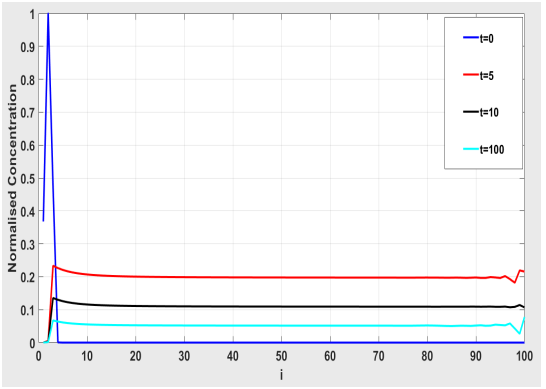

(b) $f_i(t)$ wrt i, up to $N = 100$ and $t = 100$

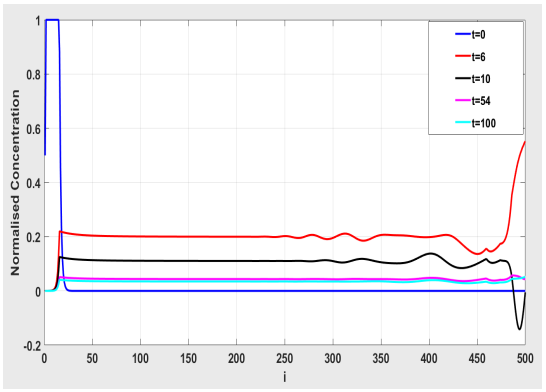

(c) $f_i(t)$ wrt i, up to $N = 500$ and $t = 100$

FIGURE 4.6: Steady-state solution for $V_{i,j} = (i + j)$

Test Case 3: Product Kernel

Now, we consider the product kernel which is given by $\beta = 1$, $\gamma = 1$, $C_V = 1$, i.e., $V_{i,j} = 2ij$. Consider the initial condition as $f_i(0) = e^{-i^2}$ with $c_1 = 1/2.73$:
The normalized solutions for $N = 30, 50$ and log-linear plot for $N = 100$ are provided at different times in Figures 4.7(a) and 4.7(b), respectively. The analytical and numerical values for f_1 are shown to be overlapping with each other in Figure 4.7(c). Similar to the previous cases, the same observation follows for the condition 4.15 and the moments that can be visualized through Figure 4.8. The steady-state behavior of the solution is presented in the Figure 4.9(a) when $N \in [1, 30]$. We observe from the Figures 4.9(b) and 4.9(c), that oscillations start to appear for a very low value of $N \approx 50$ but only for small t. We would like to mention that in the case of this kernel, the time steps also have a significant role in displaying the oscillatory behavior. One can visualize from these figures the damping behavior of the oscillations by increasing the number of time steps even for a large value of N. Similar to the previous cases, Table 4.3 summarizes the values of $M_2(t)$ for various initial conditions.

Test Case 4: Putting $\beta = 1/2$, $\gamma = 1/2$, $C_V = 4$ in (4.4), we obtain $V_{i,j} = 8i^{1/2}j^{1/2}$.

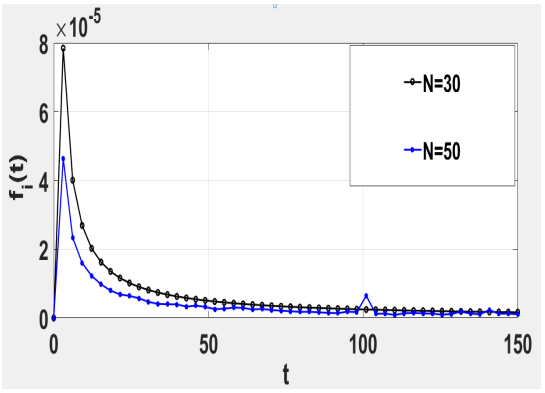

(a) $f_i(t)$ wrt t up to $t = 0, 150$

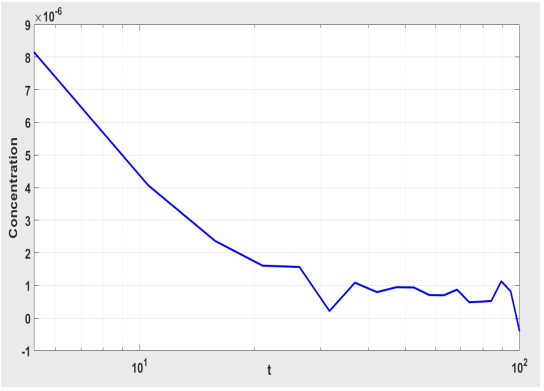

(b) Log-linear plot of $f_i(t)$ at $N = 100$

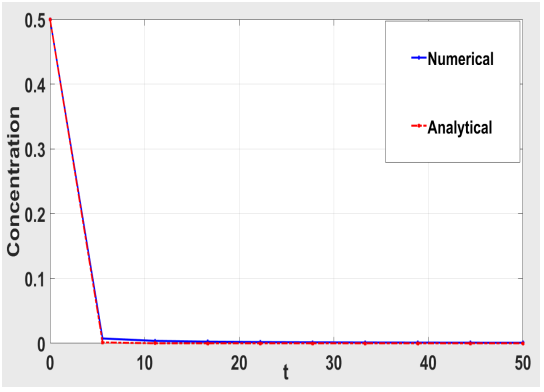

(c) f_1 plot when $N = 100$

FIGURE 4.7: Concentration plots for $V_{i,j} = 2ij$

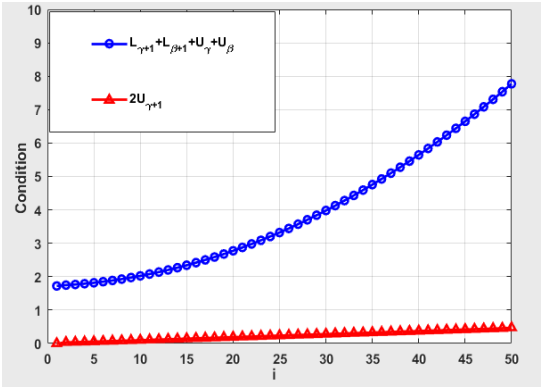

(a) Condition (4.15) plot

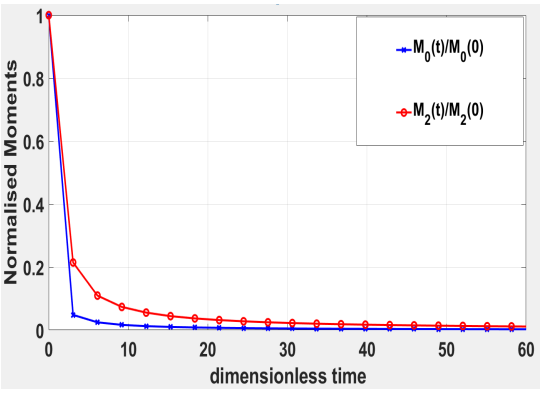

(b) Normalized moments

FIGURE 4.8: Condition (4.15) plot and normalized moments for $V_{i,j} = 2ij$

The initial condition is taken $f_i(0) = \frac{1}{2^i}$ and the steady-state solution at $i = 1$ is assumed to be equal to $f_1(t)$, i.e., $c_1 = 1/2$:

A similar type of kernel was discussed by Davidson [20] mentioned in Section 1. The normalized concentration plot of $f_i(t)$ for $N \in [1, 100]$ and its log-log plot for $N = 100$ with $t \in [0, 100]$ are shown in the Figures 4.10(a) and 4.10(b), respectively. Also, the

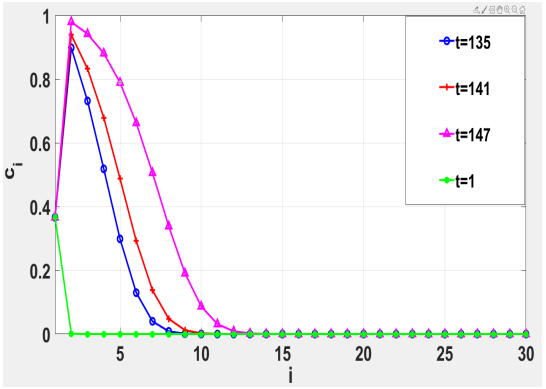

(a) c_i wrt i

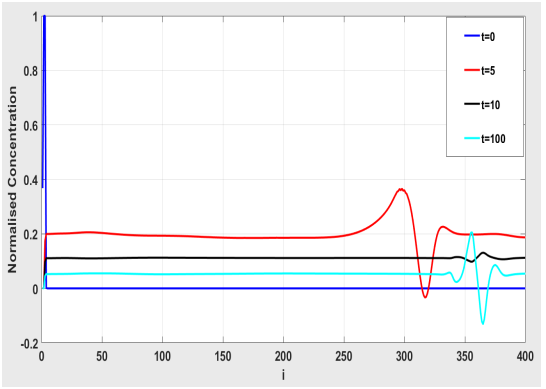

(b) $f_i(t)$ wrt i up to $N = 400$ and time step=20

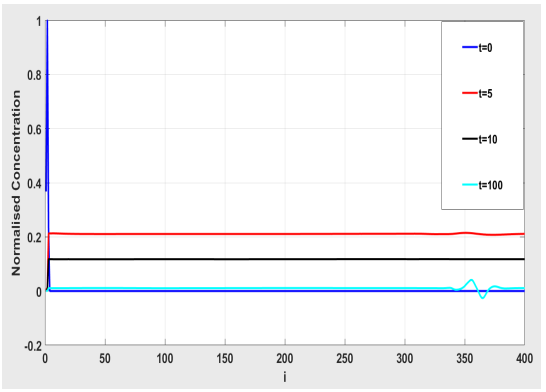

(c) $f_i(t)$ wrt i up to $N = 400$ and time step=100

FIGURE 4.9: Steady-state solution for $V_{i,j} = 2ij$

condition 4.15 holds and the normalized moments show steady-state behavior, see Figure 4.11. Figure 4.12(a) displays the steady-state solutions for different values of N and t while the oscillatory behavior are summarized in Figures 4.12(b) and 4.12(c). The oscillations arise around $N \approx 250$ for all values of t as can be observed through Figure 4.12(b). It is worth pointing out that this nature is present only at lower values of t but when t is increased up to 100, the steady-state is visible, see Figure 4.12(c). However, some oscillations can be seen at lower values of N (see Figure 4.12(b)), but when the value of N is increased, the solutions become stationary. The numerical simulations for $M_2(t)$ are reported in Table 4.4. Note that the computational time for Test cases 3 and 4 is more as compared to Test cases 1 and 2 due to high coagulation rates. Moreover, as expected, this leads to reaching steady-state conditions earlier. We also observe that the second moment $M_2(t)$ is a decreasing function of time for a particular value of N and a constant $K(T)$ can be found for every initial condition such that the second moment satisfies (4.10).

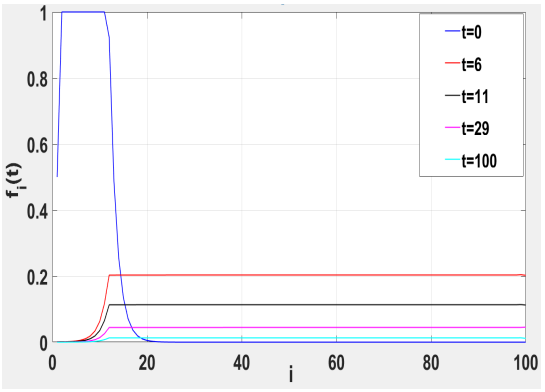

(a) f_i wrt i

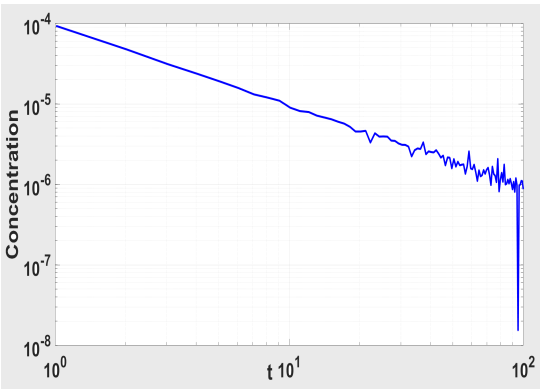

(b) Log-log plot of $f_i(t)$ when $N = 100$ and up to $t = 100$

FIGURE 4.10: Concentration plots for $V_{i,j} = 8i^{1/2}j^{1/2}$

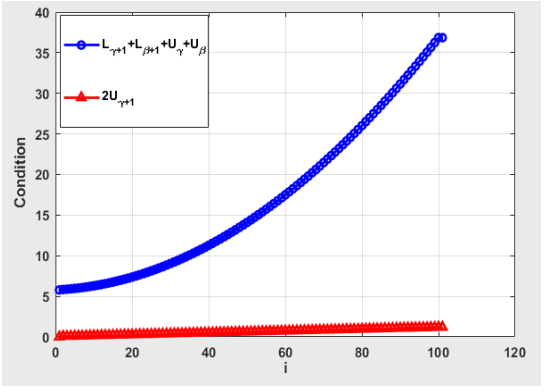

(a) Condition (4.15) plot

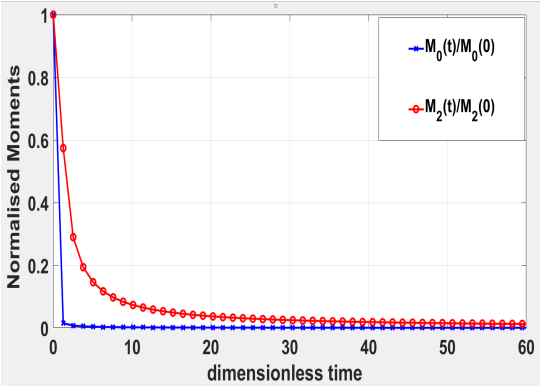

(b) Normalized moments

FIGURE 4.11: Condition (4.15) plot and normalized moments for $V_{i,j} = 8i^{1/2}j^{1/2}$

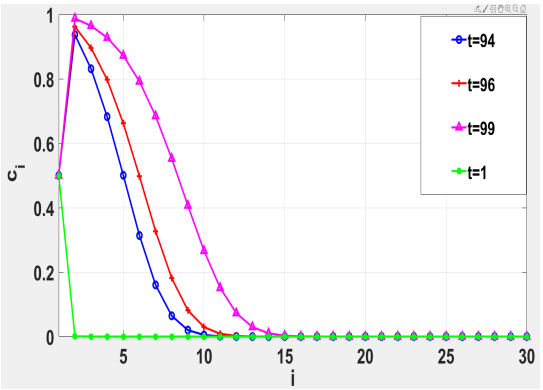

(a) c_i wrt i

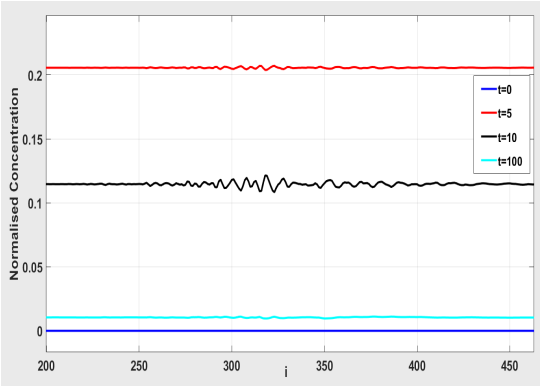

(b) $f_i(t)$ wrt i when N is from 200 to 460

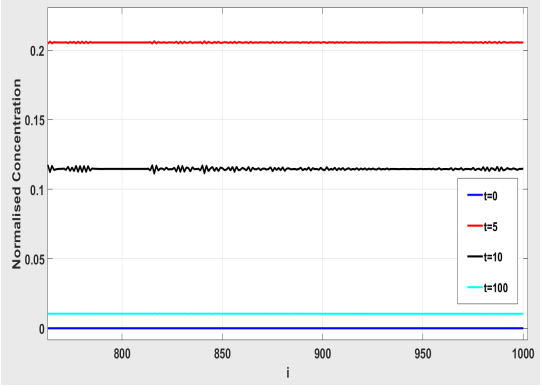

(c) $f_i(t)$ wrt i when N is from 750 to 1000

FIGURE 4.12: Steady-state solution for $V_{i,j} = 8i^{1/2}j^{1/2}$

TABLE 4.1: Values of $M_2(t)$ for different initial conditions for Test Case 1

IC	N	t	$M_2(t)$
e^{-i}	100	0	38.045
		100	17.476
		1000	1.715
	500	0	185.196
		100	438.827
		1000	43.218
e^{-i^2}	100	0	36.494
		100	17.589
		1000	1.727
	500	0	183.646
		100	440.250
		1000	43.270
$1/2^i$	100	0	55.000
		100	17.342
		1000	1.705
	500	0	255
		100	436.514
		1000	43.072

TABLE 4.2: Values of $M_2(t)$ for different initial conditions for Test Case 2

IC	N	t	$M_2(t)$
$1/2^i$	100	0	55.000
		100	.508
		1000	.015
	300	0	155
		100	1.594
		300	.556
e^{-i^2}	100	0	36.494
		100	.523
		1000	.051
	300	0	110.070
		100	1.628
		300	.539
		1000	.196
e^{-i}	100	0	38.045
		100	.515
		1000	.051
	300	0	111.620
		100	1.618
		1000	.536
		1500	.105

TABLE 4.3: Values of $M_2(t)$ for different initial conditions for Test Case 3

IC	N	t	$M_2(t)$
e^{-i^2}	50	0	18.1005
		50	.2472
		70	.1760
	70	0	25.4581
		50	.3453
		70	.2470
e^{-i}	50	0	19.6505
		50	.2472
		70	.1764
	70	0	27.6081
		50	.3451
		70	.2467
$1/2^i$	50	0	30.000
		50	.2413
		70	.1765
	70	0	40.000
		50	.3451
		70	.2470

TABLE 4.4: Values of $M_2(t)$ for different initial conditions for Test Case 4

IC	N	t	$M_2(t)$
$1/2^i$	100	0	55.000
		100	1.633
		1000	.163
	300	0	155
		100	9.075
		1000	.905
e^{-i^2}	100	0	36.494
		100	1.642
		1000	.164
	300	0	110.070
		100	9.085
		1000	.913
e^{-i}	100	0	38.045
		100	1.636
		1000	.163
	300	0	111.620
		100	9.073
		1000	.907

Chapter 5

A Novel Optimized Decomposition Method for Smoluchowski's Coagulation and Multi-Dimensional Burgers Equations[1]

In this chapter, we focus on the continuous version of Smoluchowski's equation modeling coagulation phenomenon [24] and the multi-dimensional Burgers equation [25, 32, 33]. Let us recall the coagulation equation which is written as

$$\frac{\partial u(t,x)}{\partial t} = \frac{1}{2}\int_0^x a(x-y,y)u(t,x-y)u(t,y)dy - u(t,x)\int_0^\infty a(x,y)u(t,y)dy, \tag{5.1}$$

for $x \in \mathbb{R}^+ :=]0,\infty[, t \in [0,\infty[$ and with initial datum

$$u(0,x) = u_0(x) \geq 0. \tag{5.2}$$

The one-dimensional Burgers equation [25, 31] is written as

$$\frac{\partial u}{\partial t} + u\frac{\partial u}{\partial x} = \nu\frac{\partial^2 u}{\partial x^2} + f(x,t), \tag{5.3}$$

with the initial data

$$u(x,0) = u_0(x). \tag{5.4}$$

[1]This work is published in *Journal of Computational and Applied Mathematics*, 419, 114710, 2023 and *Mathematics and Computers in Simulation*, 208, 326-350, 2023

The system of two-dimensional Burgers equation [32] is expressed as

$$\begin{aligned}\frac{\partial u}{\partial t}+u\frac{\partial u}{\partial x}+v\frac{\partial u}{\partial y}&=\frac{1}{R_e}\left(\frac{\partial^2 u}{\partial x^2}+\frac{\partial^2 u}{\partial y^2}\right),\\ \frac{\partial v}{\partial t}+u\frac{\partial v}{\partial x}+v\frac{\partial v}{\partial y}&=\frac{1}{R_e}\left(\frac{\partial^2 v}{\partial x^2}+\frac{\partial^2 v}{\partial y^2}\right),\end{aligned} \tag{5.5}$$

with the initial values

$$u(x,y,0)=f_1(x,y),\qquad v(x,y,0)=f_2(x,y),\qquad \forall (x,y)\in D \tag{5.6}$$

and boundary values

$$u(x,y,t)=g_1(x,y,t),\qquad v(x,y,t)=g_2(x,y,t),\qquad \forall (x,y)\in \partial D, \tag{5.7}$$

and the three-dimensional BE [33] is defined as

$$\frac{\partial}{\partial t}u=u\frac{\partial}{\partial x}u+\nu\left(\frac{\partial^2}{\partial x^2}u+\frac{\partial^2}{\partial y^2}u+\frac{\partial^2}{\partial z^2}u\right). \tag{5.8}$$

Recently, an article by Obidat [67] pointed out some demerits of the Adomian decomposition method (ADM) such as slow convergence [126] and inability to deal with the boundary conditions [127]. To overcome these issues, the author [67] introduced a new optimized decomposition method (ODM) for solving non-linear ordinary and partial differential equations and showed using numerical examples that ODM is much more efficient than ADM. Further, in [68], the ODM has been used to evaluate the approximated solutions for the second-order differential equations.

Therefore, it would be interesting to implement the ODM to compute the series solutions for the famous partial differential equation such as Burgers equation and integro-partial differential equations, in particular, the coagulation equation, and conduct a comparative analysis with the existing ADM [58]. So, this chapter is an attempt to introduce this method for the equations (5.1) and (5.3) and analyze the results theoretically and numerically. Additionally, as seen in the literature, the semi-analytical methods are known to be extended to multi-dimensional problems, it piques interest to develop the extension of ODM to compute the series solutions for the two and three-dimensional coupled Burgers equations.

We have considered several numerical examples and it is observed that ODM gives better agreement with the exact solution as compared to the well-established Adomian decomposition method (ADM) provided in [128] for all the cases considered for 1D Burgers equation. It is shown that the series solutions are convergent to the exact solutions in most of the cases. Moreover, by taking finite term approximations, the

numerical simulations are in excellent agreement with the analytical solutions for all the cases of 2D and 3D problems. Interestingly, ODM is able to obtain the series solution for a two-dimensional case where exact solution is not available and is validated by numerical results. In addition, the results for the coagulation equation are validated using several test cases including $a(x,y) = 1, a(x,y) = (x+y), a(x,y) = xy$ with $u(0,x) = e^{-x}$. Further, the comparison with the approximated solutions computed using ADM is shown to justify the novelty of the technique.

The chapter is organized as follows: Section 5.1 includes the preliminaries for ODM. The application of ODM to the coagulation equation, the theoretical results related to the convergence analysis, and the numerical examples are presented in Section 5.2. Section 5.3 presents the implementation of ODM to the one-dimensional Burgers equation along with the theoretical error estimates. The extension of ODM to the system of PDEs and its application to the two-dimensional BE are part of Section 5.4 and Section 5.5, respectively. The last Section 5.6 depicts the numerical test cases for one, two, and three-dimensional test cases and establishes the accuracy of the proposed method.

5.1 Optimized Decomposition Method: Preliminaries

Consider the equation of the type

$$\frac{\partial}{\partial t}u(t,x) = M[u(t,x)], \tag{5.9}$$

with the initial condition as given in (5.2) and where M is a non-linear operator in u. The solution of the above equation is written as

$$u(t,x) = u_0(x) + \mathcal{L}^{-1}\left(M[u(t,x)]\right), \tag{5.10}$$

where $\mathcal{L}^{-1}$ is the inverse operator of $\mathcal{L} = \frac{\partial}{\partial t}$. The main idea of this method revolves around obtaining a linear approximation to the non-linear problem. As in [67], under the assumption that the non-linear function $F\left(\frac{\partial}{\partial t}u, u\right) := \frac{\partial}{\partial t}u - M[u]$ can be linearized by a first-order Taylor series expansion at $t = 0$, the linear approximation to F can be obtained as

$$F\left(\frac{\partial}{\partial t}u, u\right) \approx \frac{\partial}{\partial t}u - C(x)u,$$

where

$$C(x) = \left.\frac{\partial M}{\partial u}\right|_{t=0}. \tag{5.11}$$

The above approximation leads us to a linear operator R defined as

$$R[u(t,x)] = M[u(t,x)] - C(x)u(t,x),$$

which is not easily invertible. Thanks to [67], the solution

$$u(t,x) = \sum_{k=0}^{\infty} u_k(t,x) \tag{5.12}$$

and the coefficients $u_k(t,x)$ are determined by TABLE 5.1

TABLE 5.1: Table of the coefficients for ODM

$u_0(t,x)$	$u_0(x)$
$u_1(t,x)$	$\mathcal{L}^{-1}\left(Q_0(t,x)\right)$
$u_2(t,x)$	$\mathcal{L}^{-1}\left(Q_1(t,x) - C(x)u_1(t,x)\right)$
$u_{k+1}(t,x)$	$\mathcal{L}^{-1}\left(Q_k(t,x) - C(x)(u_k(t,x) - u_{k-1}(t,x))\right), \quad k \geq 2$

where

$$Q_k(t,x) = \frac{1}{k!}\frac{d^k}{d\theta^k}\left[M\left(\sum_{i=0}^{k}\theta^i u_i(t,x)\right)\right]\Bigg|_{\theta=0}, \tag{5.13}$$

and

$$M\left[\sum_{k=0}^{\infty} u_k(t,x)\right] = \sum_{k=0}^{\infty} Q_k(t,x). \tag{5.14}$$

The following proposition discusses the condition required for the convergence of this method.

Proposition 5.1. *Let the coefficients of the series solution be determined by TABLE 5.1 and the series* $\sum_{k=0}^{\infty} u_k(t,x)$ *is convergent then* $u(t,x)$ *is the solution of equation* (5.9).

Proof. Given that

$$\sum_{k=0}^{\infty} u_k(t,x) = u_0(x) + \mathcal{L}^{-1}\Bigg(Q_0(t,x) + [Q_1(t,x) - C(x)u_1(t,x)] + [Q_2(t,x) - C(x)$$
$$(u_2(t,x) - u_1(t,x))] + \ldots + [Q_{n-1}(t,x) - C(x)(u_{n-1}(t,x) - u_{n-2}(t,x))] + \ldots\Bigg).$$

Simplifying the above equation followed by using the convergence of the series $\sum_{k=0}^{\infty} u_k(t,x)$ which ensures that $\lim_{k\to\infty} u_k = 0$, we get

$$\sum_{k=0}^{\infty} u_k(t,x) = u_0(x) + \mathcal{L}^{-1}\Big(\sum_{k=0}^{\infty} Q_k(t,x)\Big).$$

The equation (5.14) and $u(t,x) = \sum_{k=0}^{\infty} u_k(t,x)$ yield

$$u(t,x) = u_0(x) + \mathcal{L}^{-1}\Big(M\Big[\sum_{k=0}^{\infty} u_k(t,x)\Big]\Big),$$

and so $\mathcal{L}[u(t,x)] = M[u(t,x)]$. Hence, $u(t,x)$ is the solution of (5.9). □

Remark 5.2. Note that the iterative scheme for ODM reduces to ADM if $C(x) = 0$. Also, let us define the coefficients and the n-term series solutions for ADM as $v_k(t,x)$ and $\psi_n(t,x)$, respectively, where $\psi_n(t,x)$ is given as

$$\psi_n(t,x) = \sum_{k=0}^{n} v_k(t,x). \tag{5.15}$$

Remark 5.3. As explained in [67], ODM is an optimized method in the sense that the approximation $R[u] = \frac{\partial}{\partial t}u - C(x)u$ is the best linear approximation to $F(\frac{\partial}{\partial t}u, u)$ near $t = 0$, i.e, near the initial data $u(0,x)$.

5.2 ODM Implementation for Coagulation Equation

In this section, the general expression for the n-term series solution is provided for the coagulation equation (5.1). For this, define the non-linear operator M as

$$M[u(t,x)] = \frac{1}{2}\int_0^x a(x-y,y)u(t,x-y)u(t,y)dy - u(t,x)\int_0^\infty a(x,y)u(t,y)dy, \tag{5.16}$$

then using Leibnitz rule (differentiating wrt $u(t,x)$), we obtain

$$C(x) = \frac{1}{2}\int_0^x a(x-y,y)u(0,y)dy - \int_0^\infty a(x,y)u(0,y)dy. \tag{5.17}$$

Having (5.16) and (5.17), the linear operator R becomes

$$\begin{aligned} R[u(t,x)] = \frac{1}{2}\int_0^x a(x-y,y)u(t,x-y)u(t,y)dy - u(t,x)\int_0^\infty a(x,y)u(t,y)dy \\ -\Big(\frac{1}{2}\int_0^x a(x-y,y)u(0,y)dy - \int_0^\infty a(x,y)u(0,y)dy\Big)u(t,x). \end{aligned}$$

Setting $k = 0$ in (5.13) and using (5.16), the term Q_0 is written as

$$Q_0(t,x) = \left(\frac{1}{2}\int_0^x a(x-y,y)u_0(t,x-y)u_0(t,y)dy - u_0(t,x)\int_0^\infty a(x,y)u_0(t,y)dy\right),$$

so that,

$$u_1(t,x) = \mathcal{L}^{-1}\left(\frac{1}{2}\int_0^x a(x-y,y)u_0(t,x-y)u_0(t,y)dy - u_0(t,x)\int_0^\infty a(x,y)u_0(t,y)dy\right). \tag{5.18}$$

Further, $k=1$ in (5.13) yields

$$\begin{aligned} Q_1(t,x) = \frac{1}{2}\int_0^x a(x-y,y)\Big(u_0(t,x-y)u_1(t,y) + u_1(t,x-y)u_0(t,y)\Big)dy \\ - \int_0^\infty a(x,y)\Big(u_0(t,x)u_1(t,y) + u_1(t,x)u_0(t,y)\Big)dy, \end{aligned}$$

which using (5.17), gives

$$\begin{aligned} u_2(t,x) = \mathcal{L}^{-1}\Bigg(&\frac{1}{2}\int_0^x a(x-y,y)\Big(u_0(t,x-y)u_1(t,y) + u_1(t,x-y)u_0(t,y)\Big)dy \\ &- \int_0^\infty a(x,y)\Big(u_0(t,x)u_1(t,y) + u_1(t,x)u_0(t,y)\Big)dy \\ &- u_1(t,x)\Big(\frac{1}{2}\int_0^x a(x-y,y)u(0,y)dy - \int_0^\infty a(x,y)u(0,y)dy\Big)\Bigg). \end{aligned} \tag{5.19}$$

Finally, for $k \geq 2$ and only when $i+j=k$, we have

$$Q_k(t,x) = \frac{1}{2}\int_0^x a(x-y,y)\Big(\sum_{i=0}^k u_i(t,x-y)\sum_{j=0}^k u_j(t,y)\Big)dy - \int_0^\infty a(x,y)\Big(\sum_{i=0}^k u_i(t,x)\sum_{j=0}^k u_j(t,y)\Big)dy,$$

and

$$\begin{aligned} u_{k+1}(t,x) = \mathcal{L}^{-1}\Bigg(&\frac{1}{2}\int_0^x a(x-y,y)\Big(\sum_{i=0}^k u_i(t,x-y)\sum_{j=0}^k u_j(t,y)\Big)dy \\ &- \int_0^\infty a(x,y)\Big(\sum_{i=0}^k u_i(t,x)\sum_{j=0}^k u_j(t,y)\Big)dy - C(x)\Big[u_k(t,x) - u_{k-1}(t,x)\Big]\Bigg). \end{aligned} \tag{5.20}$$

Hence, the n-term series solution for (5.1) becomes

$$\begin{aligned} \phi_n(t,x) := \sum_{k=0}^n u_k(t,x) = u_0(x) + \mathcal{L}^{-1}\Bigg(&Q_0(t,x) + [Q_1(t,x) - C(x)u_1(t,x)] + [Q_2(t,x) - C(x) \\ &(u_2(t,x) - u_1(t,x))] + \ldots + [Q_{n-2}(t,x) - C(x)(u_{n-2}(t,x) - u_{n-3}(t,x))] \\ &+ [Q_{n-1}(t,x) - C(x)(u_{n-1}(t,x) - u_{n-2}(t,x))]\Bigg). \end{aligned}$$

Simplifying the above equation enables us to have

$$\begin{aligned}\phi_n(t,x) &:= u_0(x) + \mathcal{L}^{-1}\Big(\sum_{k=1}^{n} Q_{k-1}(t,x) - C(x)u_{n-1}(t,x)\Big)\\ &= u_0(x) + \mathcal{L}^{-1}\Big(M(\phi_{n-1}(t,x)) - C(x)u_{n-1}(t,x)\Big)\\ &= u_0(x) + \mathcal{L}^{-1}\Big(M\Big(\sum_{k=0}^{n-1} u_k(t,x)\Big) - C(x)u_{n-1}(t,x)\Big).\end{aligned}$$

5.2.1 Convergence Analysis

Consider the Banach space $B = (\mathcal{C}([0,T]) : L^1[0,\infty), ||\cdot||)$ with the norm defined as

$$||u|| = \sup_{s\in[0,T]} \int_0^\infty |u(s,x)|dx < \infty, \tag{5.21}$$

and $D = \{u \in B : ||u|| \leq 2L\}$, where $L > 1/2$. Using the expression of solution from (5.10) and the definition of function M from (5.16), the equation (5.1) is expressed in the following form

$$u = \mathcal{A}u, \tag{5.22}$$

where $\mathcal{A} : B \to B$ is a non-linear operator defined by

$$\mathcal{A}u = u_0(x) + \mathcal{L}^{-1}\left(M[u(t,x)]\right). \tag{5.23}$$

Now, taking into account the recursive scheme for (5.1) and using (5.23), the n-term series solution becomes

$$\phi_n = \mathcal{A}\phi_{n-1} - \int_0^t C(x)u_{n-1}(s,x)ds. \tag{5.24}$$

To establish our main findings in Theorem 5.5 below, the following theorem is required which states an important result regarding the contraction mapping of the operator $\mathcal{A}$. The result plays a significant role in proving that the sequence $\{\phi_n\}$ is a Cauchy sequence which finally proves that the series solution converges towards the exact solution.

Theorem 5.4. *Let the operator $\mathcal{A}$ be defined in (5.23) such that $a(x,y) = 1$, $\forall\ x, y \in (0,\infty)$. Then $\mathcal{A} : D \to D$ is a contraction map, i.e., $||\mathcal{A}u - \mathcal{A}u^*|| \leq \delta||u - u^*||$, $\forall\ u, u^* \in D$ if*

$$\delta = T\exp(2TL)[||u_0|| + 2TL^2 + 2TL] < 1,$$

holds, where $L > 1/2$.

Proof. To establish the contraction mapping of $\mathcal{A}$, the above equation can be written in the following equivalent form

$$\frac{\partial}{\partial t}[u(t,x)\exp[H(x,t,u)]] = \frac{1}{2}\exp[H(x,t,u)]\int_0^x a(x-y,y)u(t,x-y)u(t,y)dy,$$

where,

$$H(x,t,u) = \int_0^t \int_0^\infty a(x,y)u(s,y)dyds.$$

Thus the equivalent operator $\tilde{\mathcal{A}}$ is given by

$$\tilde{\mathcal{A}}u = u_0(x)\exp[-H(x,t,u)] + \frac{1}{2}\int_0^t \exp[H(x,s,u) - H(x,t,u)]\int_0^x a(x-y,y)u(x-y,s)u(s,y)dyds, \tag{5.25}$$

where $\tilde{A}$ maps D to itself. Let, $u, u^* \in D$ and define $W(x,s,t) = \exp[H(x,s,u) - H(x,t,u)] - \exp[H(x,s,u^*) - H(x,t,u^*)]$, then

$$\begin{aligned}\tilde{\mathcal{A}}u - \tilde{\mathcal{A}}u^* &= u_0(x)W(x,0,t) + \frac{1}{2}\int_0^t \left(W(x,s,t)\int_0^x u(s,x-y)u(s,y)dy\right)ds \\ &- \frac{1}{2}\int_0^t \left(\exp[H(x,s,u^*) - H(x,t,u^*)]\right) \\ &.\left(\int_0^x u^*(x-y,s)(u(y,s)-u^*(y,s))dy + \int_0^x u(y,s)(u(x-y,s)-u^*(x-y,s))dy\right)ds.\end{aligned} \tag{5.26}$$

We shall now obtain a bound on $W(x,0,t)$ and $W(x,s,t)$ as

$$\begin{aligned}|W(x,s,t)| &= \left|\exp\left[-\int_s^t\int_0^\infty u(\tau,y)dyd\tau\right] - \exp\left[-\int_s^t\int_0^\infty u^*(\tau,y)dyd\tau\right]\right| \\ &= \left|-\exp\left[-\int_s^t\int_0^\infty u^*(\tau,y)dyd\tau\right]\left(1-\exp\left[-\int_s^t\int_0^\infty u(\tau,y)dyd\tau + \int_s^t\int_0^\infty u^*(\tau,y)dyd\tau\right]\right)\right| \\ &\leq \exp\left[\int_s^t\int_0^\infty u^*(\tau,y)dyd\tau\right](t-s)||u-u^*||, \quad \text{using} \quad 1-\exp[-x] \leq x, \forall x \\ &\leq t\exp[2tL]||u-u^*||.\end{aligned}$$

Now, using the definition of norm (5.21), the Eqn. (5.26), one be easily expressed as

$$\begin{aligned}||\tilde{\mathcal{A}}u - \tilde{\mathcal{A}}u^*|| &\leq t\exp[2tL]||u-u^*||\left(||u_0|| + \int_0^t\left(\frac{1}{2}(||u||^2 + ||u|| + ||u^*||)\right)ds\right. \\ &\leq t\exp[2tL]||u-u^*||(||u_0|| + 2tL^2 + 2tL) \leq T\exp[2TL](||u_0|| + 2TL^2 + 2TL)||u-u^*||.\end{aligned}$$

If $\delta = T\exp[2TL](||u_0|| + 2TL^2 + 2TL) < 1$, then $\tilde{\mathcal{A}}$ is a contraction mapping on D, and so is $\mathcal{A}$. □

Theorem 5.5. *Let the coefficients of the series solution for the coagulation equation* (5.1) *be determined by the equations* (5.18)-(5.20) *and* ϕ_n *be the n-term series solution defined by* (5.24)*. Then,* ϕ_n *converges to the exact solution u with*

$$||u - \phi_m|| \leq \frac{\delta^m}{1-\delta}||u_1||, \tag{5.27}$$

if the following conditions hold

(A1) $\delta = T\exp(2TL)[||u_0||+2TL^2+2TL] < 1$*, where* $L > 1/2$*, and* $||u_1|| \leq 2L$*.*

(A2) $||u_{m-l} - u_{m-(l+1)}|| < \varepsilon$*, for* $0 \leq l \leq (m-1)$ *where* $\varepsilon = \frac{1}{n^p}$ *such that* $p > 1$*.*

(A3) $C(x) \in L^\infty(B, |\cdot|_\infty)$ *where* $|\cdot|_\infty$ *is the essential supremum norm, i.e.,* $|C(x)| \leq k$ *for some* $k \in \mathbb{R}^+$*.*

Proof. Following (5.24), consider

$$||\phi_n - \phi_m|| = \left|\left|\mathcal{A}\phi_{n-1} - \int_0^t C(x)u_{n-1}(s,x)ds - \mathcal{A}\phi_{m-1} + \int_0^t C(x)u_{m-1}(s,x)ds\right|\right|.$$

The triangle inequality gives us

$$||\phi_n - \phi_m|| \leq ||\mathcal{A}\phi_{n-1} - \mathcal{A}\phi_{m-1}|| + \left|\left|\int_0^t C(x)\left(u_{n-1}(s,x) - u_{m-1}(s,x)\right)ds\right|\right|.$$

Theorem 5.4 yield

$$||\phi_n - \phi_m|| \leq \delta||\phi_{n-1} - \phi_{m-1}|| + \left|\left|\int_0^t C(x)\left(u_{n-1}(s,x) - u_{m-1}(s,x)\right)ds\right|\right|.$$

Putting $n = m+1$ in the above expression, using $(A2)$, and further simplifications lead to

$$\begin{aligned}
||\phi_{m+1} - \phi_m|| &\leq \delta||\phi_m - \phi_{m-1}|| + \varepsilon t|C(x)|_\infty \\
&= \delta\left|\left|\mathcal{A}\phi_{m-1} - \int_0^t C(x)u_{m-1}(s,x)ds - \mathcal{A}\phi_{m-2} - \int_0^t C(x)u_{m-2}(s,x)ds\right|\right| + \varepsilon t|C(x)|_\infty \\
&\leq \delta\Big(\delta||\phi_{m-1} - \phi_{m-2}|| + \varepsilon t|C(x)|_\infty\Big) + \varepsilon t|C(x)|_\infty \\
&\vdots \\
&\leq \delta^m||\phi_1 - \phi_0|| + \varepsilon tk\left(1 + \delta + \delta^2 + \ldots + \delta^{m-1}\right).
\end{aligned}$$

Now,

$$\begin{aligned}
||\phi_n - \phi_m|| &\leq ||\phi_{m+1} - \phi_m|| + ||\phi_{m+2} - \phi_{m+1}|| + \ldots + ||\phi_n - \phi_{n-1}|| \\
&\leq [\delta^m ||\phi_1 - \phi_0|| + \varepsilon tk \left(1 + \delta + \delta^2 + \ldots + \delta^{m-1}\right)] \\
&\quad + [\delta^{m+1} ||\phi_1 - \phi_0|| + \varepsilon tk \left(1 + \delta + \delta^2 + \ldots + \delta^{m}\right)] \\
&\quad + \ldots + [\delta^{n-1} ||\phi_1 - \phi_0|| + \varepsilon tk \left(1 + \delta + \delta^2 + \ldots + \delta^{n-2}\right)] \\
&= \left(\delta^m + \delta^{m+1} + \ldots + \delta^{n-1}\right) ||\phi_1 - \phi_0|| \\
&\quad + \varepsilon tk[(1 + \delta + \delta^2 + \ldots + \delta^{m-1}) + (1 + \delta + \delta^2 + \ldots + \delta^{m}) \\
&\quad + \ldots + (1 + \delta + \delta^2 + \ldots + \delta^{n-2})] \\
&= \frac{\delta^m(1 - \delta^{n-m})}{1 - \delta} ||\phi_1 - \phi_0|| + \varepsilon tk \Big[\frac{(1 - \delta^m)}{1 - \delta} + \frac{(1 - \delta^{m+1})}{1 - \delta} + \ldots + \frac{(1 - \delta^{n-1})}{1 - \delta}\Big].
\end{aligned}$$

For a suitable t_0 and thanks to $(A1)$, the above expression becomes

$$||\phi_n - \phi_m|| \leq \frac{\delta^m}{1 - \delta} ||u_1|| + \frac{\varepsilon t_0 k}{(1 - \delta)} (n - m). \tag{5.28}$$

Finally, using $(A2)$ and $\frac{1}{n^p} < \frac{1}{m^p}$, the above expression converges to zero as $m \to \infty$. Since, $\frac{\delta^m}{1-\delta} < 1$, using $(A1)$, we have $||\phi_n - \phi_m|| \leq 2L$. Thus, $\exists$ a ϕ such that $\lim_{n\to\infty} \phi_n = \phi$ and so $u = \sum_{k=0}^{\infty} u_k = \lim_{n\to\infty} \phi_n = \phi$, which is the exact solution of (5.22). Finally, fixing m and letting $n \to \infty$ in the equation (5.28), we obtain the theoretical error bound (5.27). □

5.2.2 Numerical Examples

This section includes the implementation of ODM for several test cases of coagulation equation (5.1) considering three different kernels, i.e., constant $(a(x, y) = 1)$, sum $(a(x, y) = x + y)$ and product $(a(x, y) = xy)$ with the initial condition $u_0(x) = e^{-x}$. The calculations of the approximated solutions and other requisite computations are done with the help of MATHEMATICA©. To establish the accuracy of ODM, the series solution is compared with the available exact solution for concentration and moments. Further, the ODM results are also compared with the findings of ADM proposed in [58] and it is shown through graphs and tables of errors that ODM enjoys better estimates than ADM.

Example 5.1. *Consider the case of constant aggregation, i.e., $a(x, y) = 1$ with $u_0(x) = e^{-x}$. The exact solution in this case is given in [129] as*

$$u(t, x) = \frac{4}{(2 + t)^2} e^{-\frac{2x}{2+t}}.$$

Using the equations (5.16), (5.17) and (5.18-5.20), one gets

$$
\begin{aligned}
C(x) &= \frac{1}{2}(\sinh(x) - \cosh(x)) - \frac{1}{2}, \qquad u_0(x) = e^{-x},\\
u_1(t,x) &= \frac{te^{-x}(x-2)}{2^1 1!},\\
u_2(t,x) &= \frac{e^{-2x}t^2}{2^2 2!}(-2+x) + \frac{e^{-x}t^2}{2^2 2!}(4-5x+x^2),\\
u_3(t,x) &= \frac{e^{-3x}t^3}{2^3 3!}(-2+x) + \frac{e^{-2x}t^3}{2^3 3!}(8-8x+x^2) + (-1)^3 3!\,\frac{e^{-2x}t^2}{2^3 3!}(-2+x) + (-1)^3 2!\,\frac{e^{-x}}{2^3 3!}(-2+x)\\
&\quad + \frac{t^3 e^{-x}}{2^3 3!}(x^3 + 25x - 10x^2 - 29/2),\\
u_4(t,x) &= \frac{e^{-4x}t^4}{2^4 4!}(-2+x) + 9e^{x}(-32(-2+x) + t(23 - 20x + 2x^2)) + 9e^{2x}(-16(4-6x+x^2) +\\
&\quad tau(-101 + 138x - 26x^2 + 2x^3)) + e^{3x}(-72(15 - 20x + 4x^2)\\
&\quad + t(1073 - 2511x + 1494x^2 - 300x^3 + 18x^4))).
\end{aligned}
$$

As we proceed further, the coefficients become more complex but thanks to MATHEMATICA©, higher terms can be computed using the equation (5.20).

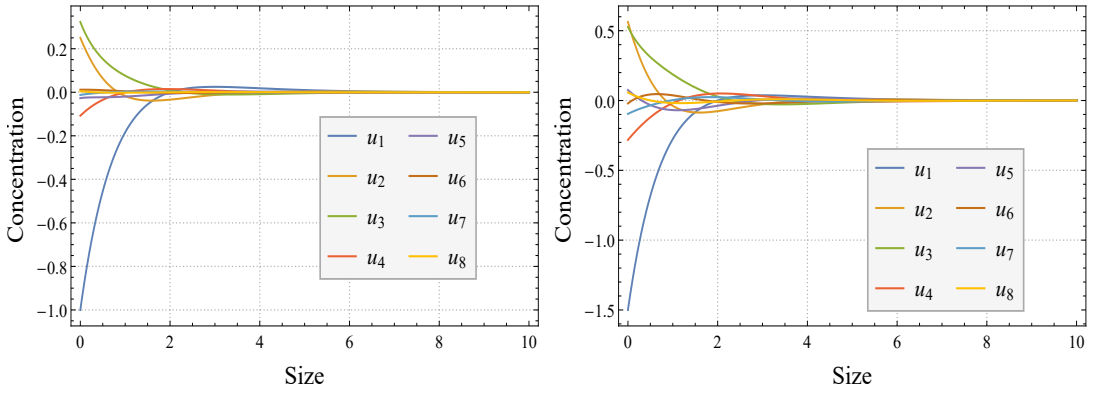

(a) Coefficients plot at $t = 1$ (b) Coefficients plot at $t = 1.5$

FIGURE 5.1: ODM coefficients plot for Example 5.1

Figure 5.1(a) and Figure 5.1(b) graphically depict the coefficients $u_k(t,x)$ of ODM for $k = 1, 2, \ldots, 8$ at $t = 1$ and $t = 1.5$, respectively. These coefficients plot help in deciding which n to choose to compute the non-negative approximate solution $\phi_n(t,x)$. For instance, at $t = 1$, the most negative value contribution is from $u_1(t,x)$ but the positive value contribution from $u_2(t,x)$ and $u_3(t,x)$ can not surpass this negative value. Further, it is easy to see that $u_4(t,x)$ and $u_5(t,x)$ are again negative, but the addition of the positive value of $u_6(t,x)$ gives the non-negative 6-term solution $\phi_6(t,x)$ as the first desired non-negative solution whose value is interestingly close to the exact solution $u(t,x)$. By following Singh et al. [58], Figure 5.2 shows the plot of the coefficients for

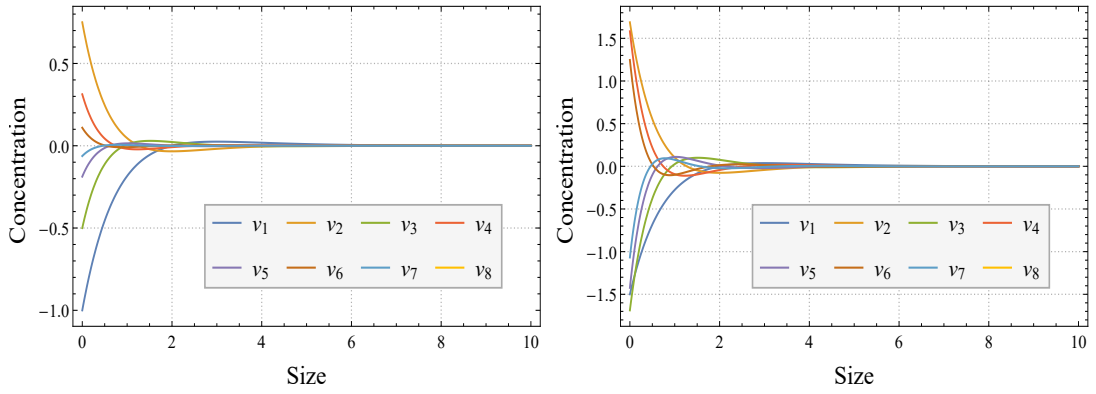

(a) Coefficients plot at $t = 1$ (b) Coefficients plot at $t = 1.5$

FIGURE 5.2: ADM coefficients plot for Example 5.1

the approximate series solutions computed using ADM at $t = 1$ and $t = 1.5$. These coefficients are denoted by $v_k(t, x)$ and it can be observed that $v_k(t, x)$ is negative for odd values of k while positive for even values of k for both values of t. This leads to the negative of $\psi_k(t, x)$ for odd k, which is not the case for the ODM coefficients for any k.

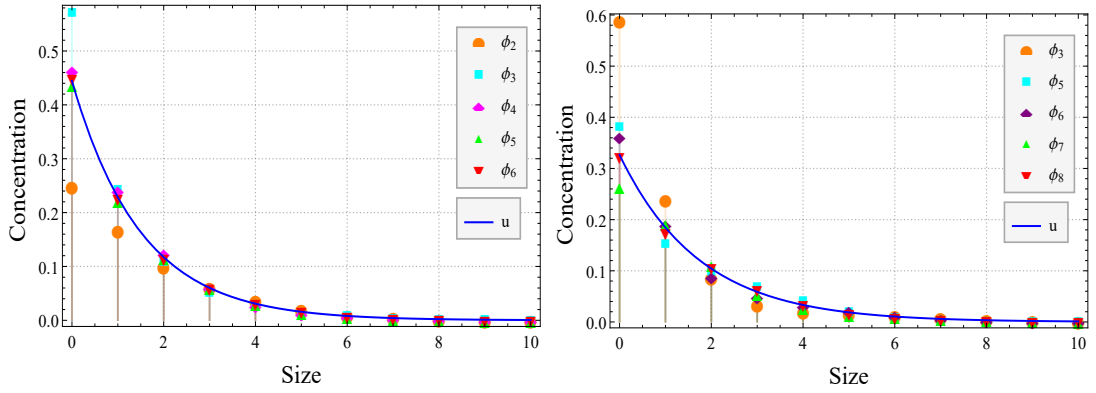

(a) at $t = 1$ (b) at $t = 1.5$

FIGURE 5.3: Series solutions using ODM at $t = 1$ and $t = 1.5$ for Example 5.1

To see these finite term solutions ϕ_n and ψ_n for various values of n, the comparison with the exact number density is provided at time $t = 1$ and $t = 1.5$ for ODM in Figure 5.3 and ADM in Figure 5.4. One can also visualize the decreasing behavior of the concentration (u, ϕ_n and ψ_n) as size increases which confirms the aggregation of particles. In addition to this, Figure 5.3 depicts that as time increases from $t = 1$ to $t = 1.5$, concentration value reduces. It is evident from Figure 5.5 that the 8-term solution ψ_8 by ADM and 6-term solution ϕ_6 by ODM are close to the exact solution $u(t, x)$ at $t = 1$. Further, at $t = 1.5$, ψ_{14} is nearest to $u(t, x)$ whereas only 8-term solution ϕ_8 is required to get the same accuracy with the exact solution. This indicates the advantage of using ODM over

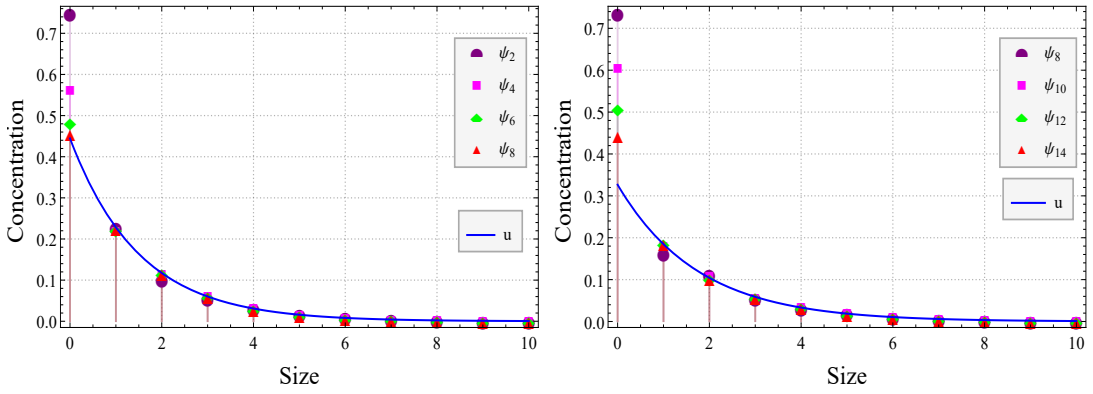

(a) $t = 1$ (b) $t = 1.5$

FIGURE 5.4: Series solutions using ADM at $t = 1$ and $t = 1.5$ for Example 5.1

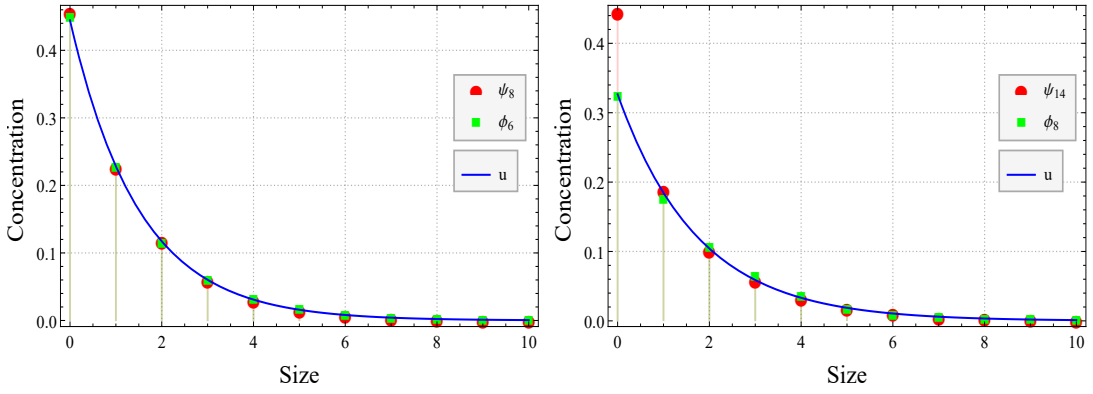

(a) Comparison of $\psi_8(t,x)$, $\phi_6(t,x)$ and $u(t,x)$ at $t = 1$ (b) Comparison of $\psi_{14}(t,x)$, $\phi_8(t,x)$ and $u(t,x)$ at $t = 1.5$

FIGURE 5.5: Comparison of ODM, ADM and exact number density at $t = 1$ and $t = 1.5$ for Example 5.1

ADM. Moving further, the efficacy of the two methods is also compared by calculating the moments of the approximated solutions and comparing them with the moments of the exact solution. The r^{th} moment of the exact solution is defined as

$$\mu_r^{Exact}(t) = \int_0^\infty x^r u(t,x)dx, \tag{5.29}$$

while for the ODM and ADM approximated solutions, it is given by

$$\mu_{r,n}^{ODM}(t) = \int_0^\infty x^r \phi_n(t,x)dx, \quad \mu_{r,n}^{ADM}(t) = \int_0^\infty x^r \psi_n(t,x)dx, \tag{5.30}$$

respectively. These moments are relevant physical quantities with zeroth moment (obtained by putting $r = 0$ in (5.29)) being the total number of clusters and the first moment ($r = 1$ in (5.29)) gives the total mass (volume) of the system. Putting $r = 2$ gives the

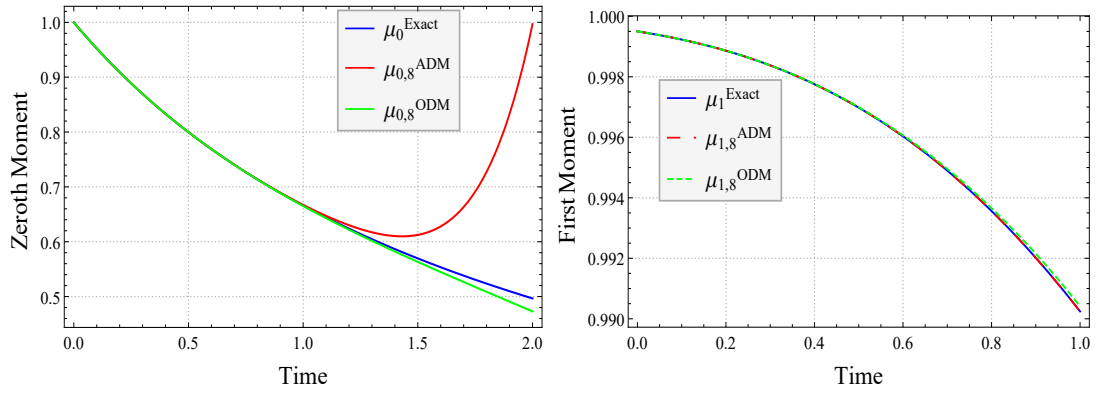

(a) Zeroth moment (b) First moment

FIGURE 5.6: Moments comparison: ODM, ADM, and exact solutions for Example 5.1

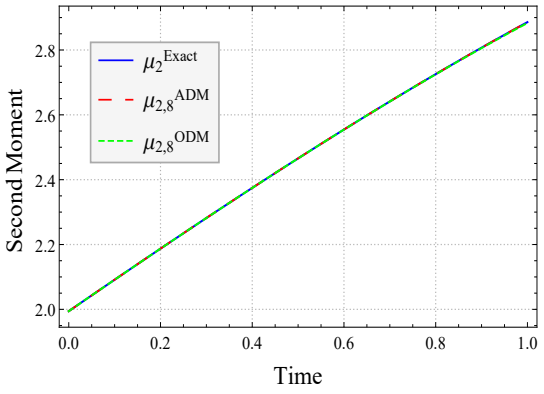

FIGURE 5.7: Second-moment comparison: ODM, ADM and exact solutions for Example 5.1

second moment which is defined as the energy dissipated by the system [22]. In Figure 5.6, the zeroth and first moments are computed using 8-term series solutions of ODM and ADM and the results are compared with the exact moments. It is well known that the number of particles in a coagulation system has a decreasing trend and is justified by the moments plotted in Figure 5.6(a). However, it is visualized here that $\mu_{0,8}^{ADM}(t)$ starts to get away from $\mu_0^{Exact}(t)$ approximately around $t = 1$ whereas $\mu_{0,8}^{ODM}(t)$ gives nice accuracy. Since Figure 5.5 concludes that ϕ_8 is closest to the exact solution u at $t = 1.5$, it is imperative that ODM will give the best approximation, but the method is performing well even when time is increased up to $t = 2$. The first and second moments using approximated solutions ϕ_8 and ψ_8 are compared with the corresponding exact moments in Figures 5.6(b) and 5.7. The increasing nature of the second moment plot, as time progresses, shows that more energy is dissipated with time. This is due to the formation of bigger particles due to the coagulation process. It needs to be mentioned here that for $i = 1, 2$, $\mu_{i,8}^{ODM}(t)$ and $\mu_{i,8}^{ADM}(t)$ estimate $\mu_i^{Exact}(t)$ very well.

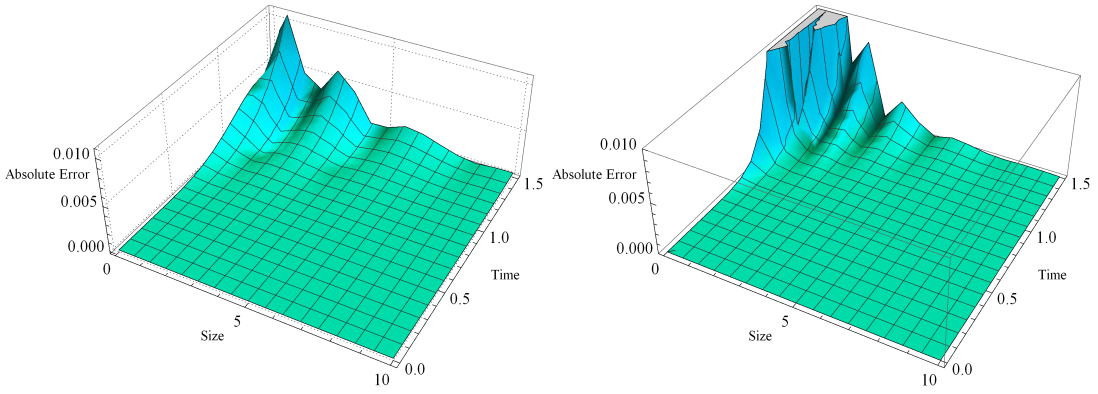

(a) ODM (b) ADM

FIGURE 5.8: Absolute error plots for ODM and ADM series solutions for Example 5.1

TABLE 5.2: Comparison of numerical errors in computing approximate solutions using ADM and ODM for Eqn (5.1) with parameters as given in Example 5.1

n	2	3	4	5	6	8
ADM at $t = 0.5$	0.023	0.006	0.002	4.5×10^{-4}	1.2×10^{-4}	8.3×10^{-6}
ODM at $t = 0.5$	0.054	0.014	0.007	0.002	4.6×10^{-4}	3.6×10^{-5}
ADM at $t = 1$	0.149	0.082	0.044	0.024	0.013	0.004
ODM at $t = 1$	0.178	0.086	0.036	0.015	0.008	0.003
ADM at $t = 1.5$	0.428	0.353	0.287	0.231	0.184	0.115
ODM at $t = 1.5$	0.328	0.230	0.010	0.075	0.060	0.027
ADM at $t = 2$	0.882	0.972	1.054	1.131	1.200	1.332
ODM at $t = 2$	0.517	0.441	0.286	0.295	0.245	0.166

The novelty of ODM can also be justified by looking at 3D plots in Figure 5.8 which provides the absolute error between the exact and the approximated number density computed using 8-term series solutions for both the methods. We also summarize the numerical errors associated with the ADM and ODM at $t = 0.5$, $t = 1$, $t = 1.5$, and $t = 2$ in TABLE 5.2. These errors are computed by dividing the interval $[0, 10]$ into N sub-intervals $[x_{i-1/2}, x_{i+1/2}], i = 1(1)N$. Each interval is represented by the mid-point $x_i = \frac{x_{i-1/2}+x_{i+1/2}}{2}$ and the error is computed using the following rule

$$\text{Error} = \sum_{i=1}^{N} |\xi_n^i - u_i| h_i, \tag{5.31}$$

where $\xi_n^i = \xi_n(t, x_i)$ and $u_i = u(t, x_i)$ are the series and exact solutions with step size $h_i = x_{i+1/2} - x_{i-1/2}$. All the computations are done by considering $N = 100$ and $h_i = 0.1$ $\forall\ i$. The table clearly shows that the error for ADM is less than ODM when $t = 0.5$. But when the value of t is increased which is a more realistic scenario, the error for ODM is seen to be lower than the error associated with the ADM. There is a significant difference in the error for ODM and ADM at $t = 2$ which claims the superiority of the novel method. Furthermore, TABLE 5.3 presents the order of convergence at $t = 2$ and it indicates that ADM has a slower rate of convergence than ODM. Although, as h tends to 0, the order of convergence for both methods approaches 1.

TABLE 5.3: Order of convergence using ADM and ODM at $t = 2$ for Eqn (5.1) with parameters as given in Example 5.1.

h	ADM	ODM
0.5		
	0.38	0.92
0.25		
	0.63	1
(0.25)/2		
	0.82	1
(0.25)/4		
	0.89	1
(0.25)/8		

Example 5.2. *The computation of ODM series solution for the aggregation parameter* $a(x, y) = (x + y)$ *with exponential initial value* $u_0(x) = e^{-x}$ *is done and the simulation results are compared with the exact solution defined in [130] as*

$$u(t, x) = \frac{e^{-t} \exp(x(e^{-t} - 2)) I_1\left(2x\sqrt{1 - e^{-t}}\right)}{x\sqrt{1 - e^{-t}}}.$$

Following equations (5.16), (5.17) and (5.18-5.20) give us

$$\begin{aligned}
C(x) &= \frac{1}{2}x(\sinh(x) - \cosh(x) - 1) - 1, \quad u_0(x) = e^{-x}, \\
u_1(t, x) &= \frac{1}{2}te^{-x}(x(x - 2) - 2), \\
u_2(t, x) &= \frac{1}{24}t^2e^{-2x}x\left(e^x(2x + 3)((x - 6)x + 6) + 3((x - 2)x - 2)\right), \\
u_3(t, x) &= \frac{1}{576}t^2e^{-3x}\left(-72e^x(x^2 - 2x - 2)(x + e^x(x + 2) + t(12((x - 2)x - 2)x^2))\right) \\
&\quad + e^{-x}(x(2x(x(x(2x^2 - 17x + 2) + 144) - 84) - 177) - 180) \\
&\quad + \frac{1}{576}t^3e^{-3x}8x^2e^x(x^3 - 9x^2 + 9x).
\end{aligned}$$

Figure 5.9 shows the comparison of the exact concentration with the approximated 10-term series solutions obtained by using ODM and ADM. In addition, it also presents the comparison between the exact and numerically approximated zeroth moment. Since the aggregation rate is more than the constant rate, it is seen that less number of particles are left at the end of the process. The number obtained after $t = 1$ is approximately the same as in the previous case after $t = 2$. The plots of the first and second moments considering ϕ_{10} and ψ_{10} are shown in Figure 5.10 along with the analytical moments. It is observed that ODM predicts all the moments better than ADM. The absolute errors for both the techniques in computing the series solutions using 10-terms are depicted in Figure 5.11. Again, one can see that ODM enjoys better estimates as compared to ADM.

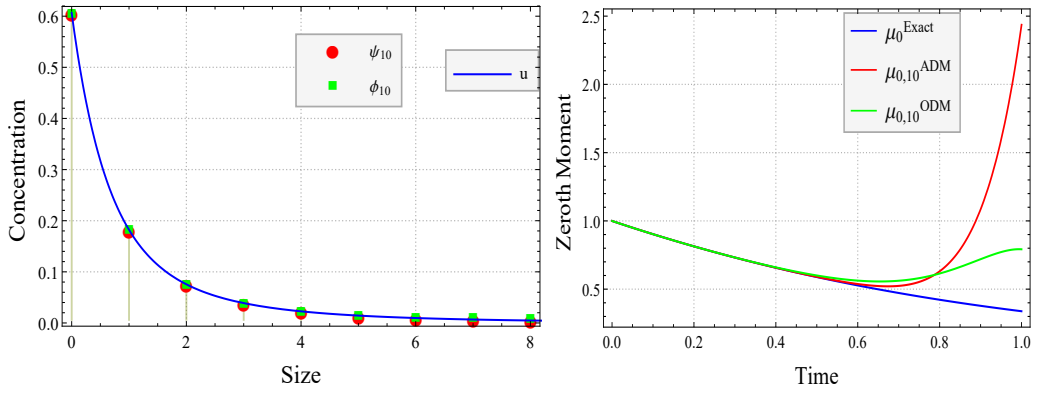

(a) Comparison of approximated and exact concentration

(b) Zeroth moment

FIGURE 5.9: Comparison of solutions and zeroth moment for Example 5.2

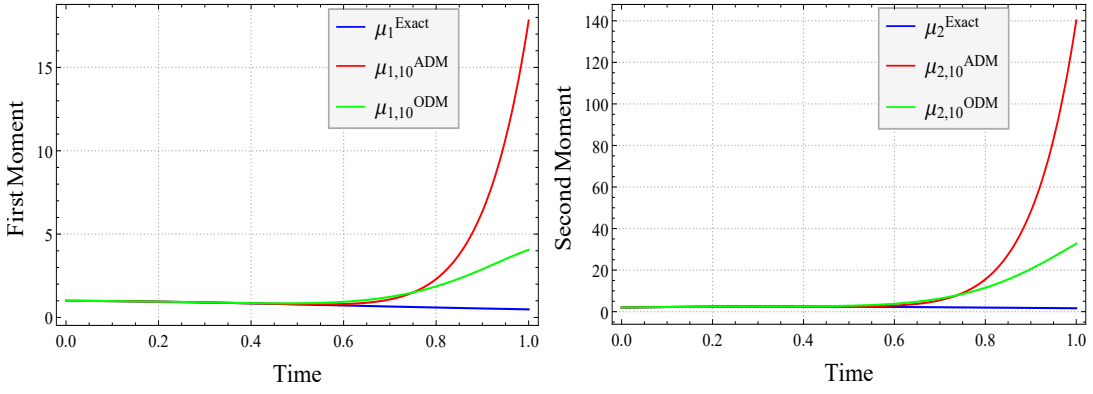

(a) First moment

(b) Second moment

FIGURE 5.10: Moments comparison: ODM, ADM and exact solutions, for Example, 5.2

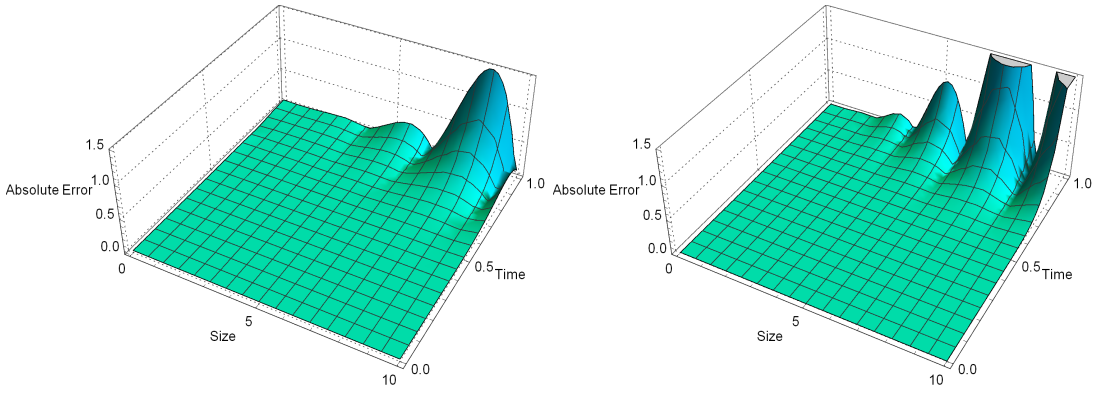

(a) ODM (b) ADM

FIGURE 5.11: Absolute error plots for ODM and ADM series solutions for Example 5.2

TABLE 5.4: Comparison of numerical errors for ADM and ODM with parameters as given in Example 5.2.

n	6	7	8	9	10	11
ADM at $t = 0.5$	0.003	0.002	0.001	0.0009	0.0006	0.0004
ODM at $t = 0.5$	0.008	0.0075	0.004	0.0043	0.002	0.002
ADM at $t = 1$	0.226	0.352	0.500	0.593	0.808	1.187
ODM at $t = 1$	0.196	0.317	0.281	0.436	0.367	0.449

Additionally, the numerical errors at $t = 0.5$ and $t = 1$ are given in TABLE 5.4 which proves that ODM is a better method to obtain an approximate solution for the Eq. (5.1) having sum aggregation rate. It is worth mentioning that the order of convergence, in this case, has similar observations as in the previous example.

Example 5.3. *Now, consider the case of product kernel $a(x, y) = xy$ with initial data $u_0(x) = e^{-x}$. For this case, the analytic number density is provided in [129] as*

$$u(t, x) = e^{-tx-x} \sum_{k=0}^{\infty} \frac{t^k x^{3k}}{\Gamma(2k+2)(k+1)!}.$$

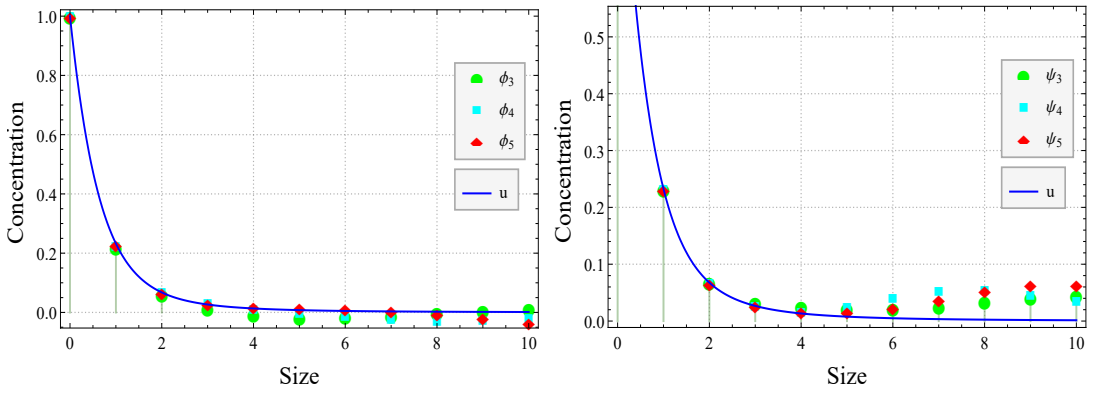

(a) ODM (b) ADM

FIGURE 5.12: Series solutions for $n = 3, 4, 5$ using ODM and ADM at $t = 0.5$ for Example 5.3

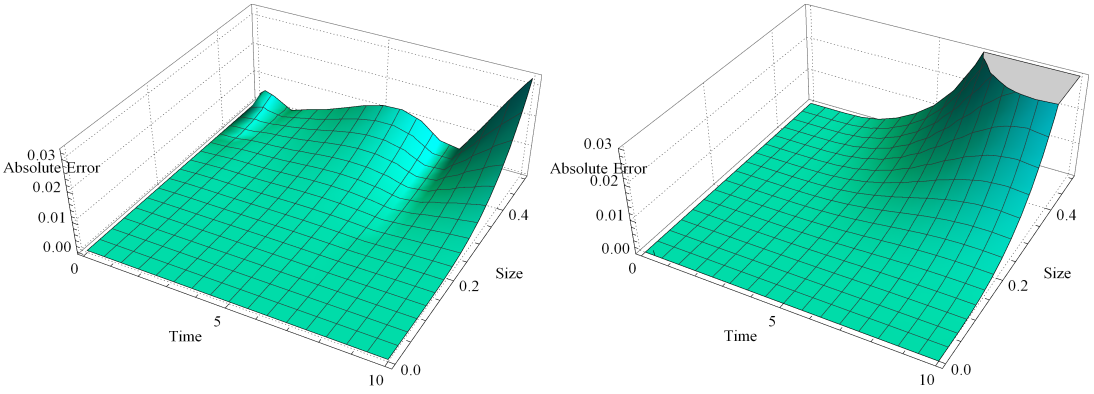

(a) ODM (b) ADM

FIGURE 5.13: Absolute error plots for ODM and ADM series solutions for Example 5.3

Using the equations (5.16), (5.17) and the recursive scheme from equations (5.18-5.20) yield

$$
\begin{aligned}
C(x) &= \frac{1}{2}\left[(x+2)(e^{-x}-1)\right], \quad u_0(x) = e^{-x}, \\
u_1(t,x) &= \frac{1}{12}te^{-x}x\left(x^2-12\right), \\
u_2(t,x) &= \frac{1}{720}t^2e^{-2x}x\left(15\left(e^x-1\right)(x+2)\left(x^2-12\right)+e^x x\left(x^4-60x^2+360\right)\right), \\
u_3(t,x) &= \frac{t^2e^{-3x}}{120960}(28(-1+e^x)x(2+x)(-15t(2+x)(-12+x^2)+e^x(-90(-12+x^2)))) \\
&\quad + \frac{t^3e^{-2x}}{120960}(28(-1+e^x)x(2+x)(-360+x(180+x(30-45x+x^3)))) \\
&\quad + \frac{t^3e^{-2x}}{120960}(-1680(264+x(240+x(120+x(38+5x))))) \\
&\quad + \frac{t^3e^{-x}}{120960}(443520-86625x+20160x^2 \\
&\quad + x^4(-10080+x^4(-3360+x^4(3696+x^4(56-148x+x^3))))).
\end{aligned}
$$

Figure 5.12 represents the approximate solutions ϕ_n and ψ_n when $n = 3, 4$ and 5. Similar to the previous examples, we notice a similar trend for concentration and moments. It is unequivocal that the ODM series solution provides a better approximation than ADM. It is mentioned in [58] that ADM needs 8-term solution to get a good agreement with the exact solution. However, here one can notice that ODM needs only 5 terms. Moving further, the absolute errors in computing ODM series solution (ϕ_5) and ADM solution (ψ_5) are presented in Figure 5.13 which clearly claims the superiority of ODM over ADM. The TABLE 5.5 depicts the comparison of error (defined in (5.31) with $N = 1000$ and $h_i = 0.01$) values for the ADM and ODM for different values of n. Again, it is noticed that the errors for ODM are lower than the errors of the solution computed using ADM. Note that, in this case as well, both ODM and ADM provide first-order convergence but the values due to ODM are slightly closer to 1 as compared to ADM which shows the superiority of ODM. The following Remark 5.6 presents some important observations regarding the advantage of the method.

TABLE 5.5: Numerical errors in computing approximated solutions using ADM and ODM at $t = 0.5$ with parameters as given in Example 5.3.

n	3	4	5
ADM	0.175	0.221	0.220
ODM	0.123	0.144	0.086

Remark 5.6. It is important to note that in the case of constant and sum kernels, when the value of t is increased, error values using ODM are significantly lower than ADM. However, for the product kernel, where the rate of aggregation is highest among all, the ODM gives better results even at lower values of t.

5.3 ODM Implementation for 1D Burgers Equation

In order to understand the implementation of ODM for the one-dimensional Burgers equation, we shall first define a non-linear operator M as

$$M[w(x,t)] = -w\frac{\partial w}{\partial x}, \tag{5.32}$$

and as a result, it gives

$$C(x) = -\frac{\partial w_0}{\partial x} - w_0\left(\frac{\frac{\partial^2 w_0}{\partial x^2}}{\frac{\partial w_0}{\partial x}}\right). \tag{5.33}$$

Using (5.32) and (5.33), the operator R can be written as

$$R[w(x,t)] = -w\frac{\partial w}{\partial x} + \left(\frac{\partial w_0}{\partial x} + w_0\left(\frac{\frac{\partial^2 w_0}{\partial x^2}}{\frac{\partial w_0}{\partial x}}\right)\right)c(x,t).$$

The definition of $Q_k(x,t)$ from equation (5.13) and M from (5.32), the following can be obtained

$$Q_0(x,t) = -w_0(x,t)\frac{\partial w_0(x,t)}{\partial x},$$

so that,

$$w_1(x,t) = \int_0^t \Big(- w_0(x,t)\frac{\partial w_0(x,t)}{\partial x} + \nu\frac{\partial^2}{\partial x^2}w_0(x,t)\Big)dt. \tag{5.34}$$

For $k \geq 1$, we have

$$Q_k(x,t) = -\sum_{i=0}^{k} w_i(x,t)\sum_{j=0}^{k}\frac{\partial w_j(x,t)}{\partial x}, \qquad \text{only when } i+j=k,$$

to give

$$w_2(x,t) = \mathcal{L}^{-1}\Big(Q_1(x,t) - C(x)w_1(x,t)\Big), \tag{5.35}$$

and for $k \geq 2$,

$$w_{k+1}(x,t) = \mathcal{L}^{-1}\Big[Q_k(x,t) + \nu\frac{\partial^2}{\partial x^2}w_{k-1}(x,t) - C(x)\Big(w_k(x,t) - w_{k-1}(x,t)\Big)\Big]. \tag{5.36}$$

Convergence Analysis

Consider the Hilbert space $H = L^2((\alpha,\beta)\times[0,T])$ with the set of applications:- $w : (\alpha,\beta)\times[0,T] \to \mathbb{R}$ with

$$\int_{(\alpha,\beta)\times[0,T]} w^2(x,s)dsdt < \infty.$$

Writing the Burgers equation in the operator form gives

$$\mathcal{B}[w] = \nu\frac{\partial^2 w}{\partial x^2} - w\frac{\partial w}{\partial x}, \tag{5.37}$$

where $\mathcal{B} : H \to H$ is an operator in H. Now, taking into account the recursive scheme, the n-term series solution $\phi_n := \sum_{k=0}^{n} w_k(x,t)$ becomes

$$\phi_n = w_0 + \mathcal{A}\phi_{n-1} - \int_0^t C(x)w_{n-1}(x,s)ds, \tag{5.38}$$

where $\mathcal{A} : H \to H := \mathcal{L}^{-1}(\mathcal{B})$. The result below plays a significant role in proving that the sequence $\{\phi_n\}$ is a Cauchy sequence which finally establishes that the series solution converges towards the exact solution.

Theorem 5.7. *The following is true for the operator $\mathcal{B}$:*

(H1) $(\mathcal{B}(w) - \mathcal{B}(v), w - v) \geq k||w - v||^2$, $k > 0, \forall w, v \in H$.

(H2) for any $M > 0$, there exists a constant $C(M) > 0$ such that for $w, v \in H$, with $||w|| \leq M$, $||v|| \leq M$, we have $(\mathcal{B}(w) - \mathcal{B}(v), w - v) \leq C(M)||w - v||||w||$, for every $w \in H$.

Proof. The proof of this theorem can be followed from (Section 6, Theorem 1 [131]). □

Theorem 5.8. *Consider $\mathcal{A}$ be an operator from a Hilbert space H to H and the truncated series solution be defined by the Eq. (5.38). Then the series solution converges to the exact solution w with*

$$||w - \phi_m|| \leq \left(\frac{\delta^{m-1} + \delta^m}{1 - \delta}\right)||w_1||, \tag{5.39}$$

if

(A1) $\exists\ 0 < \delta < 1$ *such that* $||\mathcal{A}[w_0 + w_1 + \ldots + w_k]|| \leq \delta||\mathcal{A}[w_0 + w_1 + \ldots + w_{k-1}]||$, *with* $\mathcal{A}[w_0] = w_1$ *(see [132]).*

(A2) $\{w_n\}$ *is a Cauchy sequence, i.e., for any $n > m$,* $||w_n - w_m|| < \varepsilon$, *where* $\varepsilon = \frac{1}{n^p}$ *such that $p > 1$.*

(A3) $C(x) \in L^\infty(H, |\cdot|_\infty)$ *where $|\cdot|_\infty$ is the essential supremum norm, i.e.,* $|C(x)| \leq k$ *for some $k \in \mathbb{R}^+$.*

Proof. Following (5.38), consider

$$||\phi_n - \phi_m|| = \left|\left|\mathcal{A}\phi_{n-1} - \int_0^t C(x)w_{n-1}(x,s)ds - \mathcal{A}\phi_{m-1} + \int_0^t C(x)w_{m-1}(x,s)ds\right|\right|.$$

The triangle inequality gives us

$$||\phi_n - \phi_m|| \leq ||\mathcal{A}\phi_{n-1} - \mathcal{A}\phi_{m-1}|| + \left|\left|\int_0^t C(x)\left(w_{n-1}(x,s) - w_{m-1}(x,s)\right)ds\right|\right|.$$

Theorem 5.7 and assumption $(A1)$ yield

$$\begin{aligned}||\phi_n - \phi_m|| &\leq \delta||A[w_0 + w_1 + \ldots w_{n-2}]|| + \delta||A[w_0 + w_1 + \ldots w_{m-2}]|| + \left|\left|\int_0^t C(x)\left(w_{n-1}(x,s) - w_{m-1}(x,s)\right)ds\right|\right| \\ &\leq (\delta^{n-1} + \delta^{m-1})||w_1|| + \left|\left|\int_0^t C(x)\left(w_{n-1}(x,s) - w_{m-1}(x,s)\right)ds\right|\right|.\end{aligned}$$

Using $(A2)$ and $(A3)$ lead to

$$||\phi_n - \phi_m|| \leq (\delta^{n-1} + \delta^{m-1})||w_1|| + tk\varepsilon.$$

Putting $n = m + 1$ in the above expression and further simplifications provide

$$||\phi_{m+1} - \phi_m|| \leq (\delta^m + \delta^{m-1})||w_1|| + tk\varepsilon.$$

Now,

$$\begin{aligned}
||\phi_n - \phi_m|| &\leq ||\phi_{m+1} - \phi_m|| + ||\phi_{m+2} - \phi_{m+1}|| + \ldots + ||\phi_n - \phi_{n-1}|| \\
&\leq [(\delta^m + \delta^{m-1})||w_1|| + tk\varepsilon] + [(\delta^{m+1} + \delta^m)||w_1|| + tk\varepsilon] + \ldots + [(\delta^{n-1} + \delta^{n-2})||w_1|| + tk\varepsilon] \\
&= [\delta^{m-1} + 2(\delta^m + \delta^{m+1} + \ldots + \delta^{n-2}) + \delta^{n-1}]||w_1|| + tk\varepsilon(n-m) \\
&= \left(\frac{\delta^{m-1}(1-\delta^{n-m})}{1-\delta} + \frac{\delta^m(1-\delta^{n-m-1})}{1-\delta}\right)||w_1|| + tk\varepsilon(n-m).
\end{aligned}$$

For a suitable t_0 and thanks to $(A1)$, the above expression becomes

$$||\phi_n - \phi_m|| \leq \left(\frac{\delta^{m-1} + \delta^m}{1-\delta}\right)||w_1|| + \varepsilon t_0 k(n-m). \tag{5.40}$$

Finally, using $(A2)$ and $\frac{1}{n^p} < \frac{1}{m^p}$, the above expression converges to zero as $m \to \infty$. Thus, $\exists$ a ϕ such that $\lim_{n\to\infty} \phi_n = \phi$ and so $w = \sum_{k=0}^{\infty} w_k = \lim_{n\to\infty} \phi_n = \phi$, which is the exact solution of the Burgers equation. Finally, fixing m and letting $n \to \infty$ in the equation (5.40), we obtain the theoretical error bound (5.39). □

5.4 Extension of ODM to System of PDEs

Consider the non-linear system of PDEs of the type (5.5)

$$\begin{aligned}
\frac{\partial}{\partial t}w(x,y,t) &= \nu\frac{\partial^2}{\partial x^2}w(x,y,t) + \nu\frac{\partial^2}{\partial y^2}w(x,y,t) + M_1[w(x,y,t), v(x,y,t)], \\
\frac{\partial}{\partial t}v(x,y,t) &= \nu\frac{\partial^2}{\partial x^2}v(x,y,t) + \nu\frac{\partial^2}{\partial y^2}v(x,y,t) + M_2[w(x,y,t), v(x,y,t)],
\end{aligned} \tag{5.41}$$

with the initial conditions mentioned in (5.6). The solution of the above equation is formulated as

$$\begin{aligned}
w(x,y,t) &= f_1(x,y) + \mathcal{L}^{-1}\left(\nu\frac{\partial^2}{\partial x^2}w(x,y,t) + \nu\frac{\partial^2}{\partial y^2}w(x,y,t) + M_1[w(x,y,t), v(x,y,t)]\right), \\
v(x,y,t) &= f_2(x,y) + \mathcal{L}^{-1}\left(\nu\frac{\partial^2}{\partial x^2}v(x,y,t) + \nu\frac{\partial^2}{\partial y^2}v(x,y,t) + M_2[w(x,y,t), v(x,y,t)]\right),
\end{aligned}$$

for $\mathcal{L}^{-1}$ being the inverse operator of $\mathcal{L} = \frac{\partial}{\partial t}$. Under the assumptions that the non-linear functions

$$F\left(\frac{\partial}{\partial t}w, \frac{\partial^2}{\partial x^2}w, \frac{\partial^2}{\partial y^2}w, w\right) := \frac{\partial}{\partial t}w - \nu\frac{\partial^2 w}{\partial x^2} - \nu\frac{\partial^2 w}{\partial y^2} - M_1[w, v],$$
$$G\left(\frac{\partial}{\partial t}v, \frac{\partial^2}{\partial x^2}v, \frac{\partial^2}{\partial y^2}v, v\right) := \frac{\partial}{\partial t}v - \nu\frac{\partial^2 v}{\partial x^2} - \nu\frac{\partial^2 v}{\partial y^2} - M_2[w, v],$$

can be linearized by a first-order Taylor series expansions at $t = 0$, the linear approximation to F and G can be obtained as

$$F\left(\frac{\partial}{\partial t}w, w_{xx}, w_{yy}, w\right) \approx \frac{\partial}{\partial t}w - \nu\frac{\partial^2 w}{\partial x^2} - \nu\frac{\partial^2 w}{\partial y^2} - C_1(x, y)w,$$
$$G\left(\frac{\partial}{\partial t}v, v_{xx}, v_{yy}, v\right) \approx \frac{\partial}{\partial t}v - \nu\frac{\partial^2 v}{\partial x^2} - \nu\frac{\partial^2 v}{\partial x^2} - C_2(x, y)v,$$

where we define C_i for $i = 1, 2$ as

$$C_i(x, y) = \left.\frac{\partial M_i}{\partial w}\right|_{t=0} + \left.\frac{\partial M_i}{\partial v}\right|_{t=0}. \tag{5.42}$$

Using the implicit differentiation rule, we obtain

$$\frac{\partial M_i}{\partial x} = \left(\frac{\partial M_i}{\partial w}\right)\left(\frac{\partial w}{\partial x}\right) + \left(\frac{\partial M_i}{\partial v}\right)\left(\frac{\partial v}{\partial x}\right),$$

$$\frac{\partial M_i}{\partial y} = \left(\frac{\partial M_i}{\partial w}\right)\left(\frac{\partial w}{\partial y}\right) + \left(\frac{\partial M_i}{\partial v}\right)\left(\frac{\partial v}{\partial y}\right).$$

Solving the above two equations yield

$$\frac{\partial M_i}{\partial w} = \frac{(\frac{\partial M_i}{\partial x})(\frac{\partial v}{\partial y}) - (\frac{\partial M_i}{\partial y})(\frac{\partial v}{\partial x})}{(\frac{\partial w}{\partial x})(\frac{\partial v}{\partial y}) - (\frac{\partial w}{\partial y})(\frac{\partial v}{\partial x})}, \tag{5.43}$$

and

$$\frac{\partial M_i}{\partial v} = \frac{(\frac{\partial M_i}{\partial x})(\frac{\partial w}{\partial y}) - (\frac{\partial M_i}{\partial y})(\frac{\partial w}{\partial x})}{(\frac{\partial v}{\partial x})(\frac{\partial w}{\partial y}) - (\frac{\partial w}{\partial x})(\frac{\partial v}{\partial y})}, \tag{5.44}$$

provided that

$$\left(\frac{\partial v_0}{\partial x}\frac{\partial w_0}{\partial y} - \frac{\partial w_0}{\partial x}\frac{\partial v_0}{\partial y}\right) \neq 0.$$

The above approximation leads us to the linear operators R and S that are defined as

$$R[w(x,y,t)] = M_1[w(x,y,t)] - C_1(x,y)w(x,y,t),$$
$$S[v(x,y,t)] = M_2[v(x,y,t)] - C_2(x,y)v(x,y,t),$$

which are not easily invertible. Let us define the solutions as

$$w(x,y,t) = \sum_{k=0}^{\infty} w_k(x,y,t), \qquad v(x,y,t) = \sum_{k=0}^{\infty} v_k(x,y,t) \tag{5.45}$$

and the coefficients $w_k(x,y,t)$, $v_k(x,y,t)$ are determined by the TABLES 5.6 and 5.7,

TABLE 5.6: Table of the coefficients for $w(x,y,t)$

$w_0(x,y,t)$	$f_1(x,y)$
$w_1(x,y,t)$	$\mathcal{L}^{-1}\left(\nu\frac{\partial^2}{\partial x^2}w_0(x,y,t) + \nu\frac{\partial^2}{\partial y^2}w_0(x,y,t) + Q_0(x,y,t)\right)$
$u_2(x,y,t)$	$\mathcal{L}^{-1}\left(\left(\nu\frac{\partial^2}{\partial x^2}w_1 + \nu\frac{\partial^2}{\partial y^2}w_1 + Q_1\right)(x,y,t) - \left(\nu\frac{\partial^2}{\partial x^2} + \nu\frac{\partial^2}{\partial y^2} + C_1(x,y)\right)w_1(x,y,t)\right)$
$w_{k+1}(x,y,t)$	$\mathcal{L}^{-1}\left(\left(\nu\frac{\partial^2}{\partial x^2}w_k + \nu\frac{\partial^2}{\partial y^2}w_k + Q_k\right) - \left(\nu\frac{\partial^2}{\partial x^2} + \nu\frac{\partial^2}{\partial y^2} + C_1(x,y)\right)(w_k - w_{k-1})\right), \quad k \geq 2$

TABLE 5.7: Table of the coefficients for $v(x,y,t)$

$v_0(x,y,t)$	$f_2(x,y)$
$v_1(x,y,t)$	$\mathcal{L}^{-1}\left(\nu\frac{\partial^2}{\partial x^2}v_0(x,y,t) + \nu\frac{\partial^2}{\partial y^2}v_0(x,y,t) + P_0(x,y,t)\right)$
$v_2(x,y,t)$	$\mathcal{L}^{-1}\left(\left(\nu\frac{\partial^2}{\partial x^2}v_1 + \nu\frac{\partial^2}{\partial y^2}v_1 + P_1\right)(x,y,t) - \left(\nu\frac{\partial^2}{\partial x^2} + \nu\frac{\partial^2}{\partial y^2} + C_2(x,y)\right)v_1(x,y,t)\right)$
$v_{k+1}(x,y,t)$	$\mathcal{L}^{-1}\left(\left(\nu\frac{\partial^2}{\partial x^2}v_k + \nu\frac{\partial^2}{\partial y^2}v_k + P_k\right) - \left(\nu\frac{\partial^2}{\partial x^2} + \nu\frac{\partial^2}{\partial y^2} + C_2(x,y)\right)(v_k - v_{k-1})\right), \quad k \geq 2$

where

$$Q_k(x,y,t) = \frac{1}{k!}\frac{d^k}{d\theta^k}\left[M_1\left(\sum_{i=0}^{k}\theta^i w_i(x,y,t), \sum_{i=0}^{k}\theta^i v_i(x,y,t)\right)\right]\Bigg|_{\theta=0},$$
$$P_k(x,y,t) = \frac{1}{k!}\frac{d^k}{d\theta^k}\left[M_2\left(\sum_{i=0}^{k}\theta^i w_i(x,y,t), \sum_{i=0}^{k}\theta^i v_i(x,y,t)\right)\right]\Bigg|_{\theta=0},$$

with

$$\sum_{k=0}^{\infty} Q_k(x,y,t) = M_1\left[\sum_{k=0}^{\infty} w_k(x,y,t), \sum_{k=0}^{\infty} v_k(x,y,t)\right], \tag{5.46}$$

$$\sum_{k=0}^{\infty} P_k(x,y,t) = M_2\left[\sum_{k=0}^{\infty} w_k(x,y,t), \sum_{k=0}^{\infty} v_k(x,y,t)\right]. \tag{5.47}$$

In the following proposition, the condition required for the convergence of the method is provided.

Proposition 5.9. *Let the coefficients of the series solution be determined by TABLES 5.6 and 5.7 and the series* $\sum_{k=0}^{\infty} w_k(x,y,t)$ *and* $\sum_{k=0}^{\infty} v_k(x,y,t)$ *are convergent then* $w(x,y,t)$ *and* $v(x,y,t)$ *are the solutions of the system* (5.41).

Proof. Given that

$$\begin{aligned}\sum_{k=0}^{\infty} w_k(x,y,t) = f_1(x,y) &+ \mathcal{L}^{-1}\left(\nu\frac{\partial^2}{\partial x^2} + \nu\frac{\partial^2}{\partial y^2}(w_0(x,y,t)) + Q_0(x,y,t)\right)\\ &+ \mathcal{L}^{-1}\left([Q_1(x,y,t) - C_1(x,y)w_1(x,y,t)]\right)\\ &+ \mathcal{L}^{-1}\left[Q_2(x,y,t) + \nu\frac{\partial^2}{\partial x^2} + \nu\frac{\partial^2}{\partial y^2}(w_1(x,y,t)) - C_1(x,y)(w_2(x,y,t) - w_1(x,y,t))\right]\\ &+ \ldots + \mathcal{L}^{-1}\left[Q_{n-1}(x,y,t) + \nu\frac{\partial^2}{\partial x^2} + \nu\frac{\partial^2}{\partial y^2}(w_{n-2}(x,y,t)) - C_2(x,y)(w_{n-1}(x,y,t) - w_{n-2}(x,y,t))\right] + \ldots.\end{aligned}$$

By simplifying the above equation and using the convergence of the series $\sum_{k=0}^{\infty} w_k(x,y,t)$ which guarantees that $\lim_{k\to\infty} w_k = 0$, one has

$$\sum_{k=0}^{\infty} w_k(x,y,t) = f_1(x,y) + \mathcal{L}^{-1}\left(\sum_{k=0}^{\infty}\left[\nu\frac{\partial^2}{\partial x^2}w_k(x,y,t) + \nu\frac{\partial^2}{\partial x^2}w_k(x,y,t) + Q_k(x,y,t)\right]\right).$$

The equation (5.46) and $u(x,y,t) = \sum_{k=0}^{\infty} w_k(x,y,t)$ provide

$$\begin{aligned}w(x,y,t) = f_1(x,y) &+ \mathcal{L}^{-1}\left(\nu\frac{\partial^2}{\partial x^2}\left[\sum_{k=0}^{\infty} w_k(x,y,t)\right] + \nu\frac{\partial^2}{\partial y^2}\left[\sum_{k=0}^{\infty} w_k(x,y,t)\right]\right)\\ &+ \mathcal{L}^{-1}\left(M_1\left[\sum_{k=0}^{\infty} w_k(x,y,t), \sum_{k=0}^{\infty} v_k(x,y,t)\right]\right),\end{aligned}$$

and so

$$\mathcal{L}[w(x,y,t)] = \nu\frac{\partial^2}{\partial x^2}w(x,y,t) + \nu\frac{\partial^2}{\partial y^2}w(x,y,t) + M_1[w(x,y,t), v(x,y,t)].$$

Similarly, we can prove using TABLE 5.7 and (5.47) that

$$\mathcal{L}[v(x,y,t)] = \nu\frac{\partial^2}{\partial x^2}v(x,y,t) + \nu\frac{\partial^2}{\partial y^2}v(x,y,t) + M_2[w(x,y,t), v(x,y,t)].$$

Hence, $w(x,y,t)$ and $v(x,y,t)$ are the solutions of the equation (5.41). □

5.5 ODM Implementation for 2D Burgers Equation

In order to extend the optimized decomposition method for a two-dimensional problem, we shall define two nonlinear functions M_1 and M_2 as

$$M_1[w,v] = -w\frac{\partial w}{\partial x} - v\frac{\partial w}{\partial y}, \tag{5.48}$$

and

$$M_2[w,v] = -w\frac{\partial v}{\partial x} - v\frac{\partial v}{\partial y}. \tag{5.49}$$

Using (5.43) leads to

$$\frac{\partial M_1}{\partial w} = \frac{-(\frac{\partial w}{\partial x})^2(\frac{\partial v}{\partial y}) - w(\frac{\partial^2 w}{\partial x^2})\frac{\partial v}{\partial y} - v(\frac{\partial^2 w}{\partial x \partial y})\frac{\partial v}{\partial y} + \frac{\partial w}{\partial y}\frac{\partial w}{\partial x}\frac{\partial v}{\partial x} + w(\frac{\partial^2 w}{\partial y \partial x})\frac{\partial v}{\partial x} + v(\frac{\partial^2 w}{\partial y^2})\frac{\partial v}{\partial x}}{(\frac{\partial w}{\partial x}\frac{\partial v}{\partial y} - \frac{\partial w}{\partial y}\frac{\partial v}{\partial x})},$$

$$\frac{\partial M_2}{\partial w} = \frac{-\frac{\partial w}{\partial x}\frac{\partial v}{\partial x}\frac{\partial v}{\partial y} - w(\frac{\partial^2 v}{\partial x^2})\frac{\partial v}{\partial y} - v(\frac{\partial^2 v}{\partial x \partial y})\frac{\partial v}{\partial y} + (\frac{\partial v}{\partial x})^2(\frac{\partial w}{\partial y}) + w(\frac{\partial^2 v}{\partial y \partial x})\frac{\partial v}{\partial x} + v(\frac{\partial^2 v}{\partial y^2})\frac{\partial v}{\partial x}}{(\frac{\partial w}{\partial x}\frac{\partial v}{\partial y} - \frac{\partial w}{\partial y}\frac{\partial v}{\partial x})}.$$

Similarly, using (5.44), the following can be obtained

$$\frac{\partial M_1}{\partial v} = \frac{-w(\frac{\partial^2 w}{\partial x^2})\frac{\partial w}{\partial y} - (\frac{\partial w}{\partial y})^2(\frac{\partial v}{\partial x}) - v(\frac{\partial^2 w}{\partial x \partial y})\frac{\partial w}{\partial y} + w(\frac{\partial^2 w}{\partial y \partial x})\frac{\partial w}{\partial x} + \frac{\partial w}{\partial y}\frac{\partial w}{\partial x}\frac{\partial v}{\partial y} + v(\frac{\partial^2 w}{\partial y^2})\frac{\partial w}{\partial x}}{(\frac{\partial v}{\partial x}\frac{\partial w}{\partial y} - \frac{\partial w}{\partial x}\frac{\partial v}{\partial y})},$$

$$\frac{\partial M_2}{\partial v} = \frac{-w(\frac{\partial^2 v}{\partial x^2})\frac{\partial w}{\partial y} - \frac{\partial w}{\partial y}\frac{\partial v}{\partial x}\frac{\partial v}{\partial y} - v(\frac{\partial^2 v}{\partial x \partial y})\frac{\partial w}{\partial y} + w(\frac{\partial^2 v}{\partial y \partial x})\frac{\partial w}{\partial x} + (\frac{\partial v}{\partial y})^2(\frac{\partial w}{\partial x}) + v(\frac{\partial^2 v}{\partial y^2})\frac{\partial w}{\partial x}}{(\frac{\partial v}{\partial x}\frac{\partial w}{\partial y} - \frac{\partial w}{\partial x}\frac{\partial v}{\partial y})}.$$

Finally, the equation (5.42) yields

$$\begin{aligned} C_1(x,y) = {} & \frac{-(\frac{\partial w_0}{\partial x})^2(\frac{\partial v_0}{\partial y}) - w_0(\frac{\partial^2 w_0}{\partial x^2})\frac{\partial v_0}{\partial y} - v_0(\frac{\partial^2 w_0}{\partial x \partial y})\frac{\partial v_0}{\partial y} + \frac{\partial w_0}{\partial y}\frac{\partial w_0}{\partial x}\frac{\partial v_0}{\partial x} + w_0(\frac{\partial^2 w_0}{\partial y \partial x})\frac{\partial v_0}{\partial x} + v_0(\frac{\partial^2 w_0}{\partial y^2})\frac{\partial v_0}{\partial x}}{(\frac{\partial w_0}{\partial x}\frac{\partial v_0}{\partial y} - \frac{\partial w_0}{\partial y}\frac{\partial v_0}{\partial x})} \\ & + \frac{-w_0(\frac{\partial^2 w_0}{\partial x^2})\frac{\partial w_0}{\partial y} - (\frac{\partial w_0}{\partial y})^2(\frac{\partial v_0}{\partial x}) - v_0(\frac{\partial^2 w_0}{\partial x \partial y})\frac{\partial w_0}{\partial y} + w_0(\frac{\partial^2 w_0}{\partial y \partial x})\frac{\partial w_0}{\partial x} + \frac{\partial w_0}{\partial y}\frac{\partial w_0}{\partial x}\frac{\partial v_0}{\partial y} + v_0(\frac{\partial^2 w_0}{\partial y^2})\frac{\partial w_0}{\partial x}}{(\frac{\partial v_0}{\partial x}\frac{\partial w_0}{\partial y} - \frac{\partial w_0}{\partial x}\frac{\partial v_0}{\partial y})}, \end{aligned} \tag{5.50}$$

and

$$C_2(x,y) = \frac{-\frac{\partial w_0}{\partial x}\frac{\partial v_0}{\partial x}\frac{\partial v_0}{\partial y} - w_0(\frac{\partial^2 v_0}{\partial x^2})\frac{\partial v_0}{\partial y} - v_0(\frac{\partial^2 v_0}{\partial x \partial y})\frac{\partial v_0}{\partial y} + (\frac{\partial v_0}{\partial x})^2(\frac{\partial w_0}{\partial y}) + w_0(\frac{\partial^2 v_0}{\partial y \partial x})\frac{\partial v_0}{\partial x} + v_0(\frac{\partial^2 v_0}{\partial y^2})\frac{\partial v_0}{\partial x}}{(\frac{\partial w_0}{\partial x}\frac{\partial v_0}{\partial y} - \frac{\partial w_0}{\partial y}\frac{\partial v_0}{\partial x})}$$
$$+ \frac{-w_0(\frac{\partial^2 v_0}{\partial x^2})\frac{\partial w_0}{\partial y} - \frac{\partial w_0}{\partial y}\frac{\partial v_0}{\partial x}\frac{\partial v_0}{\partial y} - v_0(\frac{\partial^2 v_0}{\partial x \partial y})\frac{\partial w_0}{\partial y} + w_0(\frac{\partial^2 v_0}{\partial y \partial x})\frac{\partial w_0}{\partial x} + (\frac{\partial v_0}{\partial y})^2(\frac{\partial w_0}{\partial x}) + v_0(\frac{\partial^2 v_0}{\partial y^2})\frac{\partial w_0}{\partial x}}{(\frac{\partial v_0}{\partial x}\frac{\partial w_0}{\partial y} - \frac{\partial w_0}{\partial x}\frac{\partial v_0}{\partial y})}, \tag{5.51}$$

provided that

$$\frac{\partial v}{\partial x}\frac{\partial w}{\partial y} - \frac{\partial w}{\partial x}\frac{\partial v}{\partial y} \neq 0. \tag{5.52}$$

Now, for $\nu = \frac{1}{R_e}$, the coefficients for $w_k(x,y,t)$ and $v_k(x,y,t)$ can be determined from the TABLES 5.6 and 5.7, respectively.

5.6 Numerical Examples for Burgers Equation

The section deals with some numerical examples to establish the applicability and accuracy of ODM to calculate the series solutions for the multi-dimensional Burgers equations. In the case of 1D problem, we have considered three test cases for inviscid BE, one for inviscid non-homogenous BE, and two for viscous Burgers equation where the exact solutions are available. In all the cases, it is established that ODM outperforms the solution proposed by ADM provided in [128]. The second subsection includes two test cases for the viscous 2D and generalized 2D BE. We have also dealt with a case of viscous 3D Burgers equation. All the computations and requisite calculations are done with the help of MATHEMATICA©.

One Dimensional Case

Example 5.4. *Consider the inviscid Burgers equation*

$$\frac{\partial w}{\partial t} + w\frac{\partial w}{\partial x} = 0, \tag{5.53}$$

with $w(x,0) = w_0(x) = ax + b$, $a \neq 0$ *and* $b \in \mathbb{R}$. *The exact solution is derived in [128] as*

$$w(x,t) = \frac{ax+b}{1+at}. \tag{5.54}$$

Using (5.33) and the equations (5.34)-(5.36) give the value of $C(x)$ and the first ten terms by ODM as

$$
\begin{aligned}
C(x) &= -a, \;\; w_0(x,t) = ax+b, \;\; w_1(x,t) = -at(ax+b), \;\; w_2(x,t) = \frac{1}{2}a^2t^2(ax+b),\\
w_3(x,t) &= -\frac{1}{2}a^2t^2(at-1)(ax+b), \;\; w_4(x,t) = \frac{1}{24}a^3t^3(9at-8)(ax+b),\\
w_5(x,t) &= -\frac{1}{120}a^3t^3(at(39at-55)+20)(ax+b), \;\; w_6(x,t) = \frac{1}{80}a^4t^4(at(21at-32)+10)(ax+b),\\
w_7(x,t) &= -\frac{a^4t^4(at(9at(41at-77)+392)-70)(ax+b)}{1680},\\
w_8(x,t) &= \frac{a^5t^5(at(3at(2427at-5072)+9296)-1344)(ax+b)}{40320},\\
w_9(x,t) &= \frac{a^5t^5(at(3at(3at(671at-1599)+3784)-3472)+336)(ax+b)}{40320},\\
w_{10}(x,t) &= \frac{a^6t^6(at(3at(at(16623at-43720)+38790)-38080)+2800)(ax+b)}{403200}.
\end{aligned}
$$

Let us denote the ODM series solution by $\phi_n(x,t)$ which is given as

$$
\begin{aligned}
\phi_n(t,x) &= \sum_{k=0}^{n} w_k(t,x) = w_0(x,t)+w_1(x,t)+w_2(x,t)+w_3(x,t)+w_4(x,t)+w_5(x,t)+\ldots\\
&= (ax+b)+(-at(ax+b))+\left(\frac{1}{2}a^2t^2(ax+b)\right)+\left(-\frac{1}{2}a^2t^2(at-1)(ax+b)\right)\\
&+\frac{1}{24}a^3t^3(9at-8)(ax+b)-\frac{1}{120}a^3t^3(at(39at-55)+20)(ax+b)+\ldots\\
&= (ax+b)\left[1-at+\left(\frac{1}{2}a^2t^2+\frac{1}{2}a^2t^2\right)-\left(\frac{1}{2}a^3t^3-\frac{1}{3}a^3t^3-\frac{1}{6}a^3t^3\right)+\ldots\right]\\
&= (ax+b)\left[1-at+a^2t^2-a^3t^3+\ldots\right].
\end{aligned}
$$

It is easy to see that the above series converges to the exact solution $w(x,t)=\frac{ax+b}{1+at}$ when $|at|<1$. For the numerical comparisons, in the later part, the Adomian coefficients are taken from the article [128] and the series solution by ADM is denoted by $\psi_n(x,t)$. Figures 5.14(a) and 5.14(c) depict the plots of the series solution of 3 terms computed using ODM and ADM, respectively, and the exact solution is presented in Figure 5.14(b) for comparison. The simulations clearly show that however, the range for both the series solutions is the same as the exact solution, the ODM solution displays more similarities with the exact solution. This claim is strengthened by the relative error plots of the series solutions in Figure 5.15. We noticed that the error corresponding to ϕ_3 is very low and has decreasing behavior for a large time while in the case of ADM, it is observed that the behavior is increasing. Finally, the absolute error for 3 and 10 terms of both ODM and ADM at a fixed value of x and $t \in [0,1]$ are plotted in Figure 5.16 which establishes the superiority of ODM by noticing that after a certain point of time, the error via ADM starts blowing up.

In addition, we have provided TABLE 5.8 which shows the numerical errors in calculating the series solutions for ODM and ADM for different values of n. The error is computed by dividing the interval $[a, b]$ into N sub-intervals $[x_{i-1/2}, x_{i+1/2}], i = 1(1)N$. Each interval is represented by the mid-point $x_i = \frac{x_{i-1/2}+x_{i+1/2}}{2}$. Define error for ODM as

$$\text{Error} := \sum_{i=1}^{N} |\phi_n^i - w_i| h_i, \tag{5.55}$$

and similarly replacing ϕ_n^i by ψ_n^i gives error for ADM. For this case, let $h_i = 1$. From the TABLE 5.8, one can easily see the advantage of using ODM over ADM as error decreases very rapidly in ODM for increasing values of n.

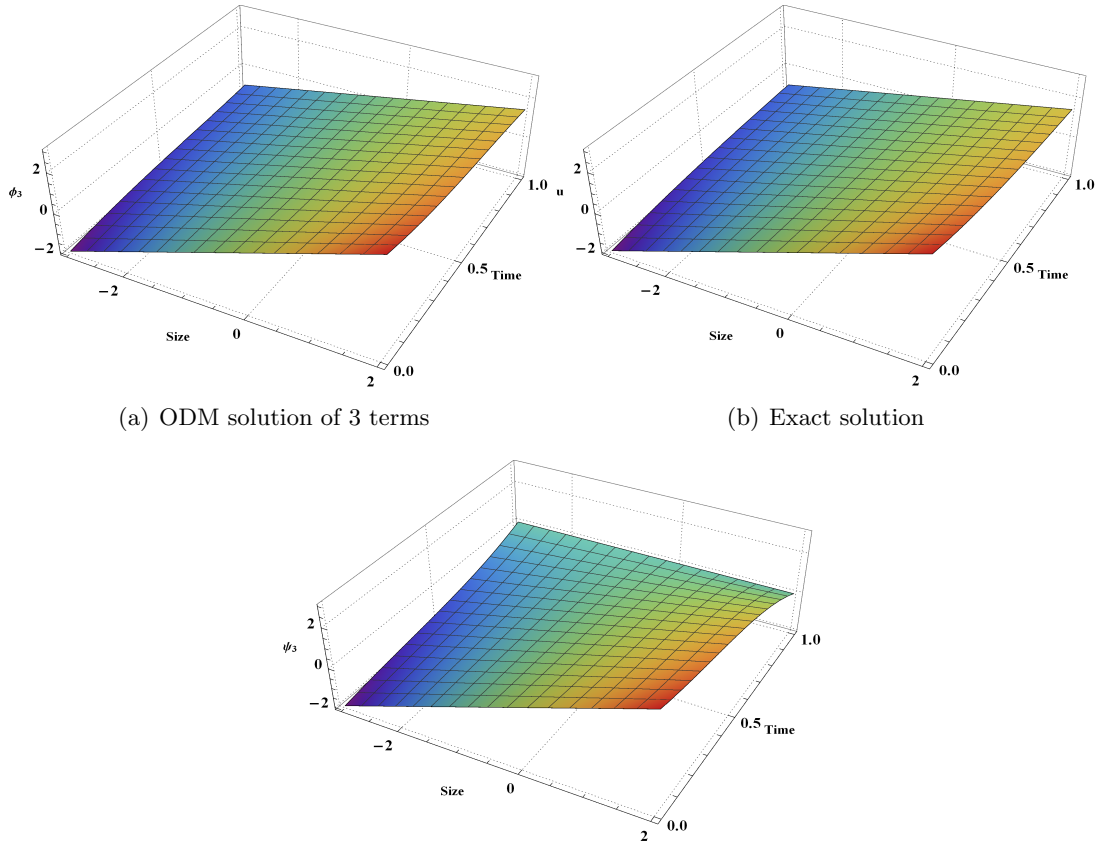

(a) ODM solution of 3 terms

(b) Exact solution

(c) ADM solution of 3 terms

FIGURE 5.14: Comparison of ODM and ADM series solutions when $a, b = 1$, x from -3 to 2 and t from 0 to 1 for Example 5.4

Example 5.5. *The example deals with computing the series solution of the inviscid 1D BE* (5.53) *with initial speed* $w_0(x) = ax^2$, $a \neq 0$ *and its comparison with the exact speed which is presented in [128] as*

$$w(x,t) = \frac{(2atx + 1) - \sqrt{4atx + 1}}{2at^2}. \tag{5.56}$$

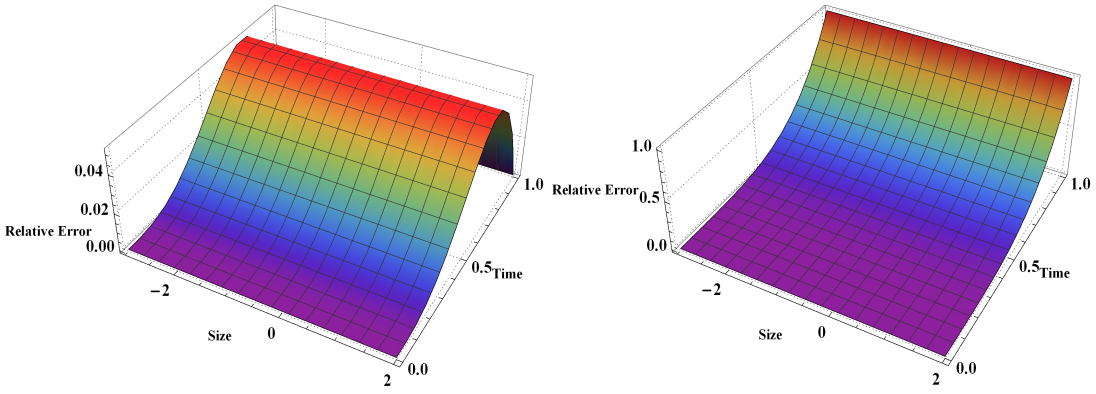

(a) Relative error for ϕ_3 (b) Relative error for ψ_3

FIGURE 5.15: Relative errors for ODM and ADM series solutions of three terms for Example 5.4

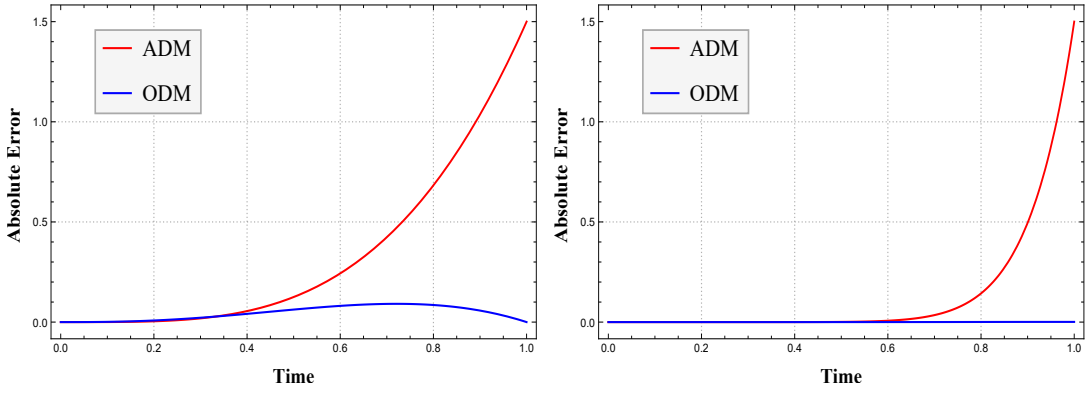

(a) Absolute error for ϕ_3 and ψ_3 at $x = 2$ (b) Absolute error for ϕ_{10} and ψ_{10} at $x = 2$

FIGURE 5.16: Absolute errors for ODM and ADM series solutions of three and ten terms at $x = 2$ for Example 5.4

TABLE 5.8: Numerical errors in computing approximate solutions using ADM and ODM for Example 5.4 at time $t = 0.5$

n	3	5	7	10	15	20
ADM	0.375	0.093	0.023	0.003	0.0009	0.0008
ODM	0.187	0.002	0.0025	0.0004	2.9×10^{-7}	7.9×10^{-10}

Again, using (5.33) and the equations (5.34)-(5.36) yield the following first few terms of the series solution as

$$C(x) = -3ax, \quad w_0(x,t) = ax^2, \quad w_1(x,t) = -2a^2tx^3, \quad w_2(x,t) = 2a^3t^2x^4,$$
$$w_3(x,t) = 3a^3t^2x^4(1-2atx), \quad w_4(x,t) = a^4t^3x^5(13atx-5),$$
$$w_5(x,t) = -\frac{1}{5}a^4t^3x^5(atx(177atx-100)+15), \quad w_6(x,t) = \frac{3}{20}a^5t^4x^6(4atx(154atx-89)+45),$$
$$w_7(x,t) = \frac{1}{20}a^5t^4x^6(atx(2atx(1731-2564atx)-711)+45).$$

Here, the value of ODM series solution leads to

$$\begin{aligned}\phi_n(t,x) &= \sum_{k=0}^{n} w_k(t,x) = w_0(x,t) + w_1(x,t) + w_2(x,t) + w_3(x,t) + w_4(x,t) + w_5(x,t) \\ &\quad + w_6(x,t) + w_7(x,t)\ldots \\ &= ax^2 - 2a^2tx^3 + (2a^3t^2x^4 + 3a^3t^2x^4) - (6a^4t^3x^5 + 5a^4t^3x^5 + 3a^4t^3x^5) \\ &\quad + (13a^5t^4x^6 + 20a^5t^4x^6 + 9a^5t^4x^6) + \ldots \\ &= ax^2 - 2a^2tx^3 + 5a^3t^2x^4 - 14a^4t^3x^5 + 42a^5t^4x^6 + \ldots.\end{aligned}$$

We noticed that the above series converges to the exact solution if we expand the series of $\sqrt{1+4z}$ and put $z = atx$. The series solutions of 5 terms computed using ODM and

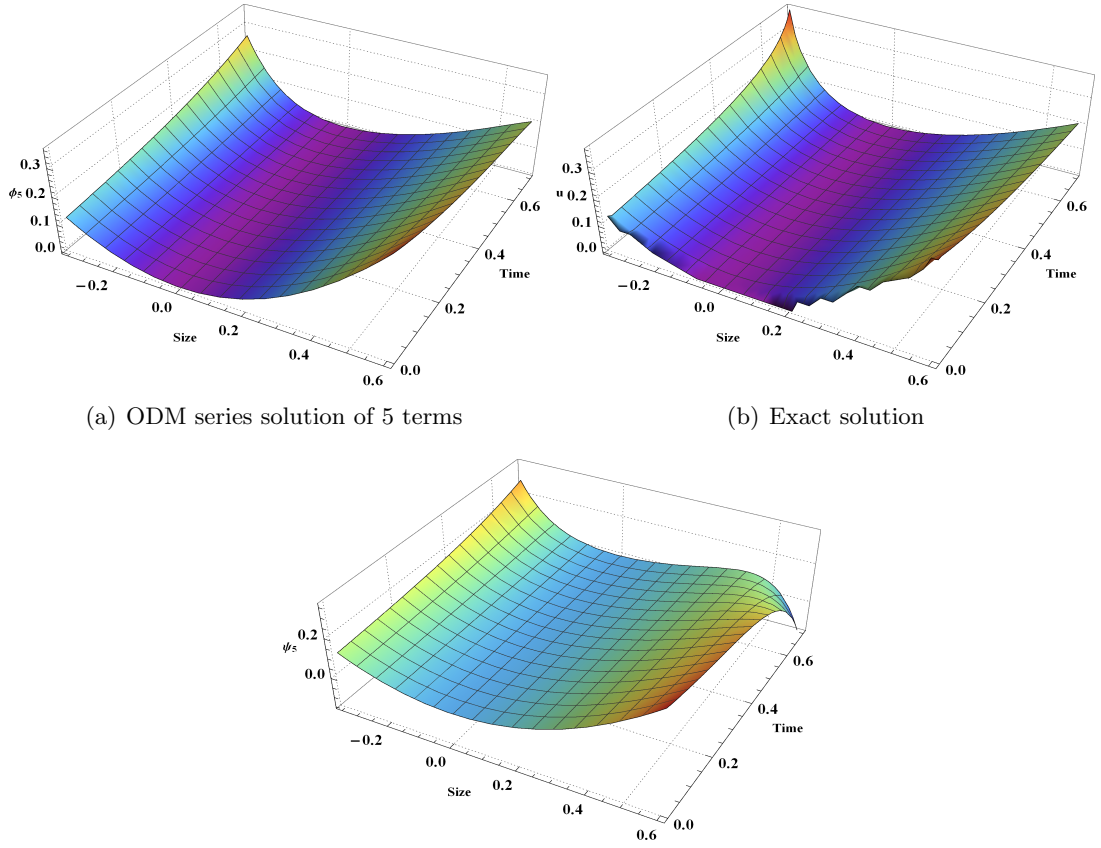

(a) ODM series solution of 5 terms

(b) Exact solution

(c) ADM series solution of 5 terms

FIGURE 5.17: Comparison of ODM and ADM series solutions when $a = 1$, x from -0.35 to 0.60 and t from 0 to 0.7 for Example 5.5

ADM along with the exact solution are visualized in Figure 5.17. The plots indicate that the ODM solution has the same range as the exact solution, whereas the solution obtained using ADM shows little similarity with the exact one. Figure 5.18 further confirms our assertion that the solution by ODM is stable and in excellent agreement

with the exact one while ADM overpredicts the results even by taking more terms in the approximated series solution. Additionally, by using formula (5.55) with $h_i = 0.1$, the numerical errors in computing the series solutions for ODM and ADM for different values of n are provided in TABLE 5.9. The table depicts that the errors in ADM are not only higher than the errors in ODM but the values keep on increasing as n progresses. Thus, indicating the superiority of ODM over ADM.

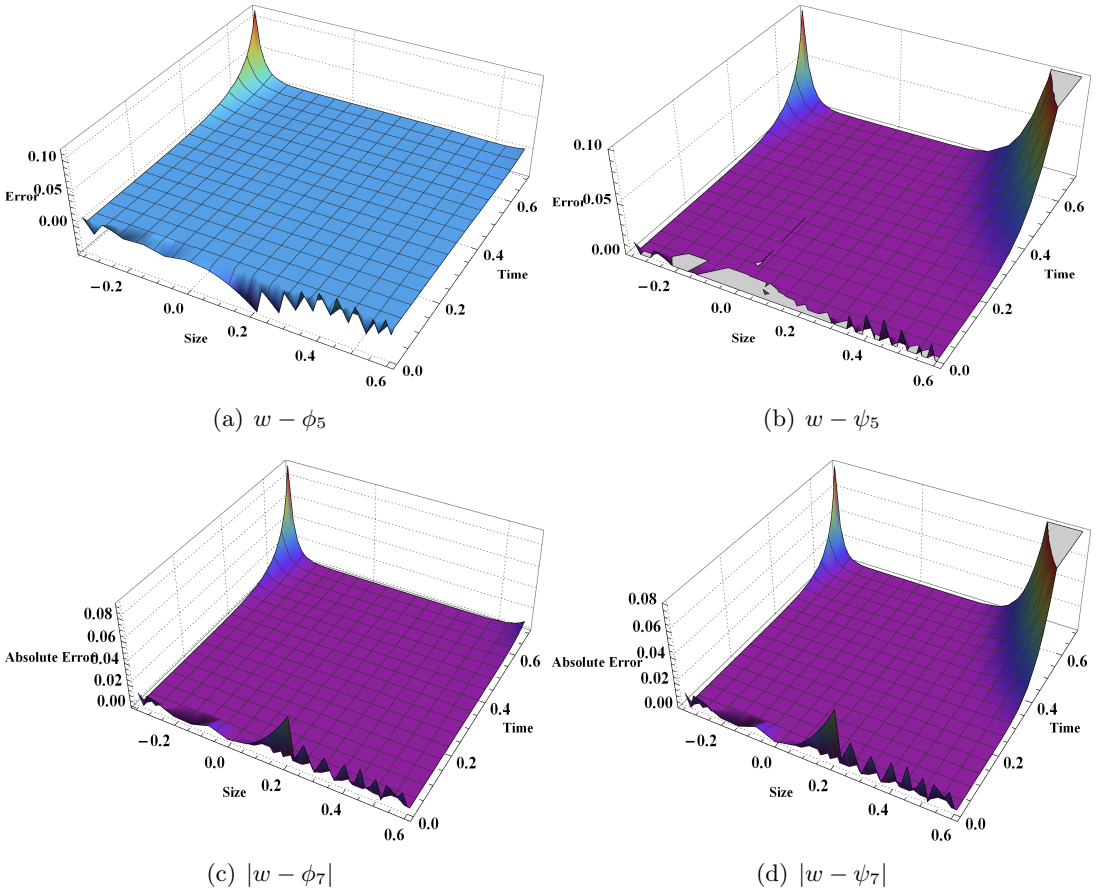

(a) $w - \phi_5$ (b) $w - \psi_5$

(c) $|w - \phi_7|$ (d) $|w - \psi_7|$

FIGURE 5.18: Errors for ODM and ADM series solutions of five and seven terms for Example 5.5

TABLE 5.9: Numerical errors in computing approximate solutions using ADM and ODM at $t = 0.7$, for Example, 5.5

n	3	5	7	10	15	20
ADM	0.032	0.034	0.044	0.085	0.4	2.3
ODM	0.018	0.012	0.0095	0.0070	0.005	0.004

Example 5.6. *Consider again the same equation (5.53) but with* $w_0(x) = \frac{ax+b}{cx+d}$, $a, c \neq 0$ *for which the exact solution is given in [128] as*

$$u(x,t) = \frac{-\sqrt{(at+d+x)^2 - 4t(ax+b)} + at + d + x}{2t}. \tag{5.57}$$

Thanks to (5.33) and the equations (5.34)-(5.36), the term $C(x)$ and the solution coefficients are computed as

$$C(x) = -\frac{(ax+b)\left(\frac{2c^2(ax+b)}{(cx+d)^3} - \frac{2ac}{(cx+d)^2}\right)}{(cx+d)\left(\frac{a}{cx+d} - \frac{c(ax+b)}{(cx+d)^2}\right)} + \frac{c(ax+b)}{(cx+d)^2} - \frac{a}{cx+d},$$

$$w_1(x,t) = \frac{t(ax+b)(bc-ad)}{(cx+d)^3}, \quad w_2(x,t) = \frac{t^2(ax+b)(bc-ad)^2}{2(cx+d)^5},$$

$$w_3(x,t) = \frac{t^2(ax+b)(bc-ad)(2acx-ad+3bc)\left(-adt+bct+(cx+d)^2\right)}{2(cx+d)^7},$$

$$w_4(x,t) = \frac{1}{24(cx+d)^9}(bc-ad)t^3(ax+b)\left(8(cx+d)^2\left(a^2\left(c^2x^2-4cdx+d^2\right)+6abc(cx-d)+6b^2c^2\right)\right)$$
$$+ t(bc-ad)\left(a^2\left(6c^2x^2-14cdx+3d^2\right)+2abc(13cx-10d)+23b^2c^2\right).$$

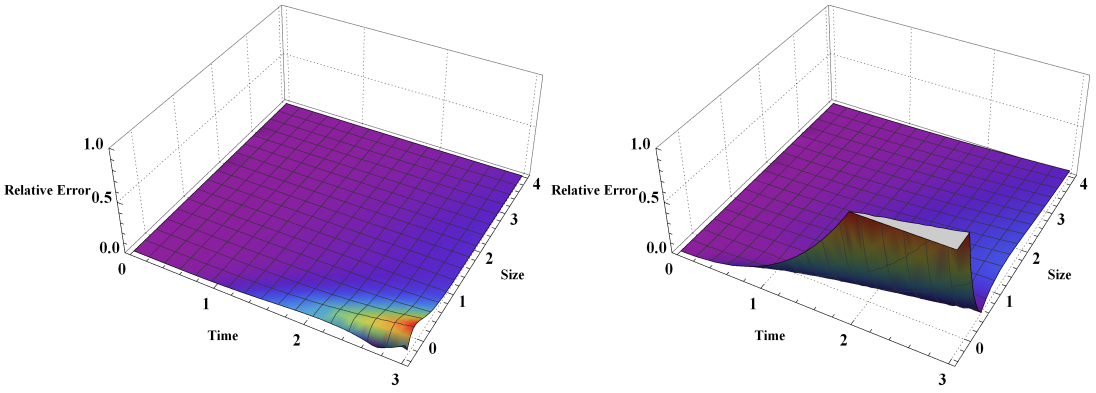

(a) Relative error for ϕ_4 (b) Relative error for ψ_4

FIGURE 5.20: Relative errors for ODM and ADM series solutions of four terms for Example 5.6

Figures 5.19(a) and 5.19(c) show the numerical simulations of the series solution by taking 4 terms using ODM and ADM, respectively and the exact solution is presented in Figure 5.19(b) for comparison. The figures depict that the ADM solution does not have the same range as the exact solution, whereas the solution obtained using ODM shows a very similar plot. The novelties of ODM over ADM can also be visualized by looking at the relative errors considering 4 term series solutions in Figure 5.20. The TABLE 5.10 depicts the comparison of the order of convergence for the approximated

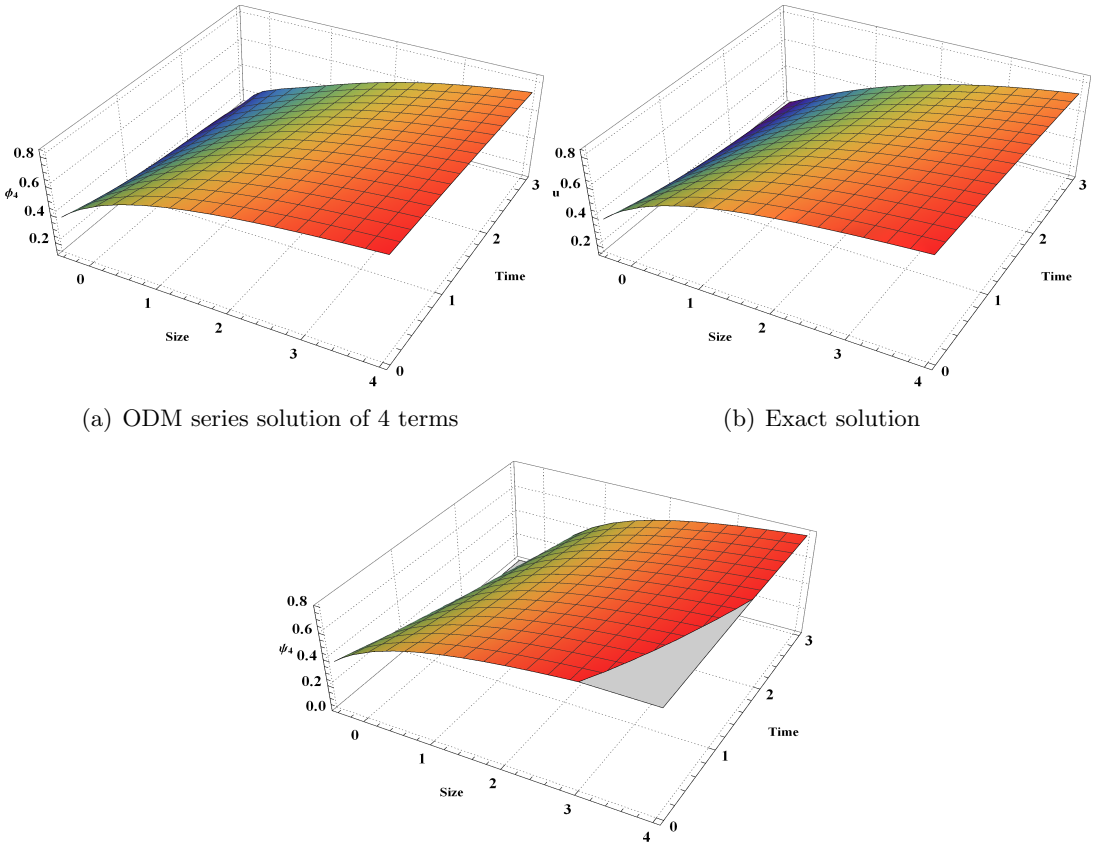

(a) ODM series solution of 4 terms

(b) Exact solution

(c) ADM series solution of 4 terms

FIGURE 5.19: Comparison of ODM and ADM series solutions of four terms when $a, b, c = 1$, $d = 2$, x from -0.40 to 4 and t from 0 to 3 for Example 5.6

solutions for $n = 10$ computed using ADM and ODM at $t = 2$, and clearly establishes ODM as a superior method to ADM.

TABLE 5.10: Comparison of the order of convergence for ten terms of ADM and ODM approximated solution at $t = 2$, for Example, 5.6

h	ADM	ODM
0.5		
	0.77	≈ 1
0.25		
	0.88	≈ 1
(0.25)/2		
	0.90	≈ 1
(0.25)/4		

Example 5.7. *Let us now consider a case of non-homogenous inviscid BE given as*

$$\frac{\partial w}{\partial t} + w\frac{\partial w}{\partial x} = f(x,t), \tag{5.58}$$

with $f(x,t) = -\sin(x+t) - \sin(2x+2t)/2$ *and initial condition* $w_0(x) = \cos x$ *for which the exact solution is presented in [133] as*

$$w(x,t) = \cos(x+t). \tag{5.59}$$

The ODM coefficients can be computed by taking $w_0(x,t) = w_0(x) + \int_0^t f(x,t)dt$, and the rest of the coefficients are expressed in the same way as in TABLE 5.1. So, we get

$$\begin{aligned}
w_0(x,t) &= \cos(x+t) + (\cos(2x+2t) - \cos 2x)/4, \quad C(x) = \sin(t+x) - \cos(t+x)\cot(t+x),\\
w_1(x,t) &= \frac{1}{8}(-\cos(t-x) + 2\cos x + 2\cos 2x - 2\cos 3x - \frac{3}{8}\cos 4x - \cos(t+x) - 2\cos(2t+2x))\\
&\quad + \frac{1}{64}(-8\cos(3t+3x) - \cos(4t+4x) + 4(t\sin(4x) + \cos(2(t+2x)) + 6\cos(t+3x))),
\end{aligned}$$

and so on. Here, the expression for $w_1(x,t)$ is too complicated and contains some terms common with $w_0(x,t)$ in the opposite sign. So, when we add $w_0(x,t)$ and $w_1(x,t)$, the only term left in $w_0(x,t)$ is $\cos(x+t)$ which is the exact solution. The other terms in $w_1(x,t)$ make a balance with values in $w_2(x,t)$ and $w_3(x,t)$ and thus we arrive at the exact solution. Another way to compute the coefficients is if we take $w_0(x,t) = \cos(x+t)$ so that we have

$$\begin{aligned}
&w_1(x,t) = \mathcal{L}^{-1}\left(-\sin(x+t) - \sin(2x+2t)/2 + \sin(t+x)\cos(t+x)\right) = 0,\\
&w_k(x,t) = 0, \quad k \geq 2.
\end{aligned}$$

So, the initial condition gives us the exact solution. It needs to be mentioned here that the same value of the coefficients are obtained via ADM in [128] and therefore, the numerical comparisons are omitted here.

Example 5.8. *Let us now consider the viscous Burgers equation*

$$\frac{\partial w}{\partial t} + w\frac{\partial w}{\partial x} = \nu\frac{\partial^2 w}{\partial x^2}, \tag{5.60}$$

with $w(x,0) = ax + b$. *The exact solution for this problem is presented in [128] and is written as*

$$w(x,t) = (ax+b)/(1+at). \tag{5.61}$$

Using (5.33) and the equations (5.34)-(5.36) give the coefficients as

$$C(x) = -a,\ \ w_0(x,t) = ax + b,\ \ w_1(x,t) = -at(ax+b),\ \ w_2(x,t) = \frac{1}{2}a^2t^2(ax+b),$$
$$w_3(x,t) = -\frac{1}{2}a^2t^2(at-1)(ax+b),\ \ w_4(x,t) = \frac{1}{24}a^3t^3(9at-8)(ax+b).$$

These coefficients are exactly the same as in Example 5.4. This is due to the initial condition considered whose second derivative is zero.

Example 5.9. *The example deals with computing the approximate solutions for the viscous Burgers equation* (5.60) *satisfying* $w_0(x) = x - 2/(x+c)$. *The solution for this problem is expressed in the Appendix of [133] as*

$$u(x,t) = \frac{x}{t} - \frac{2}{x+ct}. \tag{5.62}$$

The term $C(x)$ and the first two terms are calculated as

$$C(x) = \frac{4\left(x - \frac{2}{c+x}\right)}{(c+x)^3\left(\frac{2}{(c+x)^2}+1\right)} - \frac{2}{(c+x)^2} - 1,\quad w_0(x,t) = x - \frac{2}{c+x},$$
$$w_1(x,t) = (t-1)\left(\frac{2c}{(c+x)^2} - x\right),\quad w_2(x,t) = \frac{(t-1)^2(x(c+x)-2)\left((c+x)^2+6\right)}{2(c+x)\left((c+x)^2+2\right)}.$$

By following the same formula as in previous examples, it should be mentioned here that the higher-order coefficients can be computed using (5.34)-(5.36) and MATHEMATICA© but due to the complexity in their nature, they are omitted here. Figure 5.21 shows the error plots for series solutions ϕ_4 and ψ_4 which indicates that ADM shows a larger value of negative error. The novelty of ODM is established by looking at the absolute errors when time is increased up to $t = 2.5$ presented in Figure 5.22.

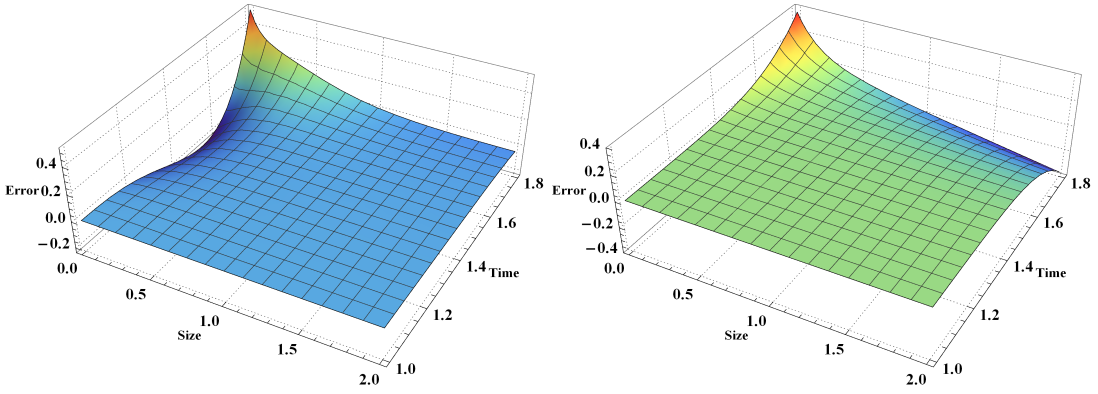

(a) $w - \phi_4$ (b) $w - \psi_4$

FIGURE 5.21: Error for ODM and ADM series solutions of four terms for Example 5.9

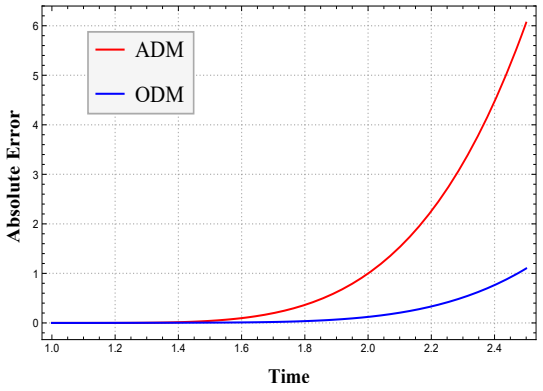

FIGURE 5.22: Error for ODM and ADM series solutions of four terms at $x = 2$ for Example 5.9

In the following subsection, we discuss two test cases for the 2D Burgers equation to show the implementation of ODM defined in Section 4, and the simulations are compared with the available analytical solutions.

Two Dimensional Case

Example 5.10. *Let us compute the series solution of the two-dimensional viscous Burgers equation obtained by putting* $\nu = 1$ *in* (5.41) *with* $f_1(x, y) = x+y$ *and* $f_2(x, y) = x-y$. *The exact solution for the equation is presented in [96] as*

$$w(x, y, t) = \frac{-2tx + x + y}{1 - 2t^2}, \quad v(x, y, t) = \frac{-2ty + x - y}{1 - 2t^2}. \tag{5.63}$$

The equations (5.50), (5.51) and the TABLES 5.6, 5.7 yield the following expressions for $C_1(x,y)$, $C_2(x,y)$, $u_k(x,y,t)$ and $v_k(x,y,t)$ upto $k=7$ as

$$
\begin{aligned}
C_1(x,y) &= -2, \quad C_2(x,y) = 0,\\
w_1(x,y,t) &= -2tx, \quad v_1(x,y,t) = -2ty,\\
w_2(x,y,t) &= 2t^2y, \quad v_2(x,y,t) = 2t^2(x-y),\\
w_3(x,y,t) &= \frac{2}{3}t^2((3-4t)x+3ty), \quad v_3(x,y,t) = \frac{2}{3}t^3(x-6y),\\
w_4(x,y,t) &= \frac{1}{3}(-2)t^3(t(x-7y)+3y), \quad v_4(x,y,t) = \frac{1}{3}t^3((11t-2)x-14ty),\\
w_5(x,y,t) &= -\frac{1}{15}t^3\left(\left(69t^2-60t+20\right)x+10t(3-8t)y\right), \quad v_5(x,y,t) = \frac{1}{15}t^4(36tx-113ty+10y),\\
w_6(x,y,t) &= \frac{1}{45}t^4(2t(15-59t)x+3(3t(49t-30)+20)y),\\
v_6(x,y,t) &= \frac{1}{45}t^4((t(311t-102)+15)x+3t(10-157t)y),\\
w_7(x,y,t) &= \frac{1}{315}t^4((t((2597-2710t)t-1197)+210)x+t(t(3931t-2100)+420)y),\\
v_7(x,y,t) &= \frac{1}{315}t^5(t(3(677t-70)x+(924-5420t)y)-105y).
\end{aligned}
$$

Let us denote the semi-analytical solutions for $w(x,y,t)$ and $v(x,y,t)$ by $\phi_n(x,y,t)$ and $\psi_n(x,y,t)$, respectively, as

$$\phi_n(x,y,t) = \sum_{k=0}^{n} w_k(x,y,t), \quad \psi_n(x,y,t) = \sum_{k=0}^{n} v_k(x,y,t).$$

The series solutions using ODM by taking five terms (ϕ_5) and seven terms (ϕ_7) at $t=0.1$ and $t=0.5$, respectively, are provided in the Figure 5.23 for $w(x,y,t)$ and in Figure 5.24 for $v(x,y,t)$. It is clearly visible that the numerical simulations are in excellent agreement with the exact solutions. The promising outcomes of ODM can be visualized by looking at the absolute error plots in Figures 5.25 and 5.26. In addition to the absolute errors, the numerical errors in computing the series solutions ϕ_n and ψ_n are depicted through TABLE 5.11 and defined as

$$\text{Error}_{2D}^{w} = ||\phi_n^i - w_i||_F, \quad \text{Error}_{2D}^{v} = ||\psi_n^i - v_i||_F. \tag{5.64}$$

Here F stands for the Frobenius norm.

TABLE 5.11: Numerical errors in computing approximate solutions using ODM for Example 5.10

n	5	7	10
ϕ_n (w)	0.004	0.005	6.01×10^{-6}
ψ_n (v)	0.0275	0.014	0.007

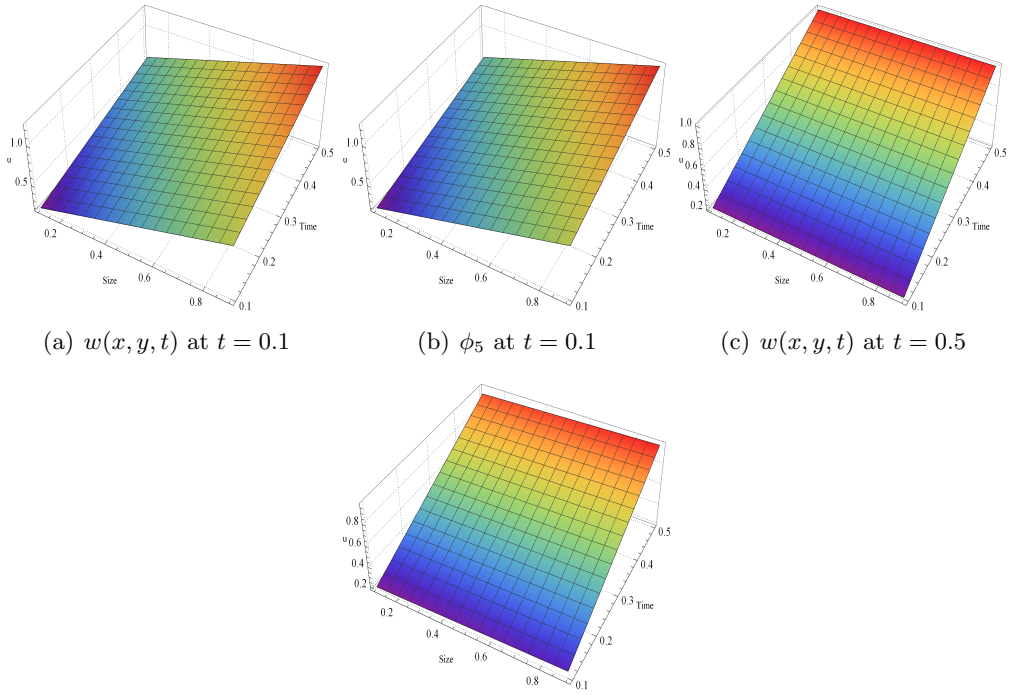

(a) $w(x, y, t)$ at $t = 0.1$ (b) ϕ_5 at $t = 0.1$ (c) $w(x, y, t)$ at $t = 0.5$

(d) ϕ_7 at $t = 0.5$

FIGURE 5.23: Comparison of ODM series solutions with exact solutions at $t = 0.1$ and $t = 0.5$ when $R_e = 1$, $x \in [0.1, 0.5]$ and $y \in [0.1, 0.5]$ for Example 5.10

Example 5.11. *The series solution of the two-dimensional viscous Burgers equation obtained by putting* $\nu = 1$ *in* (5.41) *with* $f_1(x, y) = x^2 y$ *and* $f_2(x, y) = y^2 x$ *with no exact solution are presented in this example.*

By following the equations (5.50), (5.51) and the TABLES 5.6, 5.7, the expressions for $C_1(x, y)$, $C_2(x, y)$, $w_k(x, y, t)$ and $v_k(x, y, t)$ up to $k = 3$ are obtained as

$$
\begin{aligned}
C_1(x, y) &= \frac{-4x^3y^3 - 4xy^2}{3x^2y^2} - \frac{4x^3y^3 - x^4y^2}{3x^2y^2}, \quad C_2(x, y) = -4xy - \frac{5y^2}{3}, \\
w_1(x, y, t) &= t\left(\frac{y}{50} - 3x^3y^2\right), \quad v_1(x, y, t) = t\left(\frac{x}{50} - 3x^2y^3\right), \\
w_2(x, y, t) &= \frac{t^2\left(2400x^5y^3 - 3x^4 - \left(x^3 - 4\right)y + \left(150x\left(x^3 - 4\right) - 1\right)x^2y^2\right)}{300x}, \\
v_2(x, y, t) &= \frac{1}{300}t^2y\left(1800x^3y^3 + x^2\left(3 - 750y^4\right) + 5xy - 3y^2\right),
\end{aligned}
$$

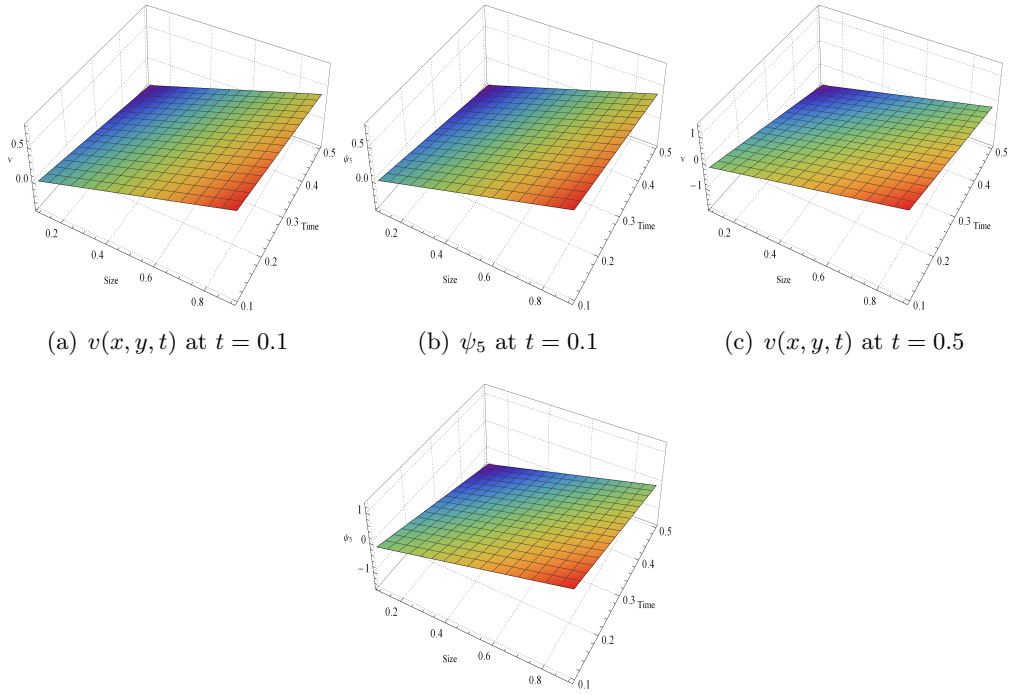

(a) $v(x, y, t)$ at $t = 0.1$ (b) ψ_5 at $t = 0.1$ (c) $v(x, y, t)$ at $t = 0.5$

(d) ψ_7 at $t = 0.5$

FIGURE 5.24: Comparison of ODM series solutions with exact solutions at $t = 0.1$ and $t = 0.5$ when $R_e = 1$, $x \in [0.1, 0.5]$ and $y \in [0.1, 0.5]$ for Example 5.10

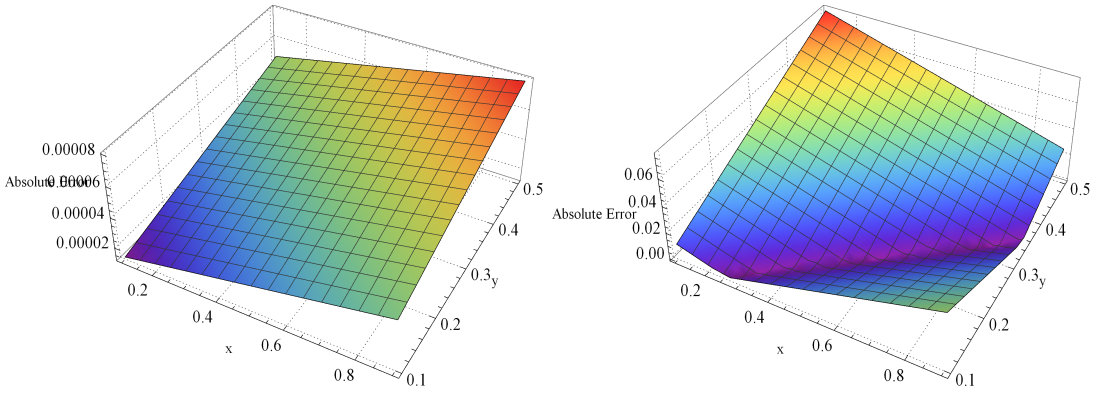

(a) $|w - \phi_5|$ at $t = 0.1$ (b) $|w - \phi_7|$ at $t = 0.5$

FIGURE 5.25: Absolute errors in ODM series solutions for computing w in Example 5.10

$$w_3(x,y,t) = -\frac{1}{18}t^3x^7y^2 - \frac{35}{18}t^3x^6y^3 - \frac{305}{9}t^3x^5y^4 + \frac{t^3x^5}{900} + \frac{5}{6}t^3x^4y^5 + \frac{4}{9}t^3x^4y^2 + \frac{121t^3x^4y}{2700} + \frac{52}{9}t^3x^3y^3$$
$$- \frac{7t^3x^3y^2}{2700} + \frac{58}{675}t^3x^2y^3 + \frac{4t^3y}{675x^2} - \frac{t^3x^2}{225} - \frac{8}{9}t^3xy^2 - \frac{2}{675}t^3xy - \frac{t^3x}{7500} + \frac{t^3y^2}{675} - \frac{1}{2}t^2x^5y^2$$
$$+ 4t^2x^4y^3 - \frac{3t^2x^3}{100} + 2t^2x^2y^2 + \frac{1}{300}t^2x^2y - \frac{7}{60}t^2xy^2 - \frac{t^2y}{75x},$$
$$v_3(x,y,t) = -\frac{1}{6}t^3x^5y^4 - \frac{83}{3}t^3x^4y^5 + \frac{15}{2}t^3x^3y^6 + \frac{2}{25}t^3x^3y^2 - \frac{1}{18}25t^3x^2y^7 + \frac{2}{3}t^3x^2y^4 + \frac{1}{900}t^3x^2y^3 + \frac{29}{540}$$
$$- \frac{t^3y^3}{225x} - \frac{t^3y^5}{180} - \frac{t^3y}{7500} + 6t^2x^3y^4 + \frac{5}{2}t^2x^2y^5 - \frac{1}{25}t^2x^2y - \frac{1}{60}t^2xy^2 - \frac{303t^2y^3}{100}.$$

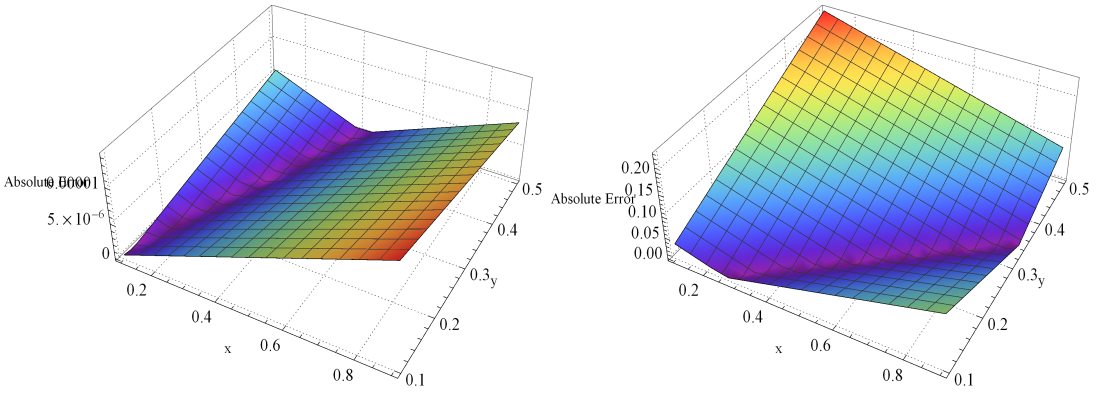

(a) $|v - \psi_5|$ at $t = 0.1$ (b) $|v - \psi_7|$ at $t = 0.5$

FIGURE 5.26: Absolute errors in ODM series solutions for computing v in Example 5.10

The other coefficients are too complex to include here but can be computed using MATHEMATICA. Figures 5.27(a)-5.27(c) depict the absolute errors among 3, 4, 5, and 6-term truncated solutions in calculating w at $t = 0.1$. They show a constant decrease in the error values, which indicates the convergence of the ODM series solution towards the exact solution. The decreasing behavior of the absolute errors of these truncated solutions in computing the value of v is represented in Figures 5.28(a)-5.28(c). This depicts that our proposed method ODM can provide solution for problems where an analytical solution is not available.

Three Dimensional Case

In this section, we shall extend ODM to a viscous 3D Burgers equation.

Example 5.12. *Consider the viscous Burgers equation* (5.8) *together with the initial condition* $w(x, y, z, 0) = x + y + z$ *and the exact solution is given in [134] as*

$$w(x, y, z, t) = \frac{(x + y + z)}{1 - t}. \tag{5.65}$$

Here,

$$M[w] = w\frac{\partial w}{\partial x}, \quad C(x) = \frac{\partial M}{\partial w}\bigg|_{t=0} = \frac{w_0(x, y, z, t)\frac{\partial^2 w_0(x,y,z,t)}{\partial x^2}}{\frac{\partial w_0(x,y,z,t)}{\partial x}} + \frac{\partial w_0(x, y, z, t)}{\partial x}.$$

By using the following TABLE 5.12, one can obtain the series solution for 3D Burgers equation. The values $Q_k(x, y, z, t)$ are defined as:

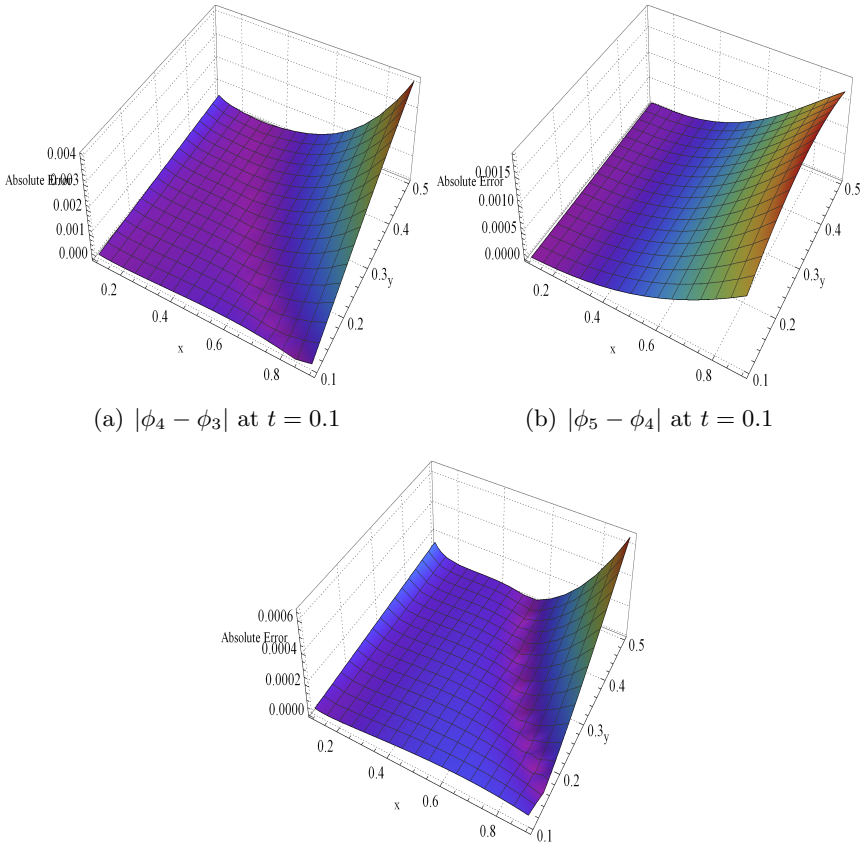

(a) $|\phi_4 - \phi_3|$ at $t = 0.1$

(b) $|\phi_5 - \phi_4|$ at $t = 0.1$

(c) $|\phi_6 - \phi_5|$ at $t = 0.1$

FIGURE 5.27: Absolute errors in ODM series solutions for computing w when $x \in [0.1, 0.9]$ and $y \in [0.1, 0.5]$ in Example 5.11

TABLE 5.12: Table of the coefficients for $w(x, y, z, t)$

$w_0(x, y, z, t)$	$w(x, y, z, 0)$
$w_1(x, y, z, t)$	$\mathcal{L}^{-1}\left(\frac{\partial^2}{\partial x^2} w_0(x, y, z, t) + \frac{\partial^2}{\partial y^2} w_0(x, y, z, t) + Q_0(x, y, z, t)\right)$
$w_2(x, y, z, t)$	$\mathcal{L}^{-1}\left(\left(\frac{\partial^2}{\partial x^2} w_1 + \frac{\partial^2}{\partial y^2} w_1 + Q_1\right)(x, y, z, t) - \left(\frac{\partial^2}{\partial x^2} + \frac{\partial^2}{\partial y^2} + C(x)\right) w_1(x, y, z, t)\right)$
$w_{k+1}(x, y, z, t)$	$\mathcal{L}^{-1}\left(\left(\frac{\partial^2}{\partial x^2} w_k + \frac{\partial^2}{\partial y^2} w_k + Q_k\right) - \left(\frac{\partial^2}{\partial x^2} + \frac{\partial^2}{\partial y^2} + C(x)\right)(w_k - w_{k-1})\right), \quad k \geq 2$

$$Q_k(x, y, z, t) = \frac{1}{k!} \frac{d^k}{d\theta^k} \left[M\left(\sum_{i=0}^{k} \theta^i w_i(x, y, z, t) \right) \right] \Bigg|_{\theta=0}. \tag{5.66}$$

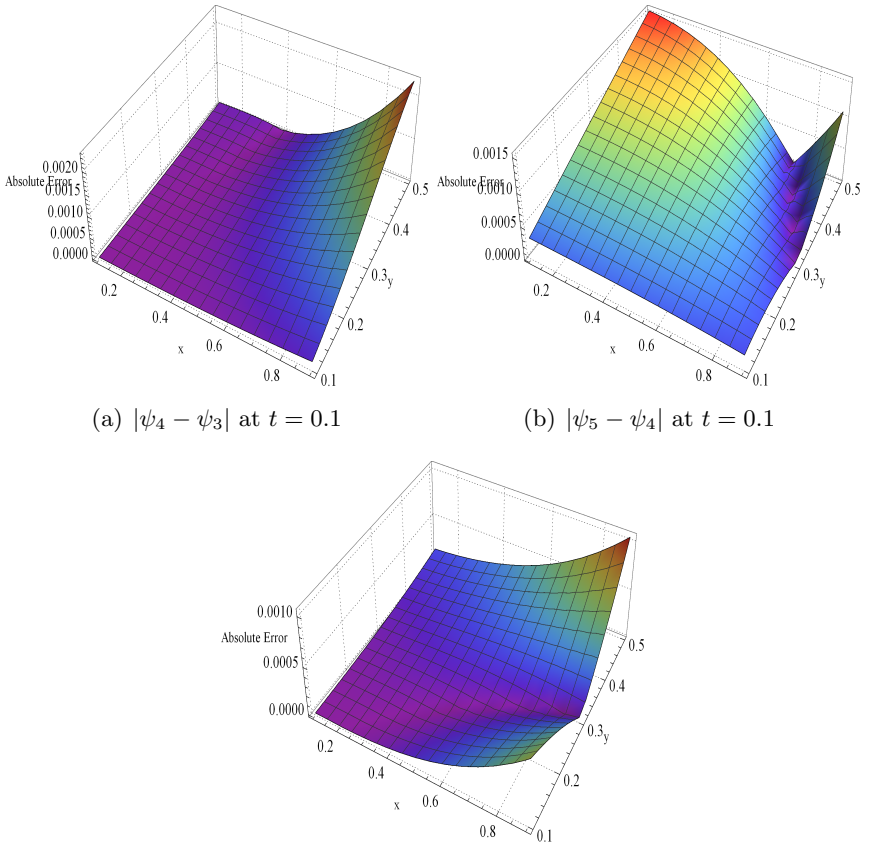

(a) $|\psi_4 - \psi_3|$ at $t = 0.1$

(b) $|\psi_5 - \psi_4|$ at $t = 0.1$

(c) $|\psi_6 - \psi_5|$ at $t = 0.1$

FIGURE 5.28: Absolute errors in ODM series solutions for computing v when $x \in [0.1, 0.9]$ and $y \in [0.1, 0.5]$ in Example 5.11

The value of $C(x)$ and the coefficients are computed as

$$
\begin{aligned}
C(x) = 1, \quad & w_0(x,y,z,t) = (x+y+z), \quad w_1(x,y,z,t) = t(x+y+z),\\
& w_2(x,y,z,t) = \frac{t^2}{2}(x+y+z), \quad w_3(x,y,z,t) = \frac{t^2}{2}(x+y+z) + \frac{t^3}{2}(x+y+z),\\
& w_4(x,y,z,t) = \frac{t^3}{3}(x+y+z) + \frac{9t^4}{24}(x+y+z),\\
& w_5(x,y,z,t) = \frac{t^3}{6}(x+y+z) + \frac{11t^4}{24}(x+y+z) + \frac{13t^5}{40}(x+y+z),\\
& w_6(x,y,z,t) = \frac{3t^4}{24}(x+y+z) + \frac{16t^5}{40}(x+y+z) + \frac{21t^5}{80}(x+y+z),\\
& w_7(x,y,z,t) = \frac{t^4}{24}(x+y+z) + \frac{392t^5}{1680}(x+y+z) + \frac{693t^6}{80}(x+y+z) + \frac{369t^7}{1680}(x+y+z).
\end{aligned}
$$

Thus, the series solution is obtained by

$$\begin{aligned}\phi_n(x,y,z,t) &= (x+y+z)\left[1+t+\left(\frac{t^2}{2}+\frac{t^2}{2}\right)+\left(\frac{t^3}{2}+\frac{t^3}{3}+\frac{t^3}{6}\right)\right]\\ &\quad+(x+y+z)\left[\left(\frac{9t^4}{24}+\frac{11t^4}{24}+\frac{3t^4}{24}+\frac{t^4}{24}\right)+\ldots\right]\\ &= (x+y+z)\left[1+t+t^2+t^3+t^4+\ldots\right]\end{aligned}$$

which converges to the exact solution $w(x,y,z,t)=\frac{(x+y+z)}{1-t}$.

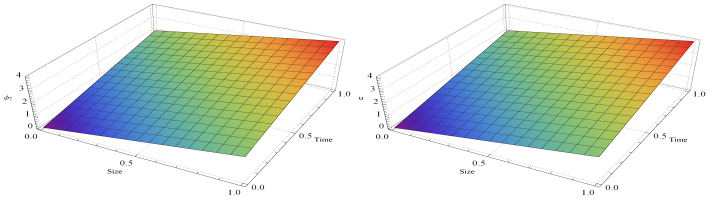

(a) ODM solution of seven terms for $z=0$ (b) Exact solution at for $z=0$

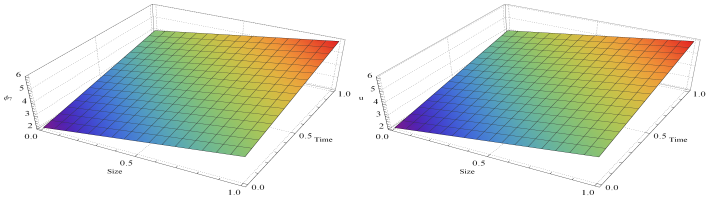

(c) ODM solution of seven terms for $z=1$ (d) Exact solution at for $z=1$

FIGURE 5.29: ODM series solution of seven terms at $t=0.5$ for x,y from 0 to 1 and $z=0,1$ for Example 5.12

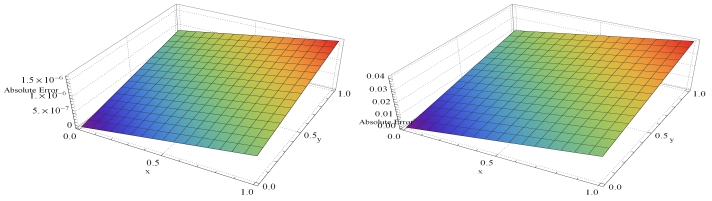

(a) $|w-\phi_3|$ at $t=0.1$ for $z=0$ (b) $|w-\phi_7|$ at $t=0.5$ for $z=0$

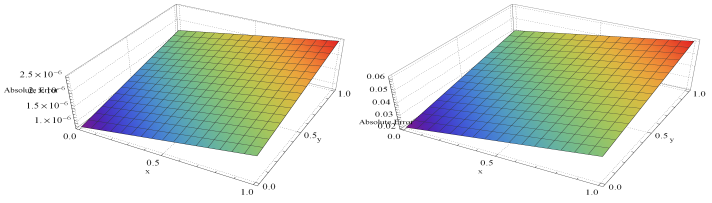

(c) $|w-\phi_3|$ at $t=0.1$ for $z=1$ (d) $|w-\phi_7|$ at $t=0.5$ for $z=1$

FIGURE 5.30: Absolute error in ODM series solution for x,y from 0 to 1 and $z=0,1$ for Example 5.12

To compare the numerical results for a three-dimensional equation, we fix two values of z, i.e., $z = 0$ and $z = 1$. It is observed that only 3 terms of the ODM series solution are needed to give an excellent similarity with the exact solution at $t = 0.1$ for both $z = 0, 1$ and when the value of t is increased, adding four extra terms gives us the desired behavior as the exact one. The absolute errors for both $t = 0.1$ and $t = 0.5$ for $z = 0, 1$ justify the accuracy of the ODM approximated solutions with exact.

Chapter 6

Laplace Transform Based Semi-Analytical Techniques for Pure Coagulation and Fragmentation Equations[1]

The focus of this chapter is the introduction of the Laplace optimized decomposition method (LODM) and Laplace Adomian decomposition method (LADM) to solve the coagulation equation

$$\frac{\partial u(x,t)}{\partial t} = \frac{1}{2}\int_0^x K(x-y,y)u(x-y,t)u(y,t)dy - \int_0^\infty K(x,y)u(x,t)u(y,t)dy, \quad (6.1)$$

and fragmentation equation

$$\frac{\partial u(x,t)}{\partial t} = \int_x^\infty b(x,y)u(y,t)\phi(y)dy - \phi(x)u(x,t), \quad (6.2)$$

respectively, where $u : J \to \mathbb{R}$ where $J =]0,\infty[\times[0,T]$ and initial datum

$$u(x,0) = u_0(x) \geq 0. \quad (6.3)$$

It has been shown in recent works [69–71] that the addition of the Laplace transformation on the ADM approach (LADM) provides better accuracy than ADM for solving fractional differential and Volterra integral equations. In 2022, Beghami et al. [72] developed a new series solution method based on ODM called the Laplace optimized decomposition method (LODM) to solve the system of partial differential equations of fractional order with great accuracy. Therefore, this study aims to solve the coagulation and fragmentation population balance equations using LODM and LADM, respectively.

[1] This chapter is under revision in Mathematical Methods in Applied Sciences.

The advantage of using the Laplace transform-based techniques is the presence of an extra time multiplier while computing the theoretical error bound which leads to lower values of error for lower t. Several numerical examples of coagulation and fragmentation problems are taken to validate the theoretical findings. It is shown that the scheme shows nice agreement with the analytical solutions.

The rest part of the chapter is organized as follows. In Section 6.1, the fundamental idea of LODM is described for the general non-linear problems and then discussed for the coagulation equation. Further, the theoretical convergence results are part of Section 6.2. Section 6.3 deals with the numerical implementations of LODM for Eq. (6.1) and LADM for Eq. (6.2) and the simulations are presented in the form of figures and tables.

6.1 Laplace Optimized Decomposition Method: Preliminaries

The concept of LODM for integro-partial differential equations is developed in this section. The following general non-linear differential equation is taken into consideration:

$$Lu(x,t) = Ru(x,t) + Nu(x,t) + h(x,t), \tag{6.4}$$

with initial condition

$$u(x,0) = f(x), \tag{6.5}$$

where $L := \frac{\partial}{\partial t}$ is linear differential operator, R is the linear operator, N is a non-linear differential operator and $h(x,t)$ is source term. Now, the procedure of LODM for the equation (6.4) is discussed in the following steps:

Step 1: Taking Laplace transform of Eq. (6.4) and using the differentiation property of Laplace transform, we acquire:

$$\mathcal{L}[u(x,t)] = \frac{f(x)}{p} + \frac{1}{p}\mathcal{L}[Ru(x,t)] + \frac{1}{p}\mathcal{L}[Nu(x,t)] + \frac{1}{p}\mathcal{L}[h(x,t)]. \tag{6.6}$$

Step 2: In terms of infinite series, LODM provides the following solution:

$$u(x,t) = \sum_{k=0}^{\infty} u_k(x,t), \tag{6.7}$$

and the nonlinear terms can be written as follows:

$$Nu(x,t) = \sum_{k=0}^{\infty} A_k(x,t), \tag{6.8}$$

where A_k, $k \geq 0$ are referred as Adomian polynomials and can be computed as given below

$$A_k(x,t) = \frac{1}{k!}\frac{d^k}{d\theta^k}\left[N\left(\sum_{i=0}^{k}\theta^i u_i(x,t)\right)\right]\Bigg|_{\theta=0}. \tag{6.9}$$

Now, to illustrate the core idea of ODM (see [67]), we take a linear approximation of the related nonlinear function. Consider,

$$F[Lu, Ru, Nu] = Lu - Ru - Nu,$$

as linear operators by linearizing the non-linear term by the first-order Taylor series expansion at $t = 0$ as follows:

$$F[Lu, Ru, Nu] \approx Lu - Ru - C(x)u,$$

where the function $C(x)$ is defined as

$$C(x) = \frac{\partial N}{\partial u}\Big|_{t=0}. \tag{6.10}$$

Step 3: The component functions $u_k(x,t), k \geq 0$ will be determined by the help of the following iteration formula

$$\begin{cases} \mathcal{L}[u_0(x,t)] & = \frac{f(x)}{p} + \frac{1}{p}\mathcal{L}[h(x,t)] \\ \mathcal{L}[u_1(x,t)] & = \frac{1}{p}\mathcal{L}[A_0(x,t) + Ru_0(x,t)] \\ \mathcal{L}[u_2(x,t)] & = \frac{1}{p}\mathcal{L}[(A_1(x,t) + Ru_1(x,t)) - (R + C(x))u_1(x,t)] \\ \mathcal{L}[u_{k+1}(x,t)] & = \frac{1}{p}\mathcal{L}[(A_k(x,t) + Ru_k(x,t)) - (R + C(x))(u_k(x,t) - u_{k-1}(x,t))], \quad k \geq 2. \end{cases}$$

Step 4: The required recursive relation is provided by applying the inverse Laplace transform to the equation generated in Step 3, as shown below

$$\begin{cases} u_0(x,t) & = \mathcal{L}^{-1}\left[\frac{f(x)}{p} + \frac{1}{p}\mathcal{L}[h(x,t)]\right] \\ u_1(x,t) & = \mathcal{L}^{-1}\left[\frac{1}{p}\mathcal{L}[A_0(x,t) + Ru_0(x,t)]\right] \\ u_2(x,t) & = \mathcal{L}^{-1}\left[\frac{1}{p}\mathcal{L}[(A_1(x,t) + Ru_1(x,t)) - (R + C(x))u_1(x,t)]\right] \\ u_{k+1}(x,t) & = \mathcal{L}^{-1}\left[\frac{1}{p}\mathcal{L}[(A_k(x,t) + Ru_k(x,t)) - (R + C(x))(u_k(x,t) - u_{k-1}(x,t))]\right], \quad k \geq 2. \end{cases} \tag{6.11}$$

Finally, if $\sum_{k=0}^{\infty} u_k(x,t)$ converges then $u(x,t) = \sum_{k=0}^{\infty} u_k(x,t)$ is the solution of the problem (6.4). Hence

$$u(x,t) = g(x,t) + \mathcal{L}^{-1}\left[\frac{1}{p}\mathcal{L}\left[R\left(\sum_{k=0}^{\infty} u_k(x,t)\right) + \sum_{k=0}^{\infty} A_k(x,t)\right]\right] \tag{6.12}$$

such that

$$g(x,t) = f(x) + \mathcal{L}^{-1}\left[\frac{1}{p}\mathcal{L}[h(x,t)]\right].$$

Remark 6.1. Comparing the expression (6.4) with the coagulation equation (6.1), one can observe that

$$Lu(x,t) = \frac{\partial u(x,t)}{\partial t}, \quad Ru(x,t) = 0, \quad h(x,t) = 0, \quad f(x) = u_0(x),$$

and

$$Nu(x,t) = \frac{1}{2}\int_0^x K(x-y,y)u(x-y,t)u(y,t)dy - \int_0^{\infty} K(x,y)u(x,t)u(y,t)dy.$$

Thus the coefficients of LODM for Eq. (6.1), with the help of relation (6.10) reduce to the following:

$$\begin{cases} u_0(x,t) & = \mathcal{L}^{-1}\left[\frac{u_0(x)}{p}\right] \\ u_1(x,t) & = \mathcal{L}^{-1}\left[\frac{1}{p}\mathcal{L}[A_0(x,t)]\right] \\ u_2(x,t) & = \mathcal{L}^{-1}\left[\frac{1}{p}\mathcal{L}[A_1(x,t) - C(x)u_1(x,t)]\right] \\ u_{k+1}(x,t) & = \mathcal{L}^{-1}\left[\frac{1}{p}\mathcal{L}[(A_k(x,t) - C(x)(u_k(x,t) - u_{k-1}(x,t))]\right], \quad k \geq 2, \end{cases} \tag{6.13}$$

where $A_k's$ are given by (6.9) and the truncated series solution of the problem is determined by the sum $\phi_n(x,t) := \sum_{k=0}^{n} u_k(x,t)$.

Remark 6.2. Comparing equation (6.2) to the Eq. (6.4), we observe that

$$Lu(x,t) = \frac{\partial u(x,t)}{\partial t}, \quad h(x,t) = 0, \quad f(x) = u(x,0), \quad Nu(x,t) = 0, \quad C(x) = 0,$$

and

$$Ru(x,t) = \int_x^\infty b(x,y)u(y,t)\phi(y)dy - \phi(x)u(x,t).$$

It is worth mentioning that LODM reduces to LADM when $C(x) = 0$. In light of this, the coefficients for LADM for Eq. (6.2) are defined as

$$\begin{cases} u_0(x,t) & = \mathcal{L}^{-1}\left[\frac{u_0(x)}{p}\right], \\ u_{k+1}(x,t) & = \mathcal{L}^{-1}\left[\frac{1}{p}\mathcal{L}[Ru_k(x,t)]\right], \quad k \geq 0. \end{cases} \tag{6.14}$$

As mentioned, the truncated series solution of the problem (6.2) is given by the sum $\psi_n(x,t) := \sum_{k=0}^{n} u_k(x,t)$.

The next part of the work deals with the theoretical convergence results for the coagulation and fragmentation problems. The theorems present the error bounds for the series solutions obtained using the approximate methods.

6.2 Theoretical Convergence Results

6.2.1 Coagulation Problem

In order to analyze the convergence result, we need to define the space $X = (C([0,T]) : L^1[0,\infty), ||\cdot||)$ with the norm

$$||u|| = \sup_{s\in[0,T]} \int_0^\infty |u(x,s)|dx < \infty, \tag{6.15}$$

and $D = \{u \in X : ||u|| \leq 2L\}$. Thanks to the values of the operators from Remark 6.1 and the Eq. (6.6), one can easily define the coagulation equation (6.1) in the operator form as

$$u = \tilde{\mathcal{N}}u, \tag{6.16}$$

where

$$\tilde{\mathcal{N}}u = u_0(x) + \mathcal{N}u,$$

and

$$\mathcal{N}u = \mathcal{L}^{-1}\left[\frac{1}{p}\mathcal{L}\left[Nu\right]\right], \tag{6.17}$$

such that $\tilde{\mathcal{N}}, \mathcal{N}, N : X \to X$ are non-linear operators where Nu is the right-hand side of Eq. (6.1). Taking into account the Eq. (6.13) and using (6.1), (6.8), and (6.17), we have the n-term series solution defined as

$$\phi_n = \tilde{\mathcal{N}}\phi_{n-1} - [tC(x)]\tilde{\mathcal{N}}u_{n-1}. \tag{6.18}$$

We shall now state and prove our main convergence result below:

Theorem 6.3. *When the coefficients $u_k(x,t)$ be determined by (6.13) and ϕ_n be defined by (6.18). Then, ϕ_n converges to u with*

$$||u - \phi_m|| \leq \frac{\Delta^{m-1}}{1-\Delta}\left[\Delta||u_1|| + Tk||u_1 - u_0||(\Delta + 1)\right], \tag{6.19}$$

when

$(A1_{agg})$ $K(x,y) = 1$, $\Delta = (T)^2\exp(2TL)[||u_0|| + 2TL^2 + 2TL] < 1$, *where* $L > 1/2$, *and* $||u_1|| \leq L$.

$(A2_{agg})$ $C(x) \in L^\infty(X, |\cdot|_\infty)$, $|\cdot|_\infty$ *is the essential supremum norm, i.e.,* $|C(x)| \leq k, k \in \mathbb{R}^+$ *and* $kT||u_1 - u_0|| \leq L/2$.

Proof. In order to prove the above assertion, we shall adopt the following steps:

Step 1: We shall prove that the operator $N : X \to X$ is a contraction mapping, i.e.,

$$||Nu - Nu^*|| \leq \delta||u - u^*|| \quad \forall \quad u, u^* \in D, \quad \delta < 1, \tag{6.20}$$

when $K(x,y) = 1$, $\delta = T\exp(2TL)[||u_0|| + 2TL^2 + 2TL] < 1$, where $L > 1/2$ and $||u_1|| \leq L$.

Proof. Similarly as in [58], to prove the contraction mapping of N, Eq. (6.1) shall be converted in an equivalent state (see [135]) with the help of the equivalent operator $\tilde{N}$ written as

$$\tilde{N}u = u_0(x)\exp[-H(x,t,u)] + \frac{1}{2}\int_0^t \exp[H(x,s,u) - H(x,t,u)]\int_0^x K(x-y,y)u(x-y,s)u(y,s)dyds,$$

where,

$$H(x,t,u) = \int_0^t \int_0^\infty K(x,y)u(y,s)dyds.$$

The rest of the proof can be followed from Theorem 3.1 in [58]. □

Step 2: Then, we shall evince that employing (6.20) and definitions as well as basic properties of Laplace and inverse Laplace transforms, the operator $\tilde{\mathcal{N}}$ is a contraction mapping, i.e.,

$$||\tilde{\mathcal{N}}u - \tilde{\mathcal{N}}u^*|| \leq \Delta||u - u^*|| \quad \forall \quad u, u^* \in D, \quad \Delta < 1, \tag{6.21}$$

when $\Delta = \delta T$.

Proof. We have

$$\begin{aligned}
||\tilde{\mathcal{N}}u - \tilde{\mathcal{N}}u^*|| &= \left|\left|\mathcal{L}^{-1}\left[\frac{1}{p}\left[\mathcal{L}\left[Nu - Nu^*\right]\right]\right]\right|\right| \\
&= \sup_{s\in[0,T]} \int_0^\infty \left[\left|\frac{1}{2\pi}\int_0^\infty \left[\frac{e^{ps}}{p}\int_0^\infty [e^{-ps}(Nu - Nu^*)]ds\right]dp\right|\right]dx \\
&\leq \frac{1}{2\pi}\int_0^\infty \left[\frac{e^{ps}}{p}\int_0^\infty \left[e^{-ps}[\sup_{[0,T]}\int_0^\infty |Nu - Nu^*|dx]\right]ds\right]dp \\
&\leq \mathcal{L}^{-1}\left[\frac{1}{p}\left[\mathcal{L}\left[\delta||u - u^*||\right]\right]\right] \\
&= \delta T||u - u^*||,
\end{aligned}$$

under the assumption that $\delta T < 1$, the result (6.21) is proved. □

Step 3: Finally, the authors indicate that the series solution ϕ_n is a Cauchy sequence under the assumption $(A2_{agg})$.

Proof. Following (6.18), consider

$$||\phi_n - \phi_m|| = \left|\left|\tilde{\mathcal{N}}\phi_{n-1} - tC(x)\tilde{\mathcal{N}}u_{n-1} - \tilde{\mathcal{N}}\phi_{m-1} + tC(x)\tilde{\mathcal{N}}u_{m-1}\right|\right|.$$

The triangle inequality gives us

$$||\phi_n - \phi_m|| \leq ||\tilde{\mathcal{N}}\phi_{n-1} - \tilde{\mathcal{N}}\phi_{m-1}|| + \left|\left|tC(x)\left[\tilde{\mathcal{N}}u_{n-1} - \tilde{\mathcal{N}}u_{m-1}\right]\right|\right|.$$

Using the result in Eq. (6.21), one can easily obtain

$$||\phi_n - \phi_m|| \leq \Delta\left[||\phi_{n-1} - \phi_{m-1}|| + ||u_{n-1} - u_{m-1}||\, t|C(x)|_\infty\right].$$

Let $n = m + 1$ in the preceding equation which yields

$$\begin{aligned}
||\phi_{m+1} - \phi_m|| &\leq \Delta||\phi_m - \phi_{m-1}|| + \Delta||u_m - u_{m-1}||\ t|C(x)|_\infty \\
&= \Delta\Big|\Big|\tilde{\mathcal{N}}\phi_{m-1} - tC(x)\tilde{\mathcal{N}}u_{m-1} - \tilde{\mathcal{N}}\phi_{m-2} + tC(x)\tilde{\mathcal{N}}u_{m-2}\Big|\Big| + \Delta||u_m - u_{m-1}||\ t|C(x)|_\infty \\
&\leq \Delta\Big(\Delta||\phi_{m-1} - \phi_{m-2}|| + \Delta||u_{m-1} - u_{m-2}||\ t|C(x)|_\infty\Big) + \Delta||u_m - u_{m-1}||\ t|C(x)|_\infty \\
&\ \ \vdots \\
&\leq \Delta^m[||\phi_1 - \phi_0|| + tk||u_1 - u_0||] + \Delta^{m-1}tk||u_1 - u_0||.
\end{aligned}$$

With the help of this, we get

$$\begin{aligned}
||\phi_n - \phi_m|| &\leq ||\phi_{m+1} - \phi_m|| + ||\phi_{m+2} - \phi_{m+1}|| + \ldots + ||\phi_n - \phi_{n-1}|| \\
&\leq \Big[\Delta^m[||\phi_1 - \phi_0|| + tk||u_1 - u_0||] + \Delta^{m-1}tk||u_1 - u_0||\Big] \\
&\quad + \Big[\Delta^{m+1}[||\phi_1 - \phi_0|| + tk||u_1 - u_0||] + \Delta^m tk||u_1 - u_0||\Big] \\
&\quad + \ldots + \Big[\Delta^{n-1}[||\phi_1 - \phi_0|| + tk||u_1 - u_0||] + \Delta^{n-2}tk||u_1 - u_0||\Big] \\
&= \frac{\Delta^m(1 - \Delta^{n-m})}{1 - \Delta}\Big[||\phi_1 - \phi_0|| + tk||u_1 - u_0||\Big] + \frac{\Delta^{m-1}(1 - \Delta^{n-m})}{1 - \Delta}tk||u_1 - u_0||.
\end{aligned}$$

Finally using $(A1_{agg})$, one can obtain

$$||\phi_n - \phi_m|| \leq \frac{\Delta^{m-1}}{1 - \Delta}\Big[\Delta||u_1|| + Tk||u_1 - u_0||(\Delta + 1)\Big]. \tag{6.22}$$

Now, using $(A2_{agg})$, the above expression converges to zero as $m \to \infty$. Hence, ϕ_n is a Cauchy sequence. Also, using $||u_1|| \leq L, kT||u_1 - u_0|| \leq L/2$, we can prove that $||\phi_n - \phi_m|| \leq 2L$. □

Therefore, there exists a ϕ so that $\lim_{n\to\infty}\phi_n = \phi$ which leads to $u = \sum_{k=0}^{\infty} u_k = \lim_{n\to\infty}\phi_n = \phi$. In the end, fixing m and taking $n \to \infty$ in the equation (6.22) lead to the requisite result (6.19). □

6.2.2 Fragmentation Problem

Consider the Banach space $X = (\mathcal{C}([0,T]) : L^1[0,\infty), ||\cdot||)$ endowed with the norm

$$||u|| = \sup_{s\in[0,T]}\int_0^\infty e^{\lambda x}|u(x,s)|dx \quad \text{for } \lambda \in \mathbb{R}^+. \tag{6.23}$$

The equation (6.2) can be written in the operator form as

$$u = \tilde{\mathcal{R}}u, \tag{6.24}$$

where

$$\tilde{\mathcal{R}}u = u_0(x) + \mathcal{R}u,$$

and

$$\mathcal{R}u = u_0(x) + \mathcal{L}^{-1}\left[\frac{1}{p}\mathcal{L}\left[Ru\right]\right], \tag{6.25}$$

such that $\tilde{\mathcal{R}}, \mathcal{R}, R : X \to X$ are linear operators where Ru is the right-hand side of (6.2). Using the Eq. (6.14) and (6.2.2), the n-term series solution is computed as

$$\psi_n := \tilde{\mathcal{R}}\psi_{n-1}. \tag{6.26}$$

The convergence result for the fragmentation equation is presented below:

Theorem 6.4. *Let ψ_n be the truncated solution defined by (6.26). Then, ψ_n converges to u with*

$$||u - \psi_m|| \leq \frac{\Phi^m}{1-\Phi}||u_1||, \tag{6.27}$$

if $\Phi := c\frac{\alpha! T^2}{\lambda^{\alpha+1}} < 1$ and $||u_1|| < \infty$.

Proof. We shall adopt the following steps one by one in order to obtain our main result.

Step 1: The operator R is contractive, i.e.,

$$||Ru - Ru^*|| \leq \rho||u - u^*||, \forall u, u^* \in X, \tag{6.28}$$

with $b(x,y) = c\frac{x^{r-1}}{y^r}$ where $c \in \mathbb{R}^+, r = 1, 2, \ldots$ and $\phi(x) \leq x^\alpha$ where $\alpha \geq 1$. Finally, λ is selected so that $\left(e^{\lambda y} - 1\right) < 1$ and $\rho := c\frac{\alpha! T}{\lambda^{\alpha+1}} < 1$.

Proof. The operator R can be expressed in the following equivalent form defined by

$$\tilde{R}u = u_0(x)\exp[-A(x,t)] + \frac{1}{2}\int_0^t \exp[A(x,s) - A(x,t)]\int_x^\infty \phi(y)b(x,y)u(y,s)dyds, \tag{6.29}$$

where, $A(x,t) = t\phi(x)$. The outline of the proof can be followed from Theorem 2.1 in the article [58]. □

Step 2: The operator $\tilde{\mathcal{R}}$ is a contraction mapping such that

$$||\tilde{\mathcal{R}}u - \tilde{\mathcal{R}}u^*|| \leq \Phi||u - u^*||, \forall u, u^* \in X, \tag{6.30}$$

when $\Phi = \rho T$.

Proof. It is certain that

$$\begin{aligned}
||\tilde{\mathcal{R}}u - \tilde{\mathcal{R}u^*}|| &= \left|\left|\mathcal{L}^{-1}\left[\frac{1}{p}\mathcal{L}\left[Ru\right]\right] - \mathcal{L}^{-1}\left[\frac{1}{p}\mathcal{L}\left[Ru^*\right]\right]\right|\right| \\
&= \sup_{s\in[0,T]} \int_0^\infty \left[e^{\lambda x}\left|\frac{1}{2\pi}\int_0^\infty \left[\frac{e^{ps}}{p}\int_0^\infty [e^{-ps}(Ru - Ru^*)]ds\right]dp\right|\right]dx \\
&\leq \frac{1}{2\pi}\int_0^\infty \left[\frac{e^{ps}}{p}\int_0^\infty \left[e^{-ps}[\sup_{[0,T]}\int_0^\infty e^{\lambda x}|Ru - Ru^*|dx]\right]dt\right]dp \\
&= \rho T||u - u^*||,
\end{aligned}$$

under the assumption that $\rho T < 1$, the result (6.30) is proved. □

Step 3: Finally, the authors indicate that the series solution ψ_n is a Cauchy sequence.

Proof. It is given that

$$||\psi_n - \psi_m|| = \left|\left|\tilde{\mathcal{R}}\psi_{n-1} - \tilde{\mathcal{R}}\psi_{m-1}\right|\right|.$$

Now, following the proof similarly as in Step 3 of Section 3.1 with $C(x) = 0$, the above assertion can be easily established. □

The completion of all the steps gives us the required result (6.27). □

6.3 Numerical Results

6.3.1 Coagulation Problem

In order to solve the aggregation equation (6.1), the fundamental LODM is applied in this part. Three test cases of constant, sum, and product kernels are considered which are useful for studying the early stages of coagulation, like in protein aggregation [7], analyzing colloidal suspensions [136], and for studying coagulation behavior in predominant particle size distributions, such as atmospheric aerosols [137]. The exponential initial condition is taken into account due to the availability of the exact solutions for the number density and moments in all the cases.

Constant Kernel

Considering $K(x,y) = 1$ in (6.1) and using Eq. (6.10) gives $C(x) = \frac{1}{2}(\sinh(x) - \cosh(x) + 1) - 1$. Following are the explicit form of the components for $u_i's$:

$$u_0 = e^{-x}, \quad u_1 = \frac{1}{2}te^{-x}(x-2), \quad u_2 = \frac{1}{8}t^2e^{-2x}\left(e^x(x-4)(x-1)+x-2\right),$$
$$u_3 = \frac{1}{96}t^2e^{-3x}\left(2t(x-2)+2e^x(t((x-8)x+8)-6(x-2))+e^{2x}\left(t\left(2(x-5)^2x-29\right)-12(x-2)\right)\right).$$

Continuing in this manner, one can compute higher order terms of the series solution with the help of MATHEMATICA©. The exact solution to this problem is provided in [138] and given as

$$u(x,t) = \frac{4e^{-\frac{2x}{t+2}}}{(t+2)^2}.$$

For numerical illustration, the exact solution and the truncated solution by LODM taking the partial sum of seven-term of the series are plotted in Figure 6.1. It can be seen that both solutions behave in a similar manner. In the beginning, there is a high density of smaller particles, and as time goes on, this density decreases (see Figure 6.1(a)). The comparison between the exact and the series approximated solutions using various terms ($n = 3, 5, 7$) at $t = 1$ is shown in Figure 6.2, along with the absolute error between the exact and seven-term truncated solutions. It can be seen that the accuracy of predicted number density can be increased by using more terms in the series approximated solution (see Figure 6.2(a)). To strengthen the novelty of the LODM, number density using the 7-term approximate solution is also compared with the finite volume approximated and exact solutions in Figure 6.3(a). The graph indicates that LODM and FVM overlap the results with the precise ones.

Moving further, the efficacy of the method can be checked by calculating the moments of the approximated solutions and comparing them with the moments of the exact solution. The r^{th} moment of the exact solution is defined as

$$\mu_r^{Exact}(t) = \int_0^\infty x^r u(x,t)dx, \tag{6.31}$$

while the approximated solutions using LODM, are given by

$$\mu^{r,n}(t) = \int_0^\infty x^r \phi_n(x,t)dx. \tag{6.32}$$

These moments are relevant physical quantities with zeroth moment (obtained by putting $r = 0$ in (6.31)) being the total number of clusters and the first moment ($r = 1$ in (6.31)) gives the total mass (volume) of the system. Putting $r = 2$ gives the second moment,

defined as the energy dissipated by the system [22]. As expected, it is observed that the series approximated solution conserves the total mass of the particles in the system and hence, plots for the first moment are omitted here as well as in the next two examples. Figure 6.3(b) represents the comparison of zeroth and second moments calculated via LODM ($\mu_{i,7}$), FVM ($\mu_{i,F}$) and exact (μ_i) solutions for $i = 0$ and 2, respectively. From this figure, it is clearly visible that all the results are overlapping with each other.

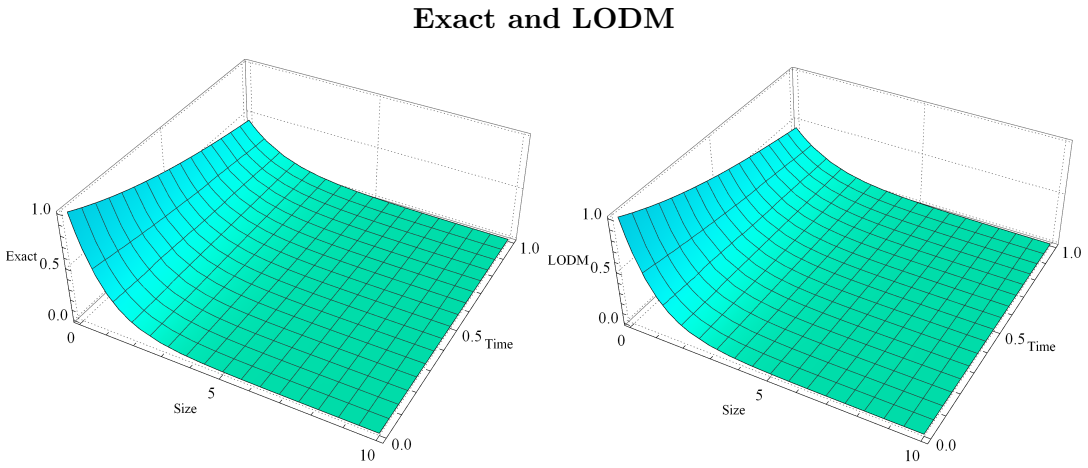

(a) Exact solution (b) LODM solution

FIGURE 6.1: Number density for constant kernel

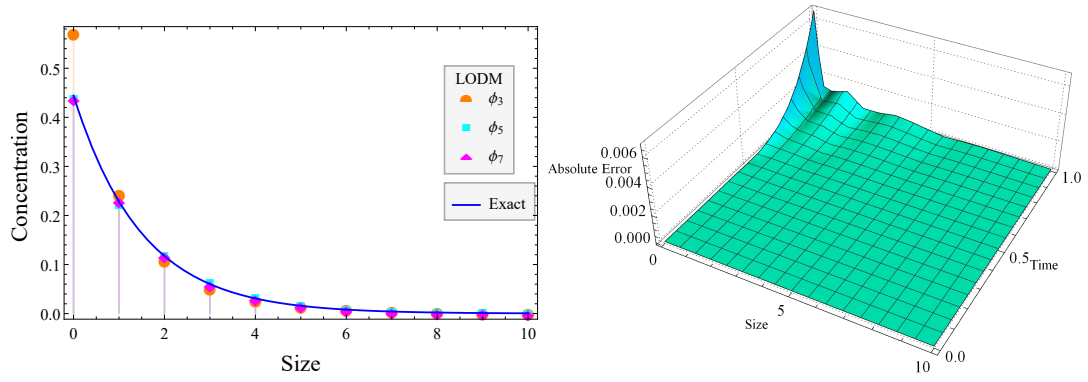

(a) LODM and exact solution (b) Absolute error.

FIGURE 6.2: Number density and absolute error for constant kernel

These numerical results are also validated by Tables 6.1-6.3 which present the values of the theoretical error bound (6.19) for three different cases. In addition, these errors are compared with the error bounds of ODM (5.27). Here, we have $||u_0||= 1, ||u_1||= \frac{T}{2}, ||u_1 - u_0||= \left(1 + \frac{T}{2}\right), |C(x)|\leq 1/2$ for large x, i.e., $k = 1/2$.

Case 1 : Let $L = 1.1$.

Choosing $T = 0.2$ provides from $(A1)$ and $(A1_{agg})$, that $\delta = 0.6 < 1$, and $\Delta = 0.1 < 1$, respectively.

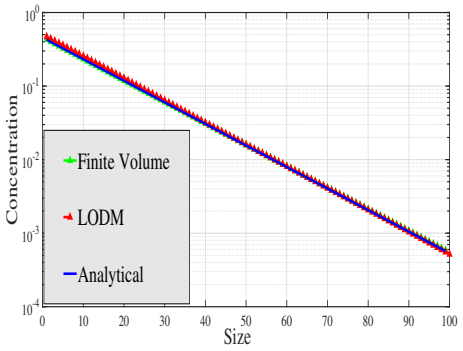

(a) Number density comparison with FVM

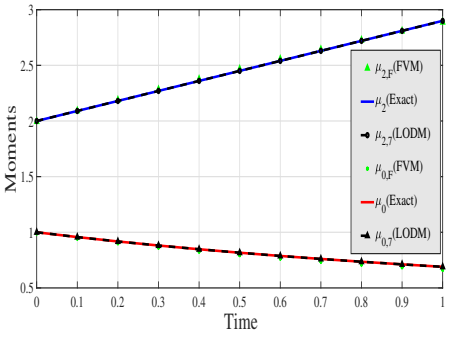

(b) Moments comparison with FVM

FIGURE 6.3: Number density and moments using LODM and FVM for constant kernel

We have, $||u_1||= 0.127 \leq 2L$ (for ODM) and
$||u_1||= 0.127 \leq L$ as well as $kT||u_1 - u_0||= 0.1 \leq L/2$ (for LODM).

Case 2 : Let $L = 2$.

Selecting $T = 0.1$ gives $\delta = 0.33 < 1$, and $\Delta = 0.03 < 1$
Now, $||u_1||= 0.063 \leq 2L$ (for ODM) and
$||u_1||= 0.063 \leq L$ as well as $kT||u_1 - u_0||= 0.05 \leq L/2$ (for LODM).

Case 3 : Let $L = 11$.

Choosing $T = 0.03$ such that we have $\delta = 0.52 < 1$, $\Delta = 0.02 < 1$.
Here, $||u_1||= 0.019 \leq 2L$ (For ODM) and
$||u_1||= 0.019 \leq L$ and $kT||u_1 - u_0||= 0.015 \leq L/2$ (for LODM).

Remark 6.5. It should be mentioned here that if we increase L (say up to $L = 101$, we can select $T = 0.01$ to get $\delta = 15.6 \not< 1$, but $\Delta = .156 < 1$ i.e., we can consider higher value of T in case of LODM. In addition, in all cases above, it is observed that we can consider $T = 0.3, 0.2, 0.08$, respectively, to obtain error estimates for LODM, but we have calculated error values for the same T for comparison. In conclusion, the significantly lower values of these errors (see [58]) for comparison) depict the excellent accuracy of our method.

TABLE 6.1: Truncation error in computing approximate solution using ODM and LODM for constant kernel for case 1

m	5	10	15	20	25	30
$\text{error}_{\text{ODM}}$	2.4×10^{-2}	1.8×10^{-3}	1.4×10^{-4}	10^-5	8.1×10^{-7}	6.2×10^{-8}
$\text{error}_{\text{LODM}}$	3.2×10^{-5}	7.8×10^{-10}	2×10^{-14}	4.6×10^{-19}	1.1×10^{-23}	2.8×10^{-28}

TABLE 6.2: Truncation error in computing approximate solution using ODM and LODM for constant kernel for case 2

m	5	10	15	20	25	30
$\text{error}_{\text{ODM}}$	4×10^{-3}	1.4×10^{-6}	5.2×10^{-9}	2×10^{-11}	7.6×10^{-14}	2.8×10^{-16}
$\text{error}_{\text{LODM}}$	6.8×10^{-8}	2.6×10^{-15}	9.8×10^{-23}	3.8×10^{-30}	1.4×10^{-37}	5.4×10^{-45}

TABLE 6.3: Truncation error in computing approximate solution using ODM and LODM for constant kernel for case 3

m	5	10	15	20	25	30
$\text{error}_{\text{ODM}}$	10^{-3}	5×10^{-5}	2×10^{-6}	7.6×10^{-8}	2.8×10^{-9}	10^{-10}
$\text{error}_{\text{LODM}}$	9.3×10^{-10}	8.4×10^{-19}	7.6×10^{-28}	6.8×10^{-37}	6.2×10^{-46}	5.6×10^{-55}

Sum Kernel

If sum kernel is taken, i.e. $K(x,y) = x + y$, this leads to $C(x) = -x + \frac{1}{2}x(\sinh(x) - \cosh(x) + 1) - 1$ and the first few components of the solution are

$$u_0 = e^{-x}, \quad u_1 = \frac{1}{2}te^{-x}(x^2 - 2x - 2), \quad u_2 = \frac{1}{24}t^2e^{-2x}x\left(e^x(2x+3)(x^2-6x+6) + 3(x^2-2x-2)\right),$$
$$u_3 = \frac{1}{576}t^2e^{-3x}\Big(e^{2x}\left(t(x(2x(x(x(x(2x-17)+2)+144)-84)-177)-180)-72\left(x^3-6x-4\right)\right)$$
$$+ 12t((x-2)x-2)x^2 + 8e^x x(x(t(x((x-9)x-3)+12)-9(x-2))+18)\Big),$$

and so on. According to [138], the exact solution to this problem is

$$u(x,t) = \frac{e^{\left(e^{-t}-2\right)x-t} I_1\left(2\sqrt{1-e^{-t}}x\right)}{\sqrt{1-e^{-t}}x},$$

where I_1 is the modified Bessel function of the first kind. Figure 6.4 illustrates the excellent agreement between the exact and truncated series solutions by using the partial sum of the seventh term in the series. In Figure 6.5(a), the comparison of the analytical and LODM solutions taking 3, 5, and 7 terms in series approximated solution is made at $t = 0.4$. The number density experiences noise over time, which can be reduced by including more terms in the series solution (see Figure 6.5(a)). Further, the absolute error is plotted in Figure 6.5(b) at different time levels. It clearly shows that the absolute error between exact and series approximated solutions is almost negligible for seven terms. Similar to the previous example, here again, it is reported from Figure 6.6(a) that the results for the number density obtained using LODM and FVM are very accurate and comparable with the analytical one.

In addition to this, the efficacy of the method can also be visualized from Figure 6.6(b), which provides the comparison of the zeroth and second moments plot for LODM and the FVM along with the exact moments. As expected, the figure demonstrates that due to the coagulation process, there is a decrease in the total number of particles and the values are very well predicted both by LODM and FVM. Further, it is visualized here that the second moment is predicted better using LODM than FVM. It is worth mentioning that both LODM and FVM yield total mass conservation.

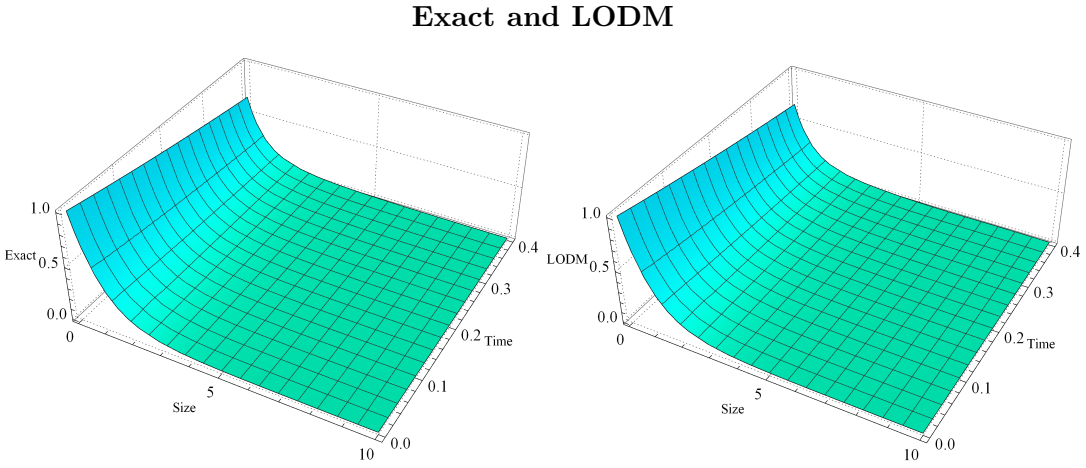

(a) Exact solution (b) LODM solution

FIGURE 6.4: Number density for sum kernel

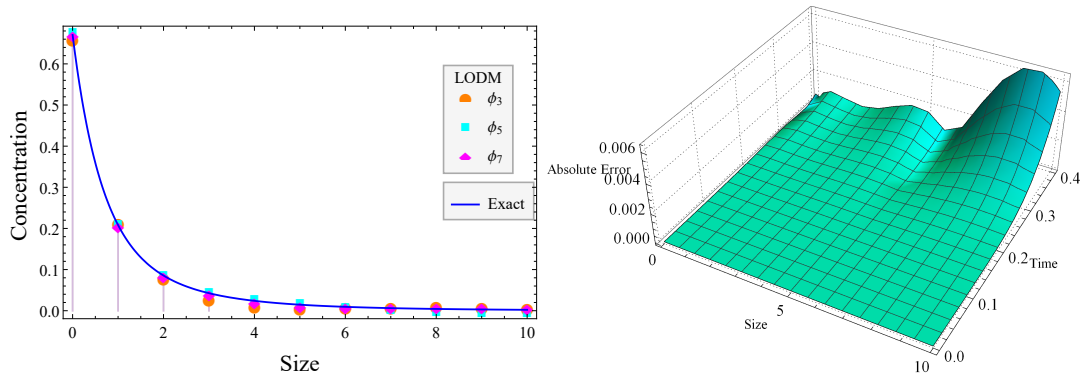

(a) LODM and Exact solution (b) Absolute Error.

FIGURE 6.5: Number density and absolute error for sum kernel

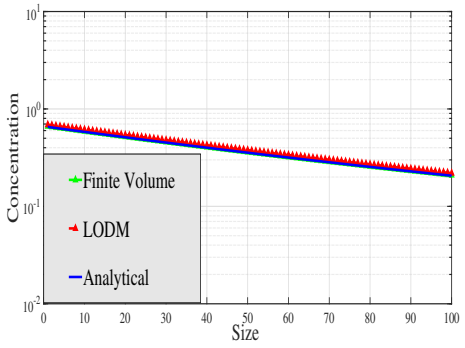

(a) Number density comparison with FVM

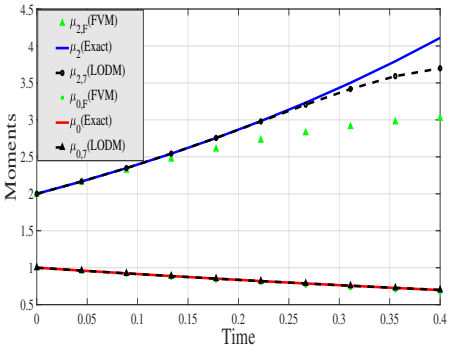

(b) Moments comparison with FVM

FIGURE 6.6: Number density and moments using LODM and FVM for sum kernel

Product Kernel

Let us consider the case of product kernel, i.e., $K(x,y) = xy$, then one can obtain $C(x) = -\frac{1}{2}e^{-x}\left(e^x - 1\right)(x+2)$ and the components $u_i's$ are

$$u_0 = e^{-x}, \quad u_1 = \frac{1}{12}xte^{-x}\left(x^2 - 12\right),$$
$$u_2 = \frac{1}{720}xt^2e^{-2x}\Big(- 15x^3 - 30x^2 + e^x\left(-45x^3 + 30x^2 + 181x - 360\right) + 180x + 360\Big).$$

Similarly, one can compute higher iterations with the software MATHEMATICA©. The exact solution to this problem is, see [129],

$$u(x,t) = e^{(-(1+t)x)}\sum_{k=0}^{\infty}\frac{t^k x^{3k}}{(k+1)!\,\Gamma(2k+1)}.$$

The Exact and truncated solutions for the density distribution function are plotted in Figure 6.7. Similar outcomes are being pursued in this case, as was shown in the previous cases. Both the LODM-based density distribution and the actual density distribution plot exhibit identical behavior. A comparison between exact and LODM-based number density functions (for $n = 3, 5$ and 7) is carried out in Figure 6.8(a) at time $t = 0.4$. It is visible that as the term in the approximated series solution increases, the truncated solution moves closer to the exact solution. In Figure 6.8(b), the absolute error is presented between the exact and LODM-based number densities, taking the partial sum of seven-term in the series approximation. The figure depicts that the error is almost zero for a shorter time. However, the error grows as time passes, which can be reduced by raising the series terms. Further, Figure 6.9(a) depicts the number density comparison of FVM and LODM with the analytical solution and it clearly indicates that both methods exhibit good agreement with the analytical concentration.

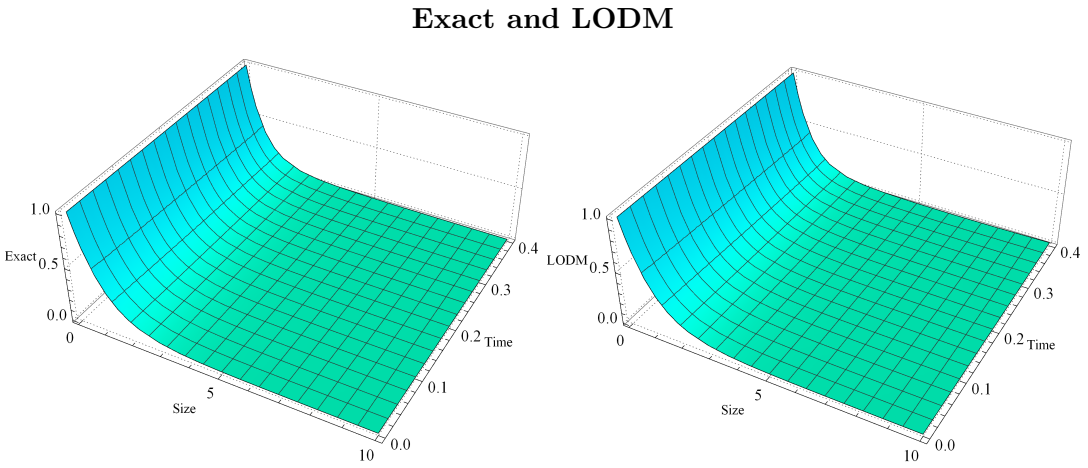

(a) Exact solution (b) LODM solution

FIGURE 6.7: Number density for product kernel

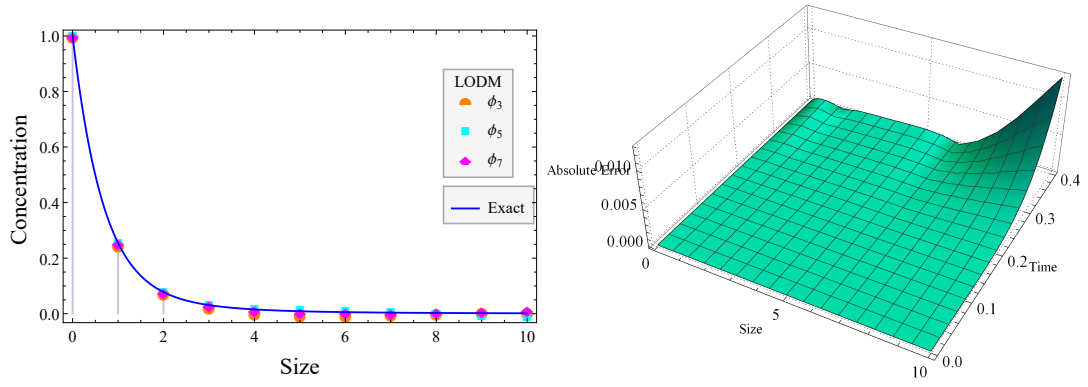

(a) LODM and Exact solution (b) Absolute Error.

FIGURE 6.8: Number density and absolute error for product kernel

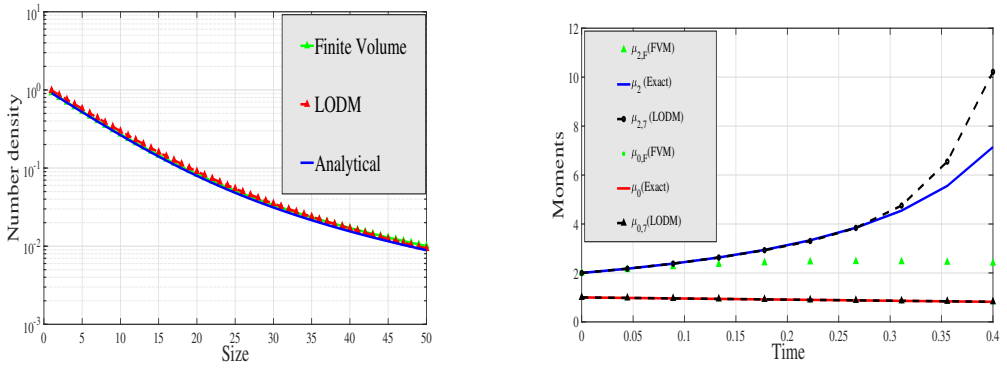

(a) Number density comparison with FVM (b) Moment comparison with FVM

FIGURE 6.9: Number density and moments using LODM and FVM for product kernel

Additionally, to verify the efficiency and accuracy of the method, zeroth and second moments for the approximated number densities computed using LODM (7-term series solution) and FVM are plotted in Figure 6.9(b) along with the exact ones. Both LODM

and FVM provide exact agreement with the precise total number of particles. However, for the second moment, LODM over-predicts the result as time progresses but it is still found to be better than the findings via FVM. It should be mentioned here that for higher rate of aggregation kernels, numerical schemes including FVM and fixed pivot technique fail to predict the second moment, see [139, 140] and further citations. Moreover, considering a higher number of terms in the semi-analytical method (which is a tedious task if not impossible to check), one can expect a better outcome. All of the above results show the novelty of the proposed method to solve this non-linear problem.

6.3.2 Fragmentation Problem

Consider the fragmentation equation (6.2) with the initial condition $u(x,0) = u_0(x) \geq 0$. We have considered four different test cases in this section which include the binary fragmentation kernel with linear and quadratic selection rates and the Austin kernel with cubic selection rate. The other parameters are provided in the following subsections. Interestingly, in all the cases, closed-form solutions are obtained using LADM.

Binary Fragmentation with Linear Selection Rate

Taking into account the fragmentation rate $b(x,y) = \frac{2}{y}$, selection rate $\phi(x) = x$ and the exponential initial condition $u_0(x) = e^{-x}$, the LODM iterations (6.14) will take the form

$$\begin{aligned} u_0 =& e^{-x}, \qquad u_1 = -tx^{-1}e^{-x}\left(x^2 - 2x\right), \\ u_2 =& \frac{(-1)^2}{2!}t^2x^0e^{-x}\left(x^2 - 4x + 2\right), \qquad u_3 = \frac{(-1)^3}{3!}t^3e^{-x}x\left(x^2 - 6x + 6\right), \end{aligned}$$

and in general,

$$u_k = \frac{(-1)^k}{k!}t^ke^{-x}x^{k-2}(x^2 - 2kx + k(k-1)), \quad k \geq 0.$$

So, the n term truncated series solution is given by

$$\psi_n = \sum_{k=0}^{n} u_k(x,t) = \sum_{k=0}^{n} \frac{(-1)^k t^k e^{-x} x^{k-2}}{k!}(x^2 - 2kx + k(k-1)). \tag{6.33}$$

In order to get the closed-form solution, taking the limiting case of (6.33) leads to

$$\lim_{n\to\infty} \psi_n = \lim_{n\to\infty} \sum_{k=0}^{n} \frac{(-1)^k t^k e^{-x} x^{k-2}}{k!}(x^2 - 2kx + k(k-1)) = (1+t)^2 e^{-(1+t)x}, \tag{6.34}$$

which is also the exact solution to the problem as provided in [141]. To validate the theoretical results, we shall calculate the theoretical error bound which confirms the efficacy of the method. For this, we have: $u_1(x,t) = te^{-x}(2-x)$, which gives

$$||u_1|| = \sup_{s\in[0,T]} \int_0^\infty se^{\lambda x - x}(2-x)dx = \frac{T(1-2\lambda}{(\lambda-1)^2},$$

and we choose $\lambda = 0.2$ and 0.1 that give two corresponding values of $T = 0.015$ and 0.0045 to compute the theoretical bound (6.27) which are presented in the following Table 6.4 as

TABLE 6.4: Theoretical error bound for binary fragmentation with linear selection rate

m	10	20	30	40	50
Error $(\lambda = 0.2)$	4.6×10^{-22}	1.5×10^{-41}	4.9×10^{-61}	1.6×10^{-80}	5.1×10^{-100}
Error $(\lambda = 0.1)$	5.3×10^{-27}	6.3×10^{-51}	7.5×10^{-75}	8.9×10^{-99}	1.1×10^{-122}

Binary Fragmentation with Quadratic Selection Rate

Considering the fragmentation rate $b(x,y) = \frac{2}{y}$, selection rate $\phi(x) = x^2$ and initial data $u_0(x) = e^{-x}$, the terms of the series solution (6.14) will be as

$$\begin{aligned}
u_0 =& e^{-x}, \quad u_1 = -te^{-x}(x^2 - 2x - 2),\\
u_2 =& \frac{(-1)^2}{2!}t^2x^2e^{-x}\left(x^2 - 4x - 4\right), \quad u_3 = \frac{(-1)^3}{3!}t^3x^4e^{-x}\left(x^2 - 6x - 6\right),\\
&\vdots\\
u_k =& \frac{(-1)^k}{k!}t^kx^{2k-2}e^{-x}\left(x^2 - 2kx - 2k\right), \quad k \geq 0.
\end{aligned}$$

So, the partial sum of n terms of the series solution is

$$\psi_n = \sum_{k=0}^{n} u_k(x,t) = \sum_{k=0}^{n} \frac{(-1)^k}{k!}t^kx^{2k-2}e^{-x}\left(x^2 - 2kx - 2k\right). \tag{6.35}$$

If we take limit $n \to \infty$ then,

$$u(x,t) = \lim_{n\to\infty} \psi_n(x,t) = (1 + 2t + 2xt)e^{-(1+xt)x},$$

which is exactly the same as the analytical solution of the problem given in [141].

Since, $u_1(x,t) = te^{-x}(2+2x-x^2)$, we have

$$||u_1|| = \sup_{s\in[0,T]} \int_0^\infty se^{\lambda x - x}(2+2x-x^2)dx = \frac{2T(\lambda^2-2\lambda)}{(\lambda-1)^3}. \tag{6.36}$$

By taking the parameters $\lambda = 0.2, 0.1$ and correspondingly $T = 0.0015, 0.0002$, the theoretical bound (6.27) is determined. These error bounds for different values of m are summarized in Table 6.5 below as

TABLE 6.5: Theoretical error bound for binary fragmentation with quadratic selection rate

m	10	20	30	40	50
Error($\lambda = 0.2$)	6.9×10^{-33}	2.2×10^{-62}	7.2×10^{-92}	2.3×10^{-121}	7.6×10^{-151}
Error($\lambda = 0.1$)	5.5×10^{-49}	5.7×10^{-93}	6×10^{-137}	6.3×10^{-181}	6.6×10^{-225}

Binary Fragmentation, Linear Selection Rate with Dirac Delta Initial Condition

Let us consider an interesting case of mono-disperse initial condition which is represented by using Dirac Delta function as $u_0(x) = \delta(x-\nu)$ along with the fragmentation rate $b(x,y) = \frac{2}{y}$ and selection rate $\phi(x) = x$. Then for a particular value of $\nu = 10$, equation (6.14) gives

$$\begin{aligned} u_0 =& \delta(x-10), \qquad u_1 = (-tx)\delta(x-10) + 2tH(10-x), \\ u_k =& \frac{(-tx)^k}{k!}\delta(x-10) + \frac{(-tx)^{k-1}}{(k-1)!}2tH(10-x) + \frac{(-tx)^{k-2}}{(k-2)!}t^2(10-x)H(10-x), \end{aligned}$$

for $H(10-x)$ being the unit step function. So, the n-term series is given by

$$\psi_n = \sum_{k=0}^{n} \frac{(-tx)^k}{k!}\delta(x-10) + \frac{(-tx)^{k-1}}{(k-1)!}2tH(10-x) + \frac{(-tx)^{k-2}}{(k-2)!}t^2(10-x)H(10-x). \tag{6.37}$$

In order to get the closed-form solution, taking the limiting case of (6.37) leads to

$$\begin{aligned} \lim_{n\to\infty}\psi_n =& \lim_{n\to\infty}\sum_{k=0}^{n} \frac{(-tx)^k}{k!}\delta(x-10) + \frac{(-tx)^{k-1}}{(k-1)!}2tH(10-x) + \frac{(-tx)^{k-2}}{(k-2)!}t^2(10-x)H(10-x), \\ =& e^{-tx}\left(\delta(x-10) + \left(t^2(10-x)+2t\right)H(10-x)\right), \end{aligned} \tag{6.38}$$

which implies that $u(x,t) = e^{-tx}\left(\delta(x-10) + \left(t^2(10-x)+2t\right)H(10-x)\right)$. Fortunately, this is also the exact solution to the problem as provided in [141]. We would like to mention here that these computations are possible for any $\nu \in \mathbb{R}$.

Austin Fragmentation Kernel, General Selection Rate with Exponential Initial Condition

Taking into account the fragmentation equation with general selection rate $\phi(x) = x^\alpha$ and a physically relevant fragmentation kernel introduced by Austin as, see [142],

$$b(x,y) = \frac{\left(\frac{\xi\gamma x^{\gamma-1}}{y^\gamma} + \frac{(1-\xi)\eta x^{\eta-1}}{y^\eta}\right)}{\left(\frac{\xi\gamma}{1+\eta}y + \frac{(1-\xi)\eta}{1+\eta}\right)},$$

with initial condition $u_0(x) = e^{-x}$. It is worth mentioning that the analytical solution to the above problem is not available in the literature. Thanks to our series approximated approach, in order to find the closed form solution, we take special case as $\alpha = 3$, $\eta = 2$, $\gamma = 2$ and $\xi = 0$ which lead to $b(x,y) = \frac{3x}{y^2}$ and $\phi(x) = x^3$.
Following the procedure as in (6.14), the coefficients of the series solution are

$$\begin{aligned}
u_0 =& e^{-x}, \qquad u_1 = -txe^{-x}(x^2-3x-3),\\
u_2 =& \frac{(-1)^2}{2!}t^2x^4e^{-x}(x^2-6x-6), \qquad u_3 = \frac{(-1)^3}{3!}t^3x^7e^{-x}(x^2-9x-9),\\
&\vdots\\
u_k =& \frac{(-1)^k}{k!}t^kx^{3k-2}e^{-x}\left(x^2-3kx-3k\right), \quad k \geq 0.
\end{aligned}$$

Hence, the partial sum of the n terms of the series solution is

$$\psi_n = \sum_{k=0}^{n} u_k(x,t) = \sum_{k=0}^{n} \frac{(-1)^k}{k!}t^kx^{3k-2}e^{-x}\left(x^2-3kx-3k\right). \tag{6.39}$$

Further, by taking the limit $n \to \infty$, we obtain

$$u(x,t) = \lim_{n\to\infty} \psi_n(x,t) = e^{-tx^3-x}\left(3tx^2+3tx+1\right). \tag{6.40}$$

By Theorem 6.4, if $\psi_n(x,t)$ converges, it will converge to the exact solution of the problem. Therefore, the limiting value of $\psi_n(x,t)$ must be the exact solution. We would like to emphasize here that the closed-form solution is obtained for a particular parameter case. However, if the problem is solvable, one can find the closed-form solution or an approximate solution in the series form for different sets of parameter values by our proposed algorithm.

Concluding Remarks and Future Scope

Concluding Remarks

This thesis work discussed in detail the theoretical, numerical, and semi-analytical approaches to deal with different forms of coagulation equations namely the Safronov-Dubovski coagulation equation (SDCE) and Smoluchowski's coagulation equation.

The theoretical analysis of the SDCE revolved around stating conditions for existence, density conservation, uniqueness, and differentiability for unbounded kernels. Our first aim was to discuss the global existence, uniqueness and density conservation of weak solutions for the unbounded kernel of the form $V_{i,j} \leq \frac{(i+j)}{\min\{i,j\}}$ for the SDCE. This kernel contains $V_{i,j} = i^{-2/3} + j^{-2/3} \ \forall \ i,j \geq 1$ which explains the 'Diffusion-controlled growth of supported metal crystallites, and $V_{i,j} = i^{1-\alpha}j^{-\alpha} + i^{-\alpha}j^{1-\alpha}$ and $V_{i,j} = (i+j)^{1-\alpha}(ij)^{-\alpha}$, where $\alpha \geq 1$. The boundedness of the first moment and finiteness of the first moment at an initial time were the only prerequisites to establish these results.

The second goal was to extend the definition of the parameter to the sum kernel $V_{i,j} \leq (i+j)$ and discuss the additional conditions under which all solutions conserve the density in the case of SDCE. Further, the first-order differentiability of the solutions was analyzed for the kernel $V_{i,j} \leq i^{\alpha} + j^{\alpha}$, $0 \leq \alpha \leq 1$ which covers the sum kernel under its umbrella. Since, it was not easy to deal with the sum coagulation parameter, we analyzed the uniqueness of the solution for the kernel $V_{i,j} \leq \min\{i^{\eta}, j^{\eta}\}$ where $0 \leq \eta \leq 2$. It was observed that these results are valid when $(\alpha+1)^{th}$ moment was bounded and its value at $t = 0$ is finite.

The numerical counterpart investigated the existence and uniqueness of the steady-state solution and its simulations considering up to bilinear growth rates for three initial data. Therefore, our third objective was to analyze the steady-state behavior and numerically analyze the solutions for the SDCE in the case of constant, sum, and product kernels, i.e., $V_{i,j} = 2, \ (i+j), \ 8i^{1/2}j^{1/2}$ & $2ij \ \forall \ i,j \geq 1$. All the results were established under the assumptions that $M_2(t)$ is bounded and the solution $f_i(t)$ is differentiable. In absence of the availability of analytical solutions, results were justified by producing numerical solutions, normalized moments, and steady-state solutions using three initial conditions $f_i(0) = \frac{1}{2^i}, f_i(0) = e^{-i}$ and $f_i(0) = e^{-i^2}$. However, it was observed that the results were replicated for taking any kernel and initial condition pair.
Interestingly, it was noticed that the oscillations arose as the value of N was increased but only when the time was low; these oscillations seemed to relax as t progressed. The oscillations appeared due to the fact that the large clusters become very efficient

at merging with small ones. As monomers are added to the system, the typical size remains fairly small until a small number of large clusters are generated. At this point, large clusters grow very rapidly by absorbing the smaller clusters, producing a pulse of mass through the space of cluster sizes. These large clusters are then removed by the cutoff, resetting the system to a state with almost no particles, and the cycle repeats. In the case of the product kernel, the aggregating system is open, so the oscillations might arise due to input at small masses and sink at large masses.

In the fourth task, we explored a semi-analytical technique known as the optimized decomposition method (ODM) to solve Smoluchowski's coagulation equation. In order to see the efficiency of this method to deal with multi-dimensional coagulation problems, we initially developed its extension to solve the 2D and 3D Burgers' equations. In addition, the theoretical investigation into the convergence analysis was also carried out for both the equations. It was observed that for the convergence of the series solution to the exact solution, two additional assumptions were required, i.e., $\{u_n\}$ should be a Cauchy sequence, and the parameter $C(x)$ must be essentially bounded. In case of the coagulation equation, the analysis included some numerical examples to establish the application and novelty of this method over ADM considering various relevant kernels with the exponential initial distribution. It was demonstrated that for the constant kernel, ODM needed fewer terms as compared to ADM for a higher value of time. Also, it predicted the behavior of the zeroth moment better than ADM. In the case of sum kernel, ODM proved to be a more reliable method for estimating the number and mass of particles in the system. Finally, we observed that ODM estimated the number density in fewer terms than ADM and both absolute and numerical error values were significantly lower than ADM for product kernel even for small values of time.
For the Burgers' equation, several test cases dealing with the 1D, 2D, and 3D problems were considered to establish the implementation of the method. In the case of 1D, the results computed using ODM were compared with the existing method ADM and it was observed that ODM proved to be a more promising method. Owing to the novelty of ODM, the method was extended to two and three dimensions that aided in calculating the approximate solutions of the 2D and 3D Burgers' equations. Interestingly, we found that ODM was able to compute the solution of a 2D Burgers' equation with no exact solution. It was visualized that the method shows excellent accuracy with the exact solution in all the cases.

Lastly, a Laplace transform-based semi-analytical approach called the Laplace optimized decomposition method (LODM) was implemented to compute the series solutions of Smoluchowski's coagulation equation. In addition to the coagulation equation, we have discussed the approximate solution for the pure fragmentation equation using the

Laplace Adomian decomposition method (LADM). We considered three cases of the coagulation parameters including the constant, sum, and product kernels with exponential initial conditions. In addition, two examples of the fragmentation kernel (binary and Austin) with three selection parameters (up to cubic) and two initial conditions (exponential and mono-disperse) were analyzed.
It was observed that in the case of the fragmentation equation, we were able to compute the closed-form solutions in all the test cases using LADM with a rate of convergence faster than the existing ADM method. However, in the case of the coagulation equation, the seven-term approximated solution computed using LODM gave excellent agreement with the exact solution and was able to predict the moments with very nice accuracy in all the cases.
The article also dealt with theoretical convergence results for both equations. It is noteworthy that in both methods, the Laplace transform provided an advantage in getting a time multiplier for the constant while establishing contraction mapping. Therefore, the theoretical error bounds obtained for both LODM and LADM were significantly improved. In conclusion, these methods proved to be very efficient in dealing with non-linear as well as linear partial integro-differential equations.

Future Scope

Based on the work done in this thesis, the possible future scopes are as follows:

- To conduct the stability analysis for the Safronov-Dubovski coagulation equation.
- To develop coupled numerical and semi-analytical methods to solve coagulation and breakage problems.
- To theoretically, numerically and semi-analytically analyze these coagulation problems in the presence of a little disturbance, i.e., the source term.
- To discuss existence and uniqueness as well as develop semi-analytical methods for multi-dimensional aggregation and breakage problems.

Bibliography

[1] Li Ge Wang, Ruihuan Ge, Xizhong Chen, Rongxin Zhou, and Han-Mei Chen. Multiscale digital twin for particle breakage in milling: From nanoindentation to population balance model. *Powder Technology*, 386:247–261, 2021.

[2] Magali Tournus, Miguel Escobedo, Wei-Feng Xue, and Marie Doumic. Insights into the dynamic trajectories of protein filament division revealed by numerical investigation into the mathematical model of pure fragmentation. *PLoS Computational Biology*, 17(9):e1008964, 2021.

[3] Suresh Pathi, Rajesh Kumar, and Vikranth Kumar Surasani. Investigation on agglomeration kinetics of acetaminophen using fluidized bed wet granulation. *Asia-Pacific Journal of Chemical Engineering*, 15(2):e2416, 2020.

[4] Oleksii S Rukhlenko, Olga A Dudchenko, Ksenia E Zlobina, and Georgy Th Guria. Mathematical modeling of intravascular blood coagulation under wall shear stress. *PloS one*, 10(7):e0134028, 2015.

[5] Panagiotis Neofytou, Maria Theodosiou, Marios G Krokidis, and Eleni K Efthimiadou. Simulation of colloidal stability and aggregation tendency of magnetic nanoflowers in biofluids. *Modelling*, 3(1):14–26, 2022.

[6] Doraiswami Ramkrishna. *Population balances: Theory and applications to particulate systems in engineering*. Elsevier, 2000.

[7] Mitja Zidar, Drago Kuzman, and Miha Ravnik. Characterisation of protein aggregation with the smoluchowski coagulation approach for use in biopharmaceuticals. *Soft matter*, 14(29):6001–6012, 2018.

[8] Dmitri O Pushkin and Hassan Aref. Bank mergers as scale-free coagulation. *Physica A: Statistical Mechanics and its Applications*, 336(3-4):571–584, 2004.

[9] Jindong Shen, M Yu, TL Chan, Can Tu, and Y Liu. Efficient method of moments for simulating atmospheric aerosol growth: Model description, verification, and application. *Journal of Geophysical Research: Atmospheres*, 125(13):e2019JD032172, 2020.

[10] Hiro-Sato Niwa. School size statistics of fish. *Journal of Theoretical Biology*, 195 (3):351–361, 1998.

[11] SI Piotrowski. The collisions of asteroids. *AcA*, 6:115–138, 1953.

[12] Nikolai Brilliantov, PL Krapivsky, Anna Bodrova, Frank Spahn, Hisao Hayakawa, Vladimir Stadnichuk, and Jürgen Schmidt. Size distribution of particles in saturn's rings from aggregation and fragmentation. *Proceedings of the National Academy of Sciences*, 112(31):9536–9541, 2015.

[13] Jonathan AD Wattis. A coagulation–disintegration model of oort–hulst cluster-formation. *Journal of Physics A: Mathematical and Theoretical*, 45(42):425001, 2012.

[14] Jane E Gross, W Graham Carlos, Charles S Dela Cruz, Philip Harber, and Shazia Jamil. Sand and dust storms: Acute exposure and threats to respiratory health. *American Journal of Respiratory and Critical Care Medicine*, 198(7):13–14, 2018.

[15] Wei Gao, Xinyan Zhang, Dawei Zhang, Qingkui Peng, Qi Zhang, and Ritsu Dobashi. Flame propagation behaviours in nano-metal dust explosions. *Powder Technology*, 321:154–162, 2017.

[16] Raymond S Bradley and John England. Volcanic dust influence on glacier mass balance at high latitudes. *Nature*, 271(5647):736–738, 1978.

[17] JH Oort, HC Van de Hulst, et al. Gas and smoke in interstellar space. *Bulletin of the Astronomical Institutes of the Netherlands*, 10(376):187–204, 1946.

[18] Viktor Sergeevich Safronov. *Evolution of the Protoplanetary Cloud and Formation of the Earth and the Planets*. Israel Program for Scientific Translations Jerusalem, 1972.

[19] PB Dubovski. A 'triangle' of interconnected coagulation models. *Journal of Physics A: Mathematical and General*, 32(5):781–798, 1999.

[20] James Davidson. Existence and uniqueness theorem for the safronov–dubovski coagulation equation. *Zeitschrift für Angewandte Mathematik und Physik ZAMP*, 65(4):757–766, 2014.

[21] Véronique Bagland. Convergence of a discrete oort–hulst–safronov equation. *Mathematical Methods in the Applied Sciences*, 28(13):1613–1632, 2005.

[22] P B Dubovski. *Mathematical theory of coagulation*. National University, 1994.

[23] MV Smoluchowski. A mathematical theory of coagulation kinetics of colloidal solutions. *Z. Phys. Chem*, 92:129–135, 1917.

[24] H Müller. To general theory of rapid coagulation. *Kolloideihefte*, 27:223–250, 1928.

[25] Johannes Martinus Burgers. A mathematical model illustrating the theory of turbulence. In *Advances in Applied Mechanics*, volume 1, pages 171–199. 1948.

[26] Julian D Cole. On a quasi-linear parabolic equation occurring in aerodynamics. *Quarterly of Applied Mathematics*, 9(3):225–236, 1951.

[27] Sergio Albeverio, Anastasia Korshunova, and Olga Rozanova. A probabilistic model associated with the pressureless gas dynamics. *Bulletin des Sciences Mathematiques*, 137(7):902–922, 2013.

[28] Ali Kurt, Yücel Çenesiz, and Orkun Tasbozan. On the solution of burgers' equation with the new fractional derivative. *Open Physics*, 13(1):355–360, 2015.

[29] Yücel Çenesiz, Dumitru Baleanu, Ali Kurt, and Orkun Tasbozan. New exact solutions of burgers' type equations with conformable derivative. *Waves in Random and Complex Media*, 27(1):103–116, 2017.

[30] Mehmet Senol, Orkun Tasbozan, and Ali Kurt. Numerical solutions of fractional burgers' type equations with conformable derivative. *Chinese Journal of Physics*, 58:75–84, 2019.

[31] Harry Bateman. Some recent researches on the motion of fluids. *Monthly Weather Review*, 43(4):163–170, 1915.

[32] Sergei E Esipov. Coupled burgers equations: a model of polydispersive sedimentation. *Physical Review E*, 52(4):3711–3718, 1995.

[33] Vineet K Srivastava and Mukesh K Awasthi. (1+ n)-dimensional burgers' equation and its analytical solution: A comparative study of hpm, adm and dtm. *Ain Shams Engineering Journal*, 5(2):533–541, 2014.

[34] https://scitechdaily.com/gigantic-collision-in-the-asteroid-belt-boosted-biodiversity-on-earth/.

[35] Miroslaw Lachowicz, Philippe Laurençot, and Dariusz Wrzosek. On the oort–hulst–safronov coagulation equation and its relation to the smoluchowski equation. *SIAM Journal on Mathematical Analysis*, 34(6):1399–1421, 2003.

[36] Philippe Laurençot. Convergence to self-similar solutions for a coagulation equation. *Zeitschrift für Angewandte Mathematik und Physik ZAMP*, 56(3):398–411, 2005.

[37] Philippe Laurençot. Self-similar solutions to a coagulation equation with multiplicative kernel. *Physica D: Nonlinear Phenomena*, 222(1-2):80–87, 2006.

[38] Véronique Bagland and Philippe Laurençot. Self-similar solutions to the oort–hulst–safronov coagulation equation. *SIAM Journal on Mathematical Analysis*, 39 (2):345–378, 2007.

[39] Govind Menon and Robert L Pego. Approach to self-similarity in smoluchowski's coagulation equations. *Communications on Pure and Applied Mathematics: A Journal Issued by the Courant Institute of Mathematical Sciences*, 57(9):1197–1232, 2004.

[40] Philippe Laurençot. Weak compactness techniques and coagulation equations. In *Evolutionary Equations with Applications in Natural Sciences*, pages 199–253. Springer, 2015.

[41] Prasanta Kumar Barik, Ankik Kumar Giri, and Philippe Laurençot. Mass-conserving solutions to the smoluchowski coagulation equation with singular kernel. *Proceedings of the Royal Society of Edinburgh: Section A Mathematics*, 150 (4):1805–1825, 2020.

[42] Philippe Laurençot. Uniqueness of mass-conserving self-similar solutions to smoluchowski's coagulation equation with inverse power law kernels. *Journal of Statistical Physics*, 171(3):484–492, 2018.

[43] Philippe Laurençot. Mass-conserving self-similar solutions to coagulation–fragmentation equations. *Communications in Partial Differential Equations*, 44 (9):773–800, 2019.

[44] IW Stewart and E Meister. A global existence theorem for the general coagulation–fragmentation equation with unbounded kernels. *Mathematical Methods in the Applied Sciences*, 11(5):627–648, 1989.

[45] Z. A. Melzak. A scalar transport equation. *Transactions of the American Mathematical Society*, 85(2):547–560, 1957.

[46] Jacek Banasiak, Wilson Lamb, and Philippe Laurençot. *Analytic methods for coagulation-fragmentation models*, volume 2. CRC Press, 2019.

[47] Jacek Banasiak. Global classical solutions of coagulation–fragmentation equations with unbounded coagulation rates. *Nonlinear Analysis: Real World Applications*, 13(1):91–105, 2012.

[48] Philippe Laurençot. Stationary solutions to coagulation-fragmentation equations. *Annales de l'Institut Henri Poincaré C, Analyse Non Linéaire*, 36(7):1903–1939, 2019.

[49] Francis Filbet and Philippe Laurençot. Numerical simulation of the smoluchowski coagulation equation. *SIAM Journal on Scientific Computing*, 25(6):2004–2028, 2004.

[50] Jean-Pierre Bourgade and Francis Filbet. Convergence of a finite volume scheme for coagulation-fragmentation equations. *Mathematics of Computation*, 77(262): 851–882, 2008.

[51] Jitendra Kumar, Jitraj Saha, and Evangelos Tsotsas. Development and convergence analysis of a finite volume scheme for solving breakage equation. *SIAM Journal on Numerical Analysis*, 53(4):1672–1689, 2015.

[52] Louis Forestier-Coste and Simona Mancini. A finite volume preserving scheme on nonuniform meshes and for multidimensional coalescence. *SIAM Journal on Scientific Computing*, 34(6):840–860, 2012.

[53] J Manafianheris. Application of the modified laplace decomposition method for solving the homogeneous smoluchowski's equation. *World Applied Sciences Journal*, 14(12):1804–1815, 2011.

[54] Daniil Aleksandrovich Stefonishin, Sergei Aleksandrovich Matveev, Aleksandr Pavlovich Smirnov, and Eugene Evgen'evich Tyrtyshnikov. Tensor decompositions for solving the equations of mathematical models of aggregation with multiple collisions of particles. *Numerical Methods and Programming (Vychislitel'nye Metody i Programmirovanie)*, 19:390–404, 2018.

[55] Jafar Biazar, Zainab Ayati, and Mohammad Reza Yaghouti. Homotopy perturbation method for homogeneous smoluchowsk's equation. *Numerical Methods for Partial Differential Equations*, 26(5):1146–1153, 2010.

[56] Gurmeet Kaur, Randhir Singh, Mehakpreet Singh, Jitendra Kumar, and Themis Matsoukas. Analytical approach for solving population balances: a homotopy perturbation method. *Journal of Physics A: Mathematical and Theoretical*, 52 (38):385201, 2019.

[57] Zakia Hammouch and Toufik Mekkaoui. A laplace-variational iteration method for solving the homogeneous smoluchowski coagulation equation. *Applied Mathematical Sciences*, 6(18):879–886, 2012.

[58] Randhir Singh, Jitraj Saha, and Jitendra Kumar. Adomian decomposition method for solving fragmentation and aggregation population balance equations. *Journal of Applied Mathematics and Computing*, 48(1):265–292, 2015.

[59] Abdelmalek Hasseine, Menwer Attarakih, Rafik Belarbi, and Hans Jörg Bart. On the semi-analytical solution of integro-partial differential equations. *Energy Procedia*, 139:358–366, 2017.

[60] Abhishek Dutta, Zehra Pınar, Denis Constales, and Turgut Öziş. Population balances involving aggregation and breakage through homotopy approaches. *International Journal of Chemical Reactor Engineering*, 16(6):20170153, 2018.

[61] Hassan Saberi Nik, Sohrab Effati, Reza Buzhabadi, and M Golchaman. Solution of the smoluchowski's equation by homotopy analysis method. *International Journal of Nonlinear Science*, 11(3):330–337, 2011.

[62] A. Hasseine, Z. Barhoum, M. Attarakih, and H.-J. Bart. Analytical solutions of the particle breakage equation by the adomian decomposition and the variational iteration methods. *Advanced Powder Technology*, 26(1):105–112, 2015.

[63] A Hasseine and H-J Bart. Adomian decomposition method solution of population balance equations for aggregation, nucleation, growth and breakup processes. *Applied Mathematical Modelling*, 39(7):1975–1984, 2015.

[64] Abdelmalek Hasseine, Samra Senouci, Menwer Attarakih, and Hand-Jörg Bart. Two analytical approaches for solution of population balance equations: particle breakage process. *Chemical Engineering & Technology*, 38(9):1574–1584, 2015.

[65] M Sommer, F Stenger, W Peukert, and NJ Wagner. Agglomeration and breakage of nanoparticles in stirred media mills—a comparison of different methods and models. *Chemical Engineering Science*, 61(1):135–148, 2006.

[66] Gurmeet Kaur, Randhir Singh, and Heiko Briesen. Approximate solutions of aggregation and breakage population balance equations. *Journal of Mathematical Analysis and Applications*, 512(2):126166, 2022.

[67] Zaid Odibat. An optimized decomposition method for nonlinear ordinary and partial differential equations. *Physica A: Statistical Mechanics and its Applications*, 541:123323, 2020.

[68] Zaid Odibat. The optimized decomposition method for a reliable treatment of ivps for second order differential equations. *Physica Scripta*, 96(9):095206, 2021.

[69] Osama H. Mohammed and Huda A. Salim. Computational methods based laplace decomposition for solving nonlinear system of fractional order differential equations. *Alexandria Engineering Journal*, 57(4):3549–3557, 2018.

[70] Najmuddin Ahmad and Balmukund Singh. Numerical solution of volterra nonlinear integral equation by using laplace adomian decomposition method. *International Journal of Applied Mathematics*, 35(1):39–48, 2022.

[71] Manzoor Ahmad, Rajshree Mishra, and Renu Jain. Analytical solution of one dimensional time fractional black-scholes equation through laplace adomian decomposition method. *Mathematics in Engineering, Science & Aerospace (MESA)*, 13(2):373–386, 2022.

[72] Wahiba Beghami, Banan Maayah, Samia Bushnaq, and Omar Abu Arqub. The laplace optimized decomposition method for solving systems of partial differential equations of fractional order. *International Journal of Applied and Computational Mathematics*, 8(2):1–18, 2022.

[73] Pei-Guang Zhang and Jian-Ping Wang. A predictor–corrector compact finite difference scheme for burgers' equation. *Applied Mathematics and Computation*, 219 (3):892–898, 2012.

[74] Yan Guo, Yu-feng Shi, and Yi-min Li. A fifth-order finite volume weighted compact scheme for solving one-dimensional burgers' equation. *Applied Mathematics and Computation*, 281:172–185, 2016.

[75] Waleed Mohamed Abd-Elhameed. Novel expressions for the derivatives of sixth kind chebyshev polynomials: Spectral solution of the non-linear one-dimensional burgers' equation. *Fractal and Fractional*, 5(2):53, 2021.

[76] Kedir Aliyi Koroche. Numerical solution of in-viscid burger equation in the application of physical phenomena: The comparison between three numerical methods. *International Journal of Mathematics and Mathematical Sciences*, 2022:8613490, 2022.

[77] Ihteram Ali, Sirajul Haq, Saud Fahad Aldosary, Kottakkaran Sooppy Nisar, and Faraz Ahmad. Numerical solution of one- and two-dimensional time-fractional burgers equation via lucas polynomials coupled with finite difference method. *Alexandria Engineering Journal*, 61(8):6077–6087, 2022.

[78] Sachin Kumar and Dia Zeidan. An efficient mittag-leffler kernel approach for time-fractional advection-reaction-diffusion equation. *Applied Numerical Mathematics*, 170:190–207, 2021.

[79] Subhankar Sil, T. Raja Sekhar, and Dia Zeidan. Nonlocal conservation laws, nonlocal symmetries and exact solutions of an integrable soliton equation. *Chaos, Solitons Fractals*, 139:110010, 2020.

[80] Farheen Sultana, Deeksha Singh, Rajesh K. Pandey, and Dia Zeidan. Numerical schemes for a class of tempered fractional integro-differential equations. *Applied Numerical Mathematics*, 157:110–134, 2020.

[81] AJ Hussein and HA Kashkool. L2-optimal order error for two-dimensional coupled burgers'equations by weak galerkin finite element method. *TWMS Journal of Applied and Engineering Mathematics*, 12(1):34–51, 2022.

[82] Xu Zhang, Yanqun Jiang, Yinggang Hu, and Xun Chen. High-order implicit weighted compact nonlinear scheme for nonlinear coupled viscous burgers' equations. *Mathematics and Computers in Simulation*, 196:151–165, 2022.

[83] Ihteram Ali, Sirajul Haq, Kottakkaran Sooppy Nisar, and Dumitru Baleanu. An efficient numerical scheme based on lucas polynomials for the study of multidimensional burgers-type equations. *Advances in Difference Equations*, 2021(1): 1–24, 2021.

[84] Wenyuan Liao. A fourth-order finite-difference method for solving the system of two-dimensional burgers' equations. *International Journal for Numerical Methods in Fluids*, 64(5):565–590, 2010.

[85] Vijitha Mukundan, Ashish Awasthi, and VS Aswin. Multistep methods for the numerical simulation of two-dimensional burgers' equation. *Differential Equations and Dynamical Systems*, 30:909–932, 2022.

[86] A Coely et al. Backlund and darboux transformations. *American Mathematical Society, Providence, Rhode Island*, pages 458–468, 2001.

[87] Tarig M Elzaki and Hwajoon Kim. The solution of burger's equation by elzaki homotopy perturbation method. *Applied Mathematical Sciences*, 8(59):2931–2940, 2014.

[88] Abdul-Majid Wazwaz. The tanh method for traveling wave solutions of nonlinear equations. *Applied Mathematics and Computation*, 154(3):713–723, 2004.

[89] A-M Wazwaz. A sine-cosine method for handling nonlinear wave equations. *Mathematical and Computer Modelling*, 40(5-6):499–508, 2004.

[90] M. Imran, D.L.C. Ching, Rabia Safdar, Ilyas Khan, M. A. Imran, and K. S. Nisar. The solutions of non-integer order burgers' fluid flowing through a round channel with semi-analytical technique. *Symmetry*, 11(8), 2019.

[91] Shabir Ahmad, Aman Ullah, Ali Akgül, and Manuel De la Sen. A novel homotopy perturbation method with applications to nonlinear fractional order kdv and

burger equation with exponential-decay kernel. *Journal of Function Spaces*, 2021, 2021.

[92] Sinan Deniz, Ali Konuralp, and Mnauel De la Sen. Optimal perturbation iteration method for solving fractional model of damped burgers' equation. *Symmetry*, 12 (6), 2020.

[93] Mohammad Partohaghighi, Ali Akgül, Jihad Asad, Rania Wannan, and Palestine Tulkarm. Solving the time-fractional inverse burger equation involving fractional heydari-hosseininia derivative. *AIMS Mathematics*, 7(9):17403–17417, 2022.

[94] Ilham Asmouh, Mofdi El-Amrani, Mohammed Seaid, and Naji Yebari. High-order isogeometric modified method of characteristics for two-dimensional coupled burgers' equations. *International Journal for Numerical Methods in Fluids*, 94: 608–631, 2022.

[95] Mustafa Inc. On numerical solution of burgers' equation by homotopy analysis method. *Physics Letters A*, 372(4):356–360, 2008.

[96] Jafar Biazar and Hossein Aminikhah. Exact and numerical solutions for non-linear burger's equation by vim. *Mathematical and Computer Modelling*, 49(7-8): 1394–1400, 2009.

[97] Saeid Abbasbandy and MT Darvishi. A numerical solution of burgers' equation by time discretization of adomian's decomposition method. *Applied Mathematics and Computation*, 170(1):95–102, 2005.

[98] Hongqing Zhu, Huazhong Shu, and Meiyu Ding. Numerical solutions of two-dimensional burgers' equations by discrete adomian decomposition method. *Computers & Mathematics with Applications*, 60(3):840–848, 2010.

[99] Mehdi Dehghan, Asgar Hamidi, and Mohammad Shakourifar. The solution of coupled burgers' equations using adomian–pade technique. *Applied Mathematics and Computation*, 189(2):1034–1047, 2007.

[100] Mayur P Bonkile, Ashish Awasthi, C Lakshmi, Vijitha Mukundan, and VS Aswin. A systematic literature review of burgers' equation with recent advances. *Pramana*, 90(6):1–21, 2018.

[101] FP Da Costa. A finite-dimensional dynamical model for gelation in coagulation processes. *Journal of Nonlinear Science*, 8(6):619–653, 1998.

[102] Walter Rudin et al. *Principles of mathematical analysis*, volume 3. McGraw-hill New York, 1976.

[103] Mícheál O'Searcoid. *Metric spaces*. Springer Science & Business Media, 2006.

[104] Halsey Lawrence Royden and Patrick Fitzpatrick. *Real analysis*, volume 32. Macmillan New York, 1988.

[105] Walter Rudin. *Real and Complex Analysis P. 2*. McGraw-Hill, 1970.

[106] Herbert Amann. *Ordinary differential equations: An introduction to nonlinear analysis*, volume 13. Walter De Gruyter, 2011.

[107] Haim Brézis. *Functional analysis, sobolev spaces and partial differential equations*, volume 2. Springer, 2011.

[108] Earl A Coddington and Norman Levinson. *Theory of ordinary differential equations*. Tata McGraw-Hill Education, 1955.

[109] Robert G Bartle and Donald R Sherbert. *Introduction to real analysis*, volume 2. Wiley New York, 2000.

[110] Gieri Simonett and Christoph Walker. On the solvability of a mathematical model for prion proliferation. *Journal of Mathematical Analysis and Applications*, 324 (1):580–603, 2006.

[111] Elena Leis and Christoph Walker. Existence of global classical and weak solutions to a prion equation with polymer joining. *Journal of Evolution Equations*, 17(4): 1227–1258, 2017.

[112] Ankik Kumar Giri and Philippe Laurençot. Weak solutions to the collision-induced breakage equation with dominating coagulation. *Journal of Differential Equations*, 280:690–729, 2021.

[113] Ankik Kumar Giri, Philippe Laurençot, and Gerald Warnecke. Weak solutions to the continuous coagulation equation with multiple fragmentation. *Nonlinear Analysis: Theory, Methods & Applications*, 75(4):2199–2208, 2012.

[114] Philippe Laurençot. On a class of continuous coagulation-fragmentation equations. *Journal of Differential Equations*, 167(2):245–274, 2000.

[115] C Dellacherie and PA Meyer. Probabilités et potentiel, chapitres ia iv, hermann. english translation: Probabilities and potential. *North-Holland Mathematics Studies*, 29, 1975.

[116] Irene Fonseca and Giovanni Leoni. *Modern methods in the calculus of variations: L^p Spaces*. Springer Science and Business Media, 2007.

[117] Po-Fang Hsieh and Yasutaka Sibuya. *Basic theory of ordinary differential equations*. Springer Science & Business Media, 2012.

[118] John M Ball and Jack Carr. The discrete coagulation-fragmentation equations: existence, uniqueness, and density conservation. *Journal of Statistical Physics*, 61 (1-2):203–234, 1990.

[119] Francis Filbet and Philippe Laurençot. Mass-conserving solutions and non-conservative approximation to the smoluchowski coagulation equation. *Archiv der Mathematik*, 83(6):558–567, 2004.

[120]

[121] Andreĭ Nikolaevich Kolmogorov and Sergeĭ Vasilevich Fomin. *Introductory real analysis*. Courier Corporation, 1975.

[122] Philippe Laurençot. The lifshitz-slyozov equation with encounters. *Mathematical Models and Methods in Applied Sciences*, 11(04):731–748, 2001.

[123] Philippe Laurençot and Stéphane Mischler. From the discrete to the continuous coagulation–fragmentation equations. *Proceedings of the Royal Society of Edinburgh Section A: Mathematics*, 132(5):1219–1248, 2002.

[124] Debdulal Ghosh, Jitraj Saha, and Jitendra Kumar. Existence and uniqueness of steady-state solution to a singular coagulation-fragmentation equation. *Journal of Computational and Applied Mathematics*, page 112992, 2020.

[125] P B Dubovski. Structural stability of disperse systems and finite nature of a coagulation front. *Journal of Experimental and Theoretical Physics*, 89(2):384–390, 1999.

[126] YC Jiao, Y Yamamoto, C Dang, and Y Hao. An aftertreatment technique for improving the accuracy of adomian's decomposition method. *Computers & Mathematics with Applications*, 43(6-7):783–798, 2002.

[127] Jihuan He. A new approach to nonlinear partial differential equations. *Communications in Nonlinear Science and Numerical Simulation*, 2(4):230–235, 1997.

[128] Dia Zeidan, Chi Kin Chau, Tzon-Tzer Lu, and Wei-Quan Zheng. Mathematical studies of the solution of burgers' equations by adomian decomposition method. *Mathematical Methods in the Applied Sciences*, 43(5):2171–2188, 2020.

[129] Mojtaba Ranjbar, Hojatollah Adibi, and Mehrdad Lakestani. Numerical solution of homogeneous smoluchowski's coagulation equation. *International Journal of Computer Mathematics*, 87(9):2113–2122, 2010.

[130] William T Scott. Analytic studies of cloud droplet coalescence. *Journal of Atmospheric Sciences*, 25(1):54–65, 1968.

[131] Jalil Manafian Heris and Isa Zamanpour. Solving burger's equation by semi-analytical and implicit method. *Statistics, Optimization & Information Computing*, 2(3):222–233, 2014.

[132] Zaid M. Odibat. A study on the convergence of variational iteration method. *Mathematical and Computer Modelling*, 51(9):1181–1192, 2010.

[133] Abdul-Majid Wazwaz. Solitary waves theory. In *Partial Differential Equations and Solitary Waves Theory*, pages 479–502. Springer, 2009.

[134] Majeed Ahmed Al-Jawary, Mustafa Mahmood Azeez, and Ghassan Hasan Radhi. Analytical and numerical solutions for the nonlinear burgers and advection–diffusion equations by using a semi-analytical iterative method. *Computers & Mathematics with Applications*, 76(1):155–171, 2018.

[135] Sonali Kaushik and Rajesh Kumar. A novel optimized decomposition method for smoluchowski's aggregation equation. *Journal of Computational and Applied Mathematics*, 419:114710, 2023.

[136] Remi Jullien and Robert Botet. Aggregation and fractal aggregates. *Ann. Telecomm.*, 41:343–short, 1987.

[137] Igor Agranovski. *Aerosols: science and technology*. John Wiley & Sons, 2011.

[138] Jitendra Kumar. *Numerical approximations of population balance equations in particulate systems*. PhD thesis, Otto-von-Guericke-Universität Magdeburg, Universitätsbibliothek, 2006.

[139] Jitendra Kumar, M Peglow, G Warnecke, S Heinrich, and L Mörl. Improved accuracy and convergence of discretized population balance for aggregation: The cell average technique. *Chemical Engineering Science*, 61(10):3327–3342, 2006.

[140] Mehakpreet Singh, Hamza Y Ismail, Themis Matsoukas, Ahmad B Albadarin, and Gavin Walker. Mass-based finite volume scheme for aggregation, growth and nucleation population balance equation. *Proceedings of the Royal Society A*, 475 (2231):20190552, 2019.

[141] Robert M Ziff and ED McGrady. The kinetics of cluster fragmentation and depolymerisation. *Journal of Physics A: Mathematical and General*, 18(15):3027–3037, 1985.

[142] Leonard G Austin. A treatment of impact breakage of particles. *Powder Technology*, 126(1):85–90, 2002.

List of Publications

1. S. Kaushik and R. Kumar, "Existence, Uniqueness and Mass Conservation for Safronov- Dubovski Coagulation Equation", *Acta Applicandae Mathematicae*, 179(1) 1-21, 2022.

   https://link.springer.com/article/10.1007/s10440-022-00497-8

2. S. Kaushik and R. Kumar,"A Novel Optimized Decomposition Method for Solving Smoluchowski's Aggregation Equation", *Journal of Computational and Applied Mathematics*, 419, 114710, 2023.

   https://www.sciencedirect.com/science/article/pii/S0377042722003594

3. S. Kaushik and R. Kumar, " Optimized Decomposition Method for Solving Multi-Dimensional Burgers' Equation", *Mathematics and Computers in Simulation*, 208, 326-350, 2023.

   https://www.sciencedirect.com/science/article/pii/S0378475423000575?dgcid=author

4. S. Kaushik and R. Kumar,"Steady-State Solution for Discrete Oort-Hulst-Safronov Coagulation Equation", *Int. J. of Dynamical Systems and Differential Equations*, 13(2), 144-163, 2023.

   https://www.inderscience.com/info/inarticle.php?artid=130311

5. S. Kaushik and R. Kumar, "Global Uniqueness Theorem for a Discrete Population Balance Model with Application in Astrophysics", *Advances in Computational Modeling and Simulation*, (Conference Proceedings) 61-73, 2022.

   https://link.springer.com/chapter/10.1007/978-981-16-7857-8˙6

6. S. Kaushik, R. Kumar, and F. P. da Costa, "Theoretical Analysis of a Discrete Population Balance Model for Sum Kernel", *Portugaliae Mathematica*, DOI-10.4171/PM/2103.

7. S. Kaushik, S. Hussain and R. Kumar, "Laplace Transform Based Semi-Analytical Techniques to Solve Pure Aggregation and Breakage Problems", *Mathematical Methods and Applied Sciences*, Under minor revision

8. S. Kaushik and R. Kumar, "Qualitative Analysis of a New Numerical Method to Solve Ordinary Differential Equations", Under review.

9. S. Kaushik and R. Kumar, "Global existence and density conservation for unbounded kernels using a non-conservative approximation for Safronov-Dubovski aggregation equation", Under review.

Conferences and Workshops

Conference Presentation

1. 4^{th} International Conference on Frontiers in Industrial and Applied Mathematics-2021- "Steady-State Solution for Discrete Oort-Hulst-Safronov Coagulation Equation" held at Sant Longowal Institute of Engineering Technology, Longowal, Punjab on December 21 - 22, 2021.

2. International Conference on Advances in Mechanics, Modeling, Computing and Statistics (ICAMMCS) - "Optimized Decomposition Method for Pure Growth Equation." organized by the Department of Mathematics on March 19-21, 2022.

3. International Conference on Dynamical Systems, Control Theory their Applications (ICDSCA) - "A New Approximation Method to Solve Pure Breakage Equation" held at IIT Roorkee on July 01-03, 2022.

Conference/Workshops Attended

1. GIAN Course on "Population Balance Equations with Applications" held at IIT Roorkee (November 26-30, 2018).

2. Indo-French Conference on Applied Mathematics (IFCAM) on "Theory and Simulation of Hyperbolic PDE's arising in Mathematical Biology and Fluid Flow" at BITS Pilani, Pilani campus (January 5-11, 2019).

3. Seven Days Workshop on Academic Writing organized by Department of Humanities and Social Sciences, BITS Pilani, Pilani campus (April 05-11, 2019).

4. West Asian Mathematical Schools (WAMS) on "Recent Developments and Applications of Partial Differential Equations, from Theory to Simulation", held at IIT Roorkee (29th August-3rd September 2019).

5. International Conference and 22nd Annual Convention of Vijñana Parishad of India on "Advances in Operations Research, Statistics and Mathematics" organized by Dept. of Mathematics, BITS Pilani, Pilani campus (December 28-30, 2019).

Brief Biography of the Supervisor

Rajesh Kumar is an Associate Professor at the Department of Mathematics, Birla Institute of Technology and Science, Pilani, Pilani Campus, India. He earned his Bachelor of Arts(H) in Mathematics from Satyawati College, Delhi University, in 2003. He completed his M.Sc.in Applied Mathematics from IIT Roorkee in 2005. Further, Prof. received the Erasmus Mundus Fellowship and went on to pursue M.Sc. in Industrial Maths and Scientific Computing (Dual Degree) from the Technical Univ. of Kaiserslautern, Germany, and Johannes Kepler Univ. Linz, Austria in 2007. He conferred his Ph.D. in 2011 from the Institute of Analysis and Numerics, Otto-von-Guericke University Magdeburg, Germany. Prof. was a Postdoctoral Fellow at MOX, Politecnico di Milano, Italy from March 2011-March 2012. He was a scientific collaborator at EPFL, Switzerland from Nov. 2011 to April 2013 and a research scientist at RICAM Linz, Austria from May 2013 to June 2014. Prof. Rajesh Kumar was a visiting Assistant Professor at IIT Bhubaneswar, India from October 2014 to July 2017 and he joined BITS Pilani as an assistant professor in July 2017. In addition, he was a visiting scientist at Univ. of Picardie Jules Verne, Amiens, France from 20th June to 15th July 2018. He was the principal organizer of the Indo-French Research Workshop on "Theory and Simulation of Hyperbolic PDEs arising in Mathematical Biology and Fluid Flow" at BITS Pilani, Pilani Campus, Rajasthan, India from 05th January to 11th January 2019 under the support of IFCAM. He has supervised several postgraduate and undergraduate students. He has published several research articles in renowned journals and presented papers and delivered lectures at several national and international conferences. Prof. Rajesh Kumar has handled several math courses at BITS Pilani, Pilani Campus, and is actively involved in graduate course development. He is also a member of many committees such as faculty recruitment, research board, senate, etc. at BITS Pilani. His research interests are Differential Equations, Nonlinear Analysis, Population Dynamics, Numerical Linear Algebra, Uncertainty Quantification, Low-Rank Approximation of Tensors, Partial-Integro Differential Equations, and Hyperbolic Conservation Laws.

Brief Biography of the Candidate

Sonali Kaushik completed her schooling with 91.6 in tenth and 92 percent in twelfth in 2009 and 2011, respectively. She conferred her Bachelor of Science(H) in Mathematics from Kirori Mal College, University of Delhi in 2014 and earned a Master's in pure Mathematics from Jamia Milia Islamia in 2016. In 2018, she qualified GATE in Mathematics (MA) with AIR 594. Then, she joined Birla Institute of Technology and Science, Pilani, Pilani Campus as an institute fellow in August 2018. In her Ph.D. journey, she has published one book chapter, five research papers in peer-reviewed journals, and presented at three national & international conferences. She has attended three workshops, two conferences and witnessed talks of three international speakers.